Multi-Scale Rock Glacier Kinematics in the Dry Andes of Argentina:

From DEMs to the State of Permafrost Using Photogrammetry

Dissertation

zur

Erlangung des Doktorgrades (Dr. rer. nat.)

der

Mathematisch-Naturwissenschaftlichen Fakultät

der

Rheinischen Friedrich-Wilhelms-Universität Bonn

Vorgelegt von

Melanie Andrea Stammler

aus Heidelberg

Bonn, Oktober 2025

Angefertigt mit Genehmigung der Mathematisch-Naturwissenschaftlichen Fakultät der Rheinischen Friedrich-Wilhelms-Universität Bonn

Gutachter/Betreuer: Prof. Dr. Lothar Schrott

Gutachter: Jun.-Prof. Dr. Jan Blöthe

Tag der Promotion: 16. Dezember 2025

Erscheinungsjahr: 2026

Table of Contents

Acknowledgements

First and foremost, I would like to thank my two supervisors Prof. Dr. Lothar Schrott and Jun.-Prof. Dr. Jan Blöthe for their supervision, support and inspiration. I still remember first learning about rock glaciers during an office visit in the research group at the end of my BSc studies and am very thankful for both of you opening doors into the rock glacier community.

This PhD journey would have been different without the presence of two other people, namely Tamara Köhler and Agostina Ortiz. Going through a PhD side by side with you in the same project was and is a privilege. Thank you for all the time – office talks, lunch breaks, conference visits, and very importantly months of fieldwork. I am so thankful that I got to know you, and for all the memories and advice shared. In addition, big thank you to you, Ago, for translating the abstract.

Further, I am extremely grateful for a network of mentors and co-authors that grew along the way. Big thanks to Rainer Bell, Diego Cusicanqui and Benjamin Robson for numerous lunch breaks, conference meet-ups, zoom calls and beautiful Erasmus stays at Bergen University. In addition, to Daniel Hölbling and Thomas Stevens who encouraged and supported my academic development outside my PhD. Further, big thank you to Anna Schoch-Baumann for your kind support. I am truly thankful to all of you always believing in my abilities and fostering personal growth.

I am extremely thankful to everyone that made the in total more than 5 month of fieldwork in the Argentinean Andes memorable and unforgettable. Next to Tamara Köhler and Agostina Ortiz, this includes: Fabian Flöck, Philipp Reichartz, Till Wenzel, Gabriele Kraus, Cristian Villaroel, Manon Cramer, Florian Wester, Rainer Bell, Kathrin Förster, and Lothar Schrott. Big thanks to Dario Trombotto Liaudat, Carla Tapia Baldis, and everyone else involved at IANIGLA-CONICET for the inspirational exchange, supporting our fieldwork, and for creating new memories during our wonderful stays in Mendoza.

When in Bonn, a wonderful working group was always up for lunch and coffee breaks. Big thank you – in addition to many already named above - to Ella Wood, Ikram Zangana, Simon Terweh and the entire KaVoMa team. Further to the 'wider-GIUB' group with Julian Antoni and Clarissa Glaser.

As a scholarship holder, I am extremely thankful to the German Academic Scholarship Foundation. Their support, non-financially and financially, definitely contributed to shaping my academic career and personal development. In addition, a big thank you to the organizers of the NFDI4Earth Academy and the participants of the first cohort. It was a true pleasure to partake and opened doors in the Earth & Data Science worlds. The inspirational aspect also holds true for the summer school 'Sensing Mountains' conducted at the University Centre Obergurgl. Big thank you to all the organizers, as well as the participants of the 2022 cohort.

One of the downsides of diving deep into the academic world is discovering its limitations. I am more than thankful to the founding team of Geomorphica as well as all the enthusiastic volunteers that I got to engage with. You truly helped me to spark positive action and provided an ecosystem to thrive. I am extremely proud of everything we have established and wish all of you only the best for your futures.

Without my friends, partner and family the time of my PhD would have been less joyful, less entertaining and certainly more stressful. Big thanks in no particular order to Carola Fank, Chikaodi Uba, Clara Fernandez-Nespral, Johanna Reineke, Sara Stücker, Ramona Schneider, Oliver Balthesen, Simon Mösch, Julian Werner, Julian Antoni, Jonas Thormann, Simon König, Kerstin König, and many more. Biggest thank you to the one urban geographer that likely knows most about rock glaciers and without whose support this PhD certainly would have been different, Michael Maday. Ein ganz großes Dankeschön gilt auch meinen Eltern, für eure unendliche Unterstützung, euren Zuspruch und euer Interesse. I am so thankful to all of you - you offered to listen when needed and kept distracting me when useful. You supported me when taking decisions, endured my niche enthusiasm, even proof-read parts of the dissertation, and gifted so many shared memories impossible to enumerate. Most of you know me for a decade or even more than two, and I am more than thankful to have you around me. You all know about my sense of humour so there we go: If I was the drone, I was only able to fly because you were my network of nodes, my solid Earth surface to fall back to.

Haeberli et al. (2006) state in their review that “Future [permafrost] studies should also appeal to the broad scientific audience that is now aware and interested in permafrost as a critical element of the Earth’s cryosphere particularly in light of its vulnerability to atmospheric warming and potential feedbacks to global climate.” I hope that almost 20 years later I can contribute to this grown and growing body of literature with an engaging dissertation that is appealing to a diverse audience. The changing mountain cryosphere is affecting everyone, independent of the respective mountain range and the proximity of oneself. Effective means of reducing vulnerabilities to arising hazards are based on a profound understanding of the periglacial and glacial domains and their complexities – calling for an accessible, innovative, diverse and interdisciplinary science along with a FAIR data management.

Summary

The high-mountain cryosphere is undergoing substantial transformation under global climate warming. In the Dry Andes of Argentina, where precipitation is scarce, glaciers and periglacial ice are critical water reserves. While glaciers rapidly lose mass and surface area, rock glaciers – landforms containing subsurface ice – respond more slowly to atmospheric forcing, temporarily buffering reduced water availability. However, limited data availability has hindered an understanding of rock glacier kinematics and their controlling factors in this region.

This PhD dissertation analyses high-resolution uncrewed aerial vehicle (UAV) surveys and satellite-based photogrammetry to investigate rock glacier surface change patterns across multiple spatial scales and time periods. At the local scale, the Dos Lenguas rock glacier (30°S, 4400 m asl) is monitored using quasi-biennial UAV flights from 2016 to 2024. While the differencing of UAV-derived digital elevation models (DEMs) reveals spatially variable vertical changes (±1.5 m) predominantly linked to compressional flow and ridge-furrow morphology, feature tracking quantifies mean horizontal velocities of 0.9 m/yr and maxima of 1.7 m/yr. Despite rising temperatures, particularly in winter, both vertical and horizontal kinematics remain stable over the eight-year observation period, likely due to the area's aridity limiting insulation effects by snow cover.

Comparisons of UAV-based DEMs and DEMs based on optical satellite imagery (Pléiades) show that when the latter are processed with the software Ames Stereo Pipeline following the strategy outlined in this dissertation, both datasets produce highly similar vertical change estimates. This comparability enables the extension of the methodology to the entire catchment, linking fine-scale UAV observations with regional-scale satellite-based analyses and expanding the surface monitoring to glaciers and debris-covered glaciers.

At the regional scale, vertical surface changes of 19 glaciers, three debris-covered glaciers, and 59 rock glaciers in the Rodeo basin are quantified for 2019 to 2025 using panchromatic, tristereo Pléiades imagery. Further, rock glacier velocity is investigated for all 47 continuously monitored rock glaciers. Glaciers exhibit pronounced surface lowering, up to -8.99 m cumulatively, with debris-covered glaciers displaying intermediate and rock glaciers minimal lowering. No regional acceleration in rock glacier velocities is observed, supporting evidence of stable permafrost conditions.

Overall, this work demonstrates stable rock glacier kinematics indicative of persistent permafrost, contrasting with the retreating glacial domain. The lack of snow cover combined with low high-altitude temperatures likely governs this stability. The study identifies key drivers of rock glacier velocity (creep, gravity, and elevation-related temperature) and evaluates climate effects based on ERA5 data (1940–2020). The findings highlight the need for long-term, continuous monitoring to capture process–response relationships in the rapidly changing high-Andean cryosphere at this critical point in time.

Keywords Cryosphere, permafrost, rock glacier kinematics, Dry Andes of Argentina, UAV monitoring, Pléiades imagery, DEMs of Difference, feature tracking, climate change

Zusammenfassung

Die Kryosphäre der Hochgebirge unterliegt aufgrund der globalen Erderwärmung erheblichen Veränderungen. In den trockenen Anden Argentiniens, wo Niederschläge selten sind, stellen Gletscher und periglaziales Eis wichtige Wasserreserven da. Während Gletscher rapide an Volumen und Fläche verlieren, reagieren Blockgletscher – Landformen, die unterhalb der Erdoberfläche Eis enthalten – langsamer auf atmosphärische Einflüsse und puffern vorübergehend verringerte Wasserverfügbarkeiten ab. Die begrenzte Verfügbarkeit von Daten behindert das Verständnis der Kinematik von Blockgletschern und ihrer Einflussfaktoren in dieser sensiblen Region.

Diese Arbeit kombiniert hochauflösende UAV-Befliegungen und satellitengestützte Photogrammetrie, um Oberflächenveränderungen von Blockgletschern über verschiedene räumliche Skalen und Zeiträume zu analysieren. Auf lokaler Ebene wird der Dos Lenguas Blockgletscher (30°S, 4400 m ü. NN) zwischen 2016 und 2024 in quasi zweijährlichem Intervall betrachtet. Aus UAV-Daten abgeleitete Differenzen digitaler Höhenmodelle (DoDs) zeigen vertikale Veränderungen bis ±1,5 m, überwiegend gesteuert durch die Oberflächenmorphologie. Feature Tracking quantifiziert mittlere horizontale Geschwindigkeiten von 0,9 m/Jahr, mit Maximalwerten von 1,7 m/Jahr. Trotz steigender Temperaturen, vor allem im Winter, bleiben vertikale und horizontale Bewegungen über acht Jahre stabil – ein Hinweis darauf, dass die extreme Trockenheit den Einfluss der nahezu ausbleibenden Schneebedeckung und damit klimatische Steuerungen abschwächt.

Vergleichende Auswertungen zeigen, dass satellitengestützte Höhenmodelle, hier basiert auf Pléiades Daten, bei Anwendung der Software Ames Stereo Pipeline eine hohe Übereinstimmung mit UAV-basierten DoDs aufweisen. Diese Vergleichbarkeit ermöglicht die Übertragung der Methode auf regionale Skalen und die Ausweitung der Analyse auf Gletscher und schuttbedeckte Gletscher.

Auf dieser Basis werden vertikale Veränderungen von 19 Gletschern, drei schuttbedeckten Gletschern und 59 Blockgletschern, sowie die Geschwindigkeiten von allen Blockgletschern mit kontinuierlichem Monitoring - 47 an der Zahl, für 2019-2025 ermittelt. Die Gletscher zeigen eine ausgeprägte Oberflächenabsenkung (bis -8,99 m kumulativ), schuttbedeckte Gletscher moderate und Blockgletscher nur geringe Senkungen. Eine Beschleunigung der Blockgletscherbewegungen ist nicht nachweisbar, was stabile Permafrostbedingungen nahelegt.

Insgesamt detektiert diese Arbeit eine stabile Kinematik der Blockgletscher, die auf stabile Permafrostbedingungen schließen lässt. Dies steht im Kontrast zu einem schrumpfenden Gletschergebiet und hebt die Relevanz des Periglazials als Wasserreserve, besonders unter einem sich erwärmenden Klima, hervor. Die fehlende Schneebedeckung in Verbindung mit auf Grund der Höhe vergleichsweise niedrigen Temperaturen werden als potenzielle Gründe für die kinematische Stabilität identifiziert. Es werden verschiedene Treiber der Blockgletschergeschwindigkeit identifiziert und exemplarisch dargestellt (permafrostbedingtes Kriechen, gravitative Bewegung und geringe Bewegung durch höhere Temperatur in Abhängigkeit von der Höhe). Zudem wird die Auswirkung des Klimas auf der Grundlage von ERA5-Daten (1940-2020) erörtert. Die Ergebnisse unterstreichen die

Notwendigkeit eines langfristigen, kontinuierlichen Monitorings von Blockgletschern, um Prozesse und die damit verbundenen Reaktionen der Blockgletscher in der sich schnell verändernden Kryosphäre der Hochanden zu diesem entscheidenden Zeitpunkt zu erfassen.

Schlagwörter Kryosphäre, Permafrost, Blockgletscherkinematik, Aride Anden Argentinas, UAV-Monitoring, Pléiades-Bilddaten, Höhenmodelldifferenzen (DEMs of Difference), Feature Tracking, Klimawandel

Resumen

La criósfera de alta montaña está experimentando una transformación sustancial debido al calentamiento climático global. En los Andes Áridos de Argentina, donde las precipitaciones son escasas, los glaciares y el hielo periglaciar constituyen reservas de agua fundamentales. Mientras los glaciares pierden masa y área superficial rápidamente, los glaciares de escombros —geoformas del relieve que contienen hielo subsuperficial— responden más lentamente a las condiciones atmosféricas, amortiguando temporalmente la reducción en la disponibilidad de agua. Sin embargo, la limitada disponibilidad de datos ha dificultado la comprensión de la dinámica de los glaciares de escombros, así como de los factores que los controlan en esta región.

Esta tesis doctoral analiza levantamientos de alta resolución mediante drones (UAV) y fotogrametría satelital para investigar los patrones de cambio superficial de glaciares de escombros en múltiples escalas espaciales y temporales. A escala local, el glaciar de escombros Dos Lenguas (30°S, 4400 m s.n.m.) se monitorea mediante vuelos cuasi-bienales de UAV entre 2016 y 2024. Mientras que la diferencia de modelos digitales de elevación (DEM) obtenidos con UAV revela cambios verticales variables espacialmente (±1,5 m), vinculados predominantemente al flujo compresional y a la morfología de crestas y surcos, el rastreo de rasgos superficiales cuantifica velocidades horizontales medias de 0,9 m/año y máximas de 1,7 m/año. A pesar del aumento de las temperaturas, especialmente en invierno, tanto la dinámica vertical como la horizontal permanecen estables durante el periodo de observación de ocho años, probablemente debido a la aridez del área que limita los efectos de la capa cobertura de nieve.

Las comparaciones entre DEM obtenidos con UAV y con imágenes Pléiades muestran que, cuando estos últimos se procesan con el software Ames Stereo Pipeline siguiendo la estrategia planteada en esta tesis, ambos conjuntos de datos producen estimaciones de cambio vertical muy similares. Esta comparabilidad permite extender la metodología a toda la cuenca, vinculando las observaciones detalladas de UAV con análisis a escala regional y ampliando el monitoreo a glaciares y glaciares cubiertos de detritos.

A escala regional, los cambios superficiales verticales de 19 glaciares, tres glaciares cubiertos de detritos y 59 glaciares de escombros en la cuenca de Rodeo se cuantifican para el periodo 2019–2025 mediante imágenes Pléiades triestéreo. Además, se investiga la velocidad de los glaciares de escombros para todos aquellos con monitoreo continuo entre 2019 y 2025, lo que lleva a un análisis de 47 glaciares de escombros. Los glaciares presentan un descenso superficial pronunciado, de hasta -8,99 m acumulados, mientras que los glaciares cubiertos de detritos muestran un descenso intermedio y los glaciares de escombros un descenso mínimo. No se observó ninguna aceleración regional en las velocidades de los glaciares de escombros, lo que respalda la evidencia de condiciones estables de permafrost.

En conjunto, este trabajo demuestra una dinámica estable de los glaciares de escombros, indicativa de permafrost persistente, en contraste con el retroceso del dominio glaciar. La ausencia de cubierta nival, combinada con bajas temperaturas en altura, probablemente explica esta estabilidad. El estudio identifica los principales factores que controlan la velocidad de los glaciares de escombros (flujo por reptación, gravedad y temperatura relacionada con la altitud) y evalúa los efectos climáticos en base a los datos de ERA5 (1940–2020). Estos hallazgos

destacan la necesidad de un monitoreo continuo y a largo plazo para captar las relaciones proceso–respuesta en la criósfera altoandina en rápida transformación en este momento crítico.

Palabras clave Criósfera, permafrost, dinámica de glaciares de escombros, Andes Áridos de Argentina, monitoreo con UAV, imágenes Pléiades, Diferencias entre DEMs, rastreo de rasgos superficiales, cambio climático.

List of Publications

Paper 1 **Stammler, M.**, Cusicanqui, D., Bell, R., Robson, B., Bodin, X., Blöthe, J., Schrott, L., 2024. Vertical surface change signals of rock glaciers: combining UAV and Pléiades imagery (Agua Negra, Argentina).7 Proceedings of the 12th International Conference on Permafrost **(**ICOP). Whitehorse / Canada. DOI: *10.52381/ICOP2024.138.1*

The open access published, peer-reviewed article is reproduced in Chapter 6 of the dissertation.

Paper 2 **Stammler, M.**, Blöthe, J., Flöck, F., Bell, R., Schrott, L., 2025. Dos Lenguas rock glacier kinematics stable despite warming trend (2016–2024): Surface changes and the role of topography and climate in the Dry Andes of Argentina. Earth Surface Processes and Landforms 50. DOI: *10.1002/esp.70151*

The open access published, peer-reviewed article is reproduced in Chapter 7 of the dissertation. It is accompanied by the following dataset publication:

Stammler, M., Blöthe, J., Flöck, F., Bell, R., Schrott, L., 2025. UAV-based optical imagery, digital elevation models and hillshades of Dos Lenguas rock glacier / Argentinean Dry Andes (30ºS, 69ºW; 2016, 2018, 2022, 2024) and daily static optical imagery (2023-2024) [dataset]. PANGAEA, DOI: *10.1594/PANGAEA.979876*

Paper 3 **Stammler, M.**, Blöthe, J., Cusicanqui, D., Ebert, S., Bell, R., Bodin, X. and Schrott, L., 2025. Glacial decline next to stable permafrost in the Dry Andes? Vertical glacier surface changes and rock glacier kinematics based on Pléiades imagery (Rodeo basin / Argentina, 2019-2025). The Cryosphere. *Submitted*.

The submitted manuscript is reproduced in Chapter 8 of the dissertation. It is accompanied by the following dataset publication:

Stammler, M., Blöthe, J., Cusicanqui, D., Ebert, S., Bell, R., Bodin, X., Schrott, L., 2025. Pléiades imagery based digital elevation models and quantified surface change for (debris-covered) glaciers and rock glaciers in the Dry Andes of Argentina (30ºS, 69ºW; 2019, 2022, 2023, 2024, 2025) [dataset]. PANGAEA. *Submitted.*

While the three papers are presented with synthesized chapters on the study area and the data and methods applied, the papers' original layout as published/submitted is appended at the very end of this document, including the papers' supplementary material.

List of Additional Publications

Jiang, Y., **Stammler, M.,** Liu, T., Hölbling, D., Stevens, T., Hu, L. 2025. "Putting arctic aeolian sand dunes in their boundaries": a CNN-based mapping approach applied in northern Sweden. Remote Sensing of Environment. *In Review*.

Bischoff, V., Petzold, P., **Stammler, M.**, 2025: 12th International Conference on Permafrost in Whitehorse/Canada: early career researchers' insight and contributions. Polarforschung. Event Report. *In Review*.

Lefebvre, A., Bosch, R., Burrows, K., Giaime, M., Goodwin, G., Lai, L. S.-H., **Stammler, M.**, Fernández, R., 2025. Geomorphica: The most accessible journal for the geomorphology community. Geomorphica, 1(1). Editorial. DOI: *10.59236/geomorphica.v1i1.54*

Stammler, M., 2024. Using drones to investigate rock glacier kinematics. Nat Rev Earth Environ., DOI: *10.1038/s43017-024-00628-9*

Stammler, M., Stevens, T., Hölbling, D., 2022. Geographic object-based image analysis (GEOBIA) of the distribution and characteristics of aeolian sand dunes in Arctic Sweden. PPP, Vol. 34, Issue 1, DOI: *10.1002/ppp.2169*

Own Contributions to the Publications

This dissertation comprehends two published peer-reviewed papers and one submitted manuscript as listed on page XV. In the following, I detail my own contributions for each of the papers. All of the papers include author contribution statements to further detail the contributions of the different co-authors.

My contributions to the paper "**Vertical surface change signals of rock glaciers: combining UAV and Pléiades imagery (Agua Negra, Argentina) (Paper 1)**" published as peer-reviewed full conference paper, compose: leading the conceptualization, co-organizing the fieldwork, conducting the analysis, facilitating collaboration to acquire the satellite imagery, and leading the investigation, the writing of the initial draft and the writing – review editing.

In detail, the investigation spans the analysis and comparison of DEMs based on UAV and Pléiades imagery for two rock glaciers – Dos Lenguas and El Paso. I acquired all UAV data and Differential Global Navigation Satellite System (DGNSS) measurements either myself or supervised student assistants while co-leading the fieldwork campaigns. I independently conducted their analysis which spans the UAV-based generation of DEMs in Agisoft Metashape Professional including workflow development (for details see below) as well as the calculation of the DEMs of Difference (DoDs). For satellite imagery, I selected Pléiades imagery as suitable input imagery based on literature review and initiated contact with co-authors to collaboratively acquire Pléiades imagery. I independently processed the Pléiades imagery in Agisoft Metashape Professional as well as Catalyst Professional, including the application of co-registration techniques. I independently investigated the DEM errors including their spatial distribution, the DEMs visual appearance, co-registration shifts, and effects of the different processing workflows on the DEMs. In addition, I compared the DoDs derived using the different software as well as between the different input imagery (UAV vs. satellite), all leading to selecting the best software approach for processing Pléiades imagery. Next to the method-oriented focus, I derived findings for rock glacier surface change on the two rock glaciers based on the UAV DEM as well as the selected Pléiades DEM and compared our findings to the literature. I independently drafted the first version of the manuscript including literature review and the generation of all figures. Further, I initiated the submission to the ICOP conference proceedings, led the review and editing stage and finalized the manuscript with comments from co-authors.

My contributions to the paper "**Dos Lenguas rock glacier kinematics stable despite warming trend (2016-2024): Surface changes and the role of topography and climate in the Dry Andes of Argentina (Paper 2)**" compose the conceptualization, co-organizing fieldwork, the methodology including methodological development, the investigation, writing of the initial draft and writing – review and editing.

After the conceptualization of the study, I acquired UAV imagery and DGNSS measurements either myself or by supervised student assistants (2022-2024). Further, I initiated contact with Meteoblue for receiving historical climatological data. The methodological development spans the workflow development for processing the UAV imagery in Agisoft Metashape Professional including co-alignment, georeferencing, and optimization as well as the generation and investigation of the UAV-based DEMs based on literature review, summer school

attendance and exchange on conferences – the two latter which I initiated participation in and for which I successfully applied for funding. The analysis further includes the calculation of vertical surface changes by DEM differencing and of volumetric changes, derivation of high-resolution hillshades for feature tracking, and quantification of data quality. These contributions are followed by the analysis of magnitude and pattern of vertical and horizontal surface changes over time, the derivation of slope and curvature rasters and the analysis of the effects of topography. In addition, the plotting of the received climatological data and the co-analysis with the vertical and horizontal surface changes. I independently drafted the manuscript and figures including reviewing literature, chose the journal, led the review and editing stage and finalized the manuscript with comments from co-authors. I initialised the publication of the paper accompanying dataset in agreement with the co-authors, chose the platform, organized the data, generated metadata, and coordinated the publication with PANGAEA.

My contributions to the paper "**Glacial decline next to stable permafrost in the Dry Andes? Vertical glacier surface changes and rock glacier kinematics based on Pléiades imagery (Rodeo basin, 2019-2025) (Paper 3)**" compose the conceptualization, the methodology including methodological development, the investigation, and writing of the initial draft and writing – review and editing.

In detail, I initiated the repeated Pléiades data-take together with co-authors, developed the workflow for co-registering clipped Pléiades-based DEMs and calculated vertical surface changes for all glaciers, debris-covered glaciers and rock glaciers in Rodeo basin (2019-2025). This includes the calculation of levels of detection (LoDs) for vertical surface change and an investigation of the data accuracy. I coordinated the feature tracking for horizontal changes with co-authors, contributed to the calculation of LoDs and independently analysed the derived horizontal changes for all rock glaciers across the catchment and across time. I validated both vertical and horizontal surface changes with DGNSS measurements taken at selected locations between 2022-2024. These data are either acquired by myself or by supervised student assistants, during fieldwork I co-organized. I independently compared the vertical and horizontal surface changes for all landforms and identified kinematic drivers, such as creep and slope. I independently drafted the manuscript and figures including reviewing literature, chose the journal, successfully applied for university internal funding of the APCs, and led the paper submission after including comments from the co-authors. Similar to Paper 2, I initialised the publication of the paper accompanying dataset, chose the platform, organized the data, generated metadata, and coordinated the submission to PANGAEA.

List of Abbreviations

ALOS PRISM Advanced Land Observing Satellite - Panchromatic Remote-sensing Instrument for Stereo Mapping

ASP Ames Stereo Pipeline

ASTER Advanced Spaceborne Thermal Emission and Reflection Radiometer

B/H Ratio Base-to-Height Ratio

CBERS-4A China-Brazil Earth Resources Satellite-4A

CMOS Complementary Metal-Oxide-Semiconductor

CP Check Point

DEM Digital Elevation Model

DoD DEM of Difference

DJI Da-Jiang Innovations

(D)GNSS (Differential) Global Navigation Satellite System

ECMWF European Centre for Medium-Range Weather Forecasts

ECV Essential Climate Variable

EMT Environmental Motion Tracking

ENSO El Niño Southern Oscillation

EP époque / time period

ERA5 ECMWF Reanalysis v5 Dataset

ERT Electrical Resistivity Tomography

FAIR Findable, accessible, interoperable, and reusable

GCP Ground Control Points

GCOS Global Climate Observing System

GeoTIFF Geographic Tagged Image File Format

GPR Ground Penetrating Radar

GTN-P Global Terrestrial Network for Permafrost

HyPERM DFG-funded project “Spatial occurrence and hydrological significance of Andean permafrost (Agua Negra, San Juan, Argentina)”

IANIGLA-CONICET Argentine Institute for Snow, Ice and Environmental Sciences

ICP Iterative Closest Point

IMU Inertial Measurement Unit

(In)SAR (Interferometric) Synthetic Aperture Radar

IPCC Intergovernmental Panel on Climate Change

ITCZ Intertropical Convergence Zone

LoD Level of Detection

MAAT Mean Annual Air Temperature

MODIS Moderate Resolution Imaging Spectroradiometer

PERMOS Swiss Permafrost Monitoring Network

PZI Permafrost Zonation Index

RGIK Rock Glacier Inventories and Kinematics

RGB Colour Space with Red, Green, and Blue

RGV Rock Glacier Velocity

RPC Rational Polynomial Coefficient

RTK Real-Time Kinematic

SfM, MVS, SfM-MVS Structure from Motion - Multi-View-Stereo

SGM Semi-Global Matching Algorithm

SPOT1-5 Satellite pour l'Observation de la Terre, satellites 1-5

SRTM Shuttle Radar Topography Mission

TA Terrain Awareness

UAV Uncrewed Aerial Vehicle

(V)LOS (Visual) Line-of-Sight

w. e. water equivalent

WGMS World Glacier Monitoring Service

WMO World Meteorological Organization

Statement on the Use of Place Names

Those geographical place names in this dissertation that are presented in their English form are presented as such for reasons of readability. This choice does not reflect the local perception of the Andean landscape, nor is it intended to diminish the cultural and linguistic significance of local place names. Rather, it represents a pragmatic decision to ensure consistency for an international readership while acknowledging the importance of local naming practices.

List of Figures

List of Tables

1. Introduction

The high mountain cryosphere exhibits pronounced sensitivity to climate changes most clearly expressed in the near-global retreat of mountain glaciers (Barry 2006). The effects of rising air temperatures on the degradation of mountain permafrost - conditions where air temperatures fall below 0°C for minimum two consecutive years - are less obvious (Hock et al. 2019; Huss et al. 2017). However, they pose a vital threat to high-mountain water resources (Arenson et al. 2022; Masiokas et al. 2020). Glacial and periglacial meltwaters impact the hydrological regimes and related sediment transport as they contribute to river runoff (Ferri et al. 2020; Masiokas et al. 2020; Pitte et al. 2022). They mitigate the effects of drought periods (Dussaillant et al. 2019) with their quantity affecting water availability essential to domestic, agricultural and economic activities (Contreras et al. 2011). Compared to glacially stored waters, periglacially stored waters express a longer and extended response time to climatic changes (Arenson et al. 2022). In times of water scarcity and global warming, this “hidden ice” is becoming an even more important future resource (ibid.). Already today, (peri)glacial runoff contribution is important in areas characterised by scarce precipitation – highlighting the hydrological significance of the Andean cryosphere which includes glaciers, debris-covered glaciers, perennial snowfields, and landforms characteristic of mountain permafrost - documented in the National Inventory of Glaciers conducted by the Argentine Institute for Snow, Ice and Environmental Sciences (IANIGLA-CONICET) in collaboration with the Argentine Ministry of the Environment and Sustainable Development (Zalazar et al. 2017).

1.1. Motivation and Relevance

The Dry Andes of Argentina (17°30'S to 35°S) are characterised by a dominant periglacial belt, hosting an exceptionally high spatial density of rock glaciers (Blöthe et al. 2021; Halla et al. 2021; Köhler et al. 2025) and other ice-containing landforms such as, e.g., block- and talus slopes (Hilbich et al. 2021; Köhler et al. 2025). Region-typical is the existence of only few glaciers at high elevation paired with the periglacial dominance – contrasting to the more southern glacially dominated Andes in Patagonia (IANIGLA-CONICET 2018). The glacial domain in the Dry Andes is in strong decline, characterised by loss of glacial volume and surface area (Dussaillant et al. 2019; Hugonnet et al. 2021; Masiokas et al. 2020; Pitte et al. 2022) and largely driven by sublimation (Ayala et al. 2016; Réveillet et al. 2020). Debris-covered glaciers in the Andes show surface lowering, however, well below the magnitude of non-covered glaciers (Ayala et al. 2025; Falaschi et al. 2021). Contrasting to studies in the European Alps and the Rocky Mountains where rock glacier velocities accelerate coincident with increasing air temperatures (Kääb and Røste 2024; Kellerer-Pirklbauer et al. 2024; Manchado et al. 2024), Dry Andean rock glacier velocities do not accelerate in recent times (Blöthe et al. 2024), elucidating stable permafrost conditions as ascertained by borehole measurements (Koenig et al. 2025). Air temperature in the Dry Andes is projected to continue rising (Pabón-Caicedo et al. 2020; Pitte et al. 2022), pressurizing present water storage quantity of the glacial and periglacial domains. A reduction of snow cover extent and albedo (Malmros et al. 2018), thus, the loss of interim water storage, is further jeopardising water availability from the high mountain region. This highlights the strong need to monitor the spatial distribution and quantity of the Dry Andean glacial and periglacial water storages at this crucial point in time.

Rock glaciers are “lobate or tongue-shaped bodies of perennially frozen unconsolidated material […] supersaturated with interstitial ice and ice lenses that move downslope” (Barsch 1996:4). The interstitial ice and ice lenses represent a periglacial water storage capability of the landform. Further, given the need of cold air temperatures for the ice component of rock glaciers to exist, rock glaciers are indicative of permafrost conditions. For example, the presence of active rock glaciers can assist in determining the lower boundary of permafrost conditions, next to inactive rock glaciers indicating that previously, permafrost conditions must have been present in the area (Brenning 2005; Gruber and Haeberli 2009; Schrott 1994). Rock glaciers express surface changes in horizontal and vertical direction, termed rock glacier kinematics. In 2022, annually measured rock glacier velocity (RGV) - the horizontal component of the kinematics - has been added to the essential climate variable (ECV) “permafrost” (Global Climate Observing System, GCOS) (RGIK 2023b; WMO et al. 2022). As rock glaciers are reported to increase with rising temperatures (Kääb and Røste 2024; Kellerer-Pirklbauer et al. 2024; Manchado et al. 2024), RGV are indicative of climate change impact on multi-decennial scale (RGIK 2023b), providing an indirect means to elucidate on the state of permafrost in the monitored region.

Cryospheric changes in the Andes and their effects are largely uncontroversial, with the Intergovernmental Panel on Climate Change’s (IPCC) 5th and 6th assessment reports outlining their relevance and effects with very high to high confidence. The reports state the retreat of the Andean cryosphere and its impact on seasonal streamflow distribution, as well as an increased risk of water supply shortages in the semi-arid regions with high confidence (Magrin et al. 2014). Further, Andean glacier loss with a 30 to 50 % reduction of the glacier surfaces since 1980 and its effect on ecosystems, water resources and livelihoods is outlined with very high confidence (Castellanos et al. 2022). This confidence in the changes and effects of the glacial and periglacial domains in the Andes along with the knowledge on the hydrological significance of the Andean cryosphere motivates integrative glacier-permafrost research on multiple spatial scales, as conducted in this dissertation.

The Dry Andes with their challenging terrain, high altitudes and remoteness cause field observations to be more resource-intense compared to more accessible mountain landscapes. Among other factors, this leads to poor data coverage of the area, e.g., lack of *in situ* data (Condom et al. 2020) and of continued, long-term rock glacier surface monitoring (Hu et al. 2025). The identified knowledge and data gaps very much contrast with the rock glaciers’ hydrological relevance in light of a changing climate (Arenson et al. 2022; Masiokas et al. 2020). It motivates closing the gaps by monitoring surface changes of Dry Andean cryospheric landforms along with publishing respective data to be findable, accessible, interoperable and reusable (FAIR). Detailed monitoring of RGV in the Dry Andes is of particular interest as it allows to elucidate on permafrost conditions in a changing cryosphere – balancing the limited availability of direct ground temperature measurements.

Remote sensing, particularly compared to *in situ* measurements, offers the possibility of scalability and higher spatial coverage by acquiring surface change information on regional or even larger spatial scale (Condom et al. 2020). Vertical and horizontal rock glacier surface changes can be detected and quantified on the basis of digital elevation models (DEMs) generated based on optical imagery (Smith et al. 2016). The steep and rough topography of the study

area with seasonal inaccessibility fosters the need for a combined on- and offsite study. This motivates a combination of uncrewed aerial vehicle (UAV) and satellite-based acquisitions for rock glacier surface change detection. On the one side, the high resolution of landform-focused UAV-based DEMs along with respective low levels of detection (LoDs) enables the investigation of low-magnitude surface changes and a detailed analysis of rock glacier surface changes within single landforms. On the other side, the generation of DEMs based on Pléiades imagery allows for increased spatial coverage, extension of the analysis to the glacial domain, as well as independence of site access for fieldwork and suitable fieldwork conditions. While this occurs at the cost of spatial resolution, it contributes to a comprehensive picture of the high-mountain cryosphere.

1.2. Objectives and Research Questions

The motivation behind this dissertation is to contribute to closing the gap that exists for knowledge on (Dry) Andean rock glacier surface kinematics, to based thereon elucidate on the current permafrost conditions in the Dry Andes and to investigate the drivers for the contrasting behaviour of rock glaciers in the Dry Andes compared to other regions on the Earth. Further, to quantify and interpret rock glacier kinematics bridging scales from within a single landform to basin coverage using different spatial resolution and data products. And finally, to foster an integrative approach by detecting and quantifying surface changes in the glacial as well as the periglacial domains contributing to a comprehensive picture of the cryospheric changes of the study area. Next to three publications, *in situ* measurements as well as image derived products are published to increase the volume of and accessibility to - particularly *in situ* - data in the Dry Andes. With its findings and data, the dissertation contributes to the Andean research efforts and community – aiming at expanding our understanding of the high-Andean cryosphere and the current state of Dry Andean permafrost conditions.

To address the above-described knowledge gap, the following research objectives are set:

1. Comparison of the suitability of UAV and Pléiades based DEMs for rock glacier surface change detection (Paper 1)
2. Investigation of horizontal and vertical rock glacier surface change on Dos Lenguas rock glacier based on high resolution UAV data (Paper 2)
3. Evaluation of potential drivers for Dos Lenguas rock glacier surface changes (Paper 2 and 3)
4. Investigation of horizontal and vertical rock glacier change on all rock glaciers in the Rodeo basin based on panchromatic Pléiades imagery (Paper 3)
5. Comparison of rock glacier surface changes and changes in the glacial domain in Rodeo basin based on panchromatic Pléiades imagery (Paper 3)
6. Evaluation of the state of permafrost elucidated on by rock glacier surface changes on Dos Lenguas and rock glaciers across the entire catchment (Paper 2 and 3)

These research objectives provide the basis for addressing the following research questions, which are examined in the three papers that constitute this dissertation (Chapters 6-8) and synthesized in the concluding chapter.

1. What is the magnitude and spatial pattern of vertical and horizontal surface changes on the Dos Lenguas rock glacier? (Paper 1, 2 and 3)
2. What is the magnitude and spatial pattern of vertical and horizontal surface changes on rock glaciers across the Rodeo basin and how representative is Dos Lenguas rock glacier? (Paper 1 and 3)
3. How do topography and climatological characteristics correlate with the magnitude and spatial pattern of these changes? (Paper 2 and 3)
4. What state of permafrost do the rock glacier surface kinematics imply for the wider region and how does the state of permafrost relate to the state of the glacial domain? (Paper 2 and 3)
5. To which degree is it possible to resolve rock glacier surface kinematics with satellite-based remote sensing compared to UAV-based investigations and which approach is most suitable in the high mountain cryosphere setting? (Paper 1, 2 and 3)

1.3. Outline and Conceptional Approach

Following the outline of motivation and objectives (Chapter 1), this dissertation proceeds with an overview on mountain permafrost and rock glaciers (Chapter 2) and recapitulates remote sensing techniques for earth surface change detection (Chapter 3). Consequently, it describes the study area (Chapter 4) and provides an overview on the data used and methods applied in this dissertation (Chapter 5).

The three papers which constitute this dissertation follow as Chapter 6 to 8. Paper 1 starts with investigating how a combination of small-scale UAV imagery and large-scale satellite imagery contributes to more comprehensive landscape assessments, as an in-depth understanding of the ongoing surface processes is scale-dependent. It ensures comparability of the UAV and Pléiades-based results in Paper 2 and 3 as well as contributes the Pléiades processing workflow to Paper 3, see Figure 1. Paper 2 continues with analysing surface changes on Dos Lenguas rock glacier located in the Dry Andes of Argentina between 2016 and 2024 based on UAV data, including an investigation of the impact of topographical and climatological forcing. With its landform focus and high-resolution, the UAV-based monitoring of rock glacier kinematics contributes transferable details on the magnitude and pattern of rock glacier surface changes and their drivers to the catchment-wide analysis in Paper 3. The third paper makes use of Pléiades (satellite) imagery to expand the spatial coverage of the rock glacier surface monitoring from a landform- to a catchment focus and widens its investigation to glaciers and debris-covered glaciers. Thereby, it ensures the representativity of Dos Lenguas rock glacier kinematics for the wider region by comparison to 46 other rock glaciers in Rodeo basin.

The dissertation concludes with a synthesis that briefly summarizes all papers, provides integrative answers to the research questions, and offers an outlook (Chapter 9), followed by an overall conclusion (Chapter 10).

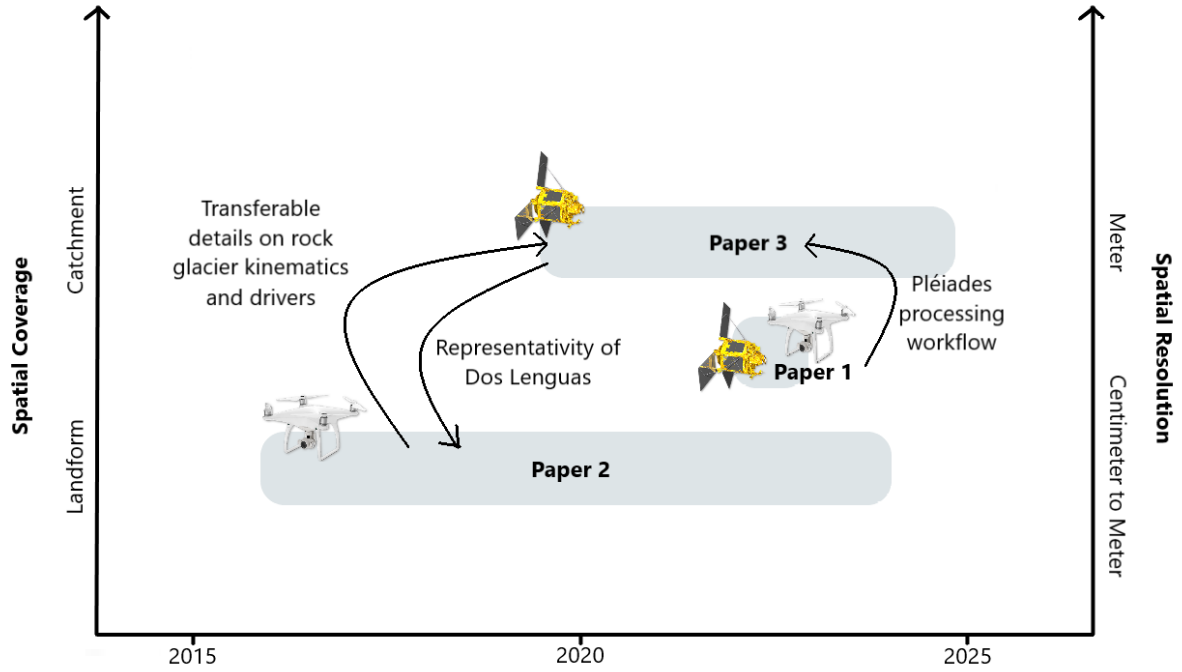

Figure 1 Rock glacier surface changes occur on a multitude of spatial and temporal scales. The possibility to survey rock glaciers with UAVs along with the availability of satellite imagery allows for addressing rock glacier surface changes at high spatial resolution and low spatial coverage focusing on Dos Lenguas rock glacier (Paper 2) and lower spatial resolution and high spatial coverage resolving rock glacier surface changes across Rodeo basin (Paper 3). A methodological comparison of UAV- and Pléiades based DEMs and the effect of software choice (Paper 1) links the two applied studies.

The foci of this dissertation and their relation to earth system science are manifold and span the delimitation of landform boundaries, use of different data and techniques to bridge spatial scale, analysis in a process-response system to derive drivers, processes and (absence of) response, and using (a set of) landform(s) in their role as climate indicators – detailed below.

Multiple components of the mountain cryosphere are referred to as 'landforms' in this dissertation. With dominant side and front slopes - hence breaks in slope (Evans 2012), particularly active rock glaciers can be seen as clearly-bounded. Their upper and root zones, which in the case of the Dry Andes are often connected to taluses, present more fuzzy boundaries. Similarly, glaciers constitute discontinuous, bounded segments internally homogeneous compared to their vicinity and decreasing in surface area and volume given the impact of climate change (Barry 2006; Evans 2012; Minár and Evans 2008). For the landforms' boundaries, this dissertation relies on the National Inventory of Glaciers, Argentina (IANIGLA-CONICET 2018).

'Topography at normal scale' (Evans 2012) relating to spatial resolutions of 2 to 20 m highlights the advances made in image acquisition, availability of high-resolution imagery and adapted processing strategies over the last 10+ years. This dissertation operates on spatial resolutions ranging from very high to high, referring to centimetres and few meters. The large footprints of the satellite imagery allow for bridging (sub-)landform to catchment scale while maintaining high spatial resolution, Figure 1. The temporal focus of less than a decade allows for a detailed monitoring of recent surface changes on annual to quasi-biennial temporal resolution. Repeated image acquisitions enable the quantification of process rates analysed in a process-response system (Chorley 1962; Chorley and Kennedy 1971; Huggett 2011).

The identification of the rock glacier's kinematic drivers is challenged by agent interconnectivity and non-linear system response (Church 2010). In addition, of a long reaction time as part of the response time, leading to a delayed system response (Arenson et al. 2022; Huggett 2011). Still, rock glacier kinematics (*process*) and their monitoring function as valuable means to identify kinematic reaction to climatic changes, e.g., increased velocities (*response*) (RGIK 2023b). Assessing a multitude of rock glaciers across a catchment with the aim of detecting a common signal of change and deciphering its meaning for the local to regional state of permafrost is in line with the hypothesis that "climate controls process(es) and process(es) control form, form is therefore a product of climate" (Thorn 1988:28), essential to climatic geomorphology.

This dissertation sets out with a focus on rock glaciers in its first two papers and finishes with a contextualisation of rock glacier changes compared to glacier and debris-covered glacier changes in its last paper contribution. This contextualization acknowledges the complexity of landform associations (Schneevoigt 2012) and addresses the differences of landform reaction to similar agents, e.g., temperature, in different domains – here the glacial and periglacial domains, respectively. The potential of interaction between the domains, discussed in Harris and Corte (1992) and described in case studies (e.g., Cusicanqui et al. 2023; Etzelmüller and Hagen 2005; Kunz and Kneisel 2020; Miesen et al. 2021) is lacking for the Dry Andes.

In summary, this chapter highlights the climatic sensitivity and hydrological relevance of the high-mountain cryosphere in the Dry Andes, the predominance of the periglacial over the glacial domain, and the role of rock glaciers as key indicators of permafrost conditions in a data-scarce region. It explains that the dissertation builds upon a framework combining geomorphological concepts, earth system science, and advances in remote sensing to address the dynamics of cryospheric landforms across multiple spatial scales. By situating glaciers, debris-covered glaciers, and rock glaciers within a process–response system, the preceding chapter has outlined how landform boundaries, the perception of spatial scale, and the complexity of interconnected systems impacts the scope of this work. As the following chapter turns specifically to mountain permafrost and rock glaciers, the focus narrows to their internal structures, modes of activity, and sensitivity to climatic drivers. This transition establishes the foundation for understanding rock glaciers and establishes the basis for the remote sensing applications and case-specific analyses developed in the following chapters.

2. Mountain Permafrost and Rock Glaciers

Mountain permafrost and rock glaciers, a surface expression of permafrost conditions, are key components of the high-altitude cryosphere and represent essential water storages (Arenson et al. 2022; Masiokas et al. 2020). Their existence is closely tied to thermal conditions, highlighting their sensitivity to changing temperatures and rendering them well-suited as indicator for climatic changes, despite changes of permafrost conditions being far less obvious than changes of the glacial domain (Hock et al. 2019; Huss et al. 2017).

2.1. Mountain Permafrost

2.1.1. Characteristics

Permafrost is thermally defined as ground that remains at or below 0°C for at least two consecutive years. Mountain permafrost, also referred to as alpine or high-mountain permafrost, is descriptive of permafrost in mountain areas (Gruber and Haeberli 2009). It is part of the mountain cryosphere which covers glaciers which by definition are not permafrost, perennial snowfields, and periglacial, often permafrost related landforms (Haeberli and Gruber 2009). In the southern hemisphere, permafrost is present in almost all ice-free areas of Antarctica (Obu et al. 2020). Further, the Andes host very extensive periglacial belts, particularly in the Dry Andes of Argentina (Gruber 2012; Schrott 1994; Köhler et al. 2025). Gruber (2012) estimates that 3'500 to 33'000 km^2 of Argentina is underlain by permafrost, exceeding the 8'484 km^2 which are covered by surface ice (IANIGLA-CONICET 2018).

The distribution of mountain permafrost is typically discontinuous and heterogeneous, exhibiting a spatial variability that contrasts sharply with the relatively continuous and predictable patterns observed in polar regions (Haeberli and Gruber 2009). Feasible conditions for the genesis of continuous permafrost in high mountain areas are very high elevation or locations with limited exposure to solar radiation. For the Dry Andes, this relates to above 5'000 m asl (Gruber 2012). In areas where permafrost is present but not continuous, it is sporadic. Permafrost presence and distribution is governed by complex interactions between topography, microclimate, solar radiation input, subsurface composition, water availability and snow cover including its redistribution by wind – all affecting ground temperature (Gruber and Haeberli 2009). Brenning (2005) determines topographic shading and the effect of massive, surrounding ice bodies as decisive factors for permafrost conditions as identified by the existence of active rock glaciers at locations where the mean annual air temperature (MAAT) is higher than the -1 to -2°C reported necessary for their development (Barsch 1996; Roer 2005).

The thickness of mountain permafrost measures decimetres to meters and is characterised by a seasonally thawing active layer located above the perennially frozen material (Haeberli et al. 2006; Humlum 1997). While the seasonal thaw-freeze cycles of the active layer contribute meltwaters to the hydrological system of the high mountain environment (Duguay et al. 2015; Halla et al. 2021), the perennially frozen ground acts as water storage (Jones et al. 2018). Today's permafrost thickness is out of equilibrium with the ground temperature conditions present (Haeberli 2000). Research in the Dry Andes of Argentina indicates ground temperatures of -7 to 7°C, depending on the site (weathered bedrock, bedrock, colluvium, glacial deposits and rock glaciers), revealing the complexity of the Andean thermal landscape (Koenig et al. 2025).

The capacity of storing and releasing water over extended periods is characteristic of mountain permafrost and particularly in arid regions essential to river runoff and groundwater recharge (Arenson et al. 2022; Geiger et al. 2014; Halla et al. 2021; Jones et al. 2018, 2019). Subsurface ice is characterised by a long reaction time compared to surface ice and, thus, a longer response time to increasing air temperature - buffering contribution to river runoff (Arenson et al. 2022). Factors influencing the duration of the response time are the thickness of the permafrost body, its thermal conductivity and ratio of the ice component compared to rock together with the availability of unfrozen water (Haeberli et al. 1993; Osterkamp and Romanovsky 1999). In light of rising temperatures, the meltwater release capacity of mountain permafrost is gaining hydrological significance compared to mountain glaciers as the latter will more rapidly continue to decrease in volume and size, critically reducing their meltwater contribution (Arenson et al. 2022; Jones et al. 2018), see Figure 2. This leads to effects on freshwater supply, solute concentrations in streamflow, irrigation and riverine ecosystem resilience (Beniston and Stoffel 2014; Castellanos et al. 2022; Magrin et al. 2014; Seelig et al. 2025). The decline in subsurface ice depends on the permafrost conditions in the area investigated – currently stable permafrost conditions in the case of the Dry Andes (Blöthe et al. 2024; Koenig et al. 2025).

Permafrost degradation occurs once the mountain permafrost's delayed reaction time to increasing air temperatures is surpassed and is mainly related to a thickening of the active layer (Trombotto and Borzotta 2009). Permafrost thaw leads to challenges surrounding the stability of the ground surface and consequent infrastructure instability (Gruber and Haeberli 2007; Kokelj et al. 2017; van der Sluijs et al. 2018). Further, it leads to the increase of natural hazards such as landslides (Gruber and Haeberli 2009; Schrott et al. 2024; Tapia Baldis and Trombotto Liaudat 2019). For a short period in time, it increases the periglacial meltwater contribution to river runoff compared to permafrost with a more intact frozen body, altering the mountain hydrosphere (Arenson et al. 2022; Jones et al. 2018).

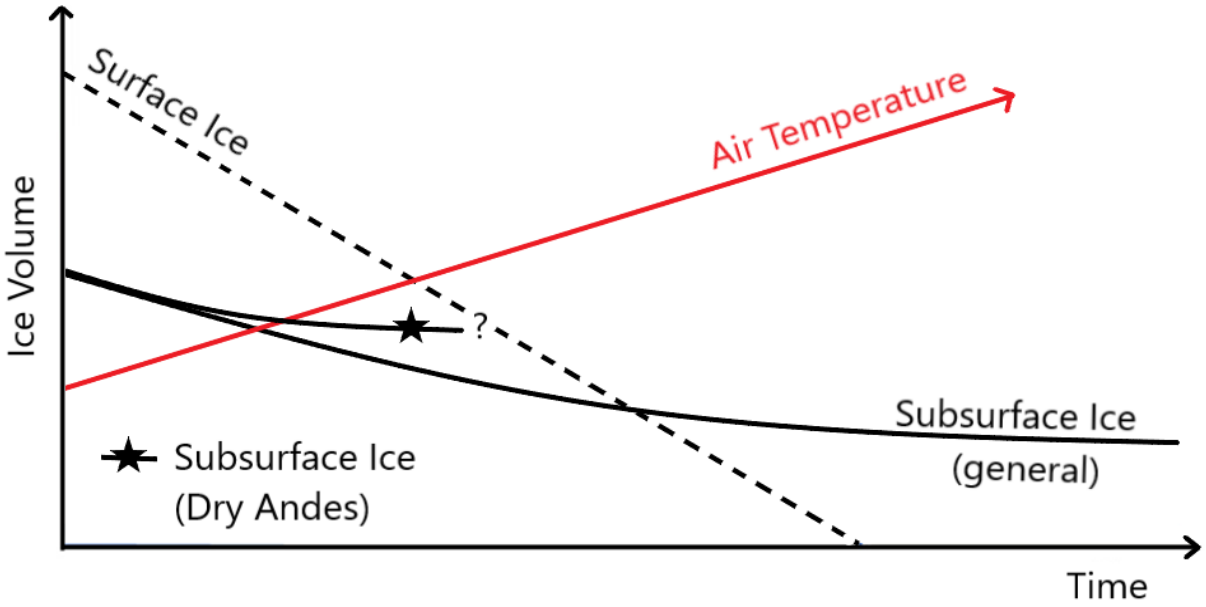

Figure 2 Changes in surface and subsurface ice volume with increasing air temperature in time. In contrast to the general perception of a gradual decrease in subsurface ice volume, rock glacier kinematics in the Dry Andes elucidate stable permafrost conditions for this region. Given the short monitoring periods in the Dry Andes, a prognosis on the future behaviour of Dry Andean subsurface ice is, however, challenging. Own illustration based on Arenson et al. (2022).

2.1.2. Monitoring techniques

The importance of monitoring permafrost occurrence, distribution and changes in its thermal state is recognized on global scale (Biskaborn et al. 2015; Smith et al. 2022). Monitoring efforts like the Global Terrestrial Network for Permafrost (GTN-P) (Biskaborn et al. 2015) and the Swiss Permafrost Monitoring Network (PERMOS 2019) provide detailed ground temperature monitoring data, although spatially biased to the northern hemisphere, particularly to Europe, (Smith et al. 2022). For the Dry Andes of Argentina, a lack of ground temperature data is particularly pronounced (Arenson et al. 2022; Koenig et al. 2025). It contrasts with mountain permafrost in the Dry Andes of Argentina having been studied systematically since the late 1970s / early 1980s (Barsch and King 1989; Barsch et al. 1994; Buk 1983; Catalano 1926; Corte 1978; Corte and Buk 1984; Götz et al. 2013; Schrott 1994, 1996, 1998; Trombotto et al. 1997; Trombotto 2000), with a main focus on permafrost thickness. The lack of *in situ* data predominantly relates to the availability of resources for costly and labour intense monitoring programs in the high, remote and less accessible, (Dry) Andes (Condom et al. 2020; Halla et al. 2021; Hilbich et al. 2021; Koenig et al. 2025; Mathys et al. 2022).

Indirect approaches that detect, monitor and quantify permafrost are of major importance given the challenges related to direct ground temperature measurements. These span geophysical methods, such as electrical resistivity tomography (ERT) and ground penetrating radar (GPR), as well as remote sensing approaches involving UAV and satellite imagery. ERT and GPR are used to infer the presence of frozen ground based on contrasts in subsurface material properties (Hauck and Vonder Mühll 2003), as applied in the Dry Andes (e.g., Croce and Milana 2002; Villarroel et al. 2020, 2022). UAV imagery is commonly used for a high-resolution monitoring of rock glacier kinematics, e.g., in Vivero et al. (2021) and the second paper of this dissertation. Optical satellite imagery as used in the third paper of this dissertation is used comparatively often in the (Dry) Andes (Blöthe et al. 2021; Falaschi et al. 2025; Robson et al. 2022; Vivero et al. 2021). Non-optical imagery and related techniques such as Interferometric Synthetic Aperture Radar (InSAR) are also applied to detect and monitor surface changes, e.g., on rock glaciers (Bodin et al. 2016; Strozzi et al. 2020; Villarroel et al. 2018). For a review on using remote sensing for glacier- and permafrost related hazards, see Kääb et al. (2005).

Modelling of permafrost occurrence and distribution represents one additional approach to observe mountain permafrost (Gruber 2012). While feasible permafrost modelling relies on the parametrisation of, e.g., solar radiation, sensible heat, surface albedo, as well as heat conduction and advection including latent heat transfer (Haeberli et al. 2006), modelling permafrost in high-mountain environments is further challenged by the mountains' complex topography. In the Andes, the paucity of long-term ground temperature data, meteorological records, and borehole measurements present significant barriers to a comprehensive modelling of permafrost presence. While studies that focus on a local spatial scale have made use of the scarce *in situ* data, often in combination with statistical proxies, there remains no consensus on a robust, validated permafrost model tailored to the Andean context (Azócar and Brenning 2010; Rangecroft et al. 2016).

2.2. Rock Glaciers

Rock glaciers are one of the landforms associated with mountain permafrost. As a geomorphic surface expression of permafrost conditions, they are indicators of past or present permafrost conditions at their location (Barsch 1992, 1996; Brenning 2005; Gruber and Haeberli 2009; RGIK 2022, 2023b; Martin and Whalley 1987; Schrott 1994). Like other permafrost related landforms, rock glaciers are present within the periglacial belts of high mountain landscapes, particularly in the Dry Andes (Blöthe et al. 2021; Halla et al. 2021; Köhler et al. 2025). For a detailed review on the nomenclature's origin, see Martin and Whalley (1987) and Roer (2005).

2.2.1. Characteristics

The formation of rock glaciers relies on a set of climatic and geological variables and is strongly impacted by sufficient and blocky debris supply, the presence or formation of ice (lenses), and temperatures that allow for the ice's persistence (Azócar and Brenning 2010; Haeberli et al. 2006; Martin and Whalley 1987). The ice's origin entertains the scientific community since the 1970s with two schools developing main hypotheses revolving around a glacier and non-glacier origin of rock glacier ice as analysed in Berthling (2011). Investigating rock glacier kinematics on recent time scales as conducted in this dissertation is not suitable for a conclusion of this dispute. Geochemical analyses to discriminate the ice's origin are challenged by their high demand on resources and are non-existent in the context of the Andes.

A layer of blocky sediments on a rock glacier's surface equivalent to a rock glacier's active layer, a core consisting of a mixture of ground ice, lithic fragments and clasts (Cicoira et al. 2021; Martin and Whalley 1987; Wahrhaftig and Cox 1959), and a shear horizon (Cicoira et al. 2021) constitute rock glaciers, Figure 3. The thickness of the active layer is determined by local meteorological characteristics, the thickness and duration of snow cover and the active's layer textural characteristics, e.g., grain size distribution (Bast et al. 2024; Haeberli et al. 2006). The core, in general, contributes 10 to 40 % to the total magnitude of creep, depending on variations in temperature and ice content (Cicoira et al. 2021; Haeberli et al. 2006). The shallow layer of the shear horizon, located below the ice-rich core, contributes 60 to 90 % of the total magnitude of creep, both annually and seasonally, and is impacted by pressurized, unfrozen water (Cicoira et al. 2021; Moore 2014). Particularly in arid regions such as the Dry Andes, the effect of the snow cover on the active layer is reduced, Paper 2, and the core may comprise less ice as portrayed in Figure 3 (Halla et al. 2021).

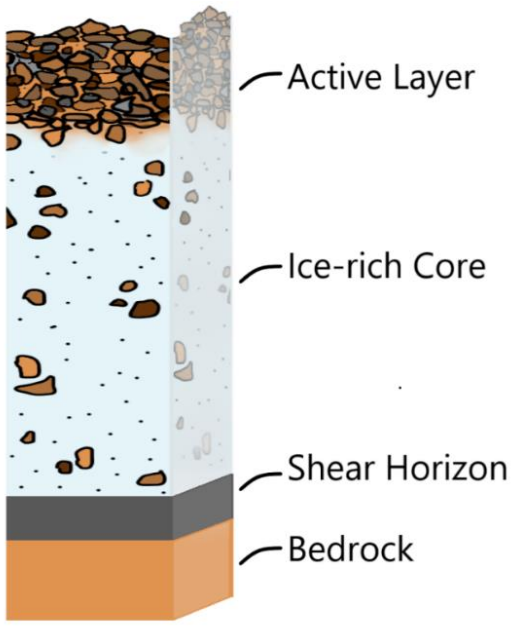

Figure 3 Generalized internal structure of a rock glacier spanning the active layer, core, and shear horizon located above debris or bedrock. The ratio of ice and rock in a rock glacier's core differs to a large degree. Own illustration based on Cicoira et al. (2021).

The states of activity of rock glaciers are active, inactive, and relict/fossil. Active rock glaciers most commonly show steep front and side slopes next to a ridge-and-furrow surface morphology, and no vegetation (Barsch 1996; Martin and Whalley 1987). In the semi-arid Andes, rock glaciers can be active up to MAATs of +1°C (Azócar and Brenning 2010; Brenning 2005). Depending on the definition, inactive rock glaciers do not maintain creep but retain ground ice next to relict/fossil rock glaciers that no longer contain ice or are an umbrella term for both (Haeberli 1985; Martin and Whalley 1987). For an exemplification of (in)active rock glaciers in the study area, see Paper 3. As suitable conditions for their formation must have existed at a certain point in time, relict/fossil rock glaciers are indicative of previous permafrost conditions (Frauenfelder and Kääb 2000; Frauenfelder et al. 2001).

Mutual (de)coupling relations are expected as rock glaciers and glaciers exist in close spatial proximity (Bodin et al. 2010; Cusicanqui et al. 2023). Examples include scenarios where geomorphic components act as mechanical agents (Etzelmüller and Hagen 2005) or where water functions as an agent of transient interaction (Miesen et al. 2021). It is hypothesized that rock glaciers with a glacier present in their vicinity exhibit surface process dynamics different from those observed in non-glacially influenced periglacial systems, such as, e.g., talus-derived rock glaciers, primarily due to the effects of glacial meltwater intruding the rock glacier and the temporary water storage thereof. Consequently, research needs to shift from analyses focused on individual landforms towards the detection and interpretation of change signals across multiple landforms and larger spatial scales, see Paper 3. To achieve an accurate and detailed understanding of surface changes and associated processes including thawing and (re)freezing of ice bodies and active layers, as well as permafrost degradation, high-resolution elevation data are indispensable (Mueting et al. 2021; Robson et al. 2022).

2.2.2. Rock glacier kinematics

Rock glacier kinematics describe the mechanical behaviour of rock glaciers expressed through surface motion and/or internal deformation processes (Hu et al. 2025). These lead to extensional and compressional flow which can mechanically thicken or thin the active layer (Haeberli et al. 2006). As a consequence of these flow dynamics, rock glacier surfaces are often characterised by a system of ridges and furrows, oriented parallel or transverse to the direction of rock glacier flow (Barsch 1996; Haeberli et al. 2006). Hence, rock glacier surface morphologies are a product of the landforms' cumulative, dynamic history and reflect the landforms' present and past internal conditions and environment (Kääb et al. 2005).

Vertical surface changes reveal volumetric variations, reflect flow dynamics, and provide insights into the morphometric complexity of rock glaciers (Kääb et al. 2005; Halla et al. 2021; Vivero and Lambiel 2024). Drivers are the above-explained flow dynamics, debris input, ice aggradation and the advance of individual ridges (Kääb et al. 2003). Next to explaining local patterns of surface variations, vertical surface change analyses elucidate on meltwater contribution to runoff (Blöthe et al. 2021; Halla et al. 2021; Vivero and Lambiel 2024).

Rock glacier velocity, the horizontal component of rock glacier surface changes, is part of the ECV "permafrost" (RGIK 2023b; WMO et al. 2022). It serves as an indicator of climate change impacts on multi-decadal timescales and supports continuous, comparable monitoring (RGIK 2023b). Rock glacier velocities are higher along a centre flow line and decrease towards the

edges (Barsch 1992, 1996). They are driven through internal deformation of the permafrost body, referred to as creep (Haeberli 1985; Jones et al. 2019). The drivers of rock glacier velocities are complex and hampered by the lack of knowledge on the landforms' internal structure (Cicoira et al. 2021; Haeberli et al. 2006). Temperature is frequently identified as a dominant factor (Kääb and Røste 2024; Marcer et al. 2021). Increased ground temperatures cause warmer frozen debris and lead to higher velocities as the reduced viscosity of warmer ice and the presence of infiltrating meltwater facilitate deformation, a behaviour explained by the Glen-Nye flow law (Arenson et al. 2007; Cicoira et al. 2021; Moore 2014). Beyond temperature, local factors including material composition (variations in the proportions of rock, ice, and air due to differences in grain size distribution), debris cover thickness, slope, ice content, internal shear horizons, water availability, and external inputs such as rockfall, also play a significant role in controlling rock glacier kinematics (Barsch 1996; Bodin et al. 2010; Cicoira et al. 2021; Hartl et al. 2023; Kääb and Reichmuth 2005; Kääb and Røste 2024).

Rock glacier velocities can show cyclic behaviour (Hartl et al. 2023), seasonal variations (Haeberli 1985; Kääb et al. 2003), and acceleration in response to changes in climatic conditions (Kääb and Røste 2024; Kellerer-Pirklbauer et al. 2024; Manchado et al. 2024). They provide valuable surface indication of subsurface processes, as they reflect variations in ground temperature and ice content (Halla et al. 2021; Jones et al. 2019; RGIK 2023b). Thus, monitoring rock glacier kinematics supports an understanding of the underlying processes, assessing climate impacts, budgeting sediment transfer or managing geohazards, as well as mass balance studies (RGIK 2022). However, despite the recognized hydrological significance of rock glaciers in the Dry Andes, long-term monitoring records from this region remain limited (Blöthe et al. 2021, 2024; Cusicanqui et al. 2025; Vivero et al. 2021). This scarcity of data stands in sharp contrast to the century-long datasets that exist for the Swiss Alps (Manchado et al. 2024) and the Rocky Mountains (Kääb and Røste 2024).

In summary, mountain permafrost in general and rock glaciers as permafrost related landform represent key components of the high-altitude cryosphere, storing solid waters that are hydrologically relevant particularly in arid regions such as the Dry Andes. The subsurface ice's longer response time to increasing air temperatures compared to surface ice underscores the components' increasing hydrological relevance. The inclusion of rock glacier velocity into the ECV permafrost highlights the suitability of rock glacier monitoring as an indirect means to decipher permafrost conditions. Despite advances in research efforts, significant regional knowledge gaps remain, particularly in the Andes, where (long-term) datasets are scarce. This gap emphasizes the need for remote approaches to more continuously monitor rock glacier surface dynamics, to enable elucidating on local permafrost conditions and to anticipate the landforms' role in future cryospheric meltwater contribution.

3. Remote Sensing of Earth Surface Change

The technical development in the last decades allows for the application of more advanced UAVs and robustly tested photogrammetric workflows. Further, it led to an increase of the resolution of satellite-based optical imagery, increasing the possibilities for monitoring rock glacier kinematics from space. Independent of a sensor's platform (e.g., UAV or satellite), overlapping optical imagery is often used for the generation of DEMs by application of photogrammetric approaches. DEMs simulate the surface morphology of an area (Xiong et al. 2021) and can be created from a multitude of datasets including spaceborne, airborne and UAV-based datasets, optical as well as synthetic aperture radar (SAR) imagery (Nelson et al. 2009). They serve as a basis for the investigation of surface changes, with a minimum of two DEMs allowing for the calculation of vertical change by DEMs of Difference (DoDs) (Williams 2012). Horizontal surface changes are commonly derived by the application of feature tracking approaches, e.g., by Schwalbe and Maas (2017).

3.1. Modes and Platforms of Remote Sensing

Remote sensing is an umbrella term for all techniques which, without direct contact, acquire information about the earth's surface. This chapter provides an overview on selected modes and platforms available.

3.1.1. Passive versus active remote sensing

Earth surface processes are regularly monitored using passive as well as active remote sensing. Passive remote sensing, e.g., spectral imaging, relies on naturally available energy to capture information about the earth's surface. Optical sensors record reflected sunlight in human-interpretable visible and infrared wavelength, such as, e.g., RGB (Red, Green, Blue) or multi-spectral imagery (Barrett 2013; Tedesco 2014). The study area's aridity as well as its extremely low cloud and vegetation cover yield highly suitable conditions for passive remote sensing. Largely uncovered terrain (no clouds, snow, vegetation), allows for non-obscured change detection and accurate co-registration. An additional benefit of passive remote sensing imagery, in contrast to radar imagery, is that the optical signal does not penetrate snow and ice, increasing suitability for cryospheric surface change detection (Berthier et al. 2014).

In contrast, active remote sensing, e.g., radar and laser altimeters, emit their own energy and measure the reflection back. Though less human-interpretable, active sensing is suitable in all weather, as well as night-time conditions (Smith and Pain 2009; Tedesco 2014). One approach applied particularly often for monitoring rock glacier velocity is spaceborne InSAR - third most applied method as found by a literature review by Hu et al. (2025). In contrast to photogrammetric approaches, InSAR measures the change in distance between the satellite-mounted sensor and the earth's surface in line-of-sight (LOS) (Bertone et al. 2022), which needs to be adjusted before comparison to monitoring efforts with other approaches. To increase comparability among InSAR-based rock glacier kinematics investigation, community guidelines have been established, e.g., for a coherent delineation of moving areas and kinematic attribution (RGIK 2023a).

3.1.2. Sensor platforms

Next to the sensors, remote sensing techniques can be divided by the platforms that the sensors are mounted on. Common examples are UAVs, airplanes, and satellites – while balloons and kites are technically also feasible (Barrett 2013; Tedesco 2014).

UAV-based imagery acquisition presents a form of near surface remote sensing, which is defined as remote sensing operated on platforms closer to the ground than crewed aircrafts or satellites. Near surface remote sensing is predominantly focused on smaller spatial scales, from parts of landforms to entire landforms. UAV-based monitoring reflects a cost-efficient means of collecting optical imagery and might be applied in areas where satellite coverage is poor (Westoby et al. 2012). Further, its high spatial resolution – both for the imagery as well as for derived products, enables detailed investigation of earth surface changes. This, next to their high accuracy, is crucial for processes where the magnitude of change is comparatively low, such as for rock glaciers (Bodin et al. 2010; Haeberli et al. 2006; Robson et al. 2022). Limitations of UAV-based imagery acquisition are the need for access to the landform(s) of interest, its sensitivity to changes in light conditions, and the restrictions to data-take caused by cloud cover and the absence of daylight. Such limitations can partially be reduced, e.g., by application of feature tracking on UAV imagery derived hillshades rather than the imagery itself as consequently, the grey shades of the hillshades compared to the RGB imagery are more consistent than the total spectral information (Dall'Asta et al. 2017; Fleischer et al. 2021). Paper 2 presents the longest UAV time series for rock glacier surface monitoring in the Andes – with very few other publications making use of UAV imagery to monitor Andean rock glacier surface changes. While Vivero and Lambiel (2024) combine UAV and other optical imagery for a quantification of rock glacier kinematics in the Dry Andes of Chile (30°S), Halla et al. (2021) investigate vertical and horizontal surface changes on Dos Lenguas rock glacier between 2016 and 2018.

Satellite-based remote sensing provides a suitable means for the investigation of earth surface changes in areas where, e.g., physical access to the landforms of interest is prohibited (Kääb et al. 2005; Schneevoigt and Schrott 2006) or ground-based observations are sparse (Schaffer et al. 2019). In addition, satellite-based imagery with its large(r) footprints allows for an increased spatial extent and enables the, often simultaneous, investigation of earth surface changes across multiple landforms. For the Dry Andes, Berthier et al. (2014) showcase the suitability of using tristereoscopic Pléiades data to investigate glacier topography and elevation changes on Agua Negra glacier, cf. Figure 5A. Ruiz and Bodin (2015) present a methodological framework for Pléiades imagery exemplified for two Andean locations and outline the benefits for glaciological and geomorphological research. As a limitation, satellite-based monitoring of earth surface change is generally of lower spatial resolution than, e.g., UAV-based investigations (Schneevoigt and Schrott 2006). It is, thus, vital to be aware of the magnitude of the targeted changes.

Indifferent of the specific location and landform, the coincident investigation of UAV- and spaceborne imagery as conducted in this dissertation enables a simultaneous quantification of, e.g., rock glacier surface changes at the highest resolution on smaller spatial scale and at lower resolution on larger spatial extent; crucial to multi-scale geomorphological investigations.

3.2. Photogrammetric Approaches for DEM Generation

3.2.1. Structure-from-motion Multi-View Stereo (SfM-MVS) photogrammetry

Structure-from-motion Multi-View Stereo (SfM-MVS) photogrammetry represents a computer vision technique and well-established method in the geosciences – particularly for change detection and geomorphological mapping (Śledź et al. 2021), with increased usage over the last decades (Carrivick et al. 2016). Today, SfM-MVS photogrammetry is the sixth most used method (out of 12) to investigate rock glacier velocity (Hu et al. 2025). To increase the comparability between studies using the method, e.g., journal guidelines detail the description of data acquisition and error reporting (James et al. 2019).

Commonly, SfM-MVS workflows are applied for generating 3D DEMs based on overlapping 2D UAV imagery (Eltner and Sofia 2020; Favalli et al. 2012; Smith et al. 2016), Figure 4. The basic photogrammetric principle that any object point on the target surface must be represented in minimum two images taken from different positions with overlapping camera fields of view to calculate a unique position in 3D space must be obliged (Bemis et al. 2014; Smith et al. 2016). While in theory few images are feasible, several hundred are suggested (Favalli et al. 2012; Smith et al. 2016). A combination of different camera inclinations increases the quality of the to-be-generated DEMs (Dai et al. 2023; James et al. 2017).

The entire workflow encompasses: image acquisition, feature detection and image matching, sparse point cloud generation via image alignment, densification of the point cloud, georeferencing with ground control points (GCPs) or onboard GNSS or inertial measurement unit (IMU) data, and the generation as well as the export of the DEM (Smith et al. 2016; Westoby et al. 2012). The MVS image matching algorithms are used to increase the density of the point cloud (James and Robson 2012). Filtering the dense point cloud is needed prior to DEM generation in cases when, e.g., vegetation, is obscuring the bare earth surface (Smith et al. 2016). For a detailed explication of all processing steps, see Bemis et al. (2014), Eltner and Sofia (2020), Smith et al. (2016) and Westoby et al. (2012).

The SfM-MVS approach applied in this dissertation with its selection of parameters and processing steps is detailed in Chapter 5.2.1.

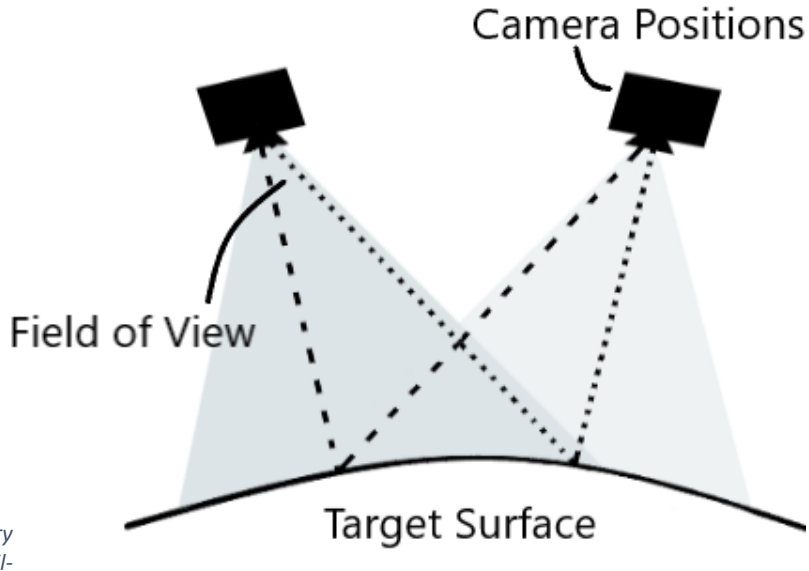

Figure 4 Basic principle of photogrammetry with the aim of 3D reconstruction. Own illustration based on Bemis et al. (2014).

Correct placement of the generated DEM is often supported by Differential Global Navigation Satellite System (DGNSS) measured GCPs used to define the model shape during bundle adjustment or to scale and orient the model (Eltner et al. 2016; James et al. 2017; Smith et al. 2016). Placed on non- and moving terrain and well-distributed across the area, their optimal number is dependent on, e.g., terrain relief, surface texture, flight height and image quality; as well as their intended use (Dai et al. 2023; James and Robson 2012; James et al. 2017).

The quality of SfM-MVS derived DEMs is strongly impacted by the acquired image quality (e.g., changes in illumination, degree of texture of an image), the image acquisition (e.g., differences in image angle, flight parameters such as altitude, speed and image overlap), and the image processing (e.g., camera calibration, alignment accuracy) (Bemis et al. 2014; Eltner et al. 2016; Favalli et al. 2012; James and Robson 2012; Smith et al. 2016; Westoby et al. 2012). The visibility and distribution of the GCPs affect DEM quality as the GCPs are important for the detection and prevention of, e.g., doming effects (James and Robson 2014). For a detailed description of SfM-MVS error sources, see Dai et al. (2023) and Eltner et al. (2016).

3.2.2. (Tri)stereo photogrammetry with satellite imagery

Spaceborne photogrammetry presents the third most common survey method (out of 12) for rock glacier velocities (Hu et al. 2025). Panchromatic (tri)stereo Pléiades imagery as input imagery is widely used, particularly in glaciology (Bagnardi et al., 2016; Beraud et al., 2023; Berthier et al., 2024). The technique relies on the precise geometry of convergent optical views, cf. Figure 4. It makes use of stereo (forward-backward) or tristereo (forward-nadir-backward) overlapping imagery of the same ground patch to generate 3D information. In contrast to SfM-MVS, classical (tri)stereo photogrammetry is originally less automated (Bemis et al. 2014; Eltner et al. 2016) and assumes *a priori* knowledge of sensor geometry, not solving for camera positions and orientations from image features automatically (Westoby et al. 2012).

Similar to UAV imagery, overlapping 2D satellite imagery is used to create 3D DEMs. Photogrammetric processing tools, such as Ames Stereo Pipeline (ASP) (Beyer et al. 2018), enable processing outside of 'black box' solutions (Shean et al. 2016). In general, crucial steps involve the rectification of the imagery, the application of a dense stereo matching technique (e.g., a semi-global matching algorithm, SGM), and the generation of DEMs. The workflow derived by Shean et al. (2016), as applied in, e.g., Cusicanqui et al. (2023), Pope et al. (2016) and this dissertation comprehends: image preprossessing, integer image correlation, sub-pixel disparity refinement, disparity filtering, stereo triangulation, and gridded DEM generation. For details of each step, see Shean et al. (2016). Instead of using GCPs and check points (CPs) measured *in situ*, satellite imagery based DEM studies often rely on the rational polynomial coefficients (RPCs) commonly delivered with the data product to orthorectify the imagery (e.g., Cusicanqui et al. 2023). Depending on the data quality, atmospheric distortions and/or sensor undulations need to be corrected for, the latter applied in, e.g., Beraud et al. (2023).

If multiple DEMs are to be compared, co-registration is required to ensure proper spatial alignment. Depending on the approach, spatial shift is corrected for in x, y, z direction (Nuth and Kääb 2011) or additionally for tilt, referring to rotational misalignments (iterative closest point (ICP), Besl and McKay 1992; Chen and Medioni 1992). Open source tools enable an automated DEM co-registration by applying the described approaches, e.g., Demcoreg (Shean et al. 2016).

4. Study Area: The Dry Andes of Argentina

The Dry Andes of Argentina (17°30'S to 35°S), which can be separated in the Desert Andes (22°S-31°S) and the Central Andes (31°S-35°S), describe an arid to semi-arid high-mountain region in western Argentina along the border to Chile. Here, the cryosphere serves as a crucial water reservoir, mitigating the effects of drought periods (Dussaillant et al. 2019) and supporting water availability through meltwater contributions to river runoff (Ferri et al. 2020; Masiokas et al. 2020; Pitte et al. 2022; Schrott and Götz 2013). Meltwaters from high-Andean catchments supply water for domestic, agricultural, and economic activities, with downstream viticulture, olive cultivation, and fruit production accounting for 35 % of the regional economy (Contreras et al. 2011). The region's aridity and increasing air temperature challenge water availability, with the risk of increasing water supply shortages determined with high confidence (Magrin et al. 2014). Therefore, identifying and quantifying solid water reserves such as ice lenses in permafrost environments is essential.

The study area of the Rodeo basin is situated in the western sector of the San Juan Province, Argentina (30°S, 69°W), Figure 5. Covering an area of 1315.7 km², its upper section is markedly influenced by the Cordillera Principal to the west (< 6947.5 m asl) and contains 19 glaciers, three debris-covered glaciers, and 59 rock glaciers (IANIGLA-CONICET 2018), Figure 5A. This distribution exemplifies the characteristic (peri)glacial landscape of the region, where only a few glaciers persist at the highest elevations, while periglacial landforms dominate (Halla et al. 2021; Köhler et al. 2025). The majority of the basin's runoff ultimately drains into the Cuesta del Viento reservoir situated in an intermontane basin between the Cordillera Principal and the Cordillera Frontal, near Rodeo at approximately 1500 m asl (Esper Angillieri 2017), Figure 5B. Due to the configuration of the valleys and the positioning of the rock glaciers closer to the valley floors, rock glaciers predominantly face east or southeast, and only infrequently north or west, Figure 5C. The current high-alpine (peri)glacial terrain in the catchment is a "geomorphic palimpsest" (Hewitt 2002), composed of relict, transitional, and replacement landforms. Within this periglacial environment, most research has concentrated on the Agua Negra catchment, a sub-basin of the upper Rodeo basin (Halla et al. 2021; Köhler et al. 2025).

Dos Lenguas rock glacier represents one of the 59 rock glaciers in the Rodeo basin, Figure 5A and Figure 6A. It is an active, westward creeping, tongue shaped, two-snouted rock glacier and corresponds to the focus of Paper 2. Located at 4400 m asl, Dos Lenguas rock glacier covers an area of 0.27 km^2 with a length and width of approximately 1500 m and 500 m. Distinctive for active rock glaciers, its surface morphology is characterised by c-shaped downward pointing ridges and furrows, detectable with UAV- and Pléiades imagery based DoDs, cf. Figure 11 and Figure 18.

The international mountain pass road no. 150 is crossing Rodeo basin, presenting anthropogenic impact on the region, connecting Jáchal in San Juan Province (Argentina) with La Serena (Coquimbo, Chile) and increasing the accessibility of the study site. The pass road reaches its highest point at slightly above 4780 m asl and is open in austral summers. Tourism predominates the pass road's use, with 10'235 vehicles and 35'586 persons passing in 2013 (Lauro et al. 2017), increased to 26'103 vehicles in 2017 and 23'703 vehicles in 2018 (Araya and Fingerhuth 2022).

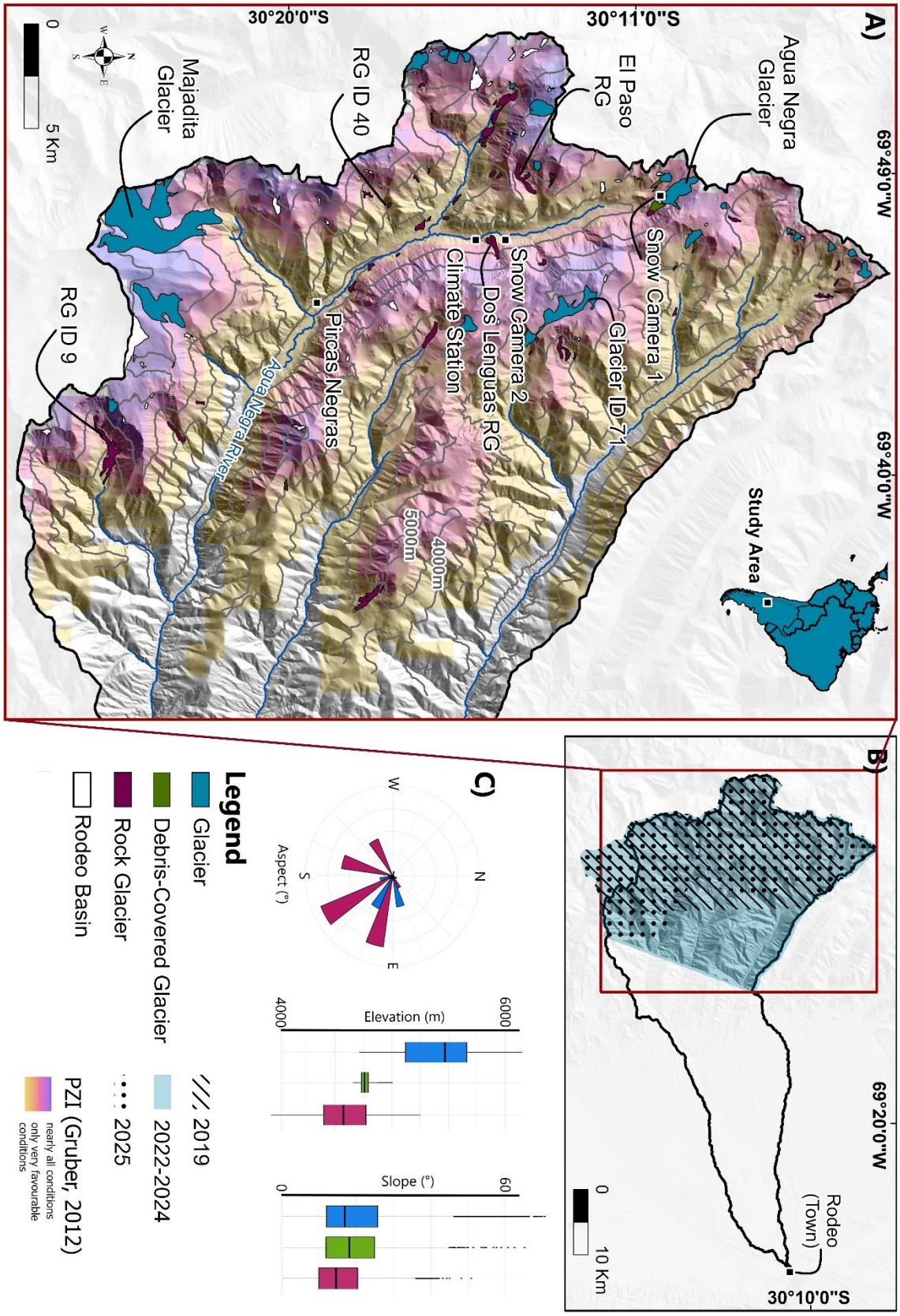

Figure 5 The study area is located in San Juan Province (30°S, 69°W) in the Dry Andes. Distribution of (debris-covered) glaciers and rock glaciers as mapped by IANIGLA-CONICET (2018) in the upper part of Rodeo basin (A). Rodeo basin including the extents of the panchromatic Pléiades imagery acquisitions (B). Aspect, elevation and slope characteristics of the (peri)glacial landforms, calculated from a 10 m Pléiades-based DEM and its derivatives (C). For the location of many place names, the climate station and static cameras, see A. The colour-scale for the landform type applies to all subfigures. PZI = Permafrost Zonation Index.

4.1. Climatological Setting

The region exhibits a semi-arid to arid climate, defined by extremely low mean annual precipitation of < 100 to 150 mm (Esper Angillieri 2017; Lauro et al. 2017). Temperatures display pronounced daily amplitudes (Schrott 1994), amounting to a MAAT of -4.9°C (1961-1990, ERA5). Solar radiation is persistently high (Croce and Milana 2002; Halla et al. 2021; Lauro et al. 2017; Lliboutry et al. 1998; Schrott 1994), causing the region-typical penitentes on glacier surfaces (Pitte et al. 2022), Figure 6B. The region's vegetation cover is minimal to absent and classified as tundra biome (Lecomte et al. 2008). Most precipitation occurs during the winter months, falling as snow or sleet above 4000 m asl (Esper Angillieri 2017; Lauro et al. 2017).

The climate can be broadly divided into the austral summer and winter, with the location of the Intertropical Convergence Zone (ITCZ) and the changing impact of the South Pacific high-pressure system from the South Atlantic system defining the seasons (Daudon et al. 2014; Garreaud 2009; Lauro et al. 2017). With altitudes of more than 6000 m asl, the Andes act as a meteorological divide (Arias et al. 2021; Schrott 1994) resulting in prevailing arid conditions on the Argentinean side of the Andes (Forte et al. 2016; Garreaud 2009; Schrott 1994). Precipitation is impacted by the El Niño Southern Oscillation (ENSO) occurrence with the warm ENSO phase promoting snow storms and an increase in cloudiness, beneficial to glacier mass balances (Forte et al. 2016; Leiva et al. 2007; Masiokas et al. 2006).

Across the Dry Andes, all cryospheric components are subject to rising temperatures (Pabón-Caicedo et al. 2020; Pitte et al. 2022). Malmros et al. (2018) find a reduction of snow cover extent and snow albedo by 13.4 ± 4 %, respectively 7.4 ± 2 % in the Central Andes slightly more south than this study area for 2000-2016 along with an average decrease of snow cover duration of 43 ± 20 days based on the analysis of daily MODIS data. For the study area, no long-term climatological records are available. The nearest climatological station is located at Capayán (4754 m asl), where air temperature measurements have been recorded since December 20th, 2016 (Pitte et al. 2022). Positioned 8.5 km north of Dos Lenguas rock glacier and directly in front of Agua Negra glacier, data from this station are likely influenced by the glacier's microclimatic effects. With the initiation of the HyPerm project (DFG, 461744503), an additional climatological station was installed 0.5 km south of Dos Lenguas, near the Agua Negra River (4160 m asl), Figure 5A. The climatological data are used in Paper 2.

4.2. Geologic-geomorphological Setting

The diversity of the Andean geology is a consequence of embedded fragments of new and old crust, granitic intrusions or partly sedimentary packages. The study area is part of the Frontal Cordillera morphotectonic geological province comprising a basement of sedimentary rocks that are part of the Tudcum Formation in addition to carboniferous rocks that are part of the Agua Negra formation (Lauro et al. 2017). Marine pelites and sandstones as well as Permo-Triassic granite and outcrops of the Choiyoi group volcanic complex are further present in the study area (Lauro et al. 2017; Lecomte et al. 2008). In detail, the Permian-Triassic Choiyoi group consists of dacites, rhyolites, tuffs, andesites and basaltic lavas, breccias and ignimbrites (Heredia et al. 2002, 2012). The basement is overlain by unconfirmed Pliocene and Cenozoic volcanic rocks (Heredia et al. 2002; Lauro et al. 2017). Precambrian or older Paleozoic metamorphic rocks and continental tertiary sediments occur in addition to the above-named geology (Reigaraz and Zambrano 1991; Schrott 1994).

The main valley of the Rodeo basin is u-shaped and indicative of Pleistocene glaciation (Lauro et al. 2017), Figure 6C. The elevation difference between the valley bottom and the upper edges of the surrounding landscape is 722 m at the northern end of the valley near Agua Negra glacier, and 1078 m at Dos Lenguas rock glacier, both based on the 2023 Pléiades DEM. In general, the valley depth is increasing with decreasing elevation. Today, the valley hosts the Agua Negra river which originates at Agua Negra glacier at an elevation of approximately 4730 m asl. Major confluences to the Agua Negra river in the upper part of the catchment are San Lorenzo river, hosting a multitude of rock glaciers and a smaller glacier in its subcatchment and Pirca river hosting the largest glacier of Rodeo basin, Majadita glacier, in its subcatchment, cf. Figure 5A. Next to glacial and periglacial landforms (IANIGLA-CONICET 2018; Köhler et al. 2024), Rodeo basin features gravitational, erosional and fluvial landforms such as landslides, gullies and alluvial cones (Lauro et al. 2017).

4.3. Glaciological Domain

Within the basin, glaciers are generally larger than rock glaciers, situated at higher elevations, and distinguished by steeper surface slopes, cf. Figure 5C and Figure 17. Glaciers in the Dry Andes of Argentina are experiencing reductions in both surface area and volume (Dussaillant et al. 2019; Hugonnet et al. 2021; Masiokas et al. 2020; Pitte et al. 2022), with sublimation playing a major role in accelerating ice loss (Ayala et al. 2016; Réveillet et al. 2020). Caro et al. (2024) identify the glaciological zone encompassing the Tapado glacier, located approximately 10 km west of Agua Negra glacier in the Chilean Andes, as the area characterised by the greatest vulnerability to reductions in glacier-based runoff across the entire Andes. For the Agua Negra glacier, cf. Figure 5A, mass balance measurements indicate a cumulative value of -3.67 m w.e. for the period 2014 to 2021 (Pitte et al. 2022). Concerning debris-covered glaciers, the thickness of the debris layer is a key control on both the rate of ice volume loss (Ferri et al. 2020) and the extent of vertical surface change. Ablation patterns are spatially heterogeneous, particularly in areas featuring supraglacial ponds and ice cliffs (Ayala et al. 2025; Bodin et al. 2010; Falaschi et al. 2021). Observations suggest that debris-covered glaciers tend to exhibit surface thinning rather than pronounced terminus retreat as a response to climate forcing (Ayala et al. 2025; Falaschi et al. 2021; Lenzano et al. 2016). From a hydrological perspective, debris-covered glaciers contribute to streamflow at levels comparable to clean-ice glaciers (Ayala et al. 2016).

Glaciological studies in the study area are centred on the Agua Negra glacier, focusing on its internal structure as well as surface area and volume changes (Berthier et al. 2014; Leiva 1999; Milana and Maturano 1999; Pitte et al. 2022).

Figure 6 Characteristic landforms of Rodeo basin. Dos Lenguas rock glacier represents one of the fastest rock glaciers in Rodeo basin (A). Agua Negra glacier is characterised by its region-typical surface morphology, the penitentes (B). U-shaped main valley of the upper Rodeo basin, viewed southward from Agua Negra glacier forefield (C). Own photos taken on February 8th 2024 (A) and March 2nd 2022 (B, C).

4.4. Permafrost Setting

(Dis)continuous permafrost conditions are present in approximately 11’000 km^2 of the Dry Andes, based on a Permafrost Zonation Index (PZI) above 0.5 (Gruber 2012). In the Rodeo basin, permafrost conditions are widespread and associated with a diverse range of ice-containing landforms, including block and talus slopes (Köhler et al. 2025), protalus ramparts (Hilbich et al. 2021), and rock glaciers (Cusicanqui et al. 2025; Halla et al. 2021; Robson et al. 2022; Villarroel et al. 2018, 2020, 2022). The active layer typically reaches depths of 2 to 3 m and may be reduced to only a few centimetres at elevations above 5000 m asl where continuous permafrost prevails (Gruber 2012; Halla et al. 2021). Recent research indicates that permafrost conditions in the Dry Andes remained stable over the past decade, as evidenced by borehole ground temperature records (Koenig et al. 2025) and observations of rock glacier kinematics (Blöthe et al. 2024).

A comparatively large body of permafrost-related studies in the Dry Andes focuses on rock glaciers, encompassing geophysical investigations (e.g., Croce and Milana 2002, 2006; Halla et al. 2021; Villarroel et al. 2020, 2022) next to studies based on remotely sensed imagery such as used in Paper 2 and 3 (e.g., Blöthe et al. 2021, 2024; Halla et al. 2021; Robson et al. 2022; Strozzi et al. 2020). Permafrost related studies in the Dry Andes that do not focus on rock glaciers report, e.g., on potentially permafrost-related rock slides (Tapia Baldis and Trombotto Liaudat 2019), seasonal frozen ground (Trombotto 2000), and ice-containing gelifluction taluses and protalus lobes (García et al. 2017), the latter on the Chilean side of the Andes.

In summary, the Rodeo basin provides a representative Dry Andean setting with a region-typical climate and geology. Changes in its glacial domain and permafrost setting are, thus, indicative of changes in the wider region. The diversity of landforms and the scarcity of long-term climatological records highlight the need for robust, multi-source datasets to characterise recent changes of the cryosphere. Consequently, the next chapter outlines the data used in this dissertation, including fieldwork-based UAV imagery and DGNSS acquisitions, as well as satellite-based Pléiades imagery. It continues to outline the methods employed which provide the basis for quantifying rock glacier kinematics as well as (debris-covered) glacier surface changes in the Dry Andes.

5. Data and Methods

The diverse topography of the study area with its steep slopes and partial physical inaccessibility drives a data-intense approach comprehensive of UAV and Pléiades imagery as well as multiple other data detailed in this chapter. The chapter continues by outlining the processing steps involved with vertical rock glacier surface change quantification by DEM differencing and horizontal rock glacier surface change quantification by feature tracking. The chapter is partly based on the second and third paper that contribute to this dissertation.

5.1. Data

5.1.1. UAV imagery (Paper 1 and 2)

During four field campaigns in the austral summers of 2016, 2018, 2022 and 2024, we obtain optical imagery with repeated UAV flights covering Dos Lenguas rock glacier and its vicinity, Table 1. The differences in data acquisition (e.g., mission type, duration of acquisition), are not intended but caused by fieldwork constraints. All imagery is acquired in sunny and windy conditions. Changing light conditions are minimized by conducting acquisitions from start to finish, wherever possible. Flight heights are decided by balancing high ground resolution, battery demand and battery weight needed to be carried in the high-mountain terrain.

For the 2016 and 2018 flights, we operate a DJI Phantom 3 Advanced in visual line-of-sight (VLOS) and 2D mode. To prevent maximum differences in ground sampling distance caused by the consistent flight height, we split the data acquisition into two overlapping parts corresponding to approximately the upper and centre zone as well as the centre zone and tongues, cf. Figure 11A. Both start with a flight height of 40 m. In 2018, imagery acquisition spans multiple days due to weather constrains. For increasing the comparability between all time periods, vertical and horizontal surface change are normalized to full years rather than keeping the time period caused by the two acquisition dates. For 2018, we select March 18th as date.

Table 1 Data characteristics for all UAV flights. TA = terrain awareness mode. All flights focus on Dos Lenguas rock glacier and its vicinity and are used in Paper 1 and 2. Our UAV imagery is published in Stammler et al. (2025b). Imagery previously used in publications (Halla et al. 2021; Stammler et al. 2024) is reprocessed with the workflow detailed in Chapter 5.2.1.

	2016	**2018**	**2022**	**2024**
UAV Model	DJI Phantom 3 Advanced		DJI Phantom 4 RTK	
Mission type	2D		TA	
Date (dd.mm.yy)	13.3.16	03.03.18 to 07.03.18	24.03.22	29.02.24
# acquired / aligned images	512 / 512	1537 / 1519	1472 / 1472	2183 / 2183
Flight altitude (m)	40 to 100		50	
Vert. / hor. Overlap (%)	60 to 70		65	70
Flight speed (m/s)	5		5.5	5
Ground res. (cm/pix)	5.56	4.76	1.55	1.39

Starting 2022 we use a Phantom 4 RTK setup in combination with a D-RTK2 mobile station in VLOS and terrain awareness (TA) mode, ensuring a constant flight altitude of 50 m over the entire rock glacier by relying on the TanDEM-X DEM (12 m, 2011–2014) as reference. Located on the moving rock glacier surface, we (re)measure and insert the coordinate of the D-RTK2 mobile station location with horizontal and vertical errors of respectively 0.01 m and 0.02 m prior to conducting the flights, Table 2. Execution of both flights with their respective sensor specifics, see Table 3, is within a single day to limit the influence of different light conditions.

Table 2 Coordinate of the D-RTK2 mobile station used 2022 and 2024. The location is (re)measured using DGNSS equipment and inserted to the DJI equipment prior to conducting the flights. All coordinates are in WGS 84 UTM zone 19S (EPSG: 32719).

	2022	**2024**
Easting	424640.993	424640.053
Northing	6653872.988	6653872.678
Elevation (m)	4370.320	4370.231

Table 3 UAV characteristics as used for image acquisition in the study area. For a discussion of their effects, see Paper 2.

	DJI Phantom 3 Advanced	**DJI Phantom 4 RTK**
Sensor	1/2.3” CMOS	1” CMOS
Effective pixels	12.4 MP	20 MP
Focal length	20 mm (35 mm equivalent)	24 mm (35 mm equivalent)
Field of view	94°	84°
Image size	4000 × 3000	5472 × 3648
Shutter type	electronic	mechanical

5.1.2. Pleiades imagery (Paper 1 and 3)

The Pléiades 1A and 1B satellites were launched on December 17th 2011 and December 2nd 2012, respectively. With a sun-synchronous orbit type and repeat cycle of 26 days, they offer panchromatic and multispectral imagery in stereo and tristereo mode with spatial resolutions of 0.5 and 2 m, respectively (ASTRIUM 2012). Achieving the (tri)stereo cover during one pass over the area, a homogeneous product which allows for the generation of most precise DEMs is acquired despite challenging topography and with suitable base-to-height (B/H) ratios comparable to other studies (e.g., Beraud et al. 2023). All Pléiades data used in this study was tasked for the upper part of Rodeo basin, Figure 5B, and for austral summers, in (tri)stereo mode and processing level 1, corresponding to the primary product (ASTRIUM 2012), Table 4.

Table 4 Data characteristics for our five (tri)stereo panchromatic Pléiades datasets tasked in processing level 1. The difference in geometry is not intended but is caused by data availability. B/H = base-to-height ratio. The number of tiles varies with the acquisitions’ extent, cf. Figure 5B.

	2019	**2022**	**2023**	**2024**	**2025**
Date(s)	17.03.19	14.02.22 22.02.22 15.02.22	13.02.23 20.02.23 14.02.23	12.02.24 19.02.24 09.03.24	02.03.25 03.03.25
Geometry	stereo	tristereo			
B/H	0.4	0.3-0.5			
Inc. Angle	< 20° (maximum)				
Cloud Cover	< 5% (maximum)				

5.1.3. DGNSS measurements (Paper 1, 2 and 3)

Marked on flat surfaces of selected large boulders (> 2 m axis) located on the rock glacier surface and surrounding terrain, 20 to 34 points per year on Dos Lenguas rock glacier, 36 points per year on El Paso rock glacier and 21 points per year in the Agua Negra glacier forefield were (re)measured using Trimble DGNSS equipment (R8 base, R2s rover, TSC3 handheld, RTK), Table 5. Difference in the date of acquisition between the UAV flights and DGNSS campaigns was kept to a minimum to ensure measurements representability. The coordinate of the base stations, one per study site, was fixed to the same coordinate for all years, Table 6. For balancing visibility of the target with the error introduced by a large marking (Smith et al. 2016), large white crosses were sprayed and small black crosses included in their centres. The 2017 to 2022, and 2024 DGNSS data measured on Dos Lenguas rock glacier are used for georeferencing and quality estimation in Paper 1 and 2 and are published in Stammler et al. (2025b). All DGNSS measurements are used for validation of the Pléiades-based results in Paper 3 and are included in the dataset accompanying Paper 3. For the DGNSS measurements' spatial distribution, see Figure 13A-C and Figure 18A, C-D.

Table 5 DGNSS measurements on Dos Lenguas rock glacier (top), El Paso rock glacier (centre) and Agua Negra glacier forefield (bottom). Hor. Acc. = Horizontal Accuracy, Ver. Acc. = Vertical Accuracy. The horizontal and vertical errors represent the mean error of all relevant DGNSS measurements, split in GCPs and CPs where indicated.

	2017	**2018**	**2022**	**2023**	**2024**
Date (dd.mm.yy)	23.02.17 & 24.02.17	01.03.18 & 02.03.18	17.03.22 & 21.03.22	16.01.23 & 12.02.23	10.02.24 & 12.02.24
# of points	16	34	20	21	15
# GCPs / CPs	12 / 4	26 / 8	15 / 5	NA	11 / 4
Mean hor. acc. GCPs / CPs (cm)	0.01 / 0.01			0.02	0.01 / 0.01
Mean ver. acc. GCPs / CPs (cm)	0.02 / 0.02			0.03	0.02 / 0.03
Date (dd.mm.yy)				01.02.23 & 02.02.23	14.02.24
# of points				36	
Mean hor. acc. (m)				0.04	0.02
Mean ver. acc. (m)				0.08	0.04
Date (dd.mm.yy)			08.03.22	17.01.23	26.02.24
# of points			21		
Mean hor. acc. (m)			0.01		
Mean ver. acc. (m)			0.02		

Table 6 Coordinates of the base stations used during the acquisition of the DGNSS measurements. Per study site, the location of the base station is fixed to the same coordinate for all acquisitions. RG = rock glacier, AN forefield = Agua Negra glacier forefield. All coordinates are in WGS 84 UTM zone 19S (EPSG: 32719).

	Dos Lenguas RG	**El Paso RG**	**AN forefield**
Easting	424101.83	422350.62	422783.389
Northing	6654084.621	6655630.667	6661216.068
Elevation (m)	4247.137	4723.248	4726.973

Due to a lack of DGNSS measurements in 2016, a set of 16 points located outside of the Dos Lenguas surface measured in 2017 was used for generating the 2016 DEM. The measurements are located on stable terrain as confirmed with mean 2017 to 2018 differences of 0.01 m ± 0.02 m (easting), -0.01 m ± 0.02 m (northing) and 0.01 m ± 0.03 m (elevation).

5.1.4. National Inventory of Glaciers, Argentina (Paper 1, 2 and 3)

Glaciers, debris-covered glaciers, rock glaciers and perennial snowfields across the Argentinean Andes and South-Atlantic islands cover an area of 8'484 km^2 and are mapped in the National Inventory of Glaciers conducted by the Argentine Institute for Snow, Ice and Environmental Sciences (IANIGLA-CONICET) in collaboration with the Argentine Ministry of the Environment and Sustainable Development (Zalazar et al. 2017). With the aim of preserving glaciers and the periglacial environment, the dataset was established based on satellite imagery and ground-truthing as requirement of the law on Minimum Standards for the Preservation of Glaciers and the Periglacial Environment (span. Régimen de Presupuestos Mínimos para la Preservación de los Glaciares y del Ambiente Periglacial) (ibid.).

All investigations of this dissertation rely on the National Inventory of Glaciers for glacial and periglacial feature boundaries of the landforms located in the study area. For all of the analyses, rock glaciers are treated indifferent of their mapped state of activity allowing to rely on measured activity rather than the visual interpretation of surface features as conducted during the establishment of the inventory (Zalazar et al. 2017). For our feature tracking approach applied directly on panchromatic Pléiades imagery, the polygons are buffered to reduce the impact of the polygon boundaries on the feature tracking outcome.

5.1.5. Climatological data (Paper 2)

A station measuring air temperature data has been operational since February 14th, 2022, recording air temperature using a HOBO sensor mounted 1.7 m above the ground. For precipitation, no *in situ* measurements are available. Snow cover spatial extent and duration is visually inspected with two SECACAM Pro Plus cameras which are set to automatically take daily imagery, installed at two different locations in the catchment, cf. Figure 5A. Location 1, close to the northern end of the Agua Negra valley at approximately 4650 m asl provides a southward overview on the valley between February 6th 2023 and February 25th 2024, comparable to Figure 6C. Location 2, at 1.5 km distance north from and with a view towards Dos Lenguas rock glacier sheds light on snow conditions at Dos Lenguas between February 16th 2023 and February 27th 2024. Location 2 is equipped with metric-labelled poles for snow height estimation.

For an investigation on longer timescale, ERA5 based air temperature at 2 m elevation (°C), precipitation amount (mm/m^2) and snowfall amount (cm/m^2) are analysed at monthly resolution for the time period 1940 to 2024. Meteoblue history+ provides tailored access to the ERA5 dataset generated by the European Centre for Medium-Range Weather Forecasts (ECMWF) (Hersbach et al. 2019), here extracted for a point in the centre area of Dos Lenguas rock glacier, Figure 11A. One year of the ERA5 based air temperature is compared to air temperature measured at the station introduced above for validation, cf. Figure 16. As no reliable local precipitation measurements for the area are available, the ERA5 precipitation is used without data-based validation except for the visual inspection of snow cover.

5.2. Methods

5.2.1. DEM generation (Paper 1, 2 and 3)

UAV-based DEMs for Dos Lenguas rock glacier are generated using SfM-MVS techniques and a standard photogrammetric workflow based on the quasi-biennial UAV missions, Table 1, in Agisoft Metashape Professional (version 2.0.4). All processing is conducted on a 13th Gen Intel(R) Core™ i9-13900K and a NVIDIA RTX A4500. All UAV imagery is reprocessed to ensure algorithm reproducibility (Hendrickx et al. 2019) and is co-aligned independent of its date of acquisition to increase comparative accuracy between the time periods (Cook and Dietze 2019; Haas et al. 2021). Highest accuracy and key and tie point limits of 40'000 and 10'000 are selected, respectively. Our optimization parameters are focal length, principal point X and Y, radial distortion coefficients k1-k3 and tangential distortion coefficients p1-p2. Additional corrections are fitted to control doming (James and Robson 2014), and no adaptive camera model fitting is applied. The aligned images are then separated based on their date of acquisition and georeferenced using the DGNSS measurements, Table 5, as GCPs and CPs, including the DGNSS measurement errors during georeferencing. For co-processing with the UAV image coordinates, DGNSS measurements are converted from WGS 84 / UTM zone 19S (EPSG: 32719) to WGS84 (EPSG: 4326) in Agisoft Metashape Professional. High-quality and moderate depth filtering are applied during depth map generation with the point cloud selected as source data during DEM generation. The DEMs are exported in GeoTIFF format. The high-resolution DEMs allow for the derivation of hillshades relevant to the feature tracking, and of slope rasters crucial for the investigation of the role of topography on rock glacier surface change.

Pléiades-based DEMs are generated at 1 m spatial resolution using our acquisitions, Table 4. We test three different software (Agisoft Metashape Professional, Catalyst Professional and ASP) aiming at determining the most suitable processing strategy for large(r)-scale application. Agisoft utilizes SfM-MVS techniques to obtain DEMs and is commonly used for the processing of UAV imagery as applied in Paper 1 and 2 (Smith et al. 2016). We test the feasibility of Agisoft for Pléiades imagery and rely on the RCPs for solving the imagery's exterior orientation. We use higher key and tie point limits than for the UAV imagery processing and build dense clouds using the 'high' quality and 'moderate' depth filtering options before generating the DEMs. Catalyst follows a traditional photogrammetric approach well used for glacial and periglacial change analysis. We create maximum overlapping epipolar images and generate DEMs using the SGM algorithm, also making use of the RCPs. In ASP, we also rely on the RPCs and follow Berthier et al. (2024) and Cusicanqui et al. (2025) using a STRM DEM as seed DEM during stereo processing and a SGM strategy. Here, either both stereo acquisitions or both pairs of the tristereo triplet are used. Given the data quality no gaps are filled due to their minimal presence and no sensor undulations are corrected.

While all three software are applied for the processing of Pléiades imagery in Paper 1, ASP and the therein used processing strategy are judged most suitable and are applied in Paper 3. In all cases, the generated DEMs correspond to multiple tiles which make up the catchment. These tiles are not mosaicked prior to, e.g., DEM generation to prevent the introduction of distortions.

5.2.2. DoD calculation for vertical change quantification (Paper 1, 2 and 3)

For UAV DEM-based DoD calculation, the spatially distributed and rasterized elevation values from subsequent UAV DEMs are resampled to equal resolution using bilinear interpolation. For Paper 2, this corresponds to the lowest resolution of all acquisitions – the 2016 data, Table 4. Previously georeferenced, the DEMs are aligned in space and are directly subtracted from one another to calculate vertical surface change. All DoDs are time-normalized to full years to establish comparability. To ensure physical meaningfulness, we calculate all surface changes also for stable terrain. Both the bias and the random component of the UAV DoD-based vertical error are assessed by calculating the mean vertical error (bias) and the standard deviation (σ, random component) of the CP residuals.

The LoD is calculated based on the propagation of the random component of vertical error between two DEMs, following the approach of Brasington et al. (2003) and Wheaton et al. (2010), Equation 1, where $\sigma\ error_{new}$ and $\sigma\ error_{old}$ refer to the random error component of the vertical errors of the newer and older DEMs used in the DoD calculation, respectively. This approach is applicable when the bias component is negligible compared to the random component. To account for cases where a systematic difference in bias exists, an additional term, where b_{new} and b_{old} denote the mean vertical error (bias) of the respective DEM, is included, Equation 2.

$$Propagated\ error = \sqrt{(\sigma\ error_{new})^2 + (\sigma\ error_{old})^2} \quad (1)$$

$$LoD = |\ b_{new} - b_{old}\ | + \sqrt{(\sigma\ error_{new})^2 + (\sigma\ error_{old})^2} \quad (2)$$

Volumetric changes are calculated based on the UAV DoDs at 11 cm resolution. For an estimation of potential error, the range between minimum and maximum volume change based on the LoD of each time period is visualized. For their calculation, see Equation 3 and 4, where pixel value and LoD depend on the time period and the pixel area is (11 cm^2) based on the data's resolution.

$$Min\ Volume\ Change\ = \sum([pixel\ value\ -\ LoD]\ *\ pixel\ area) \quad (3)$$

$$Max\ Volume\ Change\ = \sum([pixel\ value\ +\ LoD]\ *\ pixel\ area) \quad (4)$$

Pléiades-based vertical rock glacier surface change analysis is conducted on clipped Pléiades DEMs to reduce the effect of potential distortions within the generated DEM tiles, cf. Chapter 5.2.1. To clip the Pléiades DEMs, rectangular bounding boxes with minimum 500 m distance to each of the landform polygons are generated. The clipped DEMs are co-registered following Nuth and Kääb (2011) in Demcoreg (Shean et al. 2016), cf. Chapter 3.2.2. Here, the younger clipped DEM is co-registered to the older, e.g., 2022 to 2019, while masking the cryospheric landforms based on the National Inventory of Glaciers (IANIGLA-CONICET 2018), cf. Chapter 5.1.4. If available for both acquisitions, each tile is co-registered respectively, e.g., 2023T to 2022T, 2023B to 2022B, 2023R to 2022R. For specifics on the naming of the tiles, please see Paper 3. For acquisitions with different extents and/or number of tiles, co-registration is only possible where data is available and is conducted as, e.g., 2022T to 2019, 2022B to 2019, 2022R to 2019. Co-registering clipped rasters allows for an adaption to the local setting of

each landform, preventing larger distortion patterns to imprint on the DEM-based analysis while reducing processing times. Further, it enables temporal and spatial investigation of the x, y, z correction factors used during co-registration, cf. Table 12. Pléiades-based vertical surface change for the cryospheric landforms in Rodeo basin is compared as cumulative median or normalized to full years, both calculated as median for the landforms' surfaces without taking side and front slopes into account. For Pléiades-based investigations, no volumetric changes are calculated.

For the calculation of the LoDs of our Pleiades-based vertical surface changes, we extract vertical surface change at 1000 random points distributed in vicinity of each landform polygon and derive their median. Terrain outside the landform polygons is assumed stable. Having controlled vertical surface change in the areas outside the landform surfaces during co-registration, we directly accept the medians as LoDs.

5.2.3. Feature tracking for horizontal change quantification (Paper 2 and 3)

All feature tracking is conducted following the principles of the Environmental Motion Tracking (EMT) software (Schwalbe and Maas 2017). EMT matches image patches between consecutive hillshades in a two-step process, first using cross-correlation to estimate a pixel-precise shift, followed by a least-squares matching to achieve sub-pixel accuracies (ibid.).

For our landform-focus in Paper 2 we conduct feature tracking in EMT on UAV DEM-derived hillshades generated at 25 cm resolution. On the rock glacier surface, patch centres are spaced at 2 m distance, leading to a resolution of 2 m in the final rock glacier velocity dataset. Given the two-year separation of the UAV surveys, orthoimages are subject to considerable spectral differences due to varying light conditions, partial snow cover, and shadow effects between data acquisitions. The use of grey scale input for tracking surface displacement outperforms orthoimages given their independency of light conditions and capability of enhancing subtle changes, especially over longer intervals (Dall'Asta et al. 2017; Fleischer et al. 2021). To quantify the residual positional mismatch between consecutive images, 1000 randomly distributed points are placed on stable terrain outside the rock glacier. Tracking these stable points, the UAV-based analysis' LoD is quantified using the 90^{th} percentile of their apparent movement, see Blöthe et al. (2024).

To conduct feature tracking on all rock glaciers in Rodeo basin in Paper 3, the projected Pléiades panchromatic imagery at 0.5 m spatial resolution is used. Similar to the DEMs, the panchromatic orthoimages are clipped by bounding boxes to reduce the impact of distortions. For the stereo dataset, we select the first image of the pair with a view angle tilted towards south and for the tristereo datasets the second image of the triplet which is closest to nadir view (90°). We adapt the approach implemented in EMT to semi-automatically process a large quantity of rasters in python. After conducting an affine transformation for offset correction, identifiable pixels are tracked on the landform surface (no front and side slopes) using a set of equally, 5 m spaced points leading to a 5 m spatial resolution of the calculated velocities. Similarly to the UAV DEM derived hillshades, the projected panchromatic Pléiades imagery benefits from being independent of differences in light conditions (Dall'Asta et al. 2017; Fleischer et al. 2021).

LoDs for Pleiades-based horizontal surface changes are quantified by tracking surface motion at 1000 randomly distributed points located outside of the landform surface. We accept the median of the feature tracking results at these 1000 random points as LoD. Further, we track the residuals of the affine transformation during our feature tracking approach to develop a criterion for the quality of the image alignment, which directly affects the feature tracking results. We detect the correlation of these residues in x, y space and use low correlation coefficients (0 to 0.5) as indication of a high-quality feature tracking and high correlation coefficients (0.5 to 1) as indication of a poorer feature tracking quality. The implementation of the correlation coefficient of the residues that arise during feature tracking as a quality control is based on the hypothesis that high correlation is indicative of a technical error, e.g., an image distortion, while true residues are expected to be independently distributed. We include this quality criterium as a metric and as categories, cf. Table 14 and Figure 22.

5.2.4. Topographical analysis (Paper 2)

To determine the impact of topographical characteristics on horizontal and vertical surface change on Dos Lenguas rock glacier, including their change through time, we generate scatterplots with elevation and the DEM derivatives slope (6 parameter 2nd order polygon, Evans 1979) and curvature at 2 m, 5 m, and 10 m resolution. All products are resampled from their original spatial resolution (11 cm for vertical change and elevation, 2 m for horizontal change) to the respective new resolution, applying bilinear interpolation.

We calculate Pearson correlation coefficients to better understand correlations between the different rasters. Here, elevation, slope and curvature values are valid at the beginning of the respective time episode. For example, horizontal change from 2016 to 2018 is tested for correlation with the topographical characteristics for 2016, while horizontal change from 2018 to 2022 is tested for correlation with the topographical characteristics for 2018.

To summarize, the two types of optical imagery acquired using UAVs or by tasking Pléiades satellite imagery present the core datasets of this dissertation. They are used to generate DEMs, either with a high-resolution landform focus or for landforms across the entire Rodeo basin, the latter while scarifying spatial resolution. Independent of the imagery input, DEMs are essential to the quantification of vertical changes by DEM differencing, namely the generation of DoDs. The optical imagery further lies base for feature tracking, either by UAV imagery based hillshade derivation or by conducting feature tracking on the panchromatic Pléiades imagery, directly. Other datasets, such as the DGNSS measurements, support the optical imagery acting as input for georeferencing or validation data. The National Inventory of Glaciers is used for the delineation of landforms, also independent of the imagery product. Having introduced the data and methods used in this dissertation, their application across the three papers is showcased in the following chapters.

6. Vertical surface change signals of rock glaciers: combining UAV and Pléiades imagery (Agua Negra, Argentina) (Paper 1)

This chapter is based on the first publication that contributes to this dissertation. It addresses research questions 1, 2 and 5.

Stammler, M., Cusicanqui, D., Bell, R., Robson, B., Bodin, X., Blöthe, J., Schrott, L., 2024. Vertical surface change signals of rock glaciers: combining UAV and Pléiades imagery (Agua Negra, Argentina). Proceedings of the 12th International Conference on Permafrost (ICOP). Whitehorse / Canada. DOI: 10.52381/ICOP2024.138.1

As visualized in Figure 1, a combination of high-resolution UAV imagery with a landform-focus and the lower spatial resolution Pléiades imagery with a larger spatial extent of the analysis is beneficial to a comprehensive understanding of rock glacier surface changes. But how comparable are UAV- and Pléiades imagery based DEMs and which technical impact factors need to be identified? The aim of this paper is to understand the effects of different processing strategies on the visual appearance, quality and robustness of Pléiades-based DEM generation and to select the best fitting strategy.

The chapter draws on the comparison of three different software commonly used for DEM generation, namely Agisoft Metashape Professional, Catalyst Professional and ASP. It generates and compares the thereon based DEMs and DoDs for Dos Lenguas and El Paso rock glaciers and discusses the effects of the different processing strategies. Available for Dos Lenguas rock glacier, it compares the Pléiades- to UAV-based DEMs and DoDs, and the quantified rock glacier surface changes based thereon. The chapter continues to outline the findings' geomorphological relevance showcasing the similarities between the UAV- and Pléiades-based vertical rock glacier surface change and the possibility to quantify such change on El Paso rock glacier for which no UAV-based investigation is available.

To summarize, the chapter's research objectives are the generation and comparison of DEMs and DoDs based on tristereo, panchromatic Pléiades data and repeated UAV flights (austral summers 2022 and 2023), the detection of effects of different processing strategies on the generation of Pléiades DEMs through comparison of results from three software, and an evaluation of the transferability of the Pléiades-based workflow by application on El Paso rock glacier. **The research presented in this chapter is a proof of concept to allow future large(r) scale investigation.**

6.1. Results

6.1.1. DEMs based on UAV and Pléiades imagery

With a maximum UAV DEM resolution for Dos Lenguas rock glacier of 3.09 cm/pixel (2022) and 2.76 cm/pixel (2023), modelled GCP locations deviate approximately 1 cm from DGNSS measurements. The total error in x, y and z directions for 2022 is 0.6 cm, 1.0 cm, and 0.25 cm. The total error for 2023 is similar with 0.6 cm, 0.9 cm, and 0.3 cm. The DEM reproduces known points not included in the model (CPs) with a maximum distance of 10 cm. Deviations between the modelled CPs and DGNSS measurements are lower on stable terrain, and higher in the upper part of the rock glacier.

The Pléiades DEMs processed in Agisoft appear clearest and with furrows and ridges produced most similarly to the UAV DEMs, Figure 7B and Figure 8. The processed Pléiades DEM in Catalyst leads to coarser surfaces and 'flattened' microtopography, Figure 7C and Figure 8. The ASP results occur smoothest with limitations in representing boulders in the rock glaciers' upper part while portraying furrows and ridges, Figure 7D and Figure 8. None of the DEMs has voids over the target site. All Pléiades DEMs are generated with a resolution of 1 m. The offset between DEMs prior to co-registration is largest for Agisoft, followed by Catalyst and ASP, Table 7. ASP DEMs are most consistent in their offset compared to 20 DGNSS measurements (GCP/CPs), Table 8.

The spatial distribution of error (Eltner et al. 2016; James et al. 2019) is most consistent in time for the ASP DEMs, based on a comparison of the 5 highest Pléiades DEM deviations from the 20 DGNSS measurements. In 2022, errors are largest in the upper part of Dos Lenguas rock glacier (Agisoft, Catalyst), Figure 7B-C, and at the sides and front (ASP), Figure 7D. In 2023, largest errors occur at the centre, front and the sides (Agisoft), Figure 7B, and only the front and sites (Catalyst, ASP), Figure 7C-D. While differences in absolute elevation exist between processing strategies, co-registration per processing strategy is efficient, Figure 7.

Table 7 Linear co-registration shifts calculated over stable terrain between respective Pléiades DEMs, relying on RCP files for DEM generation. Co-registration of 2023 Pléiades to 2022 Pléiades DEMs following Nuth and Kääb (2011) in Demcoreg (Shean et al. 2016).

	Shift in x (m)	**Shift in y (m)**	**Shift in z (m)**
22/23 Agisoft	-35.84	15.06	15.22
22/23 Catalyst	-8.41	3.70	32.08
22/23 ASP	-0.35	-0.04	1.15

Table 8 Consistency of DEM offsets calculated as standard deviations (σ) of the differences between 20 known DGNSS points (each for 2022 and 2023) and the respective DEM, similar to Mueting et al. (2021). As we rely on the RCP files for DEM generation, none of the DGNSS measurements is included in the DEM.

	σ 2022	**σ 2023**
DGNSS to Agisoft DEM	6.46	2.48
DGNSS to Catalyst DEM	2.15	1.13
DGNSS to ASP DEM	0.83	1.02

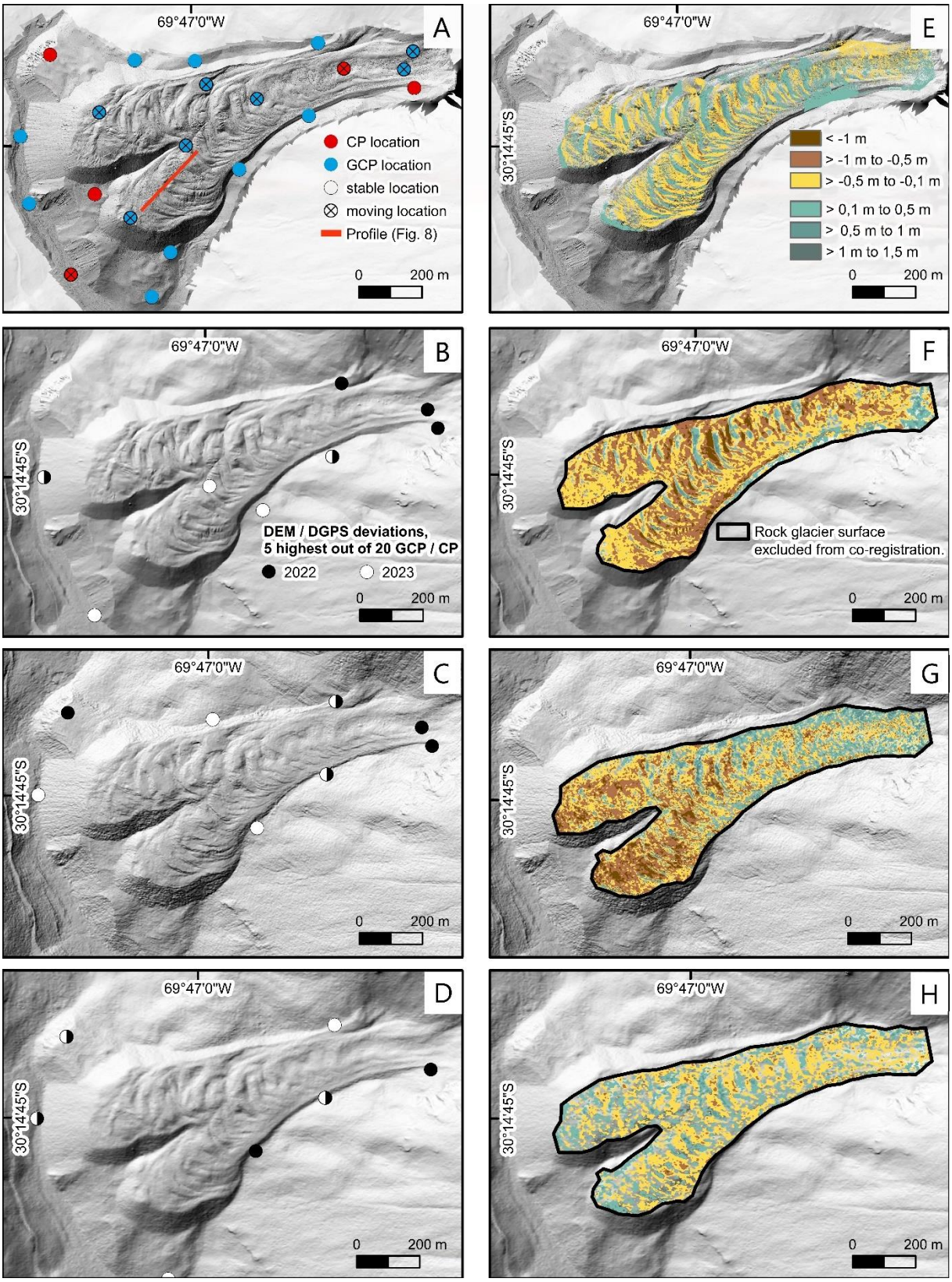

Figure 7 DEM visual appearance (2022, A-D) and vertical surface change (m, 2022-2023, E-H) of Dos Lenguas rock glacier based on UAV/Agisoft (A, E), Pléiades/Agisoft (B, F), Pléiades/Catalyst (C, G), and Pléiades/ASP (D, H). GCP/CP locations (A-D) measured in 2022 and 2023. Line in A) indicates the profile locations taken for Figure 8. The rock glacier outline (F-H) as mapped by IANIGLA-CONICET (2018) is used to exclude the rock glacier surface from co-registration. Adapted from Paper 1.

6.1.2. DoDs based on UAV and Pléiades imagery

Given its very high resolution, the UAV DoD shows magnitude and distribution of vertical surface change on Dos Lenguas rock glacier between 2022 and 2023 in most detailed manner, Figure 7E (5 cm resolution based on resampled UAV DEMs 2022 and 2023 for better comparison between UAV DEMs). The Pléiades DoD processed in Agisoft overestimates negative change throughout the entire surface of the rock glacier compared to the UAV DoD, yet appropriately represents ridges and furrows, Figure 7F. The Pléiades DoD processed in Catalyst overestimates negative change particularly towards the lower part of the rock glacier and does not adequately portray the microtopography, especially in comparison to the UAV DoD but despite being characterised by the same resolution also compared to the Pléiades DEM processed in Agisoft, Figure 7G. The processing of Pléiades imagery in ASP results in a DoD most similar to the UAV results in terms of magnitude as well as distribution of vertical surface change, Figure 7H.

Pixel frequencies for vertical surface change are unimodal and normally distributed independent of image source and processing strategy, Figure 9. Highest surface changes do not exceed ± 2 m with most changes occurring below zero. The UAV processing in Agisoft and the Pléiades processing in ASP show most similar distributions. The Pléiades processing in Agisoft and Catalyst leads to wider distributions with lower maxima, and with overall shifts to more negative values. The magnitude of calculated negative and positive surface changes between 2022 and 2023 (mean change below or above zero, uncertainty based on stable terrain for Pléiades DoDs) are higher for the Pléiades processing in Agisoft and Catalyst, and lower for the UAV processing in Agisoft and the Pléiades processing in ASP, Table 9.

Pléiades DoD based vertical surface change for El Paso rock glacier between 2022 and 2023 is similar to vertical surface change on Dos Lenguas rock glacier during the same time period. This applies to the range of the pixel frequency distribution of vertical surface changes (below ± 2 m), Figure 9 and Figure 10, the similarity of the magnitude of change of the Pléiades processing in ASP, Table 9 and Table 10, and the lower mean negative and higher mean positive changes when processing Pléiades imagery in Agisoft and Catalyst in comparison to ASP, Figure 9, Figure 10; Table 9, and Table 10.

Table 9 Mean negative and positive vertical surface changes (m) on Dos Lenguas rock glacier between 2022 and 2023. Adapted from Paper 1.

	Mean negative (m) and LoD (m)		**Mean positive (m) and LoD (m)**	
UAV Agisoft	-0.16		0.16	
Pléiades Agisoft	-0.49	± 0.09	0.24	± 0.09
Pléiades Catalyst	-0.47	±0.08	0.29	± 0.08
Pléiades ASP	-0.19	± 0.01	0.17	± 0.01

Table 10 Mean negative and positive vertical surface changes (m) on El Paso rock glacier between 2022 and 2023. Adapted from Paper 1.

	Mean negative (m) and LoD (m)		**Mean positive (m) and LoD (m)**	
Pléiades Agisoft	-0.28	± 0.04	0.22	± 0.04
Pléiades Catalyst	-0.26	± 0.03	0.24	± 0.03
Pléiades ASP	-0.19	± 0.02	0.15	± 0.02

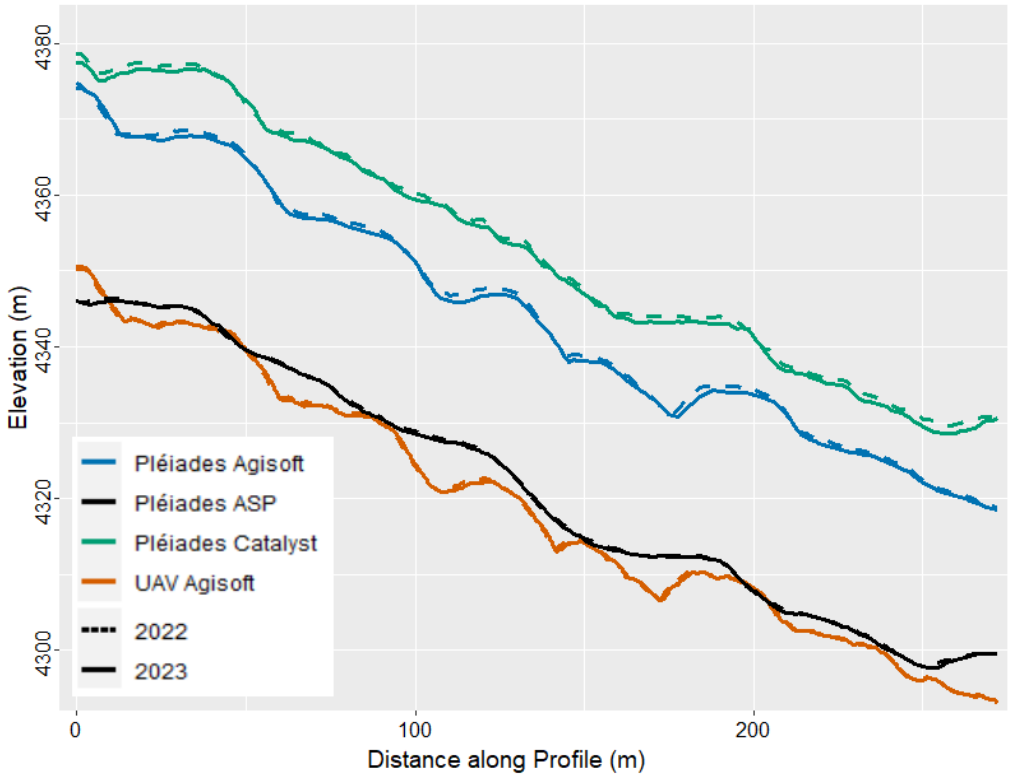

Figure 8 Surface profiles across the UAV and Pléiades DEMs on Dos Lenguas rock glacier, separated by processing strategy. For the profile location, see Figure 7A.

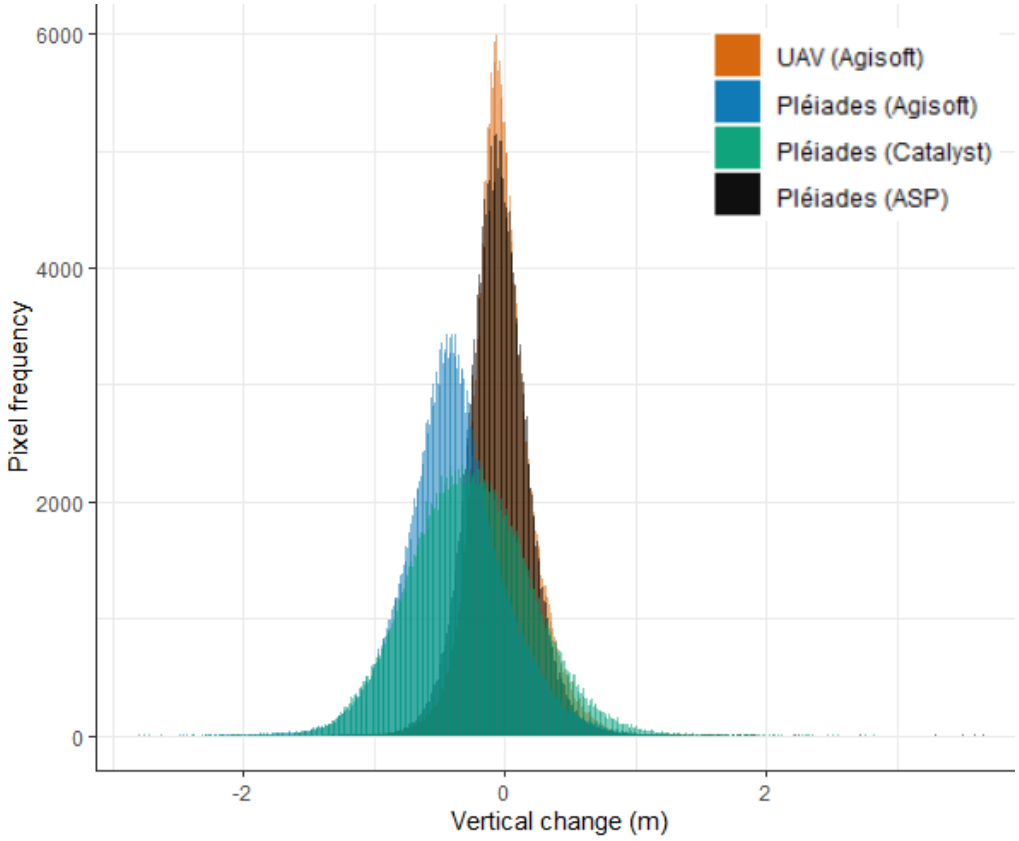

Figure 9 Vertical surface changes (m) for Dos Lenguas rock glacier (2022–2023), separated by image source and processing strategy.

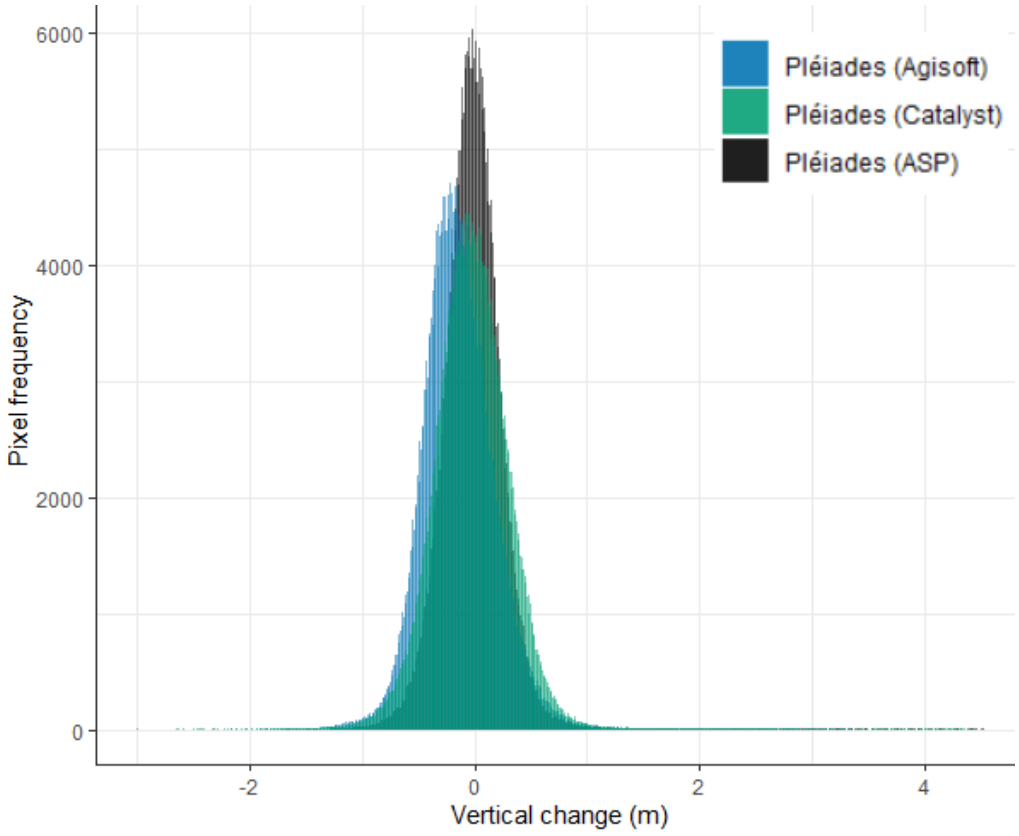

Figure 10 Vertical surface changes (m) for El Paso rock glacier (2022–2023), separated by processing strategy.

6.2. Discussion

6.2.1. Comparison of processing strategies for DEM and DoD generation

Despite using the same Pléiades imagery as input, the DEMs vary distinctively in visual appearance, Figure 7B-D, quality and robustness, Table 7 and Table 8, and absolute elevation, Figure 8. These variations caused by the three processing strategies propagate and lead to differences in calculated vertical surface change on Dos Lenguas rock glacier between 2022/2023 visually, Figure 7F-H, in pixel frequency distribution, Figure 9, and in terms of mean change values, Table 9. The differences not only hold true for Dos Lenguas but also for El Paso rock glacier, Figure 10 and Table 10.

Our processing strategy for Pléiades imagery in Agisoft outperforms the Catalyst and ASP results in reproducing coherent furrows and ridges as well as landform neighbouring ridges and erosional gullies, Figure 7B. We assume that for this reason the Agisoft Pléiades processing is the sole strategy that shows deposition on the rock glacier's orographic right-side slope, Figure 7F. Agisoft allows a combined processing of Pléiades tiles, enabling smooth transitions between overlapping tiles and direct, unrestricted investigation of rock glaciers located close to tile edges. We hypothesize that to the disadvantage; this combined processing causes distortions resulting in the shifts between the DEMs before co-registration and the poor consistency of offsets between DEMs and DGNSS measurements, Table 7 and Table 8. We interpret the inconsistency of the spatial error distribution throughout time as additional indication of low data robustness, Figure 7B. Potentially due to these limitations, the Agisoft Pléiades DoDs overestimate negative vertical surface change for the entire rock glacier, compared to the UAV results.

Our Pléiades processing strategy in Catalyst leads to 'flattened' and smoothed ridges on the DEMs, Figure 7C and Figure 8. This effect propagates to the DoD with the vertical surface change in the lower part of the rock glacier being similar in magnitude to the Pléiades based results in Agisoft but less coherent with and confined to the microtopography, Figure 7G. The maximum of the Pléiades Catalyst based pixel frequency distribution is more similar to the UAV based results than the Pléiades Agisoft processing, Figure 9. However, this is caused by the balancing of overestimation of negative changes in the lower and of positive changes in the upper part compared to the UAV DoD, Figure 7G and Table 9, hence, is no sign of quality of the dataset.

The ASP processing of Pléiades imagery clearly stands out in its similarity of the pixel frequency distribution of vertical surface change and its mean negative and positive change in comparison to the Agisoft UAV DoD, Figure 9 and Table 9. With the ability to gauge the errors of our UAV based results, we deem the ASP based results for the Pléiades data as most correct. This corresponds well to the highest overall data quality, Table 7 and Table 8 and the highest consistency of spatial error of the ASP Pléiades analysis, Figure 7D. The example highlights that Agisoft performs better when used for processing UAV imagery, than Pléiades imagery. For processing Pléiades data, ASP can clearly be attributed the best performance in terms of data quality and robustness. In terms of visualisation it lacks, e.g., the ability of reproducing single rocks on in the rock glaciers' upper zone, in comparison to the Agisoft Pléiades DEM. We hypothesize that the smoothing performed when applying the SGM algorithm is causing this difference. This might also explain the similarity of the Catalyst and ASP derived profiles, Figure 8, as in both cases SGM is used for image correlation.

Co-registration significantly reduces shifts between the 2022 and 2023 Pléiades DEMs independent of processing strategy and notably improves the quality of the DoDs. The shift that occurs for our Agisoft and Catalyst results are uncommonly high, Table 7. Rieg et al. (2018) generate Pléiades based DEMs using a SGM algorithm available in ERDAS IMAGINE along with the RPC files and, depending on study site, automatically identified and manually controlled tie points or GCPs. They investigate glaciers in the European Alps and the Khumbu Himal and encounter maximum offsets of 4 m, -3.2 m and 4.8 m in x, y and z directions. In comparison, the detected offsets for the ASP based Pléiades DEMs for Dos Lenguas rock glacier are minimal.

We decide on co-registering the 2023 to the 2022 Pléiades DEM per processing strategy to maintain independence between the photogrammetric software. We chose to not co-register the Pléiades DEMs to the UAV DEMs for a robust co-registration (UAV flights barely cover stable terrain) and to develop an UAV independent workflow for future use in larger regions. Despite well-performed co-registration of DEMs of the same processing strategy, absolute differences in elevation between the processing strategies occur, Figure 8. It is apparent that the UAV DEMs processed in Agisoft and the Pléiades DEMs processed in ASP are relatively similar in absolute elevation despite the difference in data source, in processing software and without any co-registration. We hypothesize that this is due to an unintended similarity in z values between the SRTM DEM used as seed DEM to generate the Pléiades DEM in ASP and the GCPs and CPs used for processing the UAV imagery in Agisoft.

6.2.2. Rock glacier surface change

We can confirm the ridge and furrow surface pattern as described by Halla et al. (2021) both in our UAV as well as in our Pléiades based DEMs, consequently also in all DoDs. Vertical surface change patterns are a compound signal of vertical and horizontal surface change with horizontal movements imprinting the vertical differences by shifting features, e.g., ridges, downslope from one year to the other. This results in negative change at the original location and positive change at the location downslope, Figure 7E-H. While this causes strong changes in terms of vertical surface change pattern, the horizontal movement partially equals itself in terms of net surface change balance at locations where pronounced ridges are present (Halla et al. 2021).

None of the rock glaciers investigated expresses strong net negative vertical surface changes between 2022 and 2023, based on mean positive and negative changes, Table 9 and Table 10. While this holds true for all processing strategies and data sources, we focus on the UAV processing in Agisoft and Pléiades processing in ASP given the quality of the data, Table 7 to Table 10. Halla et al. (2021) calculate UAV based annual net balances of vertical surface change on Dos Lenguas rock glacier of -0.36 m/yr for 2016-2017 and +0.27 m/yr for 2017–2018. These findings showcase interannual variability and similarities to our results.

Monnier and Kinnard (2017) calculate vertical rock glacier surface changes within Navarro complex of up to -1 m/yr based on aerial photography and spaceborne DoDs, for the period 2000 to 2014. While the Navarro complex is located approximately 200 km south of our study area, the magnitude of vertical surface change is in agreement with our Pléiades result processed in ASP, Figure 9 (minimum -1.32 m). Our UAV result processed in Agisoft exceeds these values (minimum -2.83 m). We attribute this to the difference in resolution (UAV DoD 5 cm, Pléiades DoD 1 m) and highlight the scale dependency of change values.

In the neighbouring valley west of Agua Negra catchment (La Laguna catchment, Chile), Robson et al. (2022) calculate vertical surface changes of > -0.1 m/yr on several rock glaciers between 2012 and 2020 which corresponds to the most frequent surface changes of our UAV based Agisoft and our Pléiades based ASP processed findings, Figure 9, Figure 10, Table 9 and Table 10. The presented microtopography is similar to Dos Lenguas and El Paso rock glacier surfaces.

6.3. Conclusion

We present a local analysis on Dos Lenguas rock glacier (Dry Andes/Argentina) where we compare DEMs and DoDs based on repeated UAV surveys and Pléiades acquisitions (austral summer 2022 to austral summer 2023). We derive the Pléiades based results using three software packages, namely Agisoft, Catalyst and ASP. Further, we apply the Pléiades based approach to El Paso rock glacier which is located in the same study area.

We find that the choice of processing strategy strongly affects the Pléiades based results. While Pléiades based Agisoft derived DEMs and DoDs appear more appealing visually (less noise, appropriate ridges and furrows), we find their quality in terms of offset and distortion to cause an overestimation of negative vertical rock glacier surface change. Pléiades based DEMs and DoDs processed in Catalyst ‘flatten’ the furrows and ridges on the rock glacier surface and overestimate negative surface change particularly in the lower part. The Pléiades

based results generated in ASP outperform the other processing strategies with highest consistencies of offsets to 20 known DGNSS locations, lowest shifts between DEMs before co-registration and strongest consistency of the spatial distribution of error. Pixel frequency distributions of vertical change are very similar to our UAV DoD processed in Agisoft and surface change values are in agreement with published results. Our example highlights the suitability of Agisoft for processing UAV imagery and of ASP for processing Pléiades imagery.

We can provide Pléiades based change analysis at El Paso rock glacier where we did not obtain UAV imagery. The findings allow for an interpretation of a more general behaviour in the study area. Given that the choice of software propagates to very similar impact when calculating vertical surface change for both rock glaciers, we conclude that attention should not only be focused on potential differences due to variability in co-registration techniques, but also to the choice of software for DEM generation.

A detailed analysis of surface change patterns is only possible with very high-resolution DoDs, which clearly attributes benefit to UAV based DoDs. Pléiades DoDs, however, provide insight to general surface patterns. They can, using an appropriate processing strategy, deliver surface changes similar to UAV based investigation. Given the limitations of UAV surveys imposed by high-alpine conditions, such as for example strong winds, changing weather conditions, and/or limited access; Pléiades based DoDs enable vertical surface change magnitude and pattern analysis at the cost of spatial resolution but at the gains of increased spatial coverage, “access” to previously unvisited sites, and insights beyond the limitations of fieldwork.

We conclude that tristereo Pléiades imagery provides distinguishable benefits for analysing vertical rock glacier surface changes. We highlight the need for robust co-registration and prior knowledge of the study area to carefully assess the suitability of Pléiades DoDs at a specific location. We recommend processing Pléiades data in ASP and highlight the possibility to derive visually detailed Pléiades DEMs in Agisoft. We advocate perceiving these benefits as complementation to UAV surveys, so that highest spatial coverage is achieved by the first and highest spatial resolution by the latter. In view of permafrost degradation, we are certain that an analysis on both spatial scales is relevant.

7. Dos Lenguas rock glacier kinematics stable despite warming trend (2016-2024): Surface changes and the role of topography and climate in the Dry Andes of Argentina (Paper 2)

This chapter is based on the second publication and contributes to answering research questions 1, 3, 4 and 5.

Stammler, M., Blöthe, J., Flöck, F., Bell, R., Schrott, L., 2025. Dos Lenguas rock glacier kinematics stable despite warming trend (2016–2024): Surface changes and the role of topography and climate in the Dry Andes of Argentina. Earth Surface Processes and Landforms 50. DOI: 10.1002/esp.70151.

Both, an understanding of the driving factors of rock glacier kinematics as well as the Andean state of permafrost is limited. This chapter sets out to fill these gaps by examining the surface kinematics of the Dos Lenguas rock glacier in the Dry Andes of Argentina based on high-resolution UAV datasets, cf. Table 1. The dataset represents the longest UAV time series for UAV-based rock glacier monitoring in the Dry Andes, enabling an unprecedented investigation of the magnitude and spatial patterns of rock glacier surface change, in an arid climate. SfM-MVS techniques, cf. Chapter 3.2.1, are applied to derive high-resolution DEMs followed by a calculation of volumetric changes and feature tracking to quantify horizontal change, cf. Chapters 5.2.1 to 5.2.3.

While the presented paper focuses on the magnitude and spatial pattern of vertical and horizontal surface changes on Dos Lenguas rock glacier, it aims at contributing to a better understanding of spatial and temporal rock glacier kinematics to **elucidate the current state of permafrost in vicinity of Dos Lenguas rock glacier and its implications for the wider region**. Further, the high-resolution DEMs allow for the derivation of high-resolution slope rasters used here to evaluate **the role of topography on rock glacier kinematics**. While no long-term *in situ* measurements for air temperature and precipitation are available for the region, this chapter sets out to decipher **the role of the climate** using ERA5 data.

The chapter addresses the following research questions:

- What is the magnitude and spatial pattern of vertical and horizontal surface changes on the Dos Lenguas rock glacier?
- How do topography (slope, curvature) and climatological characteristics (air temperature and precipitation) correlate with the magnitude and spatial pattern of these changes?
- What state of permafrost do the rock glacier kinematics of Dos Lenguas imply for the wider region?

7.1. Results

7.1.1. DEM and feature tracking

The error between the DGNSS-based GCPs and the generated DEMs (GCP error) and between the DGNSS points used as CPs and the generated DEMs (CP error) is highest for the 2016 dataset and lowest for the 2022 dataset, Table 11. For all time episodes, horizontal errors of the DGNSS measurements used as GCPs and CPs exceed their corresponding vertical errors, Table 5. Errors do not vary by the measurements' application as GCPs and CPs, Table 5. While differences occur between the measurement locations, no distinct spatial patterns emerge.

An investigation of the CP-based z error reveals extremely low bias for the 2018 and 2022 DEMs compared to their random error components, Table 11. For 2024, the bias is slightly higher than for 2018 and 2022 but remains lower than 50 % of the 2024 standard deviation. In contrast, the 2016 dataset exhibits a bias that exceeds the random error component. For 2022 and 2024, the mean CP errors normalized by flight height are 0.0084 % and 0.0468 %, respectively. For 2016 and 2018, non-dimensionalization by flight height is not feasible due to variable flight height, cf. Table 1.

Independent of using a DJI Phantom 3 or a DJI Phantom 4 RTK, the derived DEMs are classified as very high resolution DEMs with resolutions of 11 cm or even below, cf. Table 11. Point densities of the dense point cloud before generating the DEMs range from 0.081 points/cm^2 for the 2016 DEM to 0.105 points/cm^2 for the 2022 DEM. DEM resolutions for the 2022 and 2024 DEMs based on the Phantom 4 RTK flights exceed the resolutions of the 2016 and 2018 DEMs based on flights conducted with a DJI Phantom 3, Table 11. Suitability of our UAV imagery for alignment is high across all datasets, based on comparing the number of UAV images taken and UAV images aligned, cf. Table 1. Image characteristics such as spectral properties, presence of shadows and none to very little presence of snow is very similar across each dataset, with contrasting properties between the different datasets. LoDs for vertical change detection fall between ±4.1 cm/yr and ±27.5 cm/yr for vertical surface changes normalized to full years, depending on the DoD constituting DEMs and their error, cf. Table 11.

Using the 90th percentile of 1000 randomly distributed points outside the mapped limits of the Dos Lenguas rock glacier, we estimate the residual mismatch between image pairs to fall between 0.35 pixel (2022-2024, minimum) and 1.63 pixel (2016-2022, maximum). Given the variable epoch length, this translates to LoDs between 3.1 and 17.9 cm/yr for surface velocities obtained by feature tracking.

Table 11 DEM characteristics per data-take include GCP and CP errors, the mean vertical error and the standard deviation of the CP residuals (all in cm). For an explanation on the use of GCPs and CPs, see text. The mean vertical error quantifies the systematic bias of the DEM, whereas the standard deviation of the CP residuals reflects the random component of the vertical error.

	2016	**2018**	**2022**	**2024**
GCP error (x, y, z in cm)	10.47, 5.05, 12.39	3.44, 5.30, 3.90	1.71, 3.12, 2.81	3.87, 4.80, 4.29
CP error (x, y, z in cm)	19.91, 21.23, 15.93	2.80, 6.55, 3.51	1.53, 1.32, 1.48	4.80, 6.45, 5.33
Mean vert. CP error (cm)	-12.61	0.49	0.42	2.34
σ of CP residuals (cm)	11.25	3.72	1.59	5.53
DEM spatial resolution (cm/px)	11.0	9.51	3.09	2.89

7.1.2. Dos Lenguas vertical surface changes

Annual vertical surface changes range in their majority from 1.5 to -1.5 m with singular values reaching 1.7 m, Figure 11. The overall pattern of vertical differences is similar over the three episodes, depicting ridge-and-furrow morphology displacement. Highest magnitudes for positive and negative vertical surface changes are reached in the central area of the rock glacier surface, followed by the southern tongue. The upper zone and northern tongue, the latter specifically towards the front slope, are characterised by a lower magnitude of vertical changes. A spatially coherent positive change is visible on the southern tongue's front, see the blue area on the rock glacier's front in Figure 11.

Volumetric changes in the upper, centre, northern and southern tongue zones are predominantly negative, Figure 12. This leads to overall negative balances for the rock glacier surface in 5 out of 6 cases. In 3 out of these 5 cases, overall negative volumetric change on the southern tongue is of the highest magnitude compared to the upper, centre, and northern tongue. This pattern is consistent for the 2016-2018, 2018-2022, 2016-2024, 2016-2022 and 2018-2024 time episodes, Figure 12A, B, D-F. When pairing the 2022-2024 datasets, vertical surface changes in all zones on the rock glacier surface are positive, Figure 12C. Volumetric change on the front and side slopes is positive across all time episodes. Given the lower LoD of the 2016 dataset, the results for the 2018-2022, 2022-2024 and 2018-2024 time periods are considered to be more reliable, Figure 12.

7.1.3. Dos Lenguas horizontal surface velocities

Across all time periods (époques, EPs; 2016-2018, 2018-2022, 2022-2024, 2016-2024), the upper zone of Dos Lenguas rock glacier generally is characterised by highest values (1.5 to 2 m/yr), with a slowing trend towards the southern tongue (< 1.5 m/yr), Figure 13. The northern tongue experiences lower values (< 1 m/yr), specifically closer to the centre, in comparison to the upper, centre or southern tongue, with a drastic slow-down traversing from the centre to the northern tongue. Along the entire rock glacier and across all time episodes, the edges on both sides are characterised by lowest velocities. The mean surface velocity for the rock glacier surface without front and side slopes is 0.88 m/yr (2016-2024, LoD ±0.05 m/yr) and mean surface velocities are consistent in time (2016-2018: 0.88 m/yr with an LoD of ±0.18 m/yr, 2018-2022: 0.91 m/yr and ±0.04 m/yr, 2022-2024: 0.91 m/yr and ±0.05 m/yr). Further, the orientation of movement is consistent, with south-east-east (59.1-65.4 %, all EPs) and south-south-east (22.2-27.5 %, all EPs) representing the main directions of the rock glacier. The south-south-east direction is confined to the southern tongue and southern edge of the northern tongue, while the rest of the rock glacier is oriented in south-east-east direction.

Comparing quasi-biennial surface velocities to the 2016-2024 mean surface velocity reveals no significant change, with acceleration and deceleration to seldomly exceed the LoDs of the respective datasets, Figure 14. Detectable are a minimal increase in the upper zone for 2018-2022 (< 0.1 m/yr, Figure 14B) and a minimal increase in velocity in the tongue zone for 2022-2024 (< 0.1 m/yr, Figure 14C). In all cases, the magnitude of velocity change is minor and barely exceeds 0.1 m/yr (Figure 14F-J).

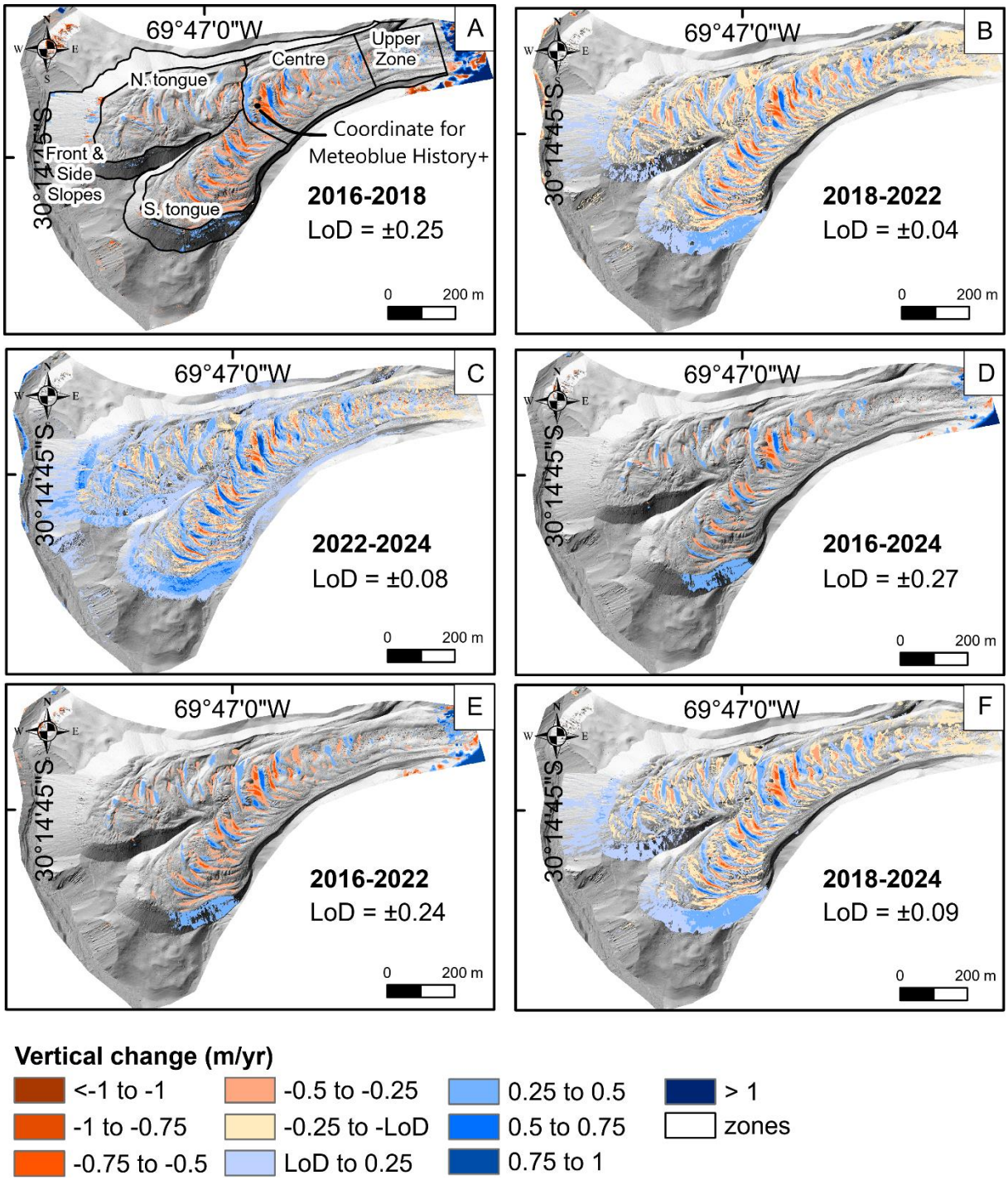

Figure 11 Vertical surface changes (m/yr) on Dos Lenguas rock glacier for the time periods 2016-2018 (A), 2018-2022 (B), 2022-2024 (C), 2016-2024 (D), 2016-2022 (E) and 2018-2024 (F), all normalized to years. UAV-based DEMs are generated at 11 cm resolution and displayed on top of the 2024 hillshade. The colour scheme of the legend is adapted to the respective LoD (m/yr). A) includes the delineation of geomorphological zones as referred to in the text. Vertical changes east of the upper zone (A, D, E) are related to the smaller extent of the 2016 flight compared to the other UAV flight campaigns. Vertical changes west of the rock glacier (B, C) are related to fluvial activity of Agua Negra River, located at the foot of Dos Lenguas rock glacier. Adapted from Paper 2.

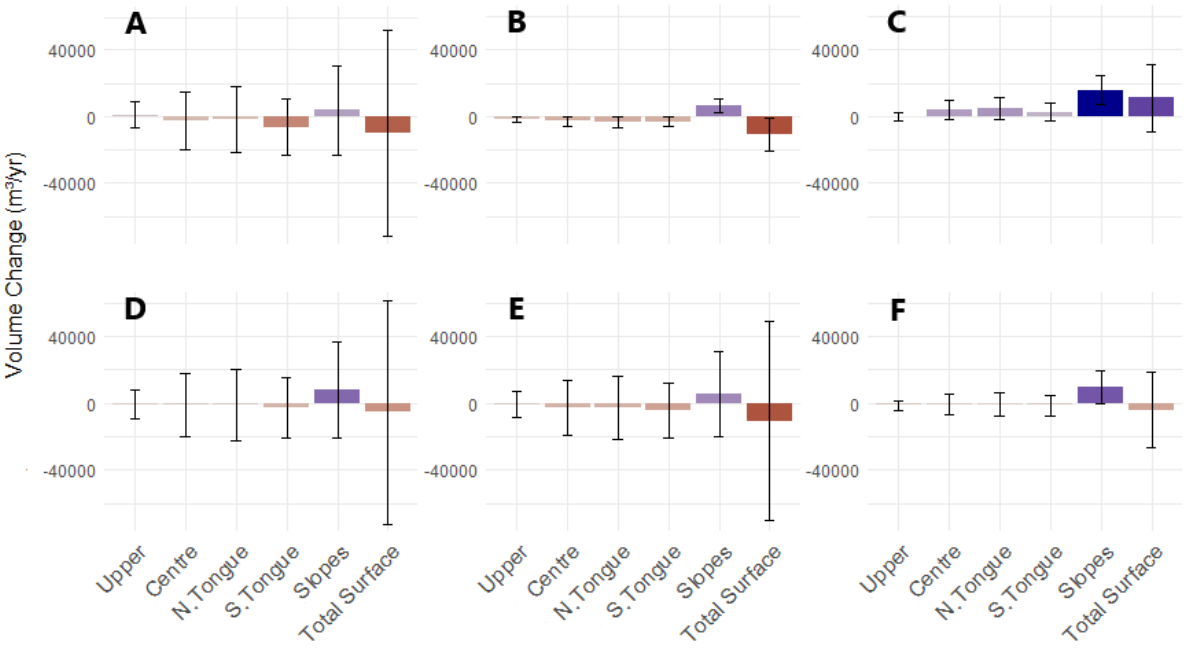

Figure 12 Volumetric changes (m^3/yr) on Dos Lenguas rock glacier for the different geomorphological zones and time periods. Periods are normalized to years and 'total surface' refers to the upper, centre and tongue zones without front and side slopes. Based on UAV imagery generated DEMs at 11 cm resolution. Whiskers indicate range between the minimum and maximum volume change based on the LoD of the respective time period. For the delineation of the geomorphological zones, see Figure 11A. For time episode specific LoDs, see Figure 11.

7.1.4. Surface kinematics and topography

Different magnitudes of horizontal rock glacier surface change are reached depending on their elevation (Figure 15A, B). This pattern is consistent through all time episodes and is independent of the resolution. Highest velocities are reached in the upper zone. At 10 m resolution, a two-grouped pattern of decreasing velocity frequencies is established in the centre of the rock glacier, Figure 15A, B. The velocity group with a lower magnitude merges with the onset of the northern tongue, and the velocity group with a higher magnitude continues to the southern tongue.

Slope decreases from the upper zone to the centre of Dos Lenguas rock glacier, Figure 15C, D. Characterised by lower slope at the beginning, the centre area increases in slope values towards the tongues. Both tongues are characterised by a similar slope at the beginning, with the slope decreasing at the northern tongue while increasing at the southern tongue.

Vertical surface changes reach the highest magnitudes in the centre area of the rock glacier, followed by the southern tongue, Figure 15E, F. Vertical surface changes on the northern tongue are of a lesser magnitude than on the southern tongue, while vertical surface change in the upper zone being of lowest magnitude. Maximum vertical surface changes, both centre and southern tongue, occur at velocities of more than 1 m/yr and less than 1.25 m/yr, vertical changes in areas with velocities below 1 m/yr or above 1.5 m/yr rarely exceed ±0.25 m/yr, Figure 15G, H.

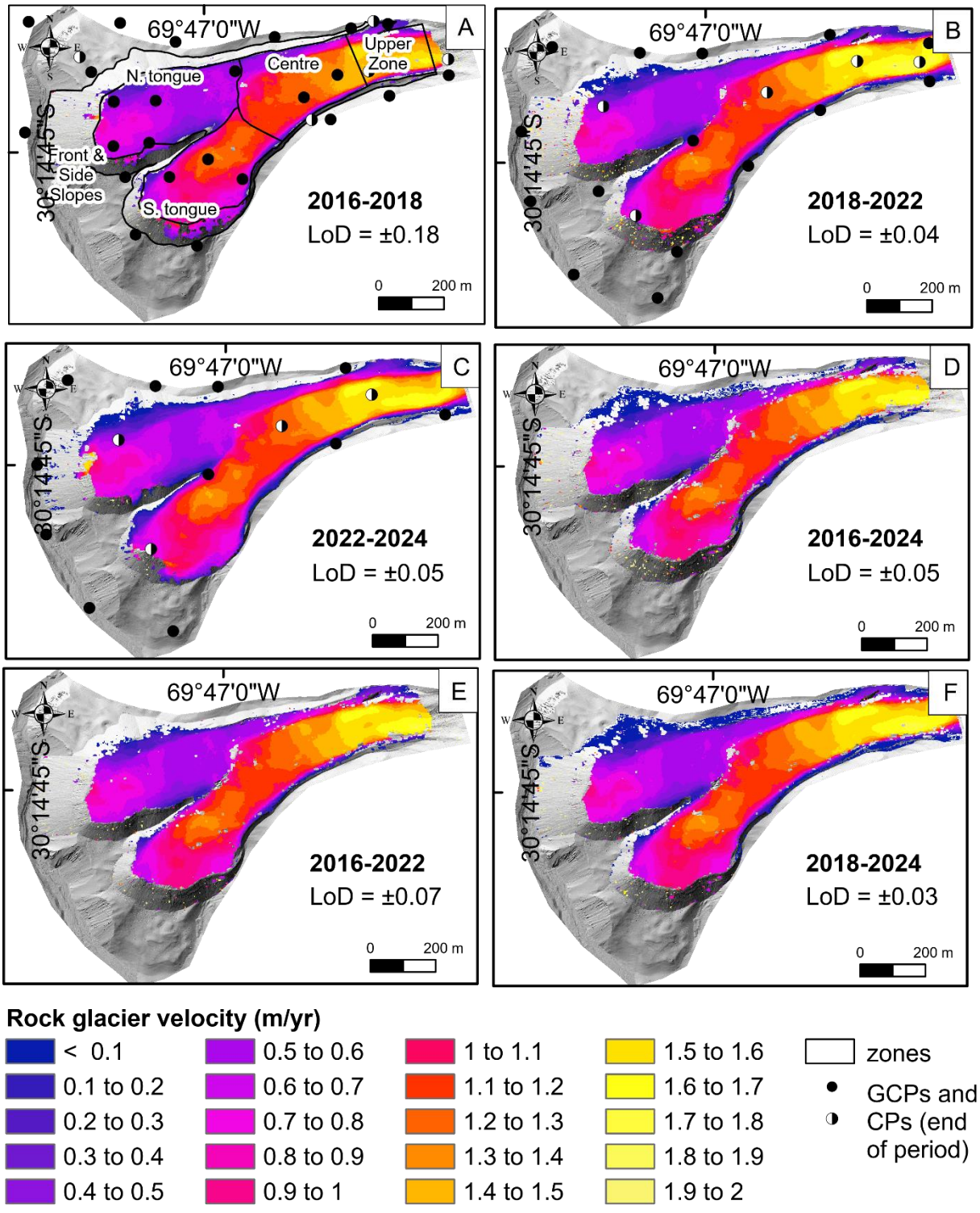

Figure 13 Surface velocities (m/yr) on Dos Lenguas rock glacier with 2 m resolution, based on feature tracking on UAV-based hillshades at 25 cm resolution. Time periods are 2016-2018 (A), 2018-2022 (B), 2022-2024 (C), 2016-2024 (D), 2016-2022 (E), and 2018-2024 (F). Surface velocities are displayed on top of the 2024 hillshade. LoDs are provided in m/yr. A), B) and C) further include the locations of DGNSS measured GCPs and CPs for the end of the period, e.g., for 2018 in A).

*Figure 14 (**next page**) Acceleration and deceleration of annual surface velocities (m/yr) on Dos Lenguas rock glacier for episodes 2016-2018 (A, F), 2018-2022 (B, G), 2022-2024 (C, H), 2016-2022 (D, I), and 2018-2024 (E, J), all normalized to years and compared to the 2016-2024 mean. LoDs are propagated by summing the squares of the individual LoDs (cf. Figure 13) and taking the square root of the result. A-E: displayed with 2 m resolution on top of the 2024 hillshade. Values within LoDs are not visualized. F-J: values correspond to velocity change on the rock glacier surface only (no front and side slopes). LoDs are indicated with grey boxes.*

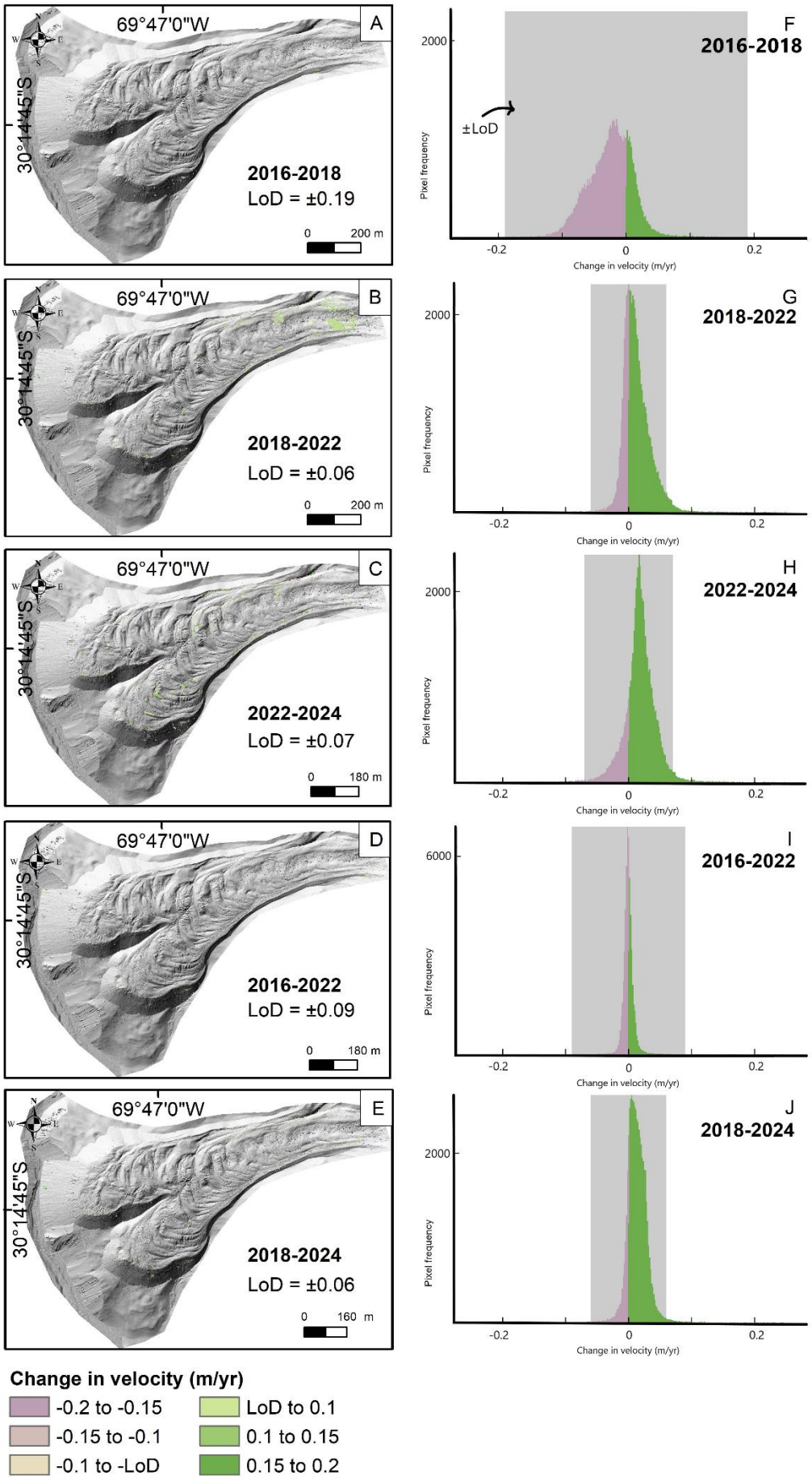

For the figure caption, see previous page.

Correlation coefficients (Pearson) calculated for upper-centre-northern (zone A) tongue and upper-centre-southern (zone B) tongue for all resolutions (2 m, 5 m, 10 m) and time episodes show strongest positive correlations between elevation and horizontal surface change (A: 0.62 to 0.71; B: 0.36 to 0.47), Figure 15. Highest values for zone A are reached for the 2016-2024 and 2016-2018 time episodes. For zone B, the correlation remains stable across time. For both zones, higher resolutions (2 m, 5 m) produce higher correlation coefficients. We find a weak but persistent positive correlation between vertical surface change and slope (A: 0.40 to 0.53; B: 0.40 to 0.55), consistent in time and increasing with higher resolutions. We find a weak negative correlation between vertical surface change and curvature at 5 m, and partially at 10 m resolution (A: -0.13 to -0.35; B: -0.11 to -0.43), stable through time.

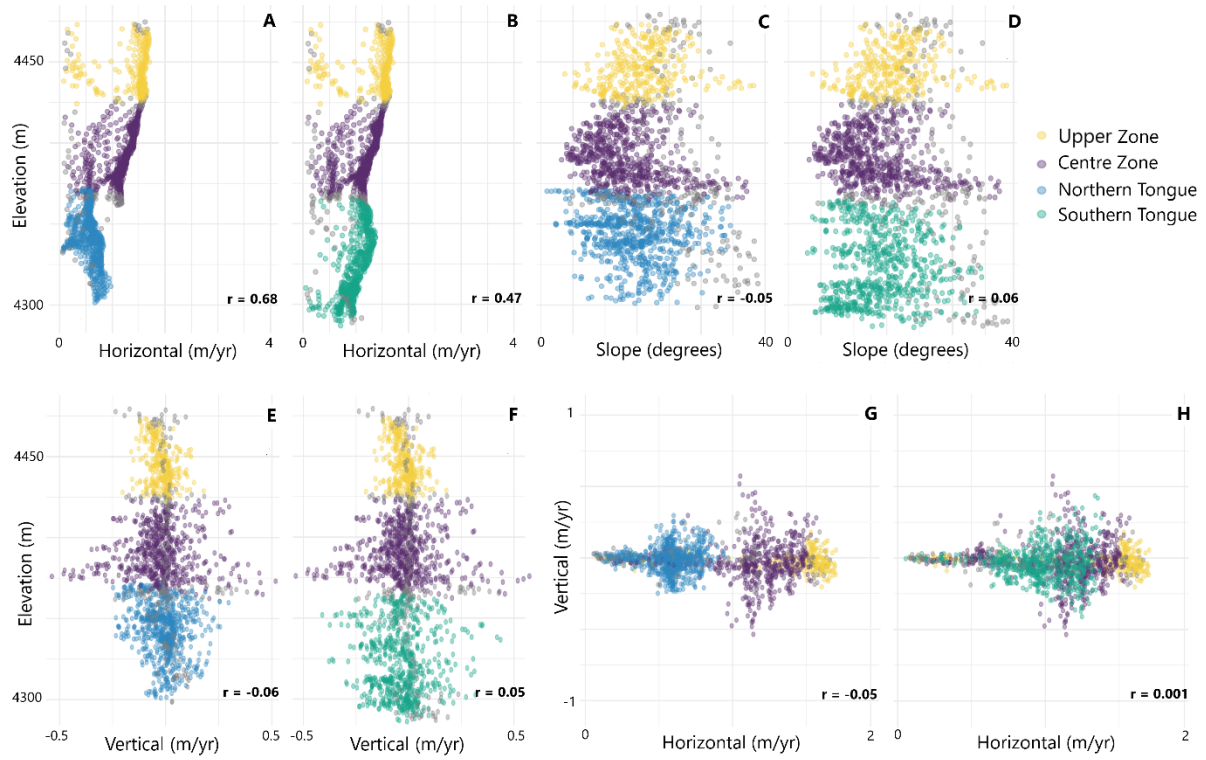

Figure 15 Dos Lenguas rock glacier kinematics and their concurrence with topographic characteristics based on 2016-2024 data at 10 m spatial resolution. For each pair, the upper and centre zones show the same data, with alteration for the northern tongue (A, C, E, G) and the southern tongue (B, D, F, H). See Figure 11A for a delineation of the geomorphological zones.

7.1.5. Climatological records

ERA5 air temperature provided through meteoblue history+ constantly falls below the temperature data measured data in front of Dos Lenguas for the same time period (February 14th 2022 to February 7th 2023), Figure 16. This deviation is larger for the austral winter months in comparison to the austral summer months. Air temperature evolution since 1940, based on the ERA5 data, shows a clear warming trend for the last decades, Figure 16B. Both austral summer and austral winter temperatures fall below their 1940-2024 mean in the 90s. While austral summer temperatures have exceeded this mean since the early 2000s, the onset of winter temperatures exceeding their mean in 2017 coincides almost with the UAV monitoring period (2016-2024, grey box). Historical ERA5 precipitation in the austral summer months is less compared to the winter months, Figure 16C-D. This is independent of precipitation occurring as rain or snow.

Based on the visible inspection of repeated optical photos, we find that snow cover is present on 14 out of 377 days at the location close to Dos Lenguas rock glacier. It does not last for more than three consecutive days (June 20th 2023 to June 23rd 2023, August 19th 2023 to August 21st 2023). Snow height at this location does not exceed 10 cm, estimated based on poles. The camera located in the upper catchment shows snow on 147 out of 386 days whereby on 104 of these days snow is present as single patches, often located at the western slope only. Similar to the UAV imagery, these photos are available in the accompanying dataset publication (Stammler et al. 2025b).

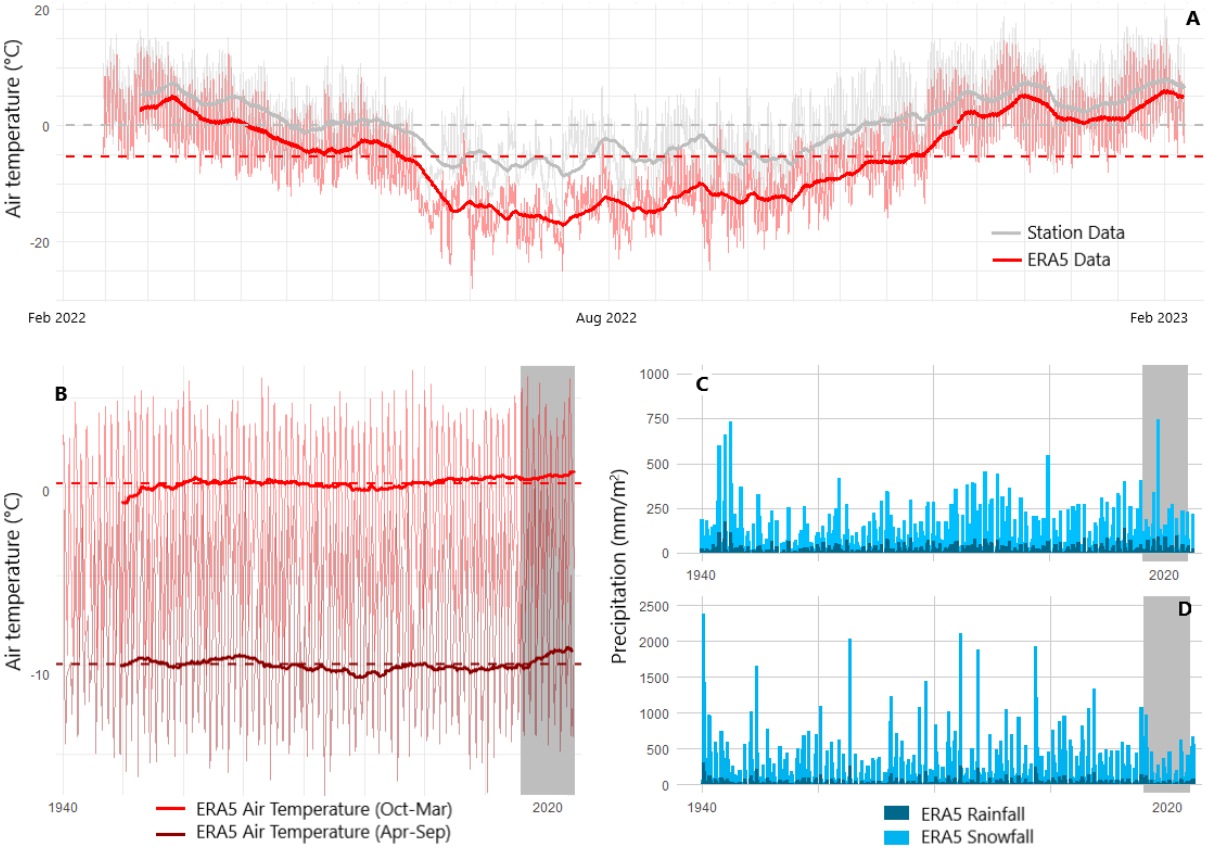

Figure 16 Air temperature and precipitation at Dos Lenguas rock glacier. Comparison of hourly ERA5 air temperature data provided through meteoblue history+ (red) to hourly measured air temperature (grey) for February 14th 2022 to February 7th 2023 (A). Dashed lines show mean colour-coded for the different datasets. Monthly ERA5 air temperature evolution over time for the October to March period (red) and April to September period (dark red) displayed as 5 year mean (solid lines) and mean temperature (dashed lines) (B). Monthly ERA5 precipitation as rainfall (dark blue) and snowfall (bright blue) for Dos Lenguas in the austral summer months (C) and the austral winter months (D). The grey boxes correspond to the time period of the UAV-based monitoring.

7.2. Discussion

7.2.1. Data quality

The error of the DEMs to the DGNSS measurements used as CPs is < 10 cm for the 2018, 2022 and 2024 DEMs, Table 11. It is higher for the 2016 dataset, coinciding with the highest GCP error and lowest resolution, Table 11. In comparison to the spatial resolution of the DEMs, the GCP and CP errors for the 2018–-2024 DEMs fall below 1 pixel. Solely the 2016 GCP error (x, z) and the 2016 CP errors range between 1 to 2 pixels. A difference between the 2016-2018 DEM quality compared to the other DEMs is expected given the variability in ground sampling distance in the 2016-2018 datasets and the poorer performance capability of the Phantom 3 Advanced to the Phantom 4 RTK in terms of, e.g., pixel depth, impact of the shutter mechanism on image quality and capability of the sensors to resolve nuances, cf. Table 3. The differences in DEM quality between the 2016 and 2018 DEMs are attributed to the few images used for the 2016 DEM generation, resulting in a lower point cloud density in combination with the error introduced by using DGNSS measurements from 2017. The measurement error is comparable for all DGNSS measurements, Table 5. Error between the 2016 selected DGNSS points measured in 2017, compared to the 2018 DGNSS points, increases total error. Testing data robustness by plotting the 2016-2022 and 2016-2024 intervals and confirmation of the comparatively low error of the 2017 measurements are, thus, essential.

When assessing the bias and the random component of the vertical CP-based errors, we find that for the 2018 and 2022 acquisitions, the bias is negligible compared to the random component, Table 11. For the 2024 acquisition, the bias is higher than for the other datasets but remains smaller than 50 % of the random component, indicating a small positive offset. Likely, this impacts the, compared to the other time episodes, slightly more positive vertical surface change in 2022-2024 leading to positive volume changes, Figure 12C. In contrast, the 2016 dataset exhibits a bias that exceeds the random error, suggesting a systematic vertical offset in the DEM. This systematic error in the 2016 dataset prevents the direct application of the error propagation formula by Brasington et al. (2003) and Wheaton et al. (2010), which assumes that DEM errors are dominated by random components with negligible bias. This systematic error in the 2016 dataset limits the quality of change detection for time periods involving this DEM. We account for the systematic error by addressing the bias in the LoD calculation, cf. Equation 4, and decide for an application of the adapted error propagation for the calculation of all DoD LoDs. As expected, the effect is almost minimal for the 2018-2022 DoD, slightly increased for DoDs involving the 2024 DEM and strongly increased for DoDs involving the 2016 DEM. The lower data quality of the 2016 datasets further leads to high uncertainty in volume calculation for time periods involving the 2016 acquisition, Figure 12A, D-E. We consider the results involving the 2016 to be reliable, given their similarities in spatial pattern and magnitude to the 2018-2022 dataset.

For all time episodes, quantified vertical and horizontal surface change is restricted to the rock glacier surface, sides and front. Otherwise, expected geomorphologically stable areas exhibit surface change below our LoDs, vertically and horizontally, Figure 11 and Figure 13. This is supported by the DGNSS points measured outside the rock glacier surface indicating high stability across all time periods (< 0.1 m/yr), cf. Figure 13A-C.

The defined 90 % percentile as LoD during feature tracking results in comparatively low LoDs in comparison to the magnitude of horizontal surface changes, Figure 13. DEM error propagates to feature tracking via hillshade generation and is accounted for by testing for stable terrain outside of the rock glacier surface during feature tracking.

7.2.2. Dos Lenguas velocities: stable in time and in agreement with published data

In Dos Lenguas rock glacier's upper zone, debris moves rapidly without compressional flow, conveying debris and potentially ice to the lower zones (Halla et al. 2021), Figure 13. In the centre of the Dos Lenguas rock glacier, compressional flow and the development of ridges and furrows increases along with a slight decrease in overall velocities. Movement in the southern half of the upper and centre zone is already faster than in the northern half, at a magnitude much smaller than after tongue separation, Figure 13 and Figure 15A, B. The main horizontal movement follows a 'streamline' from the upper to the southern tongue, with almost non-moving areas towards the edges of the rock glacier.

With our processing of the 2016 and 2018 UAV imagery, we reproduce the maximum surface velocities by Halla et al. (2021) in magnitude and pattern. In addition, we show that mean surface velocities of 0.9 m/yr, Figure 13, with maximum values of 1.7 m/yr in the upper zone, Figure 15, are consistent in time for all additional time episodes investigated in this study. Our velocities are in agreement with Strozzi et al. (2020) that quantify surface velocities for a location within Dos Lenguas upper zone ranging from 1.5 to 2 m/yr based on InSAR and offset tracking for 2015-2020, particularly when focusing on the more active areas, cf. Figure 13 and Figure 15B.

Robson et al. (2022) detect an average velocity of 0.54 ± 0.03 m/yr for rock glaciers in the La Laguna catchment (2012-2020), the neighbouring catchment on the Chilean side of the Andes, next to highlighting several rock glaciers with velocities of approximately 0.9 m/yr. While further detailed comparison is necessary, this highlights a potential for horizontal rock glacier surface change occurring with a similar magnitude on both slopes of the Andes.

With our UAV-based investigation, we detect stable surface velocity conditions on Dos Lenguas rock glacier for the time period 2016-2024 at 2 m resolution and with LoDs being low compared to the magnitude of the velocities. We find no deceleration outside our LoDs (±0.06 to ±0.19 m/yr for any of the time periods (2016-2018, 2018-2022, 2022-2024, 2016-2022, 2018-2024) and only two time periods where acceleration exceeds the LoDs of the respective time periods, but remains below 0.1 m/yr, Figure 14. This is in agreement with Blöthe et al. (2024) that find unchanged rock glacier velocities for 175 investigated rock glaciers in the Valles Calchaquíes region (Argentina) within three time episodes between 1986 and 2023 (1968-2009, 2009-2020, 2020-2023) based on optical feature tracking on historical aerial photographs, ALOS PRISM and CBERS-4A imagery.

We expect a future disconnection of the northern tongue kinematics from the rest of the rock glacier. As Halla et al. (2021) postulate an increase of ice volume for the northern tongue for 2016-2018, we argue that the decrease of velocity of the northern tongue is due to flow divergence and reduction of material through-put, coupled with a topographical effect, without a necessary decrease of ice content – as supported by the pattern and magnitude of vertical

changes being stable in time. Halla et al. (2021) assume more massive ice in the upper zone and more spatially disconnected ice in the rock glacier centre and tongues based on geophysics and four-phase modelling. We encourage repeated geophysical investigation and a thorough investigation of the coincidence of ice content and surface kinematic characteristics for an investigation of their correlation.

Hartl et al. (2023) find localized velocity increase as starting point of rock glacier destabilization on the Äußeres Hochebenkar rock glacier in the Austrian Alps. Velocities on the northern tongue of Dos Lenguas rock glacier increase towards the front, consistent across all time episodes, Figure 12. While these values are not comparable in magnitude to Hartl et al. (2023) at the moment, potential future velocity increase at the front of Dos Lenguas northern tongue including possible front failure represent great hazard potential, as a collapsed front could dam the Agua Negra River, located right next to the Dos Lenguas' front, causing potential for a consequent outburst flood and highlighting the importance of continued high-resolution monitoring.

7.2.3. Dos Lenguas vertical change: heterogeneous with predominantly negative volumetric change

The impact of the ridge and furrow system on Dos Lenguas' vertical surface change is apparent across all time episodes, Figure 11. We refrain from mean values given this heterogeneity of the vertical change distribution in space. We experience a general trend of vertical change magnitude increase in Dos Lenguas rock glacier's centre, likely related to increased compressive flow leading to the formation of higher ridges. Slope values on Dos Lenguas are high in the upper zone, lower in the centre and increase again towards the tongues, specifically the southern tongue, Figure 15C, D. We anticipate the decrease in slope in the centre to represent a knickpoint which leads to a lowering of volume through-put, resulting in high furrows and ridges, explaining the weak positive correlation between vertical change and slope. Vertical changes on the southern tongue are much higher than on the northern tongue. We relate this to the slope control as described above as well as the magnitude of the main horizontal change streamflow, Figure 13. While the northern tongue's front is characterised by gravitational movements, vertical change on the southern tongue's front indicates forward movement of the tongue, Figure 11. We explain this difference by the spatial pattern of high-magnitude surface velocity that is focused on the upper-centre-southern tongue transect, Figure 13.

Volumetric changes are overall negative for the rock glacier surface for the entire time period, Figure 12D. We interpret this as an imbalance of material input in relation to material through-put, e.g., negative balances for upper and centre zones, Figure 12, the latter visible via the continuous forward movement of the southern tongue, Figure 11. The 2022-2024 dataset strongly differs in terms of volumetric changes, displaying positive volumetric change for all geomorphological zones, Figure 12C. For horizontal surface change of rock glaciers, alternation in time of acceleration and deceleration is reported (Blöthe et al. 2024). Similarly, Vivero and Lambiel (2024) find average net elevation changes on three rock glaciers in the Western Swiss Alps to alternate between positive and negative values. Given the horizontal surface change for 2022-2024 not differing from the other time periods, cf. Figure 13C, with acceleration below 0.1 m/yr and no deceleration present, cf. Figure 14C, an investigation of volumetric change over a longer time period is needed to thoroughly ascertain this behaviour.

7.2.4. Topography: a catalysator for surface change

Slope is heterogeneously present across elevation, Figure 15C-D, with the upper zone and southern tongue being characterised by the highest slopes, and the highest horizontal changes, Figure 15A, B. We can quantify and exemplify at Dos Lenguas that slope acts as an important driver for horizontal rock glacier surface change, in agreement with the definition of rock glaciers by Barsch (1996) and many other studies. This is supported by the overall direction of flow on Dos Lenguas (south-south-east) being in agreement with the overall highest magnitudes of slope as well as the strong positive correlation of the two. In seeming contrast, high slope values at the most western location of the centre zone correspond with the lowest velocities in this unit. We argue that the higher slope values here are not related to the overall topography but to the highest ridges of the Dos Lenguas' ridge-furrow morphology, found at exactly this location.

Next to facilitating gravitational force on the rock glacier mass, knickpoints in slope control the degree of compression on the rock glacier surface. This degree of compression controls the magnitude of vertical change when observed with fixed pixel frames (impact of horizontal flow on vertical change), Figure 13. With compressional flow, vertical changes are highest (both negative and positive) while velocity decreases, Figure 15E-F. The observed weak negative correlation between vertical change and curvature is likely related to higher vertical change occurring on ridges or in furrows and not in the area of transition between both, the area with higher curvature. The correlation coefficients are higher at resolutions of 5 and 10 m, which pick up the pattern of ridges and furrows better, not obscured by, e.g., movement of big boulders.

The differences in behaviour of the tongues (lower magnitude of surface changes on northern tongue with increase in velocity towards the front; higher magnitude of velocities and vertical changes on the southern tongue stable in time) have been discussed as function of different slope and flow diversion by potential impact of bedrock topography (Halla et al. 2021; Schrott 1994). Our data attests to these discussions, cf. Figure 15A, B.

With elevation increase, we generally find higher velocities and correlation coefficients, Figure 15A, B. This pattern is impacted most by the highest velocity values occurring in the upper zone. Correlation is much higher when looking at the upper, centre and northern tongue rather than the upper centre and southern tongue, as velocities on the northern tongue are lower. We expect this behaviour not only to be driven by the high slopes in the upper zone but also by the pull force of the compressed rock glacier mass in the rock glacier centre, supported by the increasing slope values on the southern tongue.

7.2.5. Temperature: a foundation for surface change

For the time period covered by our air temperature measurements, ERA5 air temperature is constantly lower than measured at our climatological station in front of Dos Lenguas rock glacier, particularly in the austral winter, Figure 16A. We attribute this difference to the spatial resolution of the ERA5 data causing areas of an altitude higher than Dos Lenguas, and even higher than the location of our climate station, to impact the dataset. As the change patterns between the ERA5 and measured data are similar, we consider relative change within the historical time period from 1940 to 2024 to resemble real change. For observations of absolute

air temperature changes, we highlight the need for longer periods of *in situ* measured data to ensure correct temperature approximation.

We do see an overall temperature increase with ERA5 austral summer air temperatures exceeding the 1940 to 2024 mean since the 2000s. Historical precipitation (rain and snowfall) for austral summers shows no clear trend, Figure 16C. Austral winter temperatures have continuously exceeded their 1940 to 2024 mean since 2017, coinciding with the monitoring period of our study. Historical precipitation data for austral winters is reduced for the period after 2017. Austral winter precipitation, in general, is higher than austral summer precipitation. The fact that winter precipitation is more affected by change than summer precipitation is in agreement with Rivera et al. (2021) who state that the regional drought from 2000 to 2021 affected the wet season most, in Rivera et al. (2021) describing April-October.

Due to the low precipitation and strong winds in the Dry Andes, snow cover is sparse and consistently scattered as also perceived from daily images, cf. Chapter 5.1.5. With its location on the west-facing slope in the southern hemisphere, snow at the Dos Lenguas site is further exposed to higher sun activity leading to rapid melting. Insolation effects on ground temperature are, hence, not comparable to the Alps, where temperature sheltering by snow cover (Bast et al. 2024), as well as the effect of the absence thereof (Koenig et al. 2025; PERMOS 2023) have been reported. This potentially enables a more direct effect of austral winter temperatures on rock glacier velocities. We hypothesize, that the absence of snow sheltering compensates temperature increase as cold winter temperatures – despite being warmer than before – are able to thoroughly penetrate the rock glacier.

Bast et al. (2024) conclude based on a rock glacier study in the Alps that winters with little snow in combination with dry summers are beneficial for rock glacier deceleration. For Dos Lenguas, warmer and drier austral winters in combination with warmer and generally dry austral summers are beneficial for unchanged velocities, Figure 14, enabling a generally stable state. A monitoring of seasonal kinematics of Dos Lenguas rock glacier potentially offers the opportunity to study the effects of (increasingly) arid conditions on rock glacier kinematics, focusing on the role of liquid water availability.

7.2.6. Surface kinematics on Dos Lenguas: Implications for the regional state of permafrost

Dos Lenguas kinematics imply a stable state of permafrost conditions for the area. This is unexpected given increasing air temperatures in the region (Pitte et al. 2022; Pabón-Caicedo et al. 2020) and an unprecedented decrease of ice surface area and volume in the glacial domain (Pitte et al. 2022). Further, in comparison to findings on region-wide acceleration of rock glacier velocities in the Alps (Kellerer-Pirklbauer et al. 2024; Manchado et al. 2024) and North America (Kääb and Røste 2024).

Stable rock glacier velocities on Dos Lenguas are in coherence with Blöthe et al. (2024) who find unchanged rock glacier velocities for the Valles Calchaguíes region (24°S to 25°S, Argentinean Andes) for 1968-2023. This supports that rock glacier kinematics in the Dry Andes are currently stable in time and behave differently from rock glaciers in other regions of the world. We attribute the stable kinematics to the lack of snow sheltering allowing for winter

temperature penetration and the location at high altitude, with a measured mean air temperature at 0°C, Figure 16A.

Unchanged surface velocities on Dos Lenguas rock glacier elucidate stable permafrost conditions at the location for the observed period in time. This corresponds with Koenig et al. (2025) who find no clear warming indication for ground temperatures in the Andes (27°S to 34°S) based on 53 boreholes at eight locations, spanning a maximum observation period of 9 years between 2006 and 2023. Similar in length of observation to this study, the authors discuss the possibility of short-term temperature fluctuations deviating from long-term trends, highlighting the need for ongoing monitoring efforts.

7.3. Conclusion

Our UAV-based investigation of Dos Lenguas rock glacier kinematics between 2016 and 2024 allows a high spatio-temporal analysis of rock glacier kinematics. The mean rock glacier velocity for the entire Dos Lenguas surface is 0.9 m/yr (2016-2024). Spatially heterogeneous, the highest values of up to 1.7 m/yr are reached in the upper zone, with a decrease in velocity towards the centre and southern tongue. The northern tongue and northern parts of the Dos Lenguas centre are disconnected from the main spatial velocity pattern. We do not see an increase or decrease in surface velocity within the length of our 8-year study period. The majority of vertical surface changes reach ±1.5 m/yr. Highest magnitudes of vertical surface change are reached in Dos Lenguas centre and on the southern tongue.

We use scatterplot analysis and Pearson correlation coefficients to increase our understanding of forces that drive rock glacier kinematics. Analyses between rock glacier kinematics and topographic characteristics reveal a positive correlation of horizontal change and slope, highlighting the effect of gravitational forces. Further, we find the magnitude and pattern of rock glacier kinematics on Dos Lenguas to be strongly related to the location within the rock glacier surface perpendicular to and along with the flow direction (e.g., flow line vs. edges, extensional vs. compressional flow, disconnected northern vs. connected southern tongue). Vertical change and curvature are weakly, negatively correlated – supporting the impact of the ridge and furrow system. To understand the local variability of rock glacier kinematics within the landform, high-resolution UAV data – for both, horizontal and vertical changes - are essential.

We co-analyse Dos Lenguas surface changes over time with ERA5 air temperature and precipitation data to understand the observed kinematics implications for the local state of permafrost. In contrast to other regions in the world, high-resolution monitoring of Dos Lenguas rock glacier for the time period of 8 years (2016-2024) reveals horizontal surface change to be overall consistent in time, along with increasing (winter) temperatures. We attribute the lack of snow sheltering due to extremely dry conditions allowing for the penetration of winter temperatures through the rock glacier body, and the comparatively high-altitude location of Dos Lenguas (4400 m asl), the main control of absent kinematic reaction to climatological change. We highlight the importance of high-resolution monitoring for resolving the magnitude and spatial pattern of rock glacier kinematics with low levels of detection.

Our findings contribute to a better understanding of the state of permafrost in the Agua Negra catchment, next to providing potentially transferable answers to the underlying drivers of rock glacier surface changes. With ongoing air temperature increase in the Dry Andes, a (delayed)

reaction of the now-absent rock glacier kinematic response is expected in the near future. We emphasize the need for longer-term datasets of more than a decade to capture this rock glacier response and encourage an increase in monitoring efforts at this crucial point in time.

8. Glacial decline next to stable permafrost in the Dry Andes? Vertical glacier surface changes and rock glacier kinematics based on Pléiades imagery (Rodeo basin / Argentina, 2019-2025) (Paper 3)

This chapter is based on the submitted manuscript corresponding to the third contribution to this dissertation. It addresses the research questions 1, 2, 3, 4 and 5.

Stammler, M., Blöthe, J., Cusicanqui, D., Ebert, S., Bell, R., Bodin, X. and Schrott, L., 2025. Glacial decline next to stable permafrost in the Dry Andes? Vertical glacier surface changes and rock glacier kinematics based on Pléiades imagery (Rodeo basin / Argentina, 2019-2025). The Cryosphere. Submitted.

How representative are surface changes on Dos Lenguas rock glacier for other rock glaciers in the region? And how do changing rock glacier kinematics compare to surface changes occurring in the glacial domain of Rodeo basin? The submitted manuscript presented in this chapter scales up the surface change analysis to the entire Rodeo basin and to the glacial domain by using Pléiades imagery. It focuses on the investigation of the current state of the cryosphere in Rodeo basin between 2019 and 2025 by analysing vertical surface change on 19 glaciers, three debris-covered glaciers, and 59 rock glaciers, as well as horizontal surface change on, due to data coverage, 47 of the 59 rock glaciers. While our (tri)stereo, panchromatic Pléiades imagery acquisitions are used for the generation and co-registration of Pléiades-based DEMs for vertical change detection on all landforms, feature tracking is conducted directly on projected panchromatic Pléiades imagery for the quantification of rock glacier velocities.

The study increases the knowledge on the high-Andean cryosphere in a changing climate, **addresses the gap of combined and catchment wide studies for the glacial and periglacial domains**, and **contributes to the understanding of the regional solid water storages and state of permafrost in the arid environment of the Dry Andes** at a, given rising air temperatures, crucial moment in time.

The chapter addresses the following research questions:

- Which vertical surface changes can be observed on glaciers and debris-covered glaciers in Rodeo basin and how do these changes compare to vertical surface changes of the rock glaciers in the area?
- Which vertical and horizontal rock glacier surface changes can be observed across the Rodeo basin and what do these changes imply for the local permafrost conditions?
- What are the disadvantages and advantages of a Pléiades-based surface change monitoring of glaciers, debris-covered glaciers and rock glaciers in the Dry Andes?

8.1. Results

8.1.1. Co-registration, DEM differencing and feature tracking accuracies

The area's aridity and extremely limited cloud and vegetation cover yield perfectly suitable conditions for change analysis with remotely sensed optical imagery, such as Pléiades imagery. The summer conditions with very scarce and, if present, non-persistent snow coverage allow for largely uncovered terrain suitable for co-registration. For co-registration, X correction factors are of least magnitude in median through time, while Z correction factors are of highest, Table 12. A comparison of the T, B, and R tiles indicates no consistent pattern of spatial differences in co-registration factors. All correction factors used during co-registration are independent of the landform type.

Vertical surface changes as extracted at 1000 randomly distributed points surrounding the landform polygons are independent of the landform type and time period and correspond to the respective LoD of our vertical surface changes, Table 13. They vary between ±0.1 to ±10 cm/yr when compared as median for all landforms of each landform type (glaciers, debris-covered glaciers, rock glaciers). Vertical change LoDs are lower than the LoDs calculated for horizontal surface changes. Median horizontal surface change at 1000 randomly placed points in vicinity of the rock glacier surfaces range between ±16 and ±61 cm/yr and represent our LoDs for horizontal surface change. The calculated LoDs for horizontal surface change are low for the 2019-2022 and 2023-2024 time periods, compared to 2022-2023 and 2024-2025.

Correlation factors of the residues arising during our feature tracking approach range in median over time for the selected rock glaciers between 0.27 (ID44) and 0.64 (ID39), Table 14. This is representative for all polygons, with the least and highest correlation being 0.12 (ID25) and 0.66 (ID47). In total, 45 of the 57 polygons are characterised by low correlation coefficients of the residues (0 to 0.5), with 12 polygons exceeding a coefficient of 0.5 but none reaching a coefficient of 0.7. In median and independent of the different rock glacier polygons, 2023-2024 is characterised by least correlation of the residues both for the selected rock glaciers (2023-2024: 0.26) as well as all polygons (2023-2024: 0.28). Thus, three out of the four time periods are characterised by low correlation coefficients with one exceeding a coefficient of 0.5 but remaining below 0.6, both for the selection as well as for all polygons.

Table 12 Co-registration corrections in x, y, and z direction based on the approach by Nuth and Kääb (2011) as applied in Demcoreg (Shean et al. 2016). Shown as median of all co-registration factors (m) of the 81 clipped DEMs (number of landforms = 81). Medians (Mdn) per direction and time period are also provided in meter.

	Shift in X			Shift in Y			Shift in Z			Mdn
Tile	T	B	R	T	B	R	T	B	R	
2019-2022	-0.16	0.2	-0.18	0.24	0.23	0.44	1.22	1.04	2.62	0.24
2022-2023	-0.2	-0.08	0.00	-0.08	-0.01	-0.32	0.59	-0.56	-0.90	-0.08
2023-2024	0.26	-0.06	0.20	-0.47	-0.12	0.34	-0.76	0.81	0.58	0.2
2024-2025	0.05	-0.16	-	0.59	0.07	-	0.05	-1.55	-	0.05
Mdn	-0.06	-0.07	0	0.08	0.03	0.34	0.32	0.13	0.58	

Table 13 Vertical surface change (m/yr) on glaciers and debris-covered glaciers as well as vertical and horizontal surface change (m/yr) on rock glaciers shown as medians for all landforms within each category. VCh = Vertical surface change, HCh = Horizontal surface change, n = number of landforms, depending on the spatial extent of the image acquisition. LoDs for vertical and horizontal surface changes are based on the median of surface change at 1000 randomly distributed points in vicinity of the landforms, shown here as medians per landform category. For rock glacier velocities, we consider only surface change exceeding the respective LoD.

	Glaciers			Debris-c. Glaciers			Rock Glaciers					
	VCh	LoD	n	VCh	LoD	n	VCh	LoD	n	HCh	LoD	n
2019-2022	-1.28	±0.01	11	-0.09	±0.08	3	-0.01	±0.03	48	0.28	±0.16	38
2022-2023	-0.20	±0.001	18	0.02	±0.01	3	0.004	±0.003	59	0.64	±0.52	25
2023-2024	-1.50	±0.01	17	-0.22	±0.10	3	-0.01	±0.004	59	0.46	±0.17	28
2024-2025	-0.51	±0.001	17	0.16	±0.02	3	0.07	±0.001	54	0.82	±0.61	33

Table 14 Correlation coefficients for residues arising during the affine transformation of our feature tracking approach on selected rock glaciers. Rock glaciers are selected based on their size and speed (large > 0.1 km², fast > 0.2 m/yr). We treat low correlation coefficients (0 to 0.5) as criterium for a high quality of the feature tracking approach and higher correlation coefficients (0.5 to 1) as a poorer quality of the feature tracking approach.

	Large and fast RG			Small and fast RG			Small and slow RG			Mdn
IDs	ID4	ID5	ID9	ID24	ID40	ID50	ID35	ID39	ID44	
2019-2022	0.64	0.62	0.21	0.79	0.55	0.32	0.44	0.74	0.42	0.55
2022-2023	0.20	0.34	0.45	0.22	0.72	0.11	0.85	0.66	0.80	0.45
2023-2024	0.33	0.02	0.26	0.29	0.12	0.29	0.41	0.08	0.12	0.26
2024-2025	0.51	0.53	0.57	0.53	0.25	0.44	0.29	0.61	0.13	0.51
Mdn	0.42	0.43	0.35	0.41	0.40	0.30	0.42	0.64	0.27	

8.1.2. Pléiades-based vertical surface changes for (debris-covered) glaciers and rock glaciers in the Rodeo Basin

Vertical surface change across the cryospheric landforms in the Rodeo basin is highest in magnitude for glaciers, second highest for debris-covered glaciers and least for rock glaciers – independent of the time period, Figure 17A. Calculated LoDs are very low compared to the vertical surface changes on glaciers, low compared to debris-covered glaciers and vertically dynamic rock glaciers, and high compared to rock glaciers with minimal vertical surface change when calculated as median for the landforms surface, Figure 17 (whiskers) and Table 13.

All glaciers monitored in our study area are characterised by negative vertical surface changes, leading to negative cumulative vertical surface change increasing in magnitude, Figure 17A. This increase in magnitude is not linear over time and is highest for 2023-2024 (-1.50 m/yr, LoD ±0.01 m/yr) and lowest for 2022-2023 (-0.20 m/yr, LoD ±0.001 m/yr), Table 13. Cumulative vertical surface change is of highest magnitude for Agua Negra Glacier (1.09 km², 5012 m asl, 2nd largest glacier in the study area) amounting to a vertical elevation change in median for the glacier surface of -8.99 m for 2019-2025, detected with an LoD of ±0.11 m/yr. Annual vertical surface changes of Agua Negra Glacier are higher than of the largest glacier monitored

with our Pléiades imagery for the full time period (ID71, 1.80 km^2, 5335.5 m asl), Table 15. In general, smaller glaciers are characterised by higher time-normalized median vertical surface change than large glaciers, Figure 17B. Further, vertical surface change is highest in magnitude for glaciers at lower elevations, Figure 17C, and independent of slope, Figure 17D.

Only three debris-covered glaciers are present in the Rodeo basin with median vertical surface changes up to -22 cm/yr, detected with a LoD of ±10 cm, Table 15.

Rock glacier vertical surface change is minimal on Dos Lenguas and El Paso rock glaciers. This is representative for all rock glaciers monitored, Figure 17A and Table 13. Rock glacier vertical surface changes are not correlated with median elevation or slope, Figure 17C-D. However, rock glaciers in the Rodeo basin are characterised by an interannual variability of vertical surface change, with 47 rock glaciers alternating at least once between positive and negative median annual surface change between the observed time episodes (6 always negative, 4 always positive).

Table 15 Vertical surface change (VCh, m/yr) for the two largest glaciers, as median for the three debris-covered glaciers (DC = debris-covered, cf. Table 13, and for two selected rock glaciers (RG). For the location of the landforms, see Figure 5A.

	Agua Negra Glacier		Glacier ID 71		DC Glaciers (median)		Dos Lenguas RG		El Paso RG	
	VCh	LoD	VCh	LoD	VCh	LoD	VCh	LoD	VCh	LoD
2019-2022	-1.51	±0.02	-0.67	±0.04	-0.09	±0.08	-0.08	±0.04	-0.04	±0.03
2022-2023	-0.59	±0.02	-0.09	±0.02	0.02	±0.01	-0.07	±0.09	0.005	±0.01
2023-2024	-1.85	±0.01	-1.13	±0.05	-0.22	±0.10	-0.04	±0.07	0.03	±0.05
2024-2025	-2.4	±0.04	-0.48	±0.01	0.16	±0.02	-0.03	±0.03	-0.07	±0.05

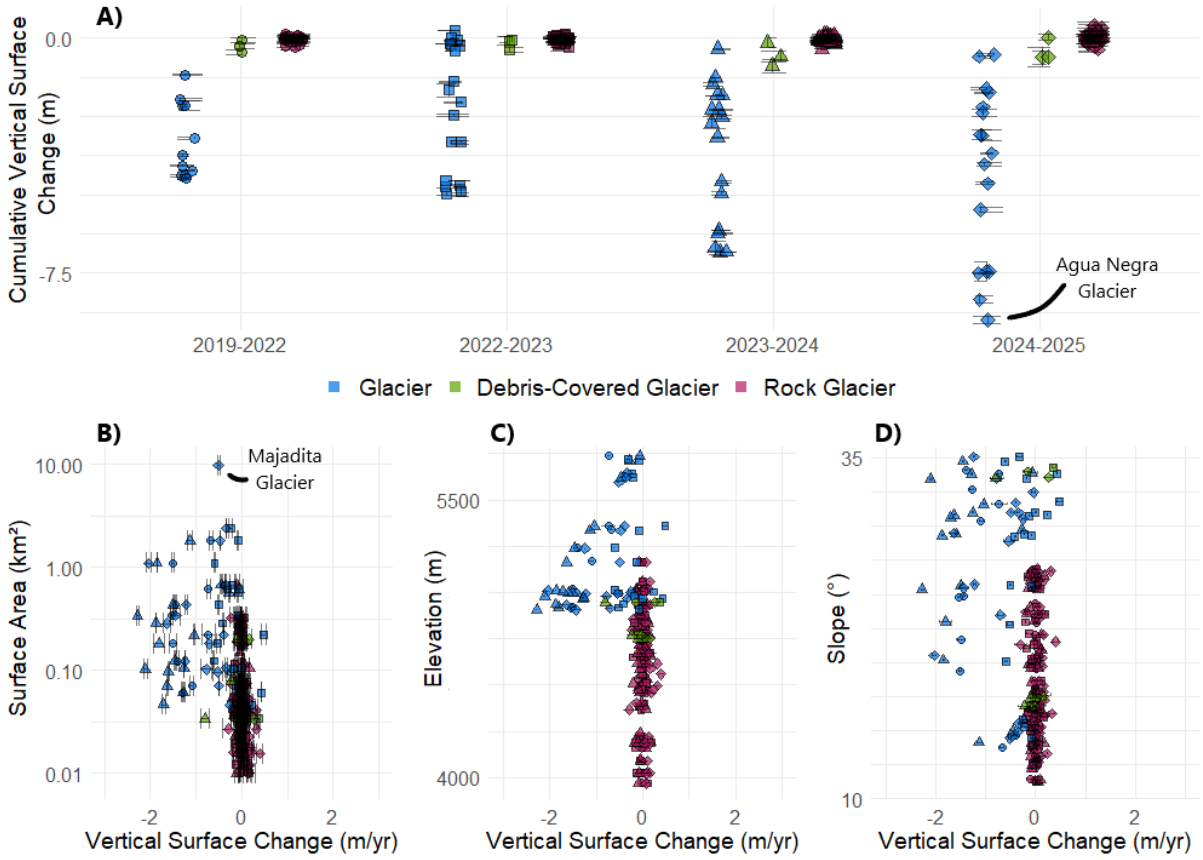

Figure 17 A) Cumulative vertical surface change for glaciers, debris-covered glaciers and rock glaciers for 2019-2025. Calculated as median vertical surface change within the landform surfaces (e.g., no rock glacier fronts) based on DEM differencing between clipped, co-registered Pléiades DEMs. The number of the landforms investigated depends on the extent of the Pléiades acquisitions. Bottom: Median annual vertical surface change normalized to full years and its concurrence with the landform surface area (B), with elevation (C) and slope (D). Elevation and slope are derived from the Pléiades-DEM at the beginning of the time period, e.g., 2019 for the 2019-2022 period. Symbol types correspond to the time periods as introduced in A). For the location of Agua Negra and Majadita Glaciers, see Figure 5A.

Spatially, time-normalized vertical surface changes on Agua Negra Glacier are heterogeneously present with highest magnitudes on its west side and towards the glacier tongue, Figure 18A. Vertical changes on the largest glacier (ID 71) are also heterogeneously present, with highest magnitudes reached in the centre and southern part, Figure 18B. The glacier located next to El Paso rock glacier exhibits vertical surface changes particularly in its centre, Figure 18C. Rock glacier vertical surface changes are spatially heterogeneous and often follow a ridge- and furrow morphology with alternating positive and negative areas, Figure 18D. Rock glacier fronts are characterised by a coherent positive vertical surface change, Figure 18C-D. For vertical surface changes of all monitored cryospheric landforms, see Figure 18E.

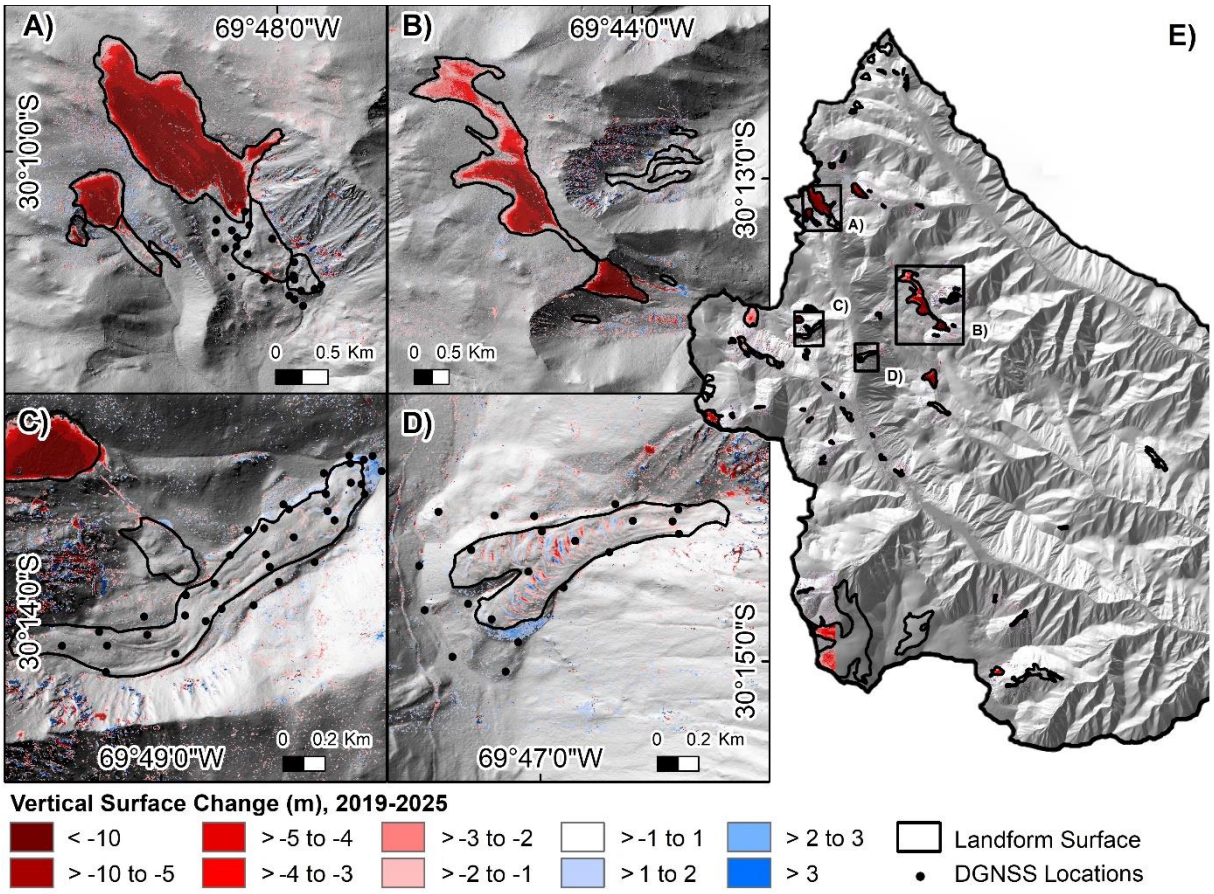

Figure 18 Vertical surface changes (m) between 2019-2025, generated by DEM differencing of co-registered Pléiades DEMs for Agua Negra Glacier and proximate landforms (A), Glacier ID 71 and proximate landforms (B), El Paso rock glacier and proximate landforms (C), and Dos Lenguas rock glacier (D). For all vertical surface change results, including the locations of A) to D), see E). Polygons based on IANIGLA-CONICET (2018). Colour-scale for vertical surface change applies to all subfigures. A), C) and D) include DGNSS locations for repeated measurements, cf. Table 5.

8.1.3. Pléiades-based rock glacier velocities for Rodeo Basin in space and time

Rock glaciers in the Rodeo basin exhibit differences in the magnitude of their horizontal surface change in space with median rock glacier surface velocities being heterogeneously present in the Rodeo basin, Figure 19. Their LoDs are independent of rock glaciers' locations, size and velocity. Out of the 47 rock glaciers, one rock glacier exceeds median velocities of > 1.25 m/yr for the time period 2019-2025 (Dos Lenguas rock glacier), while seven rock glaciers fall between 1 and 1.25 m/yr (e.g., El Paso rock glacier), and 14 fall in the classes between 0.75 to 1 m/yr and 0.5 to 0.75 m/yr, respectively. Median rock glacier surfaces velocities based on all rock glaciers are heterogenous in time, with lowest velocities in 2019-2022 and highest in 2024-2025, Table 13. Increase in velocities is not linear, with the time period 2023-2024 being characterised by second lowest velocities.

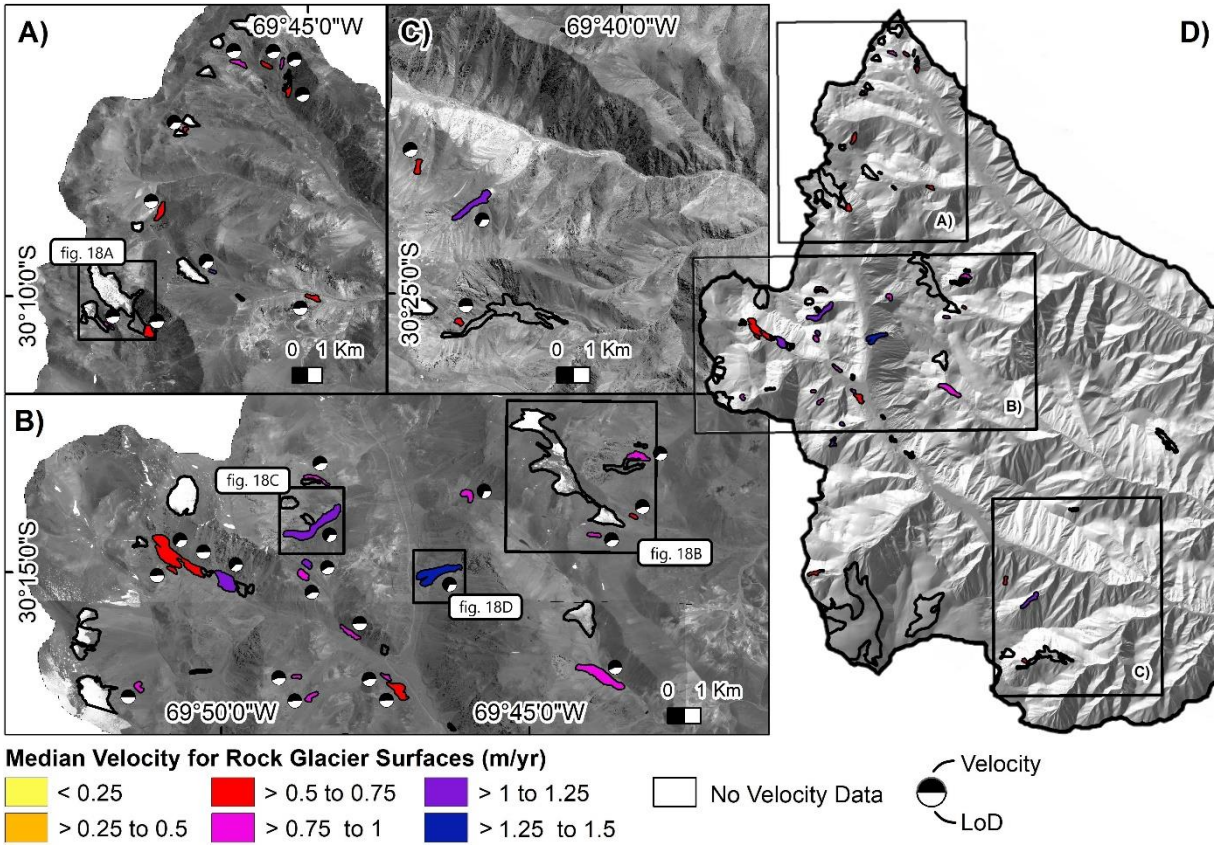

Figure 19 Median velocities (m/yr) for rock glacier surfaces between 2019-2025, categorized and normalized to years. (Peri)glacial landforms as mapped by (IANIGLA-CONICET 2018), portrayed on top of the Pléiades panchromatic orthophotos for 2024 (A-C) and a hillshade based on the 2022 Pléiades imagery (D). Ratios between the velocity (black) and LoD (white) of each landform are provided as pie charts (A-C). For specific location of the rock glaciers, see D. See black boxes referencing to Figure 18 in A) and B). Adapted from Paper 3.

While smaller rock glaciers (< 0.1 km^2) are characterised by various velocities from 0.0 to 1.23 m/yr, larger rock glaciers (> 0.1 km^2) in their vast majority exhibit velocities above 0.25 m/yr in all time periods, Figure 20A. Rock glaciers located at elevations below 4100 m asl do not exceed velocities of 0.25 m/yr, while all rock glaciers located above 4300 m asl exceed velocities of 0.09 m/yr and reach up to 1.38 m/yr, Figure 20B. Slope and rock glacier velocity are not correlated, Figure 20C. Variability of median vertical change is dependent on the time period, with 2022-2023 characterised by more negative and 2023-2024 by more positive median vertical surface changes, Figure 20D. We find three rock glacier categories in the Rodeo basin: large and fast, small and fast and small and slow rock glaciers. Large and fast rock glaciers are located at higher elevation, lower slope and are characterised by lower median vertical change. While small and fast rock glaciers are located at higher elevation and variable slope, small and slow rock glaciers are located at variable elevation and slope.

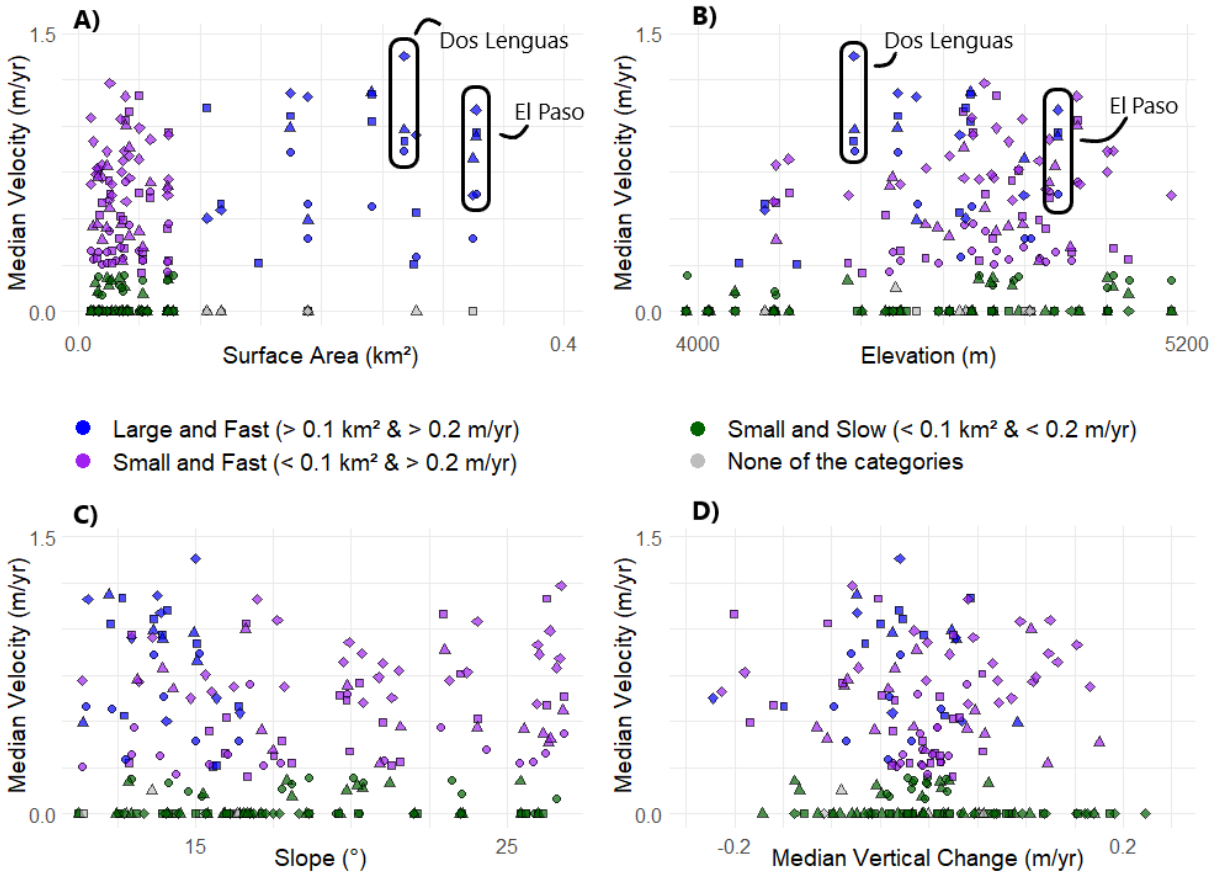

Figure 20 Median velocities for rock glacier surfaces (m/yr) and their concurrence with the rock glacier polygon size (A), median elevation (B), median slope (C) and median vertical surface change (D), all calculated for the rock glacier surfaces. Elevation and slope are calculated for the beginning of each time period, leading to variability in values and to us refraining from marking Dos Lenguas and El Paso rock glaciers in C-D. Time periods are indicated by symbols (cf. Figure 17), and rock glacier categories by colours.

Rock glacier velocities are spatially heterogeneous across the landforms, Figure 20. El Paso rock glacier (ID 5) is in its upper part characterised by linear ridges in line with the flow direction that exhibit a faster velocity than the surrounding rock glacier surface, Figure 20A. Highest velocities of up to 1.09 m/yr (2024-2025, LoD ±0.54 m/yr), are reached in its lower part. Dos Lenguas rock glacier and rock glacier ID 9 are characterised by extensional flow in the upper area and c-shaped ridge and furrow morphologies oriented perpendicular to the direction of flow, commencing in the centre area, Figure 21B-C. For both, highest velocities of up to 1.38 m/yr (2024-2025, LoD ±0.64 m/yr) and up to 1.17 m/yr (2024-2025, LoD ±0.95 m/yr) are reached in the upper part. The rock glacier with ID 40 is characterised by a lower magnitude increase in velocity in its lower part, particularly after 2024, Figure 21D. Highest magnitudes of velocities correlate with rock glacier size, Figure 21A-C compared to Figure 21D.

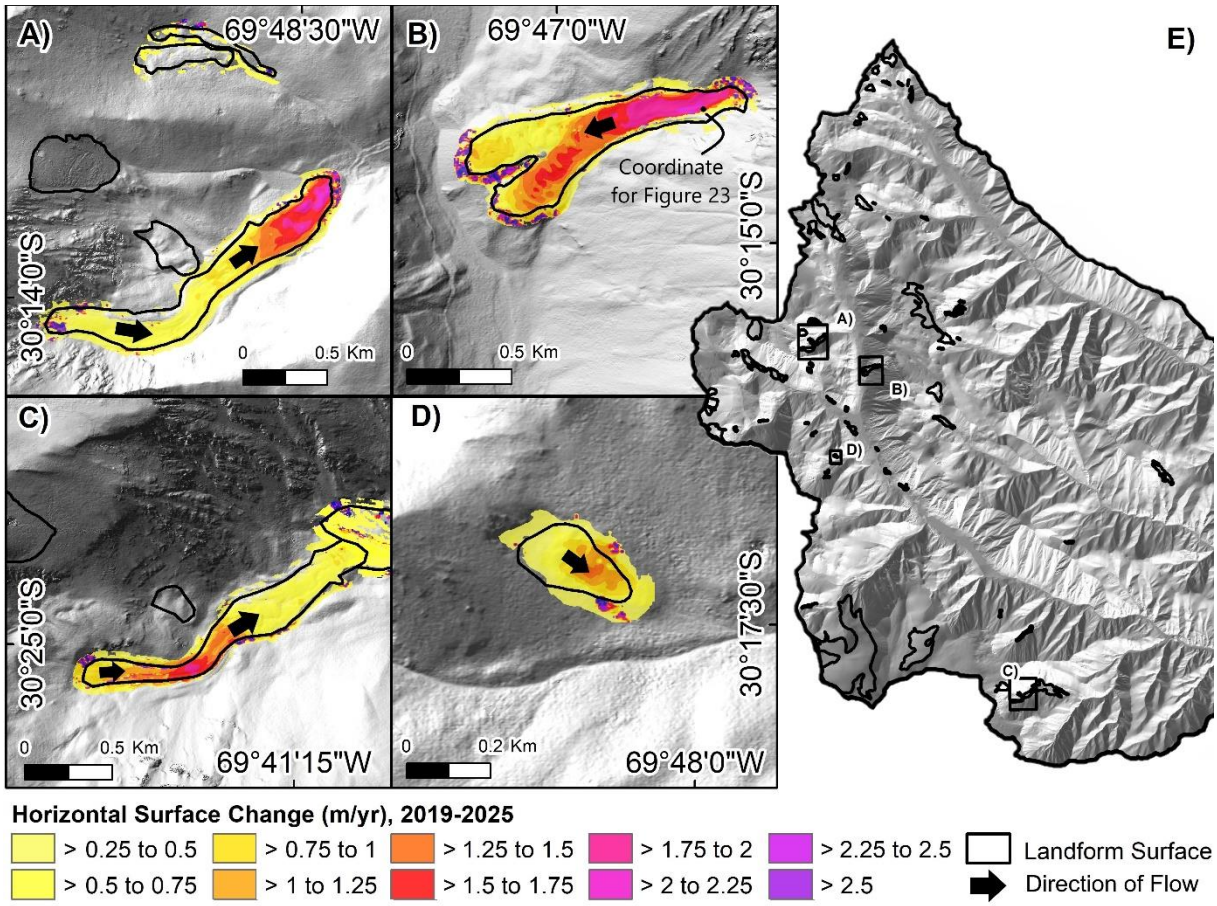

Figure 21 Magnitude and pattern of our Pléiades-based rock glacier surface velocities between 2019-2025 (m/yr) for El Paso (A), and Dos Lenguas (B) rock glaciers, as well as the rock glaciers with the IDs 9 (C), and 40 (D). Median rock glacier velocity generated based on our panchromatic Pléiades imagery and tracked on the landform surfaces with equally, 5 m spaced points. Consequent velocities at 5 m resolution are shown on a hillshade based on the 2022 Pléiades imagery together with the land-form polygons as mapped by IANIGLA-CONICET (2018). Colour-scale for horizontal surface change applies to all subfigures. Adapted from Paper 3.

Table 16 Median horizontal surface change (m/yr) reached on selected rock glaciers, compared to the median value for all rock glacier surface velocities, cf. Table 13.

	All RG surf.		El Paso		Dos Lenguas		ID9		ID40	
	HCh	LoD	HCh	LoD	HCh	LoD	HCh	LoD	HCh	LoD
2019-2022	0.28	±0.16	0.64	±0.22	0.86	±0.15	0.57	±0.23	0.44	±0.06
2022-2023	0.64	±0.52	0.97	±0.54	0.92	±0.54	1.03	±0.52	0.64	±0.37
2023-2024	0.46	±0.17	0.95	±0.50	0.98	±0.36	1.18	±0.56	0.56	±0.16
2024-2025	0.82	±0.61	1.09	±0.54	1.38	±0.64	1.17	±0.95	1.23	±0.65
Size	0.05 km^2		0.33 km^2		0.27 km^2		0.24 km^2		0.02 km^2	

The temporal evolution of rock glacier velocities for the 47 rock glaciers for which we have horizontal surface change data for all time episodes is heterogeneous, Figure 22. Particularly the smaller (< 0.1 km^2) and slower (< 0.2 m/yr) rock glaciers do not show any changes in velocity over time, e.g., IDs 46-48. Within their respective LoDs, some of the faster rock glaciers show stable velocities for 2019 to 2024 and slightly higher velocities in 2024-2025, e.g., IDs 2, 3, 49 and Dos Lenguas rock glacier. Some rock glaciers exhibit alternations between higher velocities in 2022-2023 and 2024-2025 and lower velocities in 2019-2022 and 2023-2024, e.g., IDs 8, 13, 14, 51. Not one single rock glacier is fastest for all time periods but different rock glaciers, with highest magnitudes of 0.86 m/yr in 2019-2022 (LoD ±0.15 m/yr, Dos Lenguas rock glacier), 1.16 m/yr in 2022-2023 (LoD ±0.87 m/yr, ID 23), 1.18 m/yr in 2023-2024 (LoD ±0.56 m/yr, ID 9) and 1.38 m/yr in 2024-2025 (LoD ±0.64 m/yr, Dos Lenguas rock glacier).

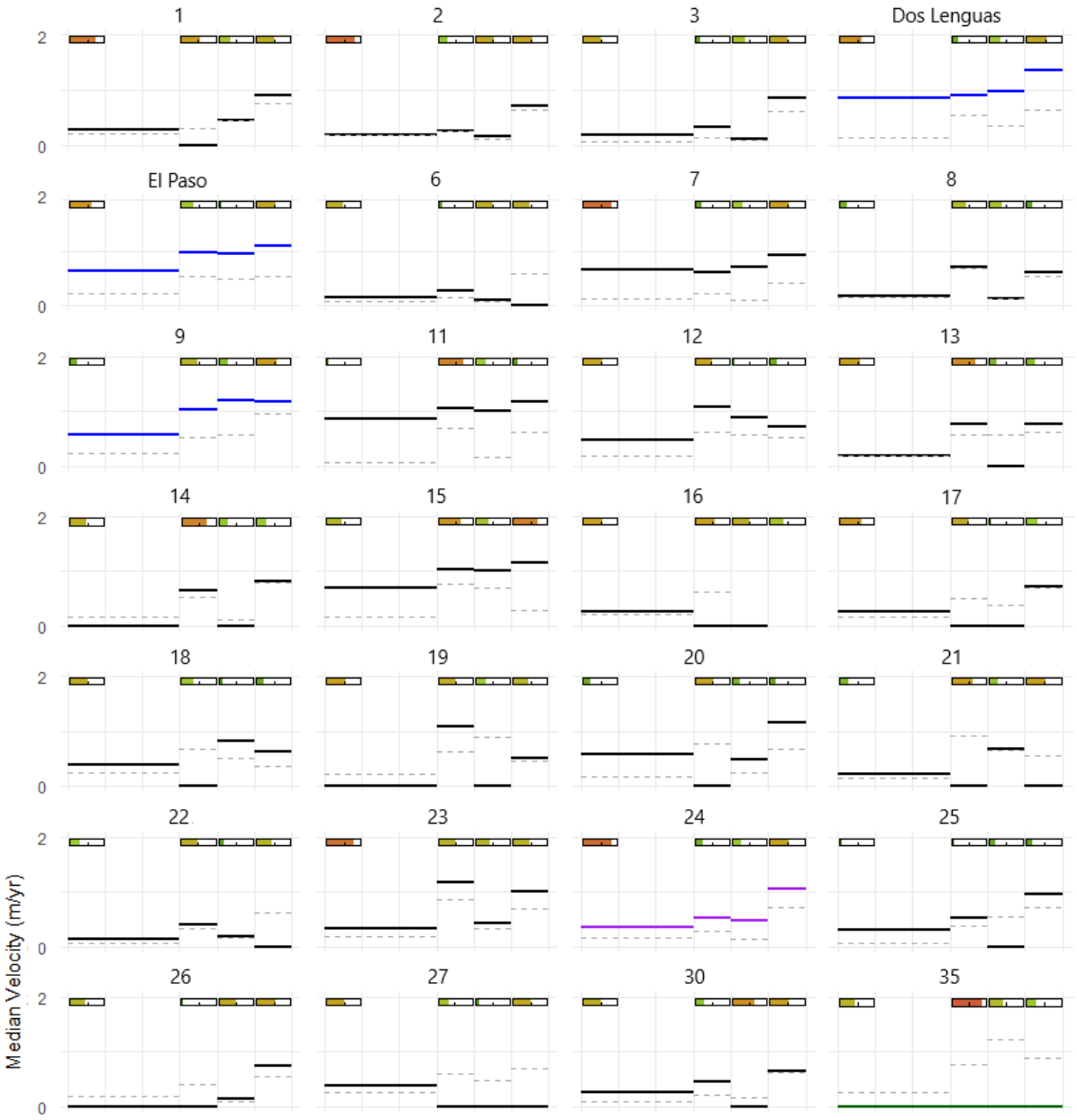

For figure caption, see next page.

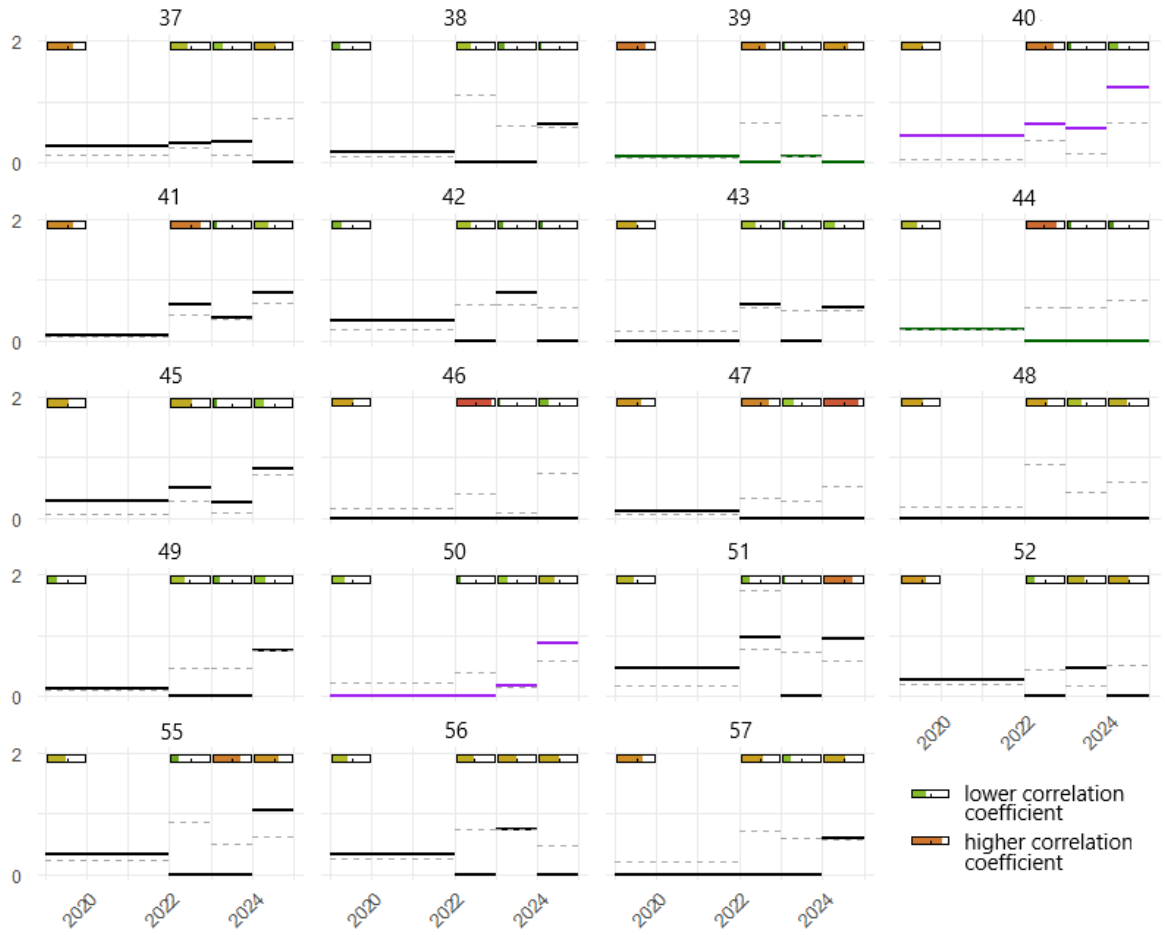

Figure 22 continued Temporal evolution of median rock glacier surface velocities (m/yr) between 2019-2025 based on feature tracking on panchromatic Pléiades imagery (solid lines, colour-coding corresponds to Figure 20). Median rock glacier velocity is calculated for the rock glacier surface based on tracked velocity at 5 m resolution. LoDs are shown as dashed lines. Residue correlation coefficients, our quality control for our feature tracking approach, are included as bars – one each per time period.

8.1.4. Comparison of Pléiades- and DGNSS-based vertical and horizontal surface changes

Our DGNSS vertical errors at all three sites (El Paso and Dos Lenguas rock glaciers and Agua Negra Glacial Forefield) range from 0.008 m to 0.028 m (2022, median 0.019 m), 0.01 m to 0.076 m (2023, median 0.021 m) and 0.009 m to 0.041 m (2024, median 0.022 m). Horizontal errors are lower than vertical errors and range from 0.005 m to 0.017 m (2022, median 0.009 m), 0.006 m to 0.036 m (2023, median 0.012 m), and 0.006 m to 0.018 m (2024, median 0.011 m). With very few exceptions on Dos Lenguas rock glacier (2023), all horizontal errors are below 0.02 m/yr and are comparable between the landforms.

Vertical DGNSS error on El Paso rock glacier is lowest in the upper part, and for the lower part higher in 2024 than in 2023. DGNSS-based vertical surface change measured on the rock glacier surface is positive with 0.16 m/yr (2023-2024; LoD ±0.03 m/yr). Outside the rock glacier surface, DGNSS-based vertical surface change is 0.3 m/yr (2023-2024; LoD ±0.03 m/yr). Pléiades-based vertical surface change on El Paso rock glacier surface deviates in median by -0.02 m (2023-2024) from the DGNSS measurement, representing a difference of less than a pixel. Outside the rock glacier surface, difference in median is higher with -0.32 m (2023-2024). For horizontal surface changes on El Paso rock glacier, DGNSS measurements on the rock glacier

surface are in median 0.66 m/yr (2023-2024, LoD ±0.11 m/yr). Outside the rock glacier surface, they are 0.07 m/yr (2023-2024, LoD ±0.11 m/yr). Given our feature tracking approach for quantifying horizontal surface changes, only DGNSS points within the landform polygon and the 50 m buffer can be compared. Pléiades-based horizontal surface change on El Paso rock glacier deviates in median -0.35 m (2023-2024) from the DGNSS measurements. Outside the rock glacier surface, difference in median is lower with 0.03 m (2023-2024).

On Dos Lenguas rock glacier, vertical errors of the DGNSS measurements are lower in the northern part than in the southern part for 2022 and 2024 and higher for 2023. DGNSS-based vertical surface change is negative at all measured points located on the Dos Lenguas rock glacier surface, and similar in magnitude for both years (2022-2023: -0.19 m/yr, LoD ±0.04 m/yr; 2023-2024: -0.21 m/yr, LoD ±0.04 m/yr). DGNSS-based vertical surface change measured outside the rock glacier are in median 0 m/yr (2022-2023, LoD ±0.03 m/yr) and 0.07 m/yr (2023-2024, LoD ±0.04 m/yr). The difference between extracted Pléiades DoD raster values and DGNSS measurements for time-normalized vertical surface change is 0.08 m (2022-2023) or 0.16 m (2023-2024) on the rock glacier surface and 0.32 m (2022-2023) or -0.47 m (2023-2024) off-surface. DGNSS-based horizontal surface changes on Dos Lenguas rock glacier are in median 0.80 m/yr (2022-2023, LoD ±0.02 m/yr) and 1.14 m/yr (2023-2024, LoD ±0.13 m/yr). Off-surface measurements result in 0.04 m/yr (2022-2023, LoD ±0.04 m/yr) and 0.04 m/yr (2023-2024, LoD ±0.11 m/yr). The difference between the DGNSS and the Pléiades-based velocities is -0.01 m (2022-2023) or 0.11 m (2023-2024) on the rock glacier surface and -0.63 m (2022-2023) or 0.01 m (2023-2024) off-surface.

In the Agua Negra Glacier forefield, vertical errors are highest and more accurate for 2022 and 2023 compared to 2024. The DGNSS measurements indicate vertical and horizontal surface stability with median vertical surface change of 0 m/yr (2022-2023, LoD ±0.02 m/yr) and 0.05 m/yr (2023-2024, LoD ±0.03 m/yr) and median horizontal surface change of 0.04 m/yr (2022-2023, LoD ±0.01 m/yr) and 0.07 m/yr (2023-2024, LoD ±0.01 m/yr). The difference between the Pléiades-based and the DGNSS based surface changes in median is minimal (vertical: 2022-2023, 0.00 m; 2023-2024, -0.18 m; horizontal: 2022-2023, 0.01 m; 2023-2024, -0.07 m).

8.2. Discussion

8.2.1. Co-registration factors, DEM, and vertical and horizontal surface change quality

The offset between the acquired panchromatic Pléiades imagery is highest in z dimension, compared to the x and y dimension, Table 12. Linear co-registration shifts calculated over stable terrain excluding the landform surfaces do not exceed ±0.20 m (x) and ±0.59 m (y), Table 12. They indicate relatively good alignment between the panchromatic Pléiades acquisitions in x and y dimension even prior to our co-registration. Co-registration for the z dimension is of higher importance with correction factors up to -1.55 m (2024-2025, tile B) and 2.62 m (2019-2022, tile R), Table 12, respectively. While our shift in z direction is high compared to the x and y component, it is low compared to Rieg et al. (2018) (offsets x, y, z of 4 m, -3.2 m and 4.8 m, Pléiades-based DEMs in ERDAS IMAGINE) and Beraud et al. (2023) (offsets x, y, z of up to -9.89 m, 7.79 m, 12.40 m, Pléiades-based DEMs in ASP). As expected, our linear shifts

are independent of the targeted location within the catchment, of time, and of the landforms type – supporting the technical nature of the need for co-registration. We do not see a difference in the magnitude of the correction factors needed to co-register the stereo dataset (2019), compared to the tri-stereo datasets (2022-2025). Based on the similarity of the 2019-2022 time period to the other time periods, cf. Figure 17, we conclude the stereo acquisition to be suitable for vertical and horizontal rock glacier surface change monitoring in the Dry Andes. In comparison, Berthier et al. (2014) conclude a moderate effect of the tristereo benefit, including the reduction of the percentage of data voids.

Artefacts or missing values in our DEMs occur in areas with steep slope. These artefacts are not related to our DEM generation but to the Pléiades data-take which includes no data values for these steep slopes due to mismatches during image correlation. In the Rodeo basin and with our processing approach, we do not see generated spikes in the DEMs as described by Ruiz and Bodin (2015). The number of artefacts in our DEMs is very small. This is mainly due to the vegetation-freeness of the study area as well as the SGM algorithm that tend to smooth the surface of the reconstructed DEMs. With a DEM resolution of 1 m, the DEMs used in this study are of higher resolution than used in other studies (e.g., Beraud et al. 2023; Falaschi et al. 2023; 2025; Pitte et al. 2022).

Related to our DEM generation workflow, vertical surface change cannot be monitored on all glaciers. This is due to limited heterogeneity of glacier surface characteristics leading to gaps in the DEMs as the photogrammetric processing fails to generate elevation information for these areas, cf. Figure 18E. According to Berthier et al. (2014), the Pléiades imagery radiometric range (12 bit) limits these effects compared to SPOT1-5 and ASTER. The effect is, however, also encountered by other studies (Beraud et al. 2023; Falaschi et al. 2023).

LoDs calculated as median vertical surface change at 1000 random points in the vicinity of the landforms leads to low LoDs in comparison to the magnitude of vertical surface changes, particularly for glaciers, cf. Table 13. Investigations of vertical surface change of rock glaciers are scarce (Vivero and Lambiel 2024), particularly for studies using Pléiades imagery (Falaschi et al. 2025). Thus, a comparison of our LoD calculation with other studies is extremely limited. For rock glacier velocities, all horizontal surface changes quantified exceed our LoDs calculated as median of 1000 random point in vicinity of the rock glaciers, Figure 21 and Figure 22. Comparatively low LoDs highlight the stability of surfaces assumed to be stable and support the suitability of panchromatic Pléiades imagery for feature tracking.

Residue correlation coefficients, here used as quality control of the feature tracking approach, are in general below 0.5 in median – independent of the respective rock glacier polygon or time period. Their variability between the time periods is higher than between the landforms, highlighting the technical nature of the correlation, cf. Table 14. The analysis of residue correlation characterises the time period 2023-2024 as particularly high in quality, not corresponding to the Pléiades tiles with the least co-registration needed, cf. Table 12. Though not fully portrayed in the residue correlation coefficient, we experience the effect of image distortion to be higher on rock glaciers located on steep slopes compared to locations closer to valley bottoms. This corresponds often with smaller landforms, as larger landforms with their elongated tongues ‘flatten’ the topography by building up bodies of rock and ice – rock glaciers.

While the use of the National Inventory of Glaciers, cf. Chapter 5.1.4, for the landform boundaries allows upscaling our analysis, it restricts the landform surface to a static measure, rather than the surface being adapted for each year. This introduces error on the calculation of median vertical and horizontal surface changes and prevents the potential detection of new landforms. We reduce the impact of the inventory by calculating vertical surface change for bounding boxes with 500 m distance to the landform polygon and with buffered polygon outlines during feature tracking. We highlight the need to display the spatial distribution of surface changes within the landform, cf. Figure 18 and Figure 21, next to the calculated statistics and agree with Ferri et al. (2020) that highlight the effect of the choice of an inventory, e.g., a national versus a global one.

8.2.2. Validation of Pléiades-based surface changes with DGNSS data

Difference of our Pléiades-based vertical change to the vertical change measured with the DGNSS equipment is of lowest magnitude for the stable forefield of Agua Negra Glacier, cf. Figure 18A. Higher difference correlates with a higher magnitude of vertical surface change dynamics at Dos Lenguas and El Paso rock glaciers, cf. Figure 18C-D. However, difference between the DGNSS measurements and the Pléiades-based vertical surface changes is of lower magnitude for the rock glacier surface compared to the DGNSS measurements located off-site the rock glacier surfaces. We hypothesize this difference to be caused by higher vertical accuracies of our DGNSS measurements located at the rock glacier surfaces compared to the surrounding terrain – paired with a very dynamic off-surface environment for El Paso rock glacier, cf. Figure 18C. Further, we hypothesize the higher accuracies of the DGNSS measurements on the rock glacier surfaces compared to their surroundings to stem from the elevated location on the surface allowing for a good connection between the DGNSS base and rover, compared to the off-surface DGNSS measurement locations partially obscured by the rock glacier body. Similar to the comparison of DGNSS- and Pléiades-derived vertical surface changes, difference between the DGNSS- and Pléiades-derived horizontal surface changes is smallest for the Agua Negra Glacier forefield. Despite low in general (all < 1 pixel), it is highest for El Paso rock glacier (-0.35 m, 2023-2024). At Dos Lenguas rock glacier, we encounter very little difference between DGNSS-based velocities and our Pléiades approach for the rock glacier surface (-0.01 m, 2022-2023 and 0.11 m, 2023-2024).

8.2.3. Vertical surface change of (debris-covered) glaciers in the Rodeo Basin

For our vertical surface changes, we find the time period 2022-2023 to contrast with rather low, partially even positive glacier vertical surface changes compared to the other time periods, cf. Table 13 and Figure 17A. Using the panchromatic Pleiades imagery, we can confirm partial snow cover in the surrounding of the majority of glaciers. The 2019, 2024 and 2025 Pléiades acquisitions are not impacted by snow, as expected in the arid study area.

Pitte et al. (2022) calculate mass balances ranging between -0.79 m w. e. (2014-2025, cumulative for entire glaciological year) and -3.67 m w.e. (2020-2021, see before) for Agua Negra Glacier based on the glaciological method (Cogley et al. 2011). Their annually repeated measurements are all negative and increase in time with one exception (2016-2017), indicating accelerated downwasting as in agreement with Dussaillant et al. (2019), Ferri et al. (2020), and Masiokas et al. (2020). Based on DEM differencing using, among others, Pléiades-based DEMs, Pitte et al. (2022) report a generalized thinning with high magnitudes at lower elevations

which we can attest with our data, cf. Figure 18A. Pitte et al. (2022) present vertical surface changes of ca. 1 m/yr between 2013-2019 in the Agua Negra centre and upper parts and changes of ca. 2 m/yr between 2013-2019 in the lower and western parts. This corresponds in magnitude with our vertical change results for Agua Negra Glacier as well as in pattern, Table 13 and Figure 18A. Pitte et al. (2022) further report a 23 % reduction of the Agua Negra surface area between 1959 to 2019. While not part of this study we highlight the suitability of panchromatic and even multispectral Pléiades imagery to continue the assessment of surface area changes using our Pléiades acquisitions, cf. Table 4.

Ayala et al. (2025) estimate a 35 % area loss of the debris-free area of Tapado glacier between 1956-2024 located in the neighbouring catchment in Chile – elucidating a similarity of glacier response on both sides of the Andes while in contrast, observing an increase of the debris-covered area of Tapado glacier which reduces comparability to Agua Negra glacier that does not have a debris-covered part.

The glacier we refer to with ID 71 as mapped by (IANIGLA-CONICET 2018), cf. Figure 18B, is split in two WGMS glacier IDs (32927, 32920). Based on geodetic method, its mean annual elevation change is attributed values ranging from -0.2 m/yr (2000-2012) to -0.5 m/yr(2009-2014) for the first WGMS ID and predominantly around -0.4 m/yr for different measurement periods between 1999 and 2019 for the second (Braun et al. 2019; Dussaillant et al. 2019; Hugonnet et al. 2021). This contrasts with our Pléiades-based quantification of surface changes, Table 15, and strongly highlights the effect of glacier surface delineation as also discussed by, e.g., by Ferri et al. (2020).

Our Pléiades-based vertical surface changes reveal glaciers at higher elevation and of larger size to be less prone to surface lowering, cf. Figure 17B-C. This is in agreement with the temperature gradient and Al-Yaari et al. (2023) that find small glaciers to be affected by more pronounced loss – supporting the suitability of our approach. We refrain from calculating glacier mass balances given our limited *in situ* knowledge on glacier ice density.

As expected, given their higher ice content compared to rock glaciers, vertical surface change is higher on the debris-covered glaciers in the Rodeo basin compared to the rock glaciers, Figure 17A. This is in agreement with Ferri et al. (2020) that find mass balances of higher magnitude for debris-covered glaciers compared to rock glaciers based on the ASTERIX method (Dussaillant et al. 2019) in the Central Andes (30°S to 37°S). For this study, however, we highlight that the three debris-covered glaciers are too little in number to draw representative conclusions upon their vertical surface change behaviour – particularly on detailed ablation patterns or the development of supraglacial ponds or ice cliffs as conducted, e.g., in Ayala et al. (2025) and Falaschi et al. (2021). Ayala et al. (2016) find similar streamflow contributions of debris-covered glaciers compared to glaciers, highlighting their hydrological significance. This significance contrasts with a strong underrepresentation of studies on debris-covered glaciers in glaciological studies (Masiokas et al. 2020).

Ferri et al. (2020) detect for the Central Andes (30°S to 37°S) highest mass balance losses for partly debris-covered glaciers, followed by clean ice glaciers and contrasting with completely debris-covered glaciers and rock glaciers characterised by almost zero mass balances (e. g., rock glaciers: -0.02 ± 0.19 m w.e. yr−1, 2000-2018). Except for the partly debris-covered

glaciers which we do not address here, this is well reflected in our results, cf. Figure 17A. It highlights the strong differences in vertical surface change behaviour between the landforms. The question here is the comparability between the meaning of vertical surface changes on glaciers and rock glaciers, which is why we focus on rock glacier velocities as indicator of (in)stability of permafrost conditions in the next chapter.

8.2.4. Rock glacier kinematics in the Rodeo Basin

For Dos Lenguas rock glacier, our Pléiades-based rock glacier vertical surface changes, Table 15, and velocities, Table 16, are in good agreement with UAV-based rock glacier vertical and horizontal surface changes for Dos Lenguas rock glacier available for 2016-2018 (Halla et al. 2021) and 2016-2024 (Stammler et al. 2025a), both in terms of magnitude, Figure 23, and pattern. In terms of pattern, highest values of 1.5 to 2 m/yr reached in the upper zone, cf. Figure 21B (Halla et al. 2021; Stammler et al. 2025a).

Strozzi et al. (2020) quantify surface velocities ranging between 1.5 to 2 m/yr (2015-2020) for the upper part of Dos Lenguas rock glacier, based on InSAR and offset tracking. These values are in good agreement with our Pléiades-based velocities, Figure 23. While we acknowledge the challenges surrounding the comparison of optical and radar imagery-based rock glacier surface change quantification (view angles, different sources of error, different time periods, etc.) and caution a detailed comparison other than the comparison of general magnitude, we highlight the inter-methodological agreement of magnitude between the UAV, Pléiades, and InSAR-based investigations.

Except for Dos Lenguas rock glacier, no other rock glaciers in Rodeo basin have been monitored for surface change. This highlights the benefit of the remotely sensed analysis and its scalability compared to, e.g., UAV-based rock glacier surface change monitoring. Median horizonal surface changes for all rock glaciers investigated in this study, Table 13 and Table 15, are in agreement in terms of magnitude with average velocities of 0.54 ± 0.03 m/yr for rock glaciers in the neighbouring La Laguna catchment (Chile) as detected by Robson et al. (2022).

We hypothesize that the three groups we identify based on our basin-wide rock glacier surface change investigation, Figure 20, are indicative of different driving mechanisms. Here, fast and large rock glaciers at high elevation and low slope are volume and creep dominated, see vertical surface change patterns in Figure 18 and velocity pattern indicative of extensional and compressional flow in Figure 21A-C. As fast and small rock glaciers concur with high elevation with most importantly high slope, we infer gravitational force to have a strong impact – supported by missing creep surface morphology in, e.g., Figure 21D. Small rock glaciers located at lower elevation with variable slope are slow to non-moving – potentially with the temperature gradient having the strongest effect on the low activity to inactivity. Fast rock glaciers, independent of their size, are characterised by coherent areas of positive vertical surface changes on the rock glaciers front, caused by the rock glaciers horizontal movement, Figure 18C-D blue area on rock glacier front.

We do not detect a regional trend in increasing rock glacier velocities in the Rodeo basin between 2019-2025, Figure 22. For many rock glaciers, including the fast and large and fast and small, the 2019-2024 period is characterised by very stable conditions, while the 2024-2025 time period is slightly higher. We cannot confirm the significance of this increase given our

LoDs and the potential of an outlier year, but can confirm no similarly high velocities for 2019-2024, rendering them unprecedented in our dataset. Thus, we highlight the strong need for continued monitoring of rock glaciers in this basin in this potentially dynamic point in time. Slow and small rock glaciers do not show any activity above the LoD, confirming our conclusion on little activity.

This lack of a regional trend in increasing velocities elucidates stable permafrost conditions in Rodeo basin during 2019-2025. While we acknowledge the limitations of our short monitoring period, we highlight the data scarcity in this region of the world – particularly also for rock glacier monitoring (Hu et al. 2025). The detected lack of a regional trend is in agreement with a longer-term monitoring (1968-2023) by Blöthe et al. (2024) who identify unchanged rock glacier velocities in the Valles Calchaguíes region (24°S to 25°S, Argentinean Andes) and Falaschi et al. (2025) who report a mixed signal of acceleration and deceleration of rock glacier velocities in Central Patagonia (47°S, Argentinean Andes) between 2018 and 2023. It contrasts with findings in the Alps (Manchado et al. 2024) or North America (Kääb and Røste 2024). Based on borehole measurements, Koenig et al. (2025) find no clear warming indication for ground temperatures in the Andes (27°S to 34°S) - further supporting the implication on permafrost conditions of our quantification of rock glacier velocities.

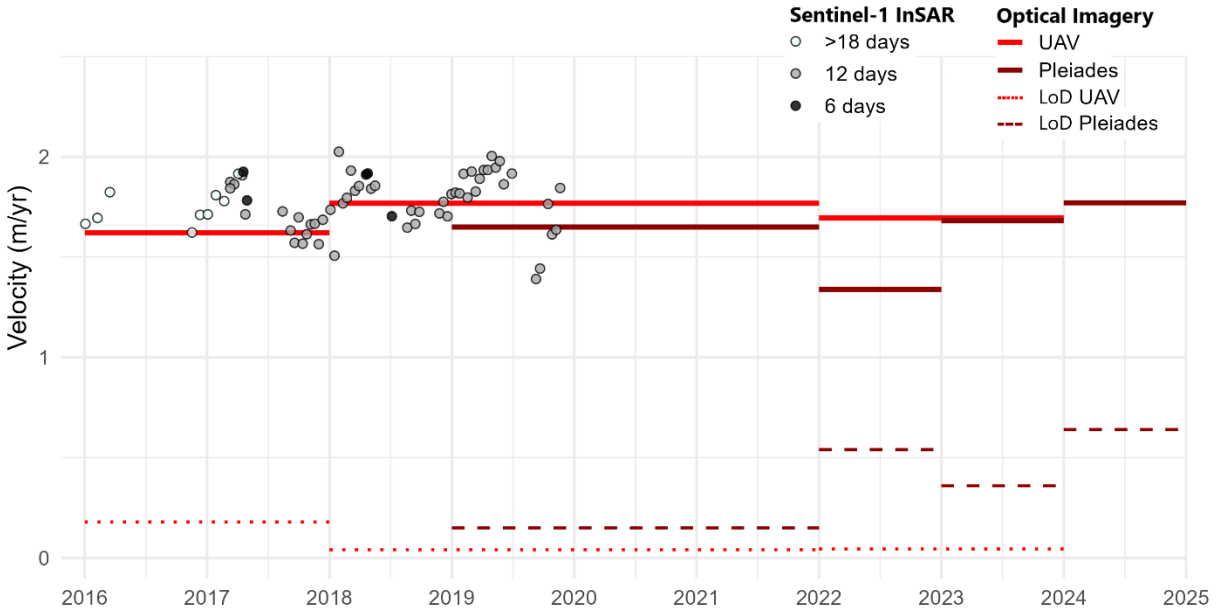

Figure 23 Inter-method comparison between our Pléiades-based rock glacier velocity compared to Sentinel-1 InSAR (Strozzi et al. 2020) and UAV-based rock glacier velocity (Stammler et al. 2025a), all for a coordinate located in the upper part of Dos Lenguas rock glacier, see Figure 21B. Note that velocities reached in the upper part of Dos Lenguas are higher than respective median values.

8.3. Conclusion

All glaciers in our study area of the Rodeo basin, located in the Dry Andes, are characterised by surface lowering. Agua Negra glacier stands out with a maximum cumulative surface lowering of -8.99 m (2019-2025). Vertical surface change based on Pléiades DEM differing confirm smaller glaciers and glaciers at lower altitude to be prone to higher vertical surface lowering. Vertical surface changes on debris-covered glaciers are of a much lesser magnitude compared to glaciers, and of a higher magnitude than rock glaciers. Rock glaciers are characterised by minimal median vertical surface changes with high variability of negative and positive balances in time.

In contrast to the decline in the glacial domain, we do not see a regional trend of increasing rock glacier velocities for 2019-2025. Rock glacier velocities are heterogeneously present across the basin, with our monitoring for the entire basin allowing for a differentiation of driving mechanisms, such as dominance by creep and volume, gravity and temperature. Monitoring 47 rock glaciers further highlights that those velocities are heterogeneously present within the landforms, with similar magnitudes of change partially reached in the upper, and partially the lower part.

Both for vertical and horizontal surface change, our validation of the Pléiades-based quantification with repeated DGNSS measurements at three selected sites with in total 78 DGNSS measurements indicate minor differences below one pixel and supports the suitability of Pléiades imagery for cryospheric landform monitoring. An inter-method comparison of the rock glacier velocities (Pléiades with UAV and InSAR) further enhances the robustness of the Pléiades approach. Pléiades imagery comes with the disadvantage of the need for tasking, particularly in areas characterised by data scarcity where archive coverage is poor. Initiatives like the Pléiades Glacier Observatory (Berthier et al. 2024) reduce this barrier by enabling access to selected image pairs and DEMs. Despite the remaining challenge in access, Pléiades imagery provides unseen opportunities specifically in remote areas where (physical) access is challenged. We find both stereo and tristereo panchromatic Pléiades acquisitions to be suitable for DEM generation at high resolution and low error, particularly with the imagery's independence from colour nuances and changing light conditions providing a suitable basis for feature tracking. The possibility to increase the spatial coverage of the surface change monitoring to, e.g., catchment scale along with the benefit of monitoring surface change across landform types enables more interdisciplinary studies in the glaciological, geomorphological and hydrological fields.

Based on our comparison of vertical and horizontal surface changes in the glacial and periglacial domains of the Rodeo basin, we conclude a delayed response of the permafrost landforms to the increasing temperatures that are leading to a decline of the glaciers and debris-covered glaciers alike. Given the hydrological significance of all meltwaters, we highlight the strong need for continued monitoring of surface changes in the glacial and periglacial domains, supported by interdisciplinary studies focusing on their potential interaction.

9. Synthesis and Outlook

This chapter presents a brief summary of the three papers and provides integrative answers to the research questions, cf. Chapter 1.2. It finishes with future directions on and the transferability of the topics and questions raised in this dissertation.

9.1. Brief summary of the three papers

Paper 1 sets out with a feasibility study to ensure a methodologically sound investigation of rock glacier kinematics on multiple scales. Rock glacier kinematics of Dos Lenguas rock glacier are quantified using UAV and Pléiades imagery. Three different software for the generation of Pléiades-based DEMs are compared, namely Agisoft Metashape Professional, Catalyst Professional and ASP. Based on data quality and robustness, ASP is selected as most suitable software for the processing of (tri)stereo panchromatic Pléiades imagery. The paper further ascertains that the Pléiades-based DoDs processed in ASP reproduce the vertical surface change quantified for Dos Lenguas rock glacier surface based on UAV imagery. This finding represents a proof of concept and allows for the investigation of rock glacier kinematics on larger spatial scale using Pléiades imagery and the selected processing strategy in ASP. The similarity in magnitude and spatial pattern of the derived vertical surface changes on Dos Lenguas rock glacier with values published in the scientific literature supports the suitability of our approach. The paper highlights the need for *in situ* knowledge and robust co-registration for effectively evaluating remotely sensed products and their derivatives. It concludes that a decision on the selection of the imagery input – UAV or Pléiades – largely depends on the research target and the therewith needed spatial resolution and spatial coverage.

Paper 2 represents an in-depth study of rock glacier kinematics on Dos Lenguas rock glacier between 2016 and 2024 using UAV imagery - presenting the longest UAV-based rock glacier surface change monitoring in the Dry Andes. The foci of the paper are three-fold: first, precisely documenting the UAV data-take, DEM and consequent DoD generation including a detailed error quantification to ascertain a robust database for the interpretation of rock glacier kinematics. Second, the quantification of Dos Lenguas vertical and horizontal rock glacier surface changes at high resolution, speaking of centimetres, for 2016-2024. And third, the interpretation of the rock glacier kinematics, elucidating their meaning for the local state of permafrost as well as the effect of topography and climate. While vertical rock glacier surface changes are highest in the rock glacier centre and range in their majority between ±1.5 m, volumetric changes are predominantly negative across the entire Dos Lenguas rock glacier surface. Rock glacier velocities are highest in the upper zone, reaching values of up to 2 m/yr. The mean surface velocity is 0.9 m/yr quantified with an LoD of ±0.05 m/yr and no increase in velocities is detected. Rock glacier velocity and elevation are positively correlated and a weak negative correlation between vertical surface change and curvature is detected. ERA5 air temperature shows a clear warming trend with summer respectively winter air temperature exceeding their 1940-2024 mean since 2000 and 2017. Visible inspection of static imagery reveals snow cover to be present on 14 of 377 days only, lasting not longer than three consecutive days. The stable rock glacier velocities detected on Dos Lenguas rock glacier are in terms of magnitude, pattern and stability in agreement with the few publications that study rock glacier kinematics in the Dry Andes. Differences of velocities within the rock glacier surface are largely controlled by slope and the specific location within the rock glacier surface. The

magnitude of vertical surface changes is controlled by compressional flow and surface topography. The lack of snow sheltering and, thus, the penetration of winter temperatures into the rock glacier body are concluded to control the absence of Dos Lenguas' kinematic response to warming air temperatures, as observed in other areas on the globe. The stable velocities elucidate currently stable permafrost conditions in the Dry Andes, a highly relevant finding for a region where water availability largely depends on mountain meltwaters. The study highlights the importance of high-resolution data in the range of centimetres to understand the local variability of rock glacier kinematics within a landform and to detect rock glacier surface changes with extremely low LoDs. It deciphers driving factors of rock glacier kinematics and contributes to a better understanding of the local state of permafrost.

Paper 3 continues with scaling up the investigation of rock glacier kinematics – in terms of spatial coverage as well as type of landform. It makes use of the processing approach tested in Paper 1 and uses (tri)stereo panchromatic Pléiades imagery to investigate vertical surface changes of all glaciers, debris-covered glaciers and rock glaciers in Rodeo basin. In addition, it quantifies horizontal surface changes of 47 of the 58 rock glaciers for which we have data for all time periods. Median annual vertical surface changes range between -0.20 and -1.50 m/yr for glaciers, -0.09 and 0.22 m/yr for debris-covered glaciers and -0.01 and 0.07 m/yr for rock glaciers. LoDs for vertical surface changes are low and never exceed ±0.08 m/yr. The cumulative vertical change is highest for Agua Negra glacier and amounts to -8.99 m for the time period 2019-2025 detected with a LoD of ±0.11 m/yr. Glacier vertical surface change is most negative in the glaciers' centre and less negative at its edges. 47 out of the 58 rock glaciers alternate between negative and positive vertical surface changes at least once between the observed time periods. Similar to our UAV-based findings for Dos Lenguas, vertical surface changes on rock glaciers are heterogeneously present across the rock glacier surfaces and mimic the ridge-and-furrow surface morphology. Rock glacier velocities in median for all rock glaciers range between 0.28 and 0.82 m/yr, detected with LoDs ranging from ±0.16 to ±0.61 m/yr. No acceleration of velocities is detected on the 47 rock glaciers. Comparison to DGNSS measurements attests a high data quality of the Pléiades-based results, while a comparison to the UAV-based surface changes as well as published InSAR-based velocities additionally support the feasibility of the Pléiades imagery-based approach. Further, published surface changes of Agua Negra glacier correspond in magnitude and pattern to our results. The paper underlines the representativity of Dos Lenguas rock glacier for rock glaciers in Rodeo basin and resolves a general, stable trend of rock glacier kinematics – proven across the entire catchment. It showcases the benefits of Pléiades imagery by monitoring 47 rock glaciers of which previously solely one was monitored, next to the potential transferability of the approach to other catchments. The paper thereby contributes to closing the gaps of catchment-wide studies and studies which address both the glacial and periglacial domains with the aim of providing a holistic understanding of the changes affecting the solid water storages in the Dry Andes in a time of rising air temperatures.

9.2. Integrative answers to the research questions

The decline of the glacial domain in terms of glacier surface area and volume is evident on global scale (Barry 2006). Permafrost is a critical element of the earth's cryosphere vulnerable to atmospheric warming (Haeberli et al. 2006). Glacial and periglacial meltwaters sustain runoff and are essential to water availability in arid regions, such as the Dry Andes (Arenson et al. 2022; Masiokas et al. 2020). Increasing air temperatures and reduced snow cover jeopardise an adequate meltwater volume (Pabón-Caicedo et al. 2020; Pitte et al. 2022; Malmros et al. 2018). It is therefore only consistent, that the IPCC states the retreat of the Andean cryosphere with its effect on streamflow contribution and an increased risk of water supply shortages with high confidence (Magrin et al. 2014), anticipating a glacier surface reduction of 30 to 50 % (Castellanos et al. 2022). Changes in the meltwater contribution to runoff affect the hydrological regime and sediment transport, freshwater supply, solute concentrations in streamflow, irrigation and riverine ecosystem resilience and the ecosystem's buffer capacity towards droughts (Beniston and Stoffel 2014; Castellanos et al. 2022; Dussaillant et al. 2019; Ferri et al. 2020; Magrin et al. 2014; Masiokas et al. 2020; Pitte et al. 2022; Seelig et al. 2025).

Hence, an in-depth investigation of solid water storages is crucial. With changes in the permafrost domain being less obvious than changes in the glacial domain (Hock et al. 2019; Huss et al. 2017) and understudied in the Dry Andes (Hu et al. 2025), the dissertation lies a focus on rock glacier kinematics. Indirect means of detecting and monitoring this surface and subsurface, 'hidden' ice are essential in the topographically challenging Dry Andes where fieldwork is resource intensive and physical access to sites is partially impossible, motivating the multi-scale and combined on- and off-site approach designed in this dissertation. This chapter provides conclusive findings based on answering the research questions stated in Chapter 1.2.

Research question 1: What is the magnitude and spatial pattern of vertical and horizontal surface changes on the Dos Lenguas rock glacier? (Paper 1, 2 and 3)

Vertical surface changes and their heterogeneous presence on Dos Lenguas rock glacier largely depict the ridge-and-furrow morphology displacement detected in all three papers: using UAV and Pléiades imagery for 2022-2023 (Paper 1), UAV imagery for 2016-2024 (Paper 2) and Pléiades imagery for 2019-2025 (Paper 3). By monitoring vertical surface change on the rock glacier front slopes in addition to the rock glacier surface, Paper 2 and 3 resolve rock glacier advancement independent of the type of imagery used, see Figure 11 and Figure 18. Vertical surface changes on Dos Lenguas rock glacier are highest in magnitude in its centre area where compressional flow is prevalent, followed by the southern tongue – determined using the high-resolution UAV imagery in Paper 2. Volumetric change is in its vast majority negative for all surface zones, cf. Figure 12. Given their heterogenous presence, vertical surface changes on Dos Lenguas rock glacier result in minimal median surface change as, e.g., calculated using Pléiades imagery, Table 13. To reduce this effect, the magnitude of vertical surface changes on Dos Lenguas rock glacier is presented as mean positive and mean negative value in Paper 1, Table 9. Their calculated mean is in agreement with the median vertical surface changes quantified using the Pléiades imagery. In the second paper we fully refrain from providing mean and median values resulting in stating that the majority of all UAV-based vertical surface changes is ±1.5 m/yr with singular values reaching ±1.7 m/yr. This is in agreement with the vertical change quantified using Pléiades imagery, cf. Figure 18.

Rock glacier velocity on Dos Lenguas is highest in its upper zone and follows a 'streamline' towards the southern tongue independent of the type of imagery used, see Figure 13 and Figure 21. Traversing from the centre to the northern tongue presents a drastic decline of velocities. Slowest velocities are present on the rock glacier (side) edges, extensional flow is present in the upper zone and compressional flow increases towards the rock glacier's centre, see Paper 2 and 3. In the case of Dos Lenguas, rock glacier velocity decreases with an increase of compressional flow. In terms of magnitude, highest values in the upper zone reach up to 2 m/yr, the mean surface velocity is 0.9 m/yr and rock glacier velocities are stable in time - determined independent of the type of imagery used, Chapter 7.1.3 and Table 16. For a direct comparison of Dos Lenguas rock glacier velocity as determined with UAV and Pléiades imagery, see Figure 23. Paper 1 does not address horizontal changes on Dos Lenguas rock glacier.

To summarise, Dos Lenguas rock glacier is characterised by vertical surface changes of ±1.5 m/yr and a median surface velocity of 0.9 m/yr which is stable in time for 2016-2024, and 2019-2025. Dos Lenguas vertical rock glacier surface changes are in agreement with Monnier and Kinnard (2017) who result with changes of up to -1 m/yr based on aerial photography and spaceborne DoDs in Navarro complex for the period 2000-2014, and Robson et al. (2022) that calculate mean vertical surface changes of > -0.1 m/yr on several rock glaciers in the neighbouring Chilean catchment La Laguna for 2012-2020. In terms of velocities, we reproduce the UAV-based Dos Lenguas surface velocities by Halla et al. (2021) as well as the feature tracking on Landsat 7/8 imagery based results by Cusicanqui et al. (2025) in magnitude and pattern. Further, our upper zone velocities independent of being generated using UAV or Pléiades imagery in Papers 2 and 3 are in agreement with the InSAR and offset tracking based upper zone velocities by Strozzi et al. (2020). The stability of our Dos Lenguas rock glacier velocities, referring to them neither accelerating nor decelerating, is in agreement with Blöthe et al. (2024).

Research question 2: What is the magnitude and spatial pattern of vertical and horizontal surface changes on rock glaciers across the Rodeo basin and how representative is Dos Lenguas rock glacier? (Paper 1 and 3)

Vertical median surface changes of all 58 rock glaciers in Rodeo basin are minimal, Table 13, not correlated with elevation or slope, Figure 17C-D, and variable in time with 47 out of the 58 alternating at least once between positive and negative vertical surface change. Vertical surface change on El Paso rock glacier is in agreement between Papers 1 and 3, cf. Table 10 and Table 15. The ridge-and-furrow morphology visible on the Dos Lenguas rock glacier surface as described for research question 1 is visible for El Paso rock glacier, Figure 18C.

Median velocities for rock glaciers in the Rodeo basin are spatially heterogeneously present across the basin and within landforms, Figure 19 and Figure 21. They also show temporal heterogeneity, such that different rock glaciers move fastest during different time periods. Median velocities for all rock glaciers in the Rodeo basin range between 0.28 and 0.82 m/yr quantified with LoDs of ±0.16 and ±0.61 m/yr, respectively, Table 13. Large and fast rock glaciers such as Dos Lenguas, El Paso and ID9 exceed median velocities of 1 m/yr, Table 16 and Figure 22. Velocities quantified for 47 rock glaciers in Rodeo basin for 2019-2025 are stable in time, Figure 22.

In comparison to other rock glaciers in Rodeo basin, Dos Lenguas is one of the fastest moving rock glaciers, representative of other large and fast rock glaciers, cf. Paper 2 and 3. Further, the Pléiades-based quantification of rock glacier velocities confirms stable velocities in time, both for Dos Lenguas and all rock glaciers investigated. Our catchment-wide vertical and horizontal rock glacier surface changes are comparable with scientific literature: Ferri et al. (2020) detect rock glacier vertical surface changes of -0.02 ± 0.19 m w.e. yr−1 for the Central Andes (30°S to 37°S) and the time period 2000-2018 while Robson et al. (2022) quantify an average rock glacier velocity of 0.54 ± 0.03 m/yr for rock glaciers in the neighbouring Chilean catchment La Laguna for 2012-2020. Further, the investigation reveals the need of satellite-based imagery for a resource-efficient large(r) scale investigation of rock glacier kinematics while spotlighting the validity of the UAV-based results, cf. Figure 1.

Research question 3: How do topography and climatological characteristics correlate with the magnitude and spatial pattern of these changes? (Paper 2 and 3)

Slope and curvature are topographical characteristics tested as potential drivers of rock glacier surface changes. Dos Lenguas' rock glacier velocities are highest in the upper zone, decrease in the centre zone and increase along the southern tongue correlating in magnitude with slope, Figure 15. This correlation is quantified by constant high Pearson correlation coefficients and determines slope as topographic catalysator of rock glacier velocity. Changes in slope further present knickpoints which decrease velocity and control the magnitude of the ridge-and-furrow pattern by compressional flow. Vertical surface changes are highest in magnitude where compressional flow has its highest impact – the rock glacier centre. This is supported by a weak negative correlation as expressed by Pearson coefficients between vertical surface change and curvature likely related to maximum vertical change occurring at the transitions between the curvature-rich ridges and furrows. In addition to rock glacier surface changes, the steep slopes of the Dos Lenguas rock glacier front facilitate gravitational processes particularly on the northern tongue, see Figure 11. Looking at rock glaciers across Rodeo basin in Paper 3, we identify three groups defined by the correspondence between rock glacier size and velocity: large and fast rock glaciers, small and fast rock glaciers and small and slow rock glaciers. Fast and large rock glaciers are located at higher elevation and lower slope compared to small and fast rock glaciers, Figure 20. In general, small and fast rock glaciers are most dominantly affected by topographic controls when looking at the role of slope on landform scale.

To consolidate, slope is the main topographical characteristic that impacts rock glacier kinematics with a catalysing effect. The effect is true for horizontal as well as vertical surface change and the magnitude of the effect depends on the specific location within the rock glacier surface, e.g., upper zone *versus* centre or streamline of velocities *versus* edges. This is in coherence with findings on the correlation of rock glacier velocities and slope as discussed, e.g., in Haeberli et al. (2006) and further found to be scale dependent. The Pléiades-based investigation on catchment scale indicates that small and fast rock glaciers are likely most affected by slope, compared to large and fast rock glaciers where the volume of the rock glacier body partially fills the valley and contributes to lowering slope at landscape scale.

Climate is investigated in terms of air temperature and precipitation. In the European Alps and Rocky Mountains, increasing air temperatures correlate with increased rock glacier velocities (Kellerer-Pirklbauer et al. 2024; Manchado et al. 2024; Kääb and Røste 2024). This behaviour comprehensive of the Glen-Nye flow law is expected, as the reduced viscosity of the warmer ice and the presence of infiltrating meltwater facilitate deformation, cf. Chapter 2.2.2. An increase of air temperature in Rodeo basin is observed based on ERA5 data validated for one year using *in situ* measured data, Figure 16. Both summer and winter temperatures increase. On first sight it is, thus, contradictive that rock glaciers in the Rodeo basin are not accelerating. Based on our findings we show that this is due to the absence of an insulating snow cover that enables the winter temperatures to penetrate the rock glacier body, cf. Chapter 7.2.5, with snow cover effects also discussed in Bast et al. (2024) and Bodin et al. (2010). Temperature influence on Dry Andean rock glaciers is evident for rock glaciers located below an elevation of 4100 m asl which are dominantly characterised by, if so, very slow velocities below our LoD, Figure 20.

To summarize, climate acts as a foundation for rock glacier kinematics. When MAATs exceed the maximum MAAT suitable for rock glaciers to be active, they become inactive, cf. Chapter 2.2.1. The Pléiades-based investigation on catchment-scale allows for the identification of such, in the case of Rodeo basin, small and slow rock glaciers. Following the Glen-Nye flow law, increased air temperatures lead to increased rock glacier velocities. We find that arid conditions and the absence of the insulating snow cover increase the impact of the temperature-related effects and lead to the investigated rock glacier velocities being stable in time, independent of the imagery type used for change quantification.

Research question 4: What state of permafrost do the surface kinematics imply for the wider region and how does the state of permafrost relate to the state of the glacial domain? (Paper 2 and 3)

Rock glacier velocities are stable on the recent temporal scale investigated in this dissertation, cf. Figure 1. This stability holds true for our high-resolution quantification of rock glacier velocities on Dos Lenguas rock glacier using UAV imagery between 2016-2024 deriving velocities at 2 m spatial resolution with LoDs ranging from ±0.03 to ±0.18 m/yr. Further, for our Pléiades-based investigation of rock glacier velocities across Rodeo basin for 2019-2025 at 5 m spatial resolution with LoDs ranging from ±0.16 to ±0.61 m/yr. Stable velocities are in agreement with Blöthe et al. (2024) who find unchanged rock glacier velocities for the Valles Calchaguíes region (24°S to 25°S, Argentinean Andes) for 1968-2023 and Falaschi et al. (2025) that report a mixed signal of acceleration and deceleration of rock glacier velocities in Central Patagonia for 2018-2023. As outlined for research question 3, changes in air temperature are associated with changes in rock glacier kinematics. Hence, unchanged surface velocities elucidate stable permafrost conditions at the location of the rock glaciers investigated for the observed period in time. With our UAV- and Pléiades based investigations we derive stable permafrost conditions in Rodeo basin. This corresponds with Koenig et al. (2025) who find no clear warming indication for ground temperatures in the Andes based on 53 boreholes at eight locations (27°S to 34°S).

Surface ice as investigated using (tri)stereo panchromatic Pléiades imagery in Paper 3 is strongly contrasting to the stable permafrost conditions. In Rodeo basin, it is in strong decline with vertical surface changes in median for all 19 investigated glaciers being negative across all time periods between 2019-2025, reaching up to -1.50 m/yr in 2023-2024 quantified with a LoD of ±0.01 m/yr. Surface lowering is highest at Agua Negra glacier and amounts to -8.99 m between 2019 and 2025, detected with an LoD of ±0.11 m/yr, Figure 18A. Debris-covered glaciers react with much lower magnitude to air temperature increase, Figure 17A. As glacier volume, however, largely outnumbers debris-covered glaciers in Rodeo basin, a decline of the glacial domain is attested. This is in agreement with glacier downwasting reported for the Andes (Dussaillant et al. 2019; Ferri et al. 2020; Masiokas et al. 2020). Surface thinning on Agua Negra glacier as quantified by Pitte et al. (2022) using Pléiades imagery is in agreement with our quantification in magnitude and pattern, cf. Table 15 and Figure 18. In Rodeo basin, we find small glaciers to be more prone to surface lowering in agreement with Al-Yaari et al. (2023).

In summary, surface ice in Rodeo basin is in strong decline as detected using (tri)stereo panchromatic Pléiades imagery for 2019-2025. Our quantification of glacier surface lowering is in magnitude and spatial pattern in agreement with published literature and contrasts with the stable permafrost conditions elucidated on by stable rock glacier velocities independent of spatial scale and type of imagery. While the contrast between the two domains is in agreement with the schematic by Arenson et al. (2022), Figure 2, the retarded reaction time of subsurface ice to rising air temperature as described in Chapter 2.1.1 is not quantifiable for rock glaciers in the Dry Andes, cf. Figure 2. If and/or when this absent response turns into a delayed response is only possible to answer by continued monitoring of rock glacier kinematics in the Dry Andes which we urge for - based on our findings and the continuously rising air temperatures in the Dry Andes of Argentina.

Research question 5: To which degree is it possible to resolve rock glacier surface kinematics with satellite-based remote sensing, compared to UAV-based investigations and which approach is most suitable in the high mountain cryosphere setting? (Paper 1, 2 and 3)

(Tri)stereo panchromatic Pléiades imagery in processing level 1, cf. Chapter 5.1.2, with a suitable processing approach provides a feasible means to resolve the magnitude of rock glacier velocities present in Rodeo basin. When balancing processing time against spatial resolution in Paper 3, we decide for a spatial resolution of the velocity dataset of 5 m. Given the 0.5 m spatial resolution of the panchromatic Pléiades imagery, achieving a higher resolution of the velocity dataset is possible. When conducting feature tracking with the UAV-based hillshades, we realize the scale dependency of horizontal processes on a rock glacier's surface. Feature tracking at very high spatial resolutions, speaking of decimetres, leads to prioritizing boulder movement over the general rock glacier velocity associated with permafrost creep. Due to this effect, we space the patch centres for feature tracking on the UAV-based hillshades with 2 m distance to each other leading to a velocity product at 2 m spatial resolution, despite the UAV DEM resolutions ranging between 2.89 and 11 cm/px, cf. Chapter 5.2.3 and Table 11. Paper 1 clearly highlights the need for selecting a suitable processing strategy for the Pléiades imagery to reduce the visual as well as processing effects on the generated DEMs and DoDs, cf. Chapters 6 and 5.2.1. Otherwise, processing effects overshadow 'true' surface movement and

prevent the correct analysis of surface changes. A comparison of Pléiades and DGNSS derived surface changes with differences of highest magnitude not exceeding -0.35 m/yr support the approach's feasibility, cf. Chapter 8.1.4. A limitation of the Pléiades-based monitoring of rock glacier velocities is its higher LoD (±0.16 to ±0.61 m/yr) compared to the UAV-based analysis (±0.03 to ±0.18 m/yr). Hence, a decision to monitor rock glacier velocities based on Pléiades imagery not necessarily comes with the cost of decreasing spatial resolution but in all cases comes with the cost of not being able to resolve slow velocities.

To summarize, satellite-based remote sensing along with a suitable processing strategy - here (tri)stereo panchromatic Pléiades imagery and our approach in ASP - is able to resolve medium to fast rock glacier velocities associated with permafrost creep at a scale comparable to UAV imagery. If an investigation of more small-scale processes on rock glacier surfaces is desired, such as tracing boulder movement, high-resolution UAV imagery is necessary. On the contrary, too high resolution of the imagery can prevent from detecting surface velocities associated with permafrost creep, highlighting the need to check the scale dependency of the process investigated. As the LoDs for Pléiades-based monitoring of rock glacier velocities are higher than the LoDs of the UAV-based investigation, the capability of resolving very slow velocities or the precise delineation of slow-moving areas within a rock glacier surface is reduced compared to an investigation based on UAV imagery.

Rock glacier vertical changes are resolvable in magnitude and pattern using panchromatic Pléiades imagery, in general patterns such as the advancement of the rock glacier front or the depiction of fast-flowing ridge-and-furrow systems comparable to UAV imagery, Figure 11 and Figure 18. The quality of the Pléiades-based quantification is validated by a comparison of the pixel frequencies of the vertical surface changes on Dos Lenguas rock glacier between 2022-2023 based on the UAV imagery processed in Agisoft following SfM-MVS techniques and the panchromatic Pléiades imagery processed in ASP following a more classic photogrammetric approach, cf. Chapter 3.2 and Figure 9. A comparison of DGNSS- to the Pléiades imagery derived surface changes at three locations supports the approach's suitability, cf. Chapter 8.1.4. In terms of LoDs, the panchromatic Pléiades imagery-based analysis is able to resolve vertical surface changes down to ±3 cm/yr, cf. Table 13, while LoDs for the UAV-based analysis range between 4 to 25 cm/yr, depending on the random component and bias of the DEM error, cf. Chapter 7.2.1. One limitation of the panchromatic Pléiades imagery-based analysis is the resolution which prevents resolving small spatially confined differences in vertical surface change on the rock glacier surface. This particularly holds true when differentiating vertical surface change in its x, y and z components by moving away from detecting vertical surface change with fixed pixels, cf. Chapter 7.2.4, as 'true' vertical change is expected to be lower than the vertical change which comprehends the horizontal component. This highlights the scale dependency of the processes investigated and calls for a detailed and robust understanding of the processes occurring in the respective study area prior to the analyses.

In summary, vertical surface changes of the magnitude present on rock glaciers in Rodeo basin can be resolved in magnitude and pattern using panchromatic, (tri)stereo Pléiades imagery when processed with our approach in ASP. The main limitation of the Pléiades-based quantification is its resolution which prevents to delineate surface areas with different vertical surface changes within a landform with high spatial resolution. The LoD of the Pléiades-based

analysis is comparable to UAV-based quantifications where the bias component of the DEM error is negligible, cf. Chapter 5.2.2. The selection of the most suitable technique in high mountain terrain depends on the research questions, objectives and the spatial and temporal resolution needed to address these as well as the potential challenges caused by a presence of clouds, vegetation and darkness. The benefits and limitations of the two different imagery types are summarized in Table 17. In agreement, Westoby et al. (2012) outline the benefits of high resolution satellite imagery over UAV imagery regarding the restrictions of UAV deployment but state the lack of active and passive sensors with resolutions high enough to remotely acquire data products that allow for an investigation of earth surface processes – impressively pointing towards the advancements made in the technical domain after 2012. We advocate for perceiving UAV- and Pléiades-based studies as complimentary, so that highest spatial resolution is achieved by the first and highest spatial coverage by the latter. In view of climate change and its effect of the glacial and periglacial domains, we are certain that an analysis on both spatial scales is relevant.

To consolidate, rock glacier kinematics – both vertical and horizontal – are resolvable with DEMs and derived products based on UAV and (tri)stereo panchromatic Pléiades imagery. The decision on which to use largely depends on the spatial and temporal resolution as well as the target objective of the research. For studies focused on permafrost creep related rock glacier surface kinematics, the choice of (tri)stereo panchromatic Pléiades imagery is recommended given its applicability on larger spatial scale and the suitability of its spatial resolution.

Table 17 Benefits and limitations of the two imagery types used in this dissertation for monitoring rock glacier surface changes in the Dry Andes of Argentina. For a comparison of the platforms and types of processing used, see Chapter 3.

	Benefits	**Limitations**
UAV	• Very high spatial resolution • Low LoDs particularly for velocities • Detailed analysis, e.g., within landforms • Independence of a data provider when acquiring the data • Dependence on fieldwork ascertains *in situ* knowledge on the study site	• Change quantification strongly dependent on the flight parameters and consequent DEM error • Dependent on physical access to, and weather conditions at the study site • Repeated data-take often limited by access and resources
Panchromatic Pléiades	• Independent of physical access, weather conditions and fieldwork limitations • RCPs allow for correct geolocalisation without georeferencing • Increase of spatial extent of the analysis is resource-efficient, including catchment wide analysis • Transferability of the processing approach to other landform types	• Change quantification is strongly dependent on the selection of the processing strategy • Co-registration needed • Only selected Pléiades imagery is provided without cost • Image foreshortening due to topography possible, depends on the target landform's location related to the satellite path

9.3. Future directions and transferability

The robust identification of stable rock glacier kinematics on Dos Lenguas as well as 47 rock glaciers in Rodeo basin allows for an investigation of the significance of the currently stable permafrost conditions on water availability, sediment transport, solute concentrations in streamflow, capacity to buffer drought, and ecosystem resilience. Currently stable permafrost conditions in the Dry Andes of Argentina ensure periglacial, subsurface water storage in the form of ice. A future direction based on the research presented in this dissertation is modelling the onset of periglacial meltwater contribution to the riverine system and its effect on the hydrological system, water availability and riverine ecosystem. Modelling this onset would increase a needed process understanding and potentially resolves if and when the currently absent periglacial response to rising air temperatures will occur in the Dry Andes of Argentina. Likely, it contributes to identifying tipping points of the Andean periglacial domain.

Seasonal monitoring of rock glacier surface changes potentially resolves freeze-thaw cycles of the permafrost's active layer. Seasonal variation of vertical surface changes is anticipated to vary more than annual change, rendering it likely resolvable with Pléiades imagery. One avenue for future work, grounded in the research presented here, is to investigate seasonal temporal resolution and thereby complementing the annual investigation of rock glacier kinematics already conducted. Increasing the temporal resolution will contribute to a more comprehensive understanding of processes occurring on rock glacier surfaces along with their drivers. Remotely sensed imagery is certainly essential to this cause given that physical access to the study site is prohibited in austral winters, along with the increased resource-demand of frequently repeating UAV acquisitions, cf. Table 17. As high-resolution satellite-borne optical imagery such as Pléiades imagery needs to be tasked for every point in time, the high temporal resolution of Sentinel-1 imagery, cf. Figure 23, could provide a feasible means to investigate seasonality of rock glacier surface dynamics in the Dry Andes of Argentina. In contrast to the imagery used in this dissertation, the Sentinel-1 satellites carry active sensors and provide SAR data, cf. Chapter 3.1.1, requiring other processing techniques from those presented – e.g., InSAR as applied by Strozzi et al. (2020). To ascertain the effect of seasonal periglacial meltwater contribution and its impact on solute concentration in streamflow (Seelig et al. 2025), water sampling at – if present – rock glacier springs and a monitoring of water levels as conducted in the project HyPerm is encouraged.

Further, the available Pléiades dataset can be used for the diversification of processes investigated on the rock glacier surfaces and surroundings, next to seasonality. These include but are not limited to quantifying rock glacier front advancement and steepening of the rock glacier front, detecting debris input onto the rock glacier, and monitoring gravitational processes on the rock glacier fronts. For glaciers, Pléiades-based investigation is not limited to surface lowering but can also serve to monitor changes in surface area. Monitoring surface changes in the glacial and periglacial domains at the same spatial and temporal resolution potentially lends the opportunity to study glacier-permafrost interaction currently missing for the (Dry) Andes - supporting the detection of cascading effects through time.

Although not analysed within the scope of this dissertation, the acquisition of UAV-based thermal imagery was tested on selected rock glaciers during the second fieldwork campaign. A DJI Mavic 3 Enterprise with an optical and thermal sensor was used for imagery acquisition. Flights

were conducted before sunrise to limit the effect of solar radiation, which is high in the Dry Andes, cf. Chapter 4. A preliminary analysis of the thermal data indicates the potential of resolving differences in surface temperature on rock glaciers using the DJI Mavic 3 Enterprise. Differences in surface temperature, however, are dominantly linked to differences in slope and the ridge-and-furrow pattern present on the rock glaciers surface. If rock glacier surface temperature is tied to the presence of ice lenses and if these can be resolved with UAV thermal imagery needs further investigation. Certainly, a detailed knowledge of the local topography and a means to correctly align high-resolution DEMs with the thermal data, e.g., by using optical GCPs that include metal which can serve as orientation for the optical and thermal image acquisition alike, are necessary.

In addition, the suitability of Sentinel-1 based coherence as a means to detect surface changes was tested in the framework of this dissertation without inclusion into the papers. Preliminary investigation finds higher coherence on slopes in the upper Rodeo basin near Dos Lenguas rock glacier, meaning values closer to 1, compared to lower coherence detected on the Dos Lenguas rock glacier surface itself. Aided by the high temporal resolution of Sentinel-1 data, coherence may provide an additional means to detect rock glacier surface changes next to an in-depth InSAR analysis. For an understanding of the magnitude resolved and the LoD inherent to this approach, further more detailed analyses are necessary.

Benefits of the (tri)stereo panchromatic Pléiades imagery-based workflow for vertical and horizontal surface change investigation and the large footprints of the Pléiades imagery are their transferability. The investigation is not limited to one landform, rock glaciers, as shown in Paper 3. Further, it is not limited to cryospheric processes and a future direction of research could be applying the Pléiades imagery-based workflow detailed in this dissertation, cf. Chapter 5.2, for the detection and investigation of, e.g., landslide or fluvial activity - either in Rodeo basin or at a different location for which (tri)stereo panchromatic Pléiades imagery was acquired. The only technical limitations to bear in mind are the magnitude and scale of the targeted processes compared to the resolution and LoDs of the Pléiades-based analysis.

10. Overall conclusion

A stable state of permafrost in the Dry Andes of Argentina is identified by monitoring rock glacier kinematics. Stability in rock glacier kinematics across multiple scales is confirmed using remotely sensed optical imagery acquired from different sensor platforms. At the landform-focused scale, high-resolution optical UAV imagery is used to quantify vertical and horizontal surface changes on Dos Lenguas rock glacier. Variations in magnitude and spatial pattern across the rock glacier surface are investigated, including the influences of topography and climate. Vertical surface changes on Dos Lenguas depict the ridge-and-furrow morphology, with most changes ranging between ±1.5 m/yr. The median rock glacier velocity for Dos Lenguas is 0.9 m/yr and shows temporal stability.

A feasibility study demonstrates that UAV- and Pléiades-based imagery provide complementary insights into rock glacier surface changes. The Pléiades-based analysis confirms the surface changes observed on Dos Lenguas and extends the investigation to 58 rock glaciers for vertical changes and 47 for horizontal changes in the Rodeo Basin. Beyond expanding the spatial extent of the analysis, the satellite-based investigation enables the quantification of glacier and debris-covered glacier surface lowering on 19 glaciers and the three debris-covered glaciers in Rodeo basin, revealing consistently negative annual median surface change. Surface lowering is highest for Agua Negra Glacier where it amounts to -8.99 m (cumulative, 2019-2025). The combined rock glacier and (debris-covered) glacier study renders a more comprehensive understanding of the changing Dry Andean cryosphere – particularly in a time of rising air temperatures, and fosters interdisciplinarity.

The combined use of UAV and Pléiades imagery is methodologically synergetic and able to resolve a large diversity of rock glacier related processes exceeding kinematics. The Pléiades workflow developed, tested and applied in this dissertation is transferable and able to empower other studies particularly in regions with low *in situ* data coverage.

As stressed on in this dissertation, rock glacier kinematics provide a suitable means for an indirect investigation of the local state of permafrost. Knowledge on the state of permafrost is essential to understand today's and to predict future periglacial contribution to river runoff and its impact on water availability both for domestic, agricultural and economic activities as well as the riverine ecosystem. Periglacial meltwater contribution is of major relevance judging the speed of decline quantified in the Rodeo basin's glacial domain. Further, the difference in rock glacier kinematic response in the Dry Andes compared to the European Alps and North America opens doors for additional process-understanding.

Thus, the dissertation calls for a future comprehensive monitoring of rock glacier kinematics in the combined Chilean-Argentinean Dry Andes based on annually repeated (tri)stereo panchromatic Pléiades imagery in the austral summers and Sentinel-1 based coherence and InSAR analysis for seasonality. The suggested approach allows for a monitoring from space independent of physical access to the landforms and resources for fieldwork. Its temporal continuity will allow to exclude short-term temperature fluctuations from long-term trends. A higher degree of the already partially automatized workflow developed in this dissertation may lead to a reduction in processing time and an increased accessibility. Where available, *in situ* DGNSS measurements and UAV-based quantifications of rock glacier surface changes

should be used for cross-validation – encouraging data sharing following the FAIR principles. It is anticipated that such continuous, long(er)-term monitoring will increase our understanding of the impact of aridity on rock glacier kinematics and will deliver crucial answers to today's and near-future water availability in the water shortage characterised Dry Andes.

On a larger and more global scale, this dissertation provides one local example of a changing cryosphere and its impact on, among many factors, water availability essential to human use and the riverine ecosystem. It resolves its complexities and interrelations on multiple spatial scales and resolutions and highlights the benefits of a combined on- and off-site study integrative of different imagery types. It attests to the global decline of glacier mass and, while detailing the current stability of the permafrost conditions in the Dry Andes based on rock glacier kinematics, emphasizes the fragility of the permafrost environment. By doing so, it spotlights the effects of climate change and related challenges on the mountain cryosphere and calls for adequate action.

Publication bibliography

Al-Yaari, Amen; Condom, Thomas; Junquas, Clementine; Rabatel, Antoine; Ramseyer, Victor; Sicart, Jean-Emmanuel et al. (2023): Climate Variability and Glacier Evolution at Selected Sites Across the World: Past Trends and Future Projections. In *Earth's Future* 11 (10). DOI: 10.1029/2023EF003618.

Araya, Alejandro; Fingerhuth, Sebastian (2022): Methodology for mitigating noise impacts of a road. Case study for the chilean route 41-CH. In *Romanian Journal of Transport Infrastructure* 11 (2), pp. 1–17. DOI: 10.2478/rjti-2022-0007.

Arenson, L.; Springman, Sarah M.; Sego, Dave C. (2007): The Rheology of Frozen Soils. In *Applied Rheology* 17 (1), 12147-1-12147-14. DOI: 10.1515/arh-2007-0003.

Arenson, Lukas U.; Harrington, Jordan S.; Koenig, Cassandra E. M.; Wainstein, Pablo A. (2022): Mountain Permafrost Hydrology—A Practical Review Following Studies from the Andes. In *Geosciences* 12 (2), p. 48. DOI: 10.3390/geosciences12020048.

Arias, Paola A.; Garreaud, René; Poveda, Germán; Espinoza, Jhan Carlo; Molina-Carpio, Jorge; Masiokas, Mariano et al. (2021): Hydroclimate of the Andes Part II: Hydroclimate Variability and Sub-Continental Patterns. In *Front. Earth Sci.* 8. DOI: 10.3389/feart.2020.505467.

ASTRIUM (2012): Pléiades Imagery User Guide. 2nd ed.

Ayala, A.; Pellicciotti, F.; MacDonell, S.; McPhee, J.; Vivero, S.; Campos, C.; Egli, P. (2016): Modelling the hydrological response of debris-free and debris-covered glaciers to present climatic conditions in the semiarid Andes of central Chile. In *Hydrol. Process.* 30 (22), pp. 4036–4058. DOI: 10.1002/hyp.10971.

Ayala, Álvaro; Robson, Benjamin; Navarro, Gonzalo; MacDonell, Shelley; Kinnard, Christophe; Vivero, Sebastián et al. (2025): Monitoring the physical processes driving the mass loss of Tapado Glacier, Dry Andes of Chile. In *J. Glaciol.* 71, e52. DOI: 10.1017/jog.2025.24.

Azócar, G. F.; Brenning, A. (2010): Hydrological and geomorphological significance of rock glaciers in the dry Andes, Chile (27°-33°S). In *Permafrost and Periglacial Processes.* 21 (1), pp. 42–53. DOI: 10.1002/ppp.669.

Barrett, Eric C. (2013): Introduction to Environmental Remote Sensing. 1st ed.: Routledge.

Barry, Roger G. (2006): The status of research on glaciers and global glacier recession: a review. In *Progress in Physical Geography: Earth and Environment* 30 (3), pp. 285–306. DOI: 10.1191/0309133306pp478ra.

Barsch, Dietrich (1992): Permafrost creep and rockglaciers. In *Permafrost and Periglacial Processes* 3 (3), pp. 175–188. DOI: 10.1002/ppp.3430030303.

Barsch, Dietrich (1996): Rockglaciers. Indicators for the Present and Former Geoecology in High Mountain Environments. Berlin, Heidelberg: Springer.

Barsch, Dietrich; Happoldt, Hans; Mäusbacher, Roland; Schrott, Lothar; Schukraft, Gerd (1994): Discharge and fluvial sediment transport in a semi-arid high mountain catchment, Agua Negra, San Juan, Argentina. In *Dynamics and Geomorphology of Mountain Rivers* 52, pp. 213–224. DOI: 10.1007/BFb0117841.

Barsch, Dietrich; King, Lorenz (1989): Origin and geoelectrical resistivity of rockglaciers in semi-arid subtropical mountains (Andes of Mendoza, Argentinia). In *zfg* 33 (2), pp. 151–163. DOI: 10.1127/zfg/33/1989/151.

Bast, Alexander; Kenner, Robert; Phillips, Marcia (2024): Short-term cooling, drying, and deceleration of an ice-rich rock glacier. In *The Cryosphere* 18 (7), pp. 3141–3158. DOI: 10.5194/tc-18-3141-2024.

Bemis, Sean P.; Micklethwaite, Steven; Turner, Darren; James, Mike R.; Akciz, Sinan; Thiele, Sam T.; Bangash, Hasnain Ali (2014): Ground-based and UAV-Based photogrammetry: A multi-scale, high-resolution mapping tool for structural geology and paleoseismology. In *Journal of Structural Geology* 69, pp. 163–178. DOI: 10.1016/j.jsg.2014.10.007.

Beniston, Martin; Stoffel, Markus (2014): Assessing the impacts of climatic change on mountain water resources. In *The Science of the total environment* 493, pp. 1129–1137. DOI: 10.1016/j.scitotenv.2013.11.122.

Beraud, Luc; Cusicanqui, Diego; Rabatel, Antoine; Brun, Fanny; Vincent, Christian; Six, Delphine (2023): Glacier-wide seasonal and annual geodetic mass balances from Pléiades stereo images: application to the Glacier d'Argentière, French Alps. In *J. Glaciol.* 69 (275), pp. 525–537. DOI: 10.1017/jog.2022.79.

Berthier, E.; Vincent, C.; Magnússon, E.; Gunnlaugsson, Á. Þ.; Pitte, P.; Le Meur, E. et al. (2014): Glacier topography and elevation changes derived from Pléiades sub-meter stereo images. In *The Cryosphere* 8 (6), pp. 2275–2291. DOI: 10.5194/tc-8-2275-2014.

Berthier, Etienne; Lebreton, Jérôme; Fontannaz, Delphine; Hosford, Steven; Belart, Joaquin Munoz Cobo; Brun, Fanny et al. (2024): The Pléiades Glacier Observatory: high resolution digital elevation models and ortho-imagery to monitor glacier change. In *The Cryosphere* 18, pp. 5551–5571. DOI: 10.5194/tc-18-5551-2024.

Berthling, Ivar (2011): Beyond confusion: Rock glaciers as cryo-conditioned landforms. In *Geomorphology* 131 (3-4), pp. 98–106. DOI: 10.1016/j.geomorph.2011.05.002.

Bertone, Aldo; Barboux, Chloé; Bodin, Xavier; Bolch, Tobias; Brardinoni, Francesco; Caduff, Rafael et al. (2022): Incorporating InSAR kinematics into rock glacier inventories: insights from 11 regions worldwide. In *The Cryosphere* 16 (7), pp. 2769–2792. DOI: 10.5194/tc-16-2769-2022.

Besl, Paul J.; McKay, Neil D. (1992): Method for registration of 3-D shapes. In *Proceedings Sensor Fusion IV: Control Paradigms and Data Structures* 1611, pp. 586–606. DOI: 10.1117/12.57955.

Beyer, Ross A.; Alexandrov, Oleg; McMichael, Scott (2018): The Ames Stereo Pipeline: NASA's Open Source Software for Deriving and Processing Terrain Data. In *Earth and Space Science* 5 (9), pp. 537–548. DOI: 10.1029/2018EA000409.

Biskaborn, B. K.; Lanckman, J.-P.; Lantuit, H.; Elger, K.; Streletskiy, D. A.; Cable, W. L.; Romanovsky, V. E. (2015): The new database of the Global Terrestrial Network for Permafrost (GTN-P). In *Earth Syst. Sci. Data* 7 (2), pp. 245–259. DOI: 10.5194/essd-7-245-2015.

Blöthe, Jan Henrik; Falaschi, Daniel; Vivero, Sebastián; Tadono, Takeo (2024): Rock Glacier Kinematics in the Valles Calchaquíes Region, Northwestern Argentina, From Multi-Temporal Aerial and Satellite Imagery (1968–2023). In *Permafrost and Periglacial Processes*, ppp.2260. DOI: 10.1002/ppp.2260.

Blöthe, Jan Henrik; Halla, Christian; Schwalbe, Ellen; Bottegal, Estefania; Trombotto Liaudat, Dario; Schrott, Lothar (2021): Surface velocity fields of active rock glaciers and ice-debris complexes in the Central Andes of Argentina. In *Earth Surface Processes and Landforms* 46 (2), pp. 504–522. DOI: 10.1002/esp.5042.

Bodin, X.; Rojas, F.; Brenning, A. (2010): Status and evolution of the cryosphere in the Andes of Santiago (Chile, 33.5°S.). In *Geomorphology* 118 (3-4), pp. 453–464. DOI: 10.1016/j.geomorph.2010.02.016.

Bodin, Xavier; Echelard, Thomas; Trombotto, Dario; Vivero, Sebastián; Pitte, Pierre (2016): Rock glacier activity and distribution in the semi-arid Andes of Chile and Argentina detected from dInSAR. In *Proceedings of the XI International Conference on Permafrost, Potsdam, Germany*, pp. 20–24.

Brasington, James; Langham, Joe; Rumsby, Barbara (2003): Methodological sensitivity of morphometric estimates of coarse fluvial sediment transport. In *Geomorphology* 53 (3-4), pp. 299–316. DOI: 10.1016/S0169-555X(02)00320-3.

Braun, Matthias H.; Malz, Philipp; Sommer, Christian; Farías-Barahona, David; Sauter, Tobias; Casassa, Gino et al. (2019): Constraining glacier elevation and mass changes in South America. In *Nature Clim Change* 9 (2), pp. 130–136. DOI: 10.1038/s41558-018-0375-7.

Brenning, Alexander (2005): Geomorphological, hydrological and climatic significance of rock glaciers in the Andes of Central Chile (33–35°S). In *Permafrost and Periglacial Processes* 16 (3), pp. 231–240. DOI: 10.1002/ppp.528.

Buk, E. (1983): Glaciares de escombros y su significación hidrológica. In *Acta Geocriogéna* 1, pp. 22–38.

Caro, Alexis; Condom, Thomas; Rabatel, Antoine; Champollion, Nicolas; García, Nicolás; Saavedra, Freddy (2024): Hydrological response of Andean catchments to recent glacier mass loss. In *The Cryosphere* 18 (5), pp. 2487–2507. DOI: 10.5194/tc-18-2487-2024.

Carrivick, Jonathan L.; Smith, Mark W.; Quincey, Duncan J. (2016): Structure from Motion in the Geosciences: John Wiley & Sons.

Castellanos, E.; Lemos, M. F.; Astigarraga, L.; Chacón, N.; Cuvi, N.; Huggel, C. et al. (2022): Central and South America. In H.-O. Pörtner, D. C. Roberts, M. Tignor, E. S. Poloczanska, K. Mintenbeck, A. Alegría et al. (Eds.): Climate Change 2022: Impacts, Adaptation and Vulnerability. Contribution of Working Group II to the Sixth Assessment Report of the Intergovernmental Panel on Climate Change. IPCC. Cambridge, UK, New York, USA.

Catalano, Luciano R. (1926): Contribución al Conocimiento de los Fenómenos Geofísicos Atmosféricos (en base a observaciones efectuadas en la Puna de Atacama, territorio nacional de Los Andes). Ministerio de Agricultura. Dirección General de Minas, Geología e Hidrología (Ministerio de Agricultura. Dirección General de Minas, Geología e Hidrología).

Chen, Yang; Medioni, Gérard (1992): Object modelling by registration of multiple range images. In *Image and Vision Computing* 10 (3), pp. 145–155. DOI: 10.1016/0262-8856(92)90066-c.

Chorley, R. J. (1962): Geomorphology and general systems theory. Theoretical papers in the hydrologic and geomorphic sciences (USGS Numbered Series. Professional Paper, 500-B).

Chorley, Richard J.; Kennedy, Barbara A. (1971): Physical geography. A systems approach. London: Prentice-Hall.

Church, Michael (2010): The trajectory of geomorphology. In *Progress in Physical Geography: Earth and Environment* 34 (3), pp. 265–286. DOI: 10.1177/0309133310363992.

Cicoira, Alessandro; Marcer, Marco; Gärtner-Roer, Isabelle; Bodin, Xavier; Arenson, Lukas U.; Vieli, Andreas (2021): A general theory of rock glacier creep based on in-situ and remote sensing observations. In *Permafrost and Periglacial Processes* 32 (1), pp. 139–153. DOI: 10.1002/ppp.2090.

Cogley, J. G.; R. Hock; L.A. Rasmussen; A.A. Arendt; A. Bauder, R. BraithwaiteJ.; P. Jansson et al. (2011): Glossary of glacier mass balance and related terms. Paris, France (IHP-VII Technical Documents in Hydrology No. 86, IACS Contribution No. 2, UNESCO-IHP). Available online at https://wgms.ch/downloads/Cogley_etal_2011.pdf.

Condom, Thomas; Martínez, Rodney; Pabón, José Daniel; Costa, Felipe; Pineda, Luis; Nieto, Juan Jose et al. (2020): Climatological and Hydrological Observations for the South American Andes: In situ Stations, Satellite, and Reanalysis Data Sets. In *Front. Earth Sci.* 8, Article 92, p. 509192. DOI: 10.3389/feart.2020.00092.

Contreras, Sergio; Jobbágy, Esteban G.; Villagra, Pablo E.; Nosetto, Marcelo D.; Puigdefábregas, Juan (2011): Remote sensing estimates of supplementary water consumption by arid ecosystems of central Argentina. In *Journal of Hydrology* 397 (1-2), pp. 10–22. DOI: 10.1016/j.jhydrol.2010.11.014.

Corte, Arturo E. (1978): Rock glaciers as permafrost bodies with a debris cover as an active layer. A hydrological approach. Andes of Mendoza, Argentine. In *Proceedings of the Third International Conference on Permafrost, Edmonton, Canada*, pp. 262–269. Available online at https://pascal-francis.inist.fr/vibad/index.php?action=getrecorddetail&idt=pascalgeodebrgm7920260379.

Corte, Arturo E.; Buk, E. (1984): El marco criogénico para la hidrología cordillerana. In *Jornadas de Hi.*

Croce, C.; Milana, J. P. (2006): Electrical Tomography applied to image the 3D extent of the permafrost of three different Rock Glaciers of the Arid Andes of Argentina. In *Geophysical Research Abstracts* 8 (03026).

Croce, Flavia A.; Milana, Juan P. (2002): Internal structure and behaviour of a rock glacier in the Arid Andes of Argentina. In *Permafrost and Periglacial Processes.* 13 (4), pp. 289–299. DOI: 10.1002/ppp.431.

Cusicanqui, Diego; Bodin, Xavier; Duvillard, Pierre-Allain; Schoeneich, Philippe; Revil, André; Assier, Alain et al. (2023): Glacier, permafrost and thermokarst interactions in Alpine terrain:

Insights from seven decades of reconstructed dynamics of the Chauvet glacial and periglacial system (Southern French Alps). In *Earth Surface Processes and Landforms* 48 (13), pp. 2595–2612. DOI: 10.1002/esp.5650.

Cusicanqui, Diego; Lacroix, Pascal; Bodin, Xavier; Robson, Benjamin Aubrey; Kääb, Andreas; MacDonell, Shelley (2025): Detection and reconstruction of rock glacier kinematics over 24 years (2000–2024) from Landsat imagery. In *The Cryosphere* 19 (7), pp. 2559–2581. DOI: 10.5194/tc-19-2559-2025.

Dai, Wen; Zheng, Guanghui; Antoniazza, Gilles; Zhao, Fei; Chen, Kai; Lu, Wangda; Lane, Stuart N. (2023): Improving UAV-SfM photogrammetry for modelling high-relief terrain: Image collection strategies and ground control quantity. In *Earth Surface Processes and Landforms* 48 (14), pp. 2884–2899. DOI: 10.1002/esp.5665.

Dall'Asta, Elisa; Forlani, Gianfranco; Roncella, Riccardo; Santise, Marina; Diotri, Fabrizio; Di Morra Cella, Umberto (2017): Unmanned Aerial Systems and DSM matching for rock glacier monitoring. In *ISPRS Journal of Photogrammetry and Remote Sensing* 127, pp. 102–114. DOI: 10.1016/j.isprsjprs.2016.10.003.

Daudon, Dominique; Moreiras, Stella Maris; Beck, Elise (2014): Multi Hazard Scenarios in the Mendoza/San Juan Provinces, Cuyo Region Argentina. In *Procedia Economics and Finance* 18, pp. 560–567. DOI: 10.1016/s2212-5671(14)00976-9.

Duguay, M. A.; Edmunds, A.; Arenson, L.; Wainstein, P. A. (2015): Quantifying the significance of the hydrological contribution of a rock glacier – A review. In. GEOQuébec 2015. 68th Canadian Geotechnical Conference, 7th Canadian Permafrost Conference. Richmond, BC, Canada.

Dussaillant, I.; Berthier, E.; Brun, F.; Masiokas, M.; Hugonnet, R.; Favier, V. et al. (2019): Two decades of glacier mass loss along the Andes. In *Nat. Geosci.* 12 (10), pp. 802–808. DOI: 10.1038/s41561-019-0432-5.

Eltner, Anette; Kaiser, Andreas; Castillo, Carlos; Rock, Gilles; Neugirg, Fabian; Abellán, Antonio (2016): Image-based surface reconstruction in geomorphometry – merits, limits and developments. In *Earth Surf. Dynam.* 4 (2), pp. 359–389. DOI: 10.5194/esurf-4-359-2016.

Eltner, Anette; Sofia, Giulia (2020): Structure from motion photogrammetric technique. In: Remote Sensing of Geomorphology, vol. 23: Elsevier (Developments in Earth Surface Processes), pp. 1–24.

Esper Angillieri, María Yanina (2017): Permafrost distribution map of San Juan Dry Andes (Argentina) based on rock glacier sites. In *Journal of South American Earth Sciences* 73, pp. 42–49. DOI: 10.1016/j.jsames.2016.12.002.

Etzelmüller, Bernd; Hagen, Jon Ove (2005): Glacier-permafrost interaction in Arctic and alpine mountain environments with examples from southern Norway and Svalbard. In *SP* 242 (1), pp. 11–27. DOI: 10.1144/GSL.SP.2005.242.01.02.

Evans, I. S. (1979): An Integrated System of Terrain Analysis & Slope Mapping: Department of Geography, University of Durham.

Evans, Ian S. (2012): Geomorphometry and landform mapping: What is a landform? In *Geomorphology* 137 (1), pp. 94–106. DOI: 10.1016/j.geomorph.2010.09.029.

Falaschi, Daniel; Bhattacharya, Atanu; Guillet, Gregoire; Huang, Lei; King, Owen; Mukherjee, Kriti et al. (2023): Annual to seasonal glacier mass balance in High Mountain Asia derived from Pléiades stereo images: examples from the Pamir and the Tibetan Plateau. In *The Cryosphere* 17 (12), pp. 5435–5458. DOI: 10.5194/tc-17-5435-2023.

Falaschi, Daniel; Blöthe, Jan; Berthier, Etienne; Tadono, Takeo; Villalba, Ricardo (2025): Monitoring recent (2018–2023) glacier and rock glacier changes in Central Patagonia using high-resolution Pléiades and ALOS PRISM satellite data. In *Front. Earth Sci.* 13, Article 1601249, p. 1601249. DOI: 10.3389/feart.2025.1601249.

Falaschi, Daniel; Rivera, Andrés; Lo Vecchio Repetto, Andrés; Moragues, Silvana; Villalba, Ricardo; Rastner, Philipp et al. (2021): Evolution of Surface Characteristics of Three Debris-Covered Glaciers in the Patagonian Andes From 1958 to 2020. In *Front. Earth Sci.* 9, Article 671854, p. 671854. DOI: 10.3389/feart.2021.671854.

Favalli, M.; Fornaciai, A.; Isola, I.; Tarquini, S.; Nannipieri, L. (2012): Multiview 3D reconstruction in geosciences. In *Computers & Geosciences* 44, pp. 168–176. DOI: 10.1016/j.cageo.2011.09.012.

Ferri, Lidia; Dussaillant, Inés; Zalazar, Laura; Masiokas, Mariano H.; Ruiz, Lucas; Pitte, Pierre et al. (2020): Ice Mass Loss in the Central Andes of Argentina Between 2000 and 2018 Derived From a New Glacier Inventory and Satellite Stereo-Imagery. In *Frontiers in Earth Science* 8, p. 530997. DOI: 10.3389/feart.2020.530997.

Fleischer, Fabian; Haas, Florian; Piermattei, Livia; Pfeiffer, Madlene; Heckmann, Tobias; Altmann, Moritz et al. (2021): Multi-decadal (1953–2017) rock glacier kinematics analysed by high-resolution topographic data in the upper Kaunertal, Austria. In *The Cryosphere* 15 (12), pp. 5345–5369. DOI: 10.5194/tc-15-5345-2021.

Forte, Ana P.; Villarroel, Cristian D.; Esper Angillieri, María Y. (2016): Impact of natural parameters on rock glacier development and conservation in subtropical mountain ranges. Northern sector of the Argentine Central Andes. In *The Cryosphere Discussions*, pp. 1–24. DOI: 10.5194/tc-2016-232.

Frauenfelder, Regula; Haeberli, Wilfried; Hoelzle, Martin; Maisch, Max (2001): Using relict rockglaciers in GIS-based modelling to reconstruct Younger Dryas permafrost distribution patterns in the Err-Julier area, Swiss Alp. In *Norsk Geografisk Tidsskrift - Norwegian Journal of Geography* 55 (4), pp. 195–202. DOI: 10.1080/00291950152746522.

Frauenfelder, Regula; Kääb, Andreas (2000): Towards a palaeoclimatic model of rock-glacier formation in the Swiss Alps. In *Ann. Glaciol.* 31, pp. 281–286. DOI: 10.3189/172756400781820264.

García, Ayôn; Ulloa, Christopher; Amigo, Gonzalo; Milana, Juan Pablo; Medina, Catherine (2017): An inventory of cryospheric landforms in the arid diagonal of South America (high Central Andes, Atacama region, Chile). In *Quaternary International* 438, pp. 4–19. DOI: 10.1016/j.quaint.2017.04.033.

Garreaud, R. D. (2009): The Andes climate and weather. In *Advances in Geosciences* 22, pp. 3–11. DOI: 10.5194/adgeo-22-3-2009.

Geiger, Stuart T.; Daniels, J. Michael; Miller, Scott N.; Nicholas, Joseph W. (2014): Influence of Rock Glaciers on Stream Hydrology in the La Sal Mountains, Utah. In *Arctic, Antarctic, and Alpine Research* 46 (3), pp. 645–658. DOI: 10.1657/1938-4246-46.3.645.

Götz, J.; Otto, J.-C.; Schrott, L. (2013): Postglacial sediment storage and rockwall retreat in a semi-closed inner-Alpine sedimentary basin (Gradenmoos, Hohe Tauern, Austria). In *Geografia Fisica e Dinamica Quaternaria* 36 (1), pp. 63–80. DOI: 10.4461/GFDQ.2013.36.5.

Gruber, S. (2012): Derivation and analysis of a high-resolution estimate of global permafrost zonation. In *The Cryosphere* 6 (1), pp. 221–233. DOI: 10.5194/tc-6-221-2012.

Gruber, Stephan; Haeberli, Wilfried (2007): Permafrost in steep bedrock slopes and its temperature-related destabilization following climate change. In *Journal of Geophysical Research* 112 (F2). DOI: 10.1029/2006JF000547.

Gruber, Stephan; Haeberli, Wilfried (2009): Mountain Permafrost. In Rosa Margesin (Ed.): Permafrost Soils: Springer, Berlin, Heidelberg, pp. 33–44.

Haeberli, W. (1985): Creep of mountain permafrost: internal structure and flow of alpine rock glaciers. In *Mitteilungen der Versuchsanstalt fur Wasserbau, Hydrologie und Glaziologie an der Eidgenossischen Technischen Hochschule Zurich* 77.

Haeberli, W.; Guodong, Cheng; Gorbunov, A. P.; Harris, S. A. (1993): Mountain permafrost and climatic change. In *Permafrost and Periglacial Processes* 4 (2), pp. 165–174. DOI: 10.1002/ppp.3430040208.

Haeberli, Wilfried (2000): Modern Research Perspectives Relating to Permafrost Creep and Rock Glaciers: A Discussion. In *Permafrost and Periglacial Processes* 11 (4), pp. 290–293. DOI: 10.1002/1099-1530(200012)11:4<290::AID-PPP372>3.0.CO;2-0.

Haeberli, Wilfried; Gruber, Stephan (2009): Global Warming and Mountain Permafrost. In Rosa Margesin (Ed.): Permafrost Soils. Berlin, Heidelberg: Springer (16), 205-218.

Haeberli, Wilfried; Hallet, Bernard; Arenson, Lukas; Elconin, Roger; Humlum, Ole; Kääb, Andreas et al. (2006): Permafrost creep and rock glacier dynamics. In *Permafrost and Periglacial Processes* 17 (3), pp. 189–214. DOI: 10.1002/ppp.561.

Halla, Christian; Blöthe, Jan Henrik; Tapia Baldis, Carla; Trombotto, Dario; Hilbich, Christin; Hauck, Christian; Schrott, Lothar (2021): Ice content and interannual water storage changes of an active rock glacier in the dry Andes of Argentina. In *The Cryosphere* 15, pp. 1187–1213. DOI: 10.5194/tc-15-1187-2021.

Harris, Stuart A.; Corte, Arturo E. (1992): Interactions and relations between mountain permafrost, glaciers, snow and water. In *Permafrost and Periglacial Processes* 3 (2), pp. 103–110. DOI: 10.1002/ppp.3430030207.

Hartl, Lea; Zieher, Thomas; Bremer, Magnus; Stocker-Waldhuber, Martin; Zahs, Vivien; Höfle, Bernhard et al. (2023): Multi-sensor monitoring and data integration reveal cyclical destabilization of the Äußeres Hochebenkar rock glacier. In *Earth Surf. Dynam.* 11 (1), pp. 117–147. DOI: 10.5194/esurf-11-117-2023.

Hauck, Christian; Vonder Mühll, Daniel (2003): Evaluation of gephysical techniques for application in mountain permafrost studies. In *Zeitschrift für Geomorphologie, NF Suppl., Bd* 132, pp. 161–190.

Heredia, N.; Rodríguez Fernández, L.R; Gallastegui, G.; Busquets, P.; Colombo, F. (2002): Geological setting of the Argentine Frontal Cordillera in the flat-slab segment (30°00'–31°30'S latitude). In *Journal of South American Earth Sciences* 15 (1), pp. 79–99. DOI: 10.1016/S0895-9811(02)00007-X.

Heredia, Nemesio; Farias, Pedro; García-Sansegundo, Joaquín; Giambiagi, Laura (2012): The Basement of the Andean Frontal Cordillera in the Cordón del Plata (Mendoza, Argentina): Geodynamic Evolution. In *andgeo* 39 (2). DOI: 10.5027/andgeoV39n2-a03.

Hersbach, H.; Bell, W.; Berrisford, P.; Horányi, A.; Muñoz-Sabater, J.; Radu, N. R. (2019): Global reanalysis: goodbye ERA-Interim, hello ERA5 | ECMWF Newsletter. In *European Centre for Medium-Range Weather Forecasts*, 04/2019. Available online at https://www.ecmwf.int/en/elibrary/81046-global-reanalysis-goodbye-era-interim-hello-era5, checked on 4/4/2025.

Hewitt, K. (2002): Landscape Assemblages and Transitions in Cold Regions. In K. Hewitt, M. L. Byrne, M. English, G. Young (Eds.): Landscapes of Transition. 1st ed.: Springer.

Hilbich, C.; Hauck, C.; Mollaret, C.; Wainstein, P. A.; Arenson, L. (2021): Towards accurate quantification of ice content in permafrost of the Central Andes – Part 1: Geophysics-based estimates from three different regions. In *The Cryosphere* 16. DOI: 10.5194/tc-16-1845-2022.

Hock, R.; G. Rasul; C. Adler; B. Cáceres; S. Gruber; Y. Hirabayashi et al. (2019): High Mountain Areas. In H.-O. Pörtner, D. C. Roberts, V. Masson-Delmotte, P. Zhai, M. Tignor, E. Poloczanska et al. (Eds.): IPCC Special Report on the Ocean and Cryosphere in a Changing Climate. Cambridge, UK and New York, NY, USA: Cambridge University Press.

Hu, Yan; Arenson, Lukas U.; Barboux, Chloé; Bodin, Xavier; Cicoira, Alessandro; Delaloye, Reynald et al. (2025): Rock Glacier Velocity: An Essential Climate Variable Quantity for Permafrost. In *Reviews of Geophysics* 63 (1). DOI: 10.1029/2024RG000847.

Huggett, Richard John (2011): Fundamentals of Geomorphology: Routledge.

Hugonnet, Romain; McNabb, Robert; Berthier, Etienne; Menounos, Brian; Nuth, Christopher; Girod, Luc et al. (2021): Accelerated global glacier mass loss in the early twenty-first century. In *Nature* 592 (7856), pp. 726–731. DOI: 10.1038/s41586-021-03436-z.

Humlum, Ole (1997): Active layer thermal regime at three rock glaciers in Greenland. In *Permafrost and Periglacial Processes* 8 (4), pp. 383–408. DOI: 10.1002/(SICI)1099-1530(199710/12)8:4<383::AID-PPP265>3.0.CO;2-V.

Huss, M.; Bookhagen, B.; Huggel, C.; Jacobsen, D.; Bradley, R. S.; Clague, J. J. et al. (2017): Toward mountains without permanent snow and ice. In *Earth's Future* 5 (5), pp. 418–435. DOI: 10.1002/2016EF000514.

IANIGLA-CONICET (2018): ANIGLA-Inventario Nacional de Glaciares y Ambiente Periglacial. Informe de la subcuenca del río Blanco.Cuenca del río San Juan. With assistance of Ministerio de Ambiente y Desarrollo Sustentable de la Nación.

James, M. R.; Robson, S. (2012): Straightforward reconstruction of 3D surfaces and topography with a camera: Accuracy and geoscience application. In *J. Geophys. Res.* 117 (F3), Article 2011JF002289. DOI: 10.1029/2011JF002289.

James, M. R.; Robson, S.; d'Oleire-Oltmanns, S.; Niethammer, U. (2017): Optimising UAV topographic surveys processed with structure-from-motion: Ground control quality, quantity and bundle adjustment. In *Geomorphology* 280, pp. 51–66. DOI: 10.1016/j.geomorph.2016.11.021.

James, Mike R.; Chandler, Jim H.; Eltner, Anette; Fraser, Clive; Miller, Pauline E.; Mills, Jon P. et al. (2019): Guidelines on the use of structure-from-motion photogrammetry in geomorphic research. In *Earth Surface Processes and Landforms* 44 (10), pp. 2081–2084. DOI: 10.1002/esp.4637.

James, Mike R.; Robson, Stuart (2014): Mitigating systematic error in topographic models derived from UAV and ground-based image networks. In *Earth Surface Processes and Landforms* 39 (10), pp. 1413–1420. DOI: 10.1002/esp.3609.

Jones, D. B.; Harrison, S.; Anderson, K.; Betts, R. A. (2018): Mountain rock glaciers contain globally significant water stores. In *Scientific reports* 8 (1), p. 2834. DOI: 10.1038/s41598-018-21244-w.

Jones, Darren B.; Harrison, Stephan; Anderson, Karen; Whalley, W. Brian (2019): Rock glaciers and mountain hydrology: A review. In *Earth-Science Reviews* 193, pp. 66–90. DOI: 10.1016/j.earscirev.2019.04.001.

Kääb, A.; Huggel, C.; Fischer, L.; Guex, S.; Paul, F.; Roer, I. et al. (2005): Remote sensing of glacier- and permafrost-related hazards in high mountains: an overview. In *Nat. Hazards Earth Syst. Sci.* 5 (4), pp. 527–554. DOI: 10.5194/nhess-5-527-2005.

Kääb, A.; Kaufmann, V.; Ladstätter, R.; Eiken, T. (2003): Rock glacier dynamics: implications from high-resolution measurements of surface velocity fields. In M. Phillips, S. Springman, L. Arenson (Eds.): Permafrost. Proceedings of the 8th International Conference on Permafrost: Swets & Zeitlinger.

Kääb, A.; Reichmuth, T. (2005): Advance mechanisms of rock glaciers. In *Permafrost and Periglacial Processes* 16 (2), pp. 187–193. DOI: 10.1002/ppp.507.

Kääb, Andreas; Røste, Julie (2024): Rock glaciers across the United States predominantly accelerate coincident with rise in air temperatures. In *Nat Commun* 15 (1), p. 7581. DOI: 10.1038/s41467-024-52093-z.

Kellerer-Pirklbauer, Andreas; Bodin, Xavier; Delaloye, Reynald; Lambiel, Christophe; Gärtner-Roer, Isabelle; Bonnefoy-Demongeot, Mylène et al. (2024): Acceleration and interannual variability of creep rates in mountain permafrost landforms (rock glacier velocities) in the European Alps in 1995–2022. In *Environ. Res. Lett.* 19 (3), p. 34022. DOI: 10.1088/1748-9326/ad25a4.

Koenig, Cassandra E. M.; Hilbich, Christin; Hauck, Christian; Arenson, Lukas U.; Wainstein, Pablo (2025): Thermal state of permafrost in the Central Andes (27–34° S). In *The Cryosphere* 19 (7), pp. 2653–2676. DOI: 10.5194/tc-19-2653-2025.

Köhler, Tamara; Schoch-Baumann, Anna; Bell, Rainer; Buckel, Johannes; Ortiz, Diana Agostina; Trombotto Liaudat, Dario; Schrott, Lothar (2025): Expanding cryospheric landform inventories – quantitative approaches for underestimated periglacial block- and talus slopes in the Dry Andes of Argentina. In *Front. Earth Sci.* 13, Article 1534410, p. 1534410. DOI: 10.3389/feart.2025.1534410.

Köhler, Tamara; Schoch-Baumann, Anna; Bell, Rainer; Ortiz, Diana Agostina; Reichartz, Philipp; Schrott, Lothar; Trombotto Liaudat, Dario (2024): Underestimated permafrost landforms – block and talus slope distribution in the Dry Andes of Argentina. In *Proceedings of the 12th International Conference on Permafrost*. DOI: 10.52381/ICOP2024.151.1.

Kokelj, Steven V.; Lantz, Trevor C.; Tunnicliffe, Jon; Segal, Rebecca; Lacelle, Denis (2017): Climate-driven thaw of permafrost preserved glacial landscapes, northwestern Canada. In *Geology* 45 (4), pp. 371–374. DOI: 10.1130/G38626.1.

Kunz, Julius; Kneisel, Christof (2020): Glacier–Permafrost Interaction at a Thrust Moraine Complex in the Glacier Forefield Muragl, Swiss Alps. In *Geosciences* 10 (6), p. 205. DOI: 10.3390/geosciences10060205.

Lauro, Carolina; Moreiras, Stella M.; Junquera, Sebastian; Vergara, Ivan; Toural, Rafael; Wolf, Johannes; Tutzer, Ruben (2017): Summer rainstorm associated with a debris flow in the Amarilla gully affecting the international Agua Negra Pass (30°20'S), Argentina. In *Environ Earth Sci* 76 (5), pp. 1–12. DOI: 10.1007/s12665-017-6530-z.

Lecomte, Karina L.; Milana, Juan Pablo; Formica, Stella M.; Depetris, Pedro J. (2008): Hydrochemical appraisal of ice- and rock-glacier meltwater in the hyperarid Agua Negra drainage basin, Andes of Argentina. In *Hydrological Processes* 22 (13), pp. 2180–2195. DOI: 10.1002/hyp.6816.

Leiva, J. C.; Cabrera, G. A.; Lenzano, L. E. (2007): 20 years of mass balances on the Piloto glacier, Las Cuevas river basin, Mendoza, Argentina. In *Global and Planetary Change* 59 (1-4), pp. 10–16. DOI: 10.1016/j.gloplacha.2006.11.018.

Leiva, Juan Carlos (1999): Recent fluctuations of the Argentinian glaciers. In *Global and Planetary Change* 22 (1-4), pp. 169–177. DOI: 10.1016/s0921-8181(99)00034-x.

Lenzano, María Gabriela; Lenzano, Luis; Barón, Jorge; Lannutti, Esteban; Durand, Marcelo; Trombotto Liaudat, Dario (2016): Thinning of the Horcones inferior debris-covered glacier, derived from five ablation seasons by semi-continuous GNSS geodetic surveys (Mt. Aconcagua, Argentina). In *andgeo* 43 (1), p. 47. DOI: 10.5027/andgeoV43n1-a03.

Lliboutry, L.; Williams, R.; Ferrigno, Jane G. (1998): Glaciers of Chile and Argentina. Edited by Geological Survey professional paper. United States Gov. Print. Off. Washington.

Magrin, G. O.; Marengo, J. A.; Boulanger, J.-P.; Buckeridge, M. S.; Castellanos, G.; Poveda, Germán et al. (2014): Central and South America. In V. R. Barros, C. B. Field, D. J. Dokken, M. D. Mastrandrea, K. J. Mach, T. E. Bilir et al. (Eds.): Climate Change 2014: Impacts, Adaption, and Vulnerability. Part B: Regional Aspects. Contribution of Working Group II to the Fifth Assessment Report of the Intergovernmental Panel on Climate Change. IPCC. Cambridge, UK, New York, USA, pp. 1499–1566.

Malmros, Jeppe K.; Mernild, Sebastian H.; Wilson, Ryan; Tagesson, Torbern; Fensholt, Rasmus (2018): Snow cover and snow albedo changes in the central Andes of Chile and Argentina from daily MODIS observations (2000–2016). In *Remote Sensing of Environment* 209, pp. 240–252. DOI: 10.1016/j.rse.2018.02.072.

Manchado, Alberto Muñoz-Torrero; Allen, Simon; Cicoira, Alessandro; Wiesmann, Samuel; Haller, Ruedi; Stoffel, Markus (2024): 100 years of monitoring in the Swiss National Park reveals overall decreasing rock glacier velocities. In *Commun Earth Environ* 5 (1). DOI: 10.1038/s43247-024-01302-0.

Marcer, Marco; Cicoira, Alessandro; Cusicanqui, Diego; Bodin, Xavier; Echelard, Thomas; Obregon, Renée; Schoeneich, Philippe (2021): Rock glaciers throughout the French Alps accelerated and destabilised since 1990 as air temperatures increased. In *Commun Earth Environ* 2 (1). DOI: 10.1038/s43247-021-00150-6.

Martin, H. E.; Whalley, W. B. (1987): Rock glaciers. part 1: rock glacier morphology: classification and distribution. In *Progress in Physical Geography: Earth and Environment* 11 (2), pp. 260–282. DOI: 10.1177/030913338701100205.

Masiokas, M. H.; Rabatel, A.; Rivera, A.; Ruiz, L.; Pitte, P.; Ceballos, J. L. et al. (2020): A Review of the Current State and Recent Changes of the Andean Cryosphere. In *Front. Earth Sci.* 8, Article 99. DOI: 10.3389/feart.2020.00099.

Masiokas, Mariano H.; Villalba, Ricardo; Luckman, Brian H.; Le Quesne, Carlos; Aravena, Juan Carlos (2006): Snowpack Variations in the Central Andes of Argentina and Chile, 1951–2005: Large-Scale Atmospheric Influences and Implications for Water Resources in the Region. In *Journal of Climate* 19 (24), pp. 6334–6352. DOI: 10.1175/JCLI3969.1.

Mathys, Tamara; Hilbich, Christin; Arenson, Lukas U.; Wainstein, Pablo A.; Hauck, Christian (2022): Towards accurate quantification of ice content in permafrost of the Central Andes – Part II: an upscaling strategy of geophysical measurements to the catchment scale at two study sites. In *The Cryosphere* 16, pp. 2595–2615. DOI: 10.5194/tc-16-2595-2002.

Miesen, Floreana; Dahl, Svein Olaf; Schrott, Lothar (2021): Evidence of glacier-permafrost interactions associated with hydro-geomorphological processes and landforms at Snøhetta, Dovrefjell, Norway. In *Geografiska Annaler: Series A, Physical Geography* 103 (3), pp. 273–302. DOI: 10.1080/04353676.2021.1955539.

Milana, Juan Pablo; Maturano, Aníbal (1999): Application of Radio Echo Sounding at the arid Andes of Argentina: the Agua Negra Glacier. In *Global and Planetary Change* 22 (1-4), pp. 179–191. DOI: 10.1016/S0921-8181(99)00035-1.

Minár, Jozef; Evans, Ian S. (2008): Elementary forms for land surface segmentation: The theoretical basis of terrain analysis and geomorphological mapping. In *Geomorphology* 95 (3-4), pp. 236–259. DOI: 10.1016/j.geomorph.2007.06.003.

Monnier, Sébastien; Kinnard, Christophe (2017): Pluri-decadal (1955–2014) evolution of glacier–rock glacier transitional landforms in the central Andes of Chile (30–33° S). In *Earth Surf. Dynam.* 5 (3), pp. 493–509. DOI: 10.5194/esurf-5-493-2017.

Moore, Peter L. (2014): Deformation of debris-ice mixtures. In *Rev. Geophys.* 52 (3), pp. 435–467. DOI: 10.1002/2014RG000453.

Mueting, A.; Bookhagen, B.; Strecker, M. R. (2021): Identification of Debris-Flow Channels Using High-Resolution Topographic Data: A Case Study in the Quebrada del Toro, NW Argentina. In *JGR Earth Surface* 126 (12). DOI: 10.1029/2021JF006330.

Nelson, A.; Reuter, H. I.; Gessler, P. (2009): Chapter 3 DEM Production Methods and Sources. In: Geomorphometry - Concepts, Software, Applications, vol. 33: Elsevier (Developments in Soil Science), pp. 65–85.

Nuth, C.; Kääb, A. (2011): Co-registration and bias corrections of satellite elevation data sets for quantifying glacier thickness change. In *The Cryosphere* 5 (1), pp. 271–290. DOI: 10.5194/tc-5-271-2011.

Obu, Jaroslav; Westermann, Sebastian; Vieira, Gonçalo; Abramov, Andrey; Balks, Megan Ruby; Bartsch, Annett et al. (2020): Pan-Antarctic map of near-surface permafrost temperatures at 1 km 2 scale. In *The Cryosphere* 14 (2), pp. 497–519. DOI: 10.5194/tc-14-497-2020.

Osterkamp, T. E.; Romanovsky, V. E. (1999): Evidence for warming and thawing of discontinuous permafrost in Alaska. In *Permafrost and Periglacial Processes* 10 (1), pp. 17–37. DOI: 10.1002/(SICI)1099-1530(199901/03)10:1<17::AID-PPP303>3.0.CO;2-4.

Pabón-Caicedo, José Daniel; Arias, Paola A.; Carril, Andrea F.; Espinoza, Jhan Carlo; Borrel, Lluís Fita; Goubanova, Katerina et al. (2020): Observed and Projected Hydroclimate Changes in the Andes. In *Front. Earth Sci.* 8, Article 61. DOI: 10.3389/feart.2020.00061.

PERMOS (2019): Permafrost in Switzerland 2014/2015 to 2017/2018, Glaciological Report No. 16-19. Edited by J. Noetzli, C. Pellet, B. Staub. Cryospheric Commission of the Swiss Academy of Sciences. Available online at doi.org/10.13093/permos-rep-2019-16-19.

PERMOS (2023): Swiss Permafrost Bulletin 2022. Annual report #4 on permafrost observation in the Swiss Alps. 4th ed. Edited by J. Noetzli, Cécile Pellet. Available online at 10.13093/permos-bull-23.

Pitte, Pierre; Masiokas, Mariano; Gargantini, Hernán; Ruiz, Lucas; Berthier, Etienne; Ferri Hidalgo, Lidia et al. (2022): Recent mass-balance changes of Agua Negra glacier (30°S) in the Desert Andes of Argentina. In *J. Glaciol.* 68 (272), pp. 1197–1209. DOI: 10.1017/jog.2022.22.

Pope, A.; Scambos, T. A.; Moussavi, M.; Tedesco, M.; Willis, M.; Shean, D.; Grigsby, S. (2016): Estimating supraglacial lake depth in West Greenland using Landsat 8 and comparison with other multispectral methods. In *The Cryosphere* 10 (1), pp. 15–27. DOI: 10.5194/tc-10-15-2016.

Rangecroft, Sally; Suggitt, Andrew J.; Anderson, Karen; Harrison, Stephan (2016): Future climate warming and changes to mountain permafrost in the Bolivian Andes. In *Climatic Change* 137 (1), pp. 231–243. DOI: 10.1007/s10584-016-1655-8.

Reigaraz, A. C.; Zambrano, J. J. (1991): Unidades morfoestructurales y fenómenos neotectónicos en El norte de la província de Mendoza (Andes Centrales argentinos entre 32° y 34° de latitud sur). In *Bamberger Geografische Schriften* 11, pp. 1–21.

Réveillet, Marion; MacDonell, Shelley; Gascoin, Simon; Kinnard, Christophe; Lhermitte, Stef; Schaffer, Nicole (2020): Impact of forcing on sublimation simulations for a high mountain catchment in the semiarid Andes. In *The Cryosphere* 14 (1), pp. 147–163. DOI: 10.5194/tc-14-147-2020.

RGIK (2022): IPA Action Group: Rock glacier inventories and kinematics. 22 Newsletter (04.02.3022): Rock glacier velocity as an associated parameter of ECV Permafrost. Available online at https://www.unifr.ch/geo/geomorphology/en/research/ipa-action-group-rock-glacier/, updated on 6/30/2023, checked on 6/30/2023.

RGIK (2023a): InSAR-based kinematic attribute in rock glacier inventories. Practical InSAR Guidelines v.4.0. IPA Action Group Rock glacier inventories and kinematics, pp °1-33.

RGIK (2023b): Rock Glacier Velocity as an associated parameter of ECV Permafrost. Baseline Concepts. IPA Action Group Rock glacier inventories and kinematics, pp°1-12.

Rieg, Lorenzo; Klug, Christoph; Nicholson, Lindsey; Sailer, Rudolf (2018): Pléiades Tri-Stereo Data for Glacier Investigations—Examples from the European Alps and the Khumbu Himal. In *Remote Sensing* 10 (10), p. 1563. DOI: 10.3390/rs10101563.

Rivera, Juan A.; Otta, Sebastián; Lauro, Carolina; Zazulie, Natalia (2021): A Decade of Hydrological Drought in Central-Western Argentina. In *Front. Water* 3, Article 640544. DOI: 10.3389/frwa.2021.640544.

Robson, Benjamin Aubrey; MacDonell, Shelley; Ayala, Álvaro; Bolch, Tobias; Nielsen, Pål Ringkjøb; Vivero, Sebastián (2022): Glacier and rock glacier changes since the 1950s in the La Laguna catchment, Chile. In *The Cryosphere* 16 (2), pp. 647–665. DOI: 10.5194/tc-16-647-2022.

Roer, Isabelle (2005): Rock glacier kinematics in a high mountain geosystem. Dissertation. University of Bonn, Bonn, Germany. Department of Geography.

Ruiz, L.; Bodin, Xavier (2015): Analysis and improvement of surface representativeness of high resolution Pléiades DEMs: Examples from glaciers and rock glaciers in two areas of the Andes. In *Geomorphometry.org*. DOI: 10.13140/RG.2.1.4328.2963.

Schaffer, Nicole; MacDonell, Shelley; Réveillet, Marion; Yáñez, Eduardo; Valois, Rémi (2019): Rock glaciers as a water resource in a changing climate in the semiarid Chilean Andes. In *Regional Environmental Change* 19 (5), pp. 1263–1279. DOI: 10.1007/s10113-018-01459-3.

Schneevoigt, N. J.; Schrott, L. (2006): Linking geomorphic systems theory and remote sensing: a conceptual approach to Alpine landform detection (Reintal, Bavarian Alps, Germany). In *Geogr. Helv.* 61 (3), pp. 181–190. DOI: 10.5194/gh-61-181-2006.

Schneevoigt, Nora Jennifer (2012): Remote Sensing in Geomorphological and Glaciological Research. Dissertation. University of Oslo, Oslo, Norway. Department of Geosciences, Faculty of Mathematics and Natural Sciences.

Schrott, Lothar (1994): Die Solarstrahlung als steuernder Faktor im Geosystem der subtropischen semiariden Hochanden (Agua Negra, San Juan, Argentinien). In *Heidelberger Geographische Arbeiten* 94.

Schrott, Lothar (1996): Some geomorphological-hydrological aspects of rock glaciers in the Andes (San Juan, Argentina). In *Zeitschrift für Geomorphologie. Supplementband* 104, pp. 161–173.

Schrott, Lothar (1998): The hydrological significance of high mountain permafrost and its relation to solar radiation. A case study in the high Andes of San Juan, Argentina. In *Bamberger Geographische Schriften* 15, pp. 71–84.

Schrott, Lothar; Bell, Rainer; Blöthe, Jan Henrik (2024): Chapter 5 - Mountain hazards and permafrost degradation. In Stefan Schneiderbauer, Paola Fontanella Pisa, John F. Shroder, Joerg Szarzynski (Eds.): Safeguarding Mountain Social-Ecological Systems: Elsevier, pp. 31–41.

Schrott, Lothar; Götz, Joachim (2013): The periglacial environment in the semiarid and arid Andes of Argentina - hydological significance and research frontiers. In : Forschen im Gebirge / Investigating the mountains / investigando las Montanas, vol. 5.

Schwalbe, Ellen; Maas, Hans-Gerd (2017): The determination of high-resolution spatio-temporal glacier motion fields from time-lapse sequences. In *Earth Surf. Dynam.* 5 (4), pp. 861–879. DOI: 10.5194/esurf-5-861-2017.

Seelig, Simon; Krainer, Karl; Tropper, Peter; Pettauer, Michael; Leis, Albrecht; Wagner, Thomas et al. (2025): Origin and Evolution of High Nickel Concentrations in Rock Glacier Springs. In *ACS EST Water*, Article acsestwater.5c00542. DOI: 10.1021/acsestwater.5c00542.

Shean, David E.; Alexandrov, Oleg; Moratto, Zachary M.; Smith, Benjamin E.; Joughin, Ian R.; Porter, Claire; Morin, Paul (2016): An automated, open-source pipeline for mass production of digital elevation models (DEMs) from very-high-resolution commercial stereo satellite imagery. In *ISPRS Journal of Photogrammetry and Remote Sensing* 116, pp. 101–117. DOI: 10.1016/j.isprsjprs.2016.03.012.

Śledź, Szymon; Ewertowski, Marek W.; Piekarczyk, Jan (2021): Applications of unmanned aerial vehicle (UAV) surveys and Structure from Motion photogrammetry in glacial and periglacial geomorphology. In *Geomorphology* 378, p. 107620. DOI: 10.1016/j.geomorph.2021.107620.

Smith, M. J.; Pain, C. F. (2009): Applications of remote sensing in geomorphology. In *Progress in Physical Geography: Earth and Environment* 33 (4), pp. 568–582. DOI: 10.1177/0309133309346648.

Smith, M. W.; Carrivick, J. L.; Quincey, D. J. (2016): Structure from motion photogrammetry in physical geography. In *Progress in Physical Geography: Earth and Environment* 40 (2), pp. 247–275. DOI: 10.1177/0309133315615805.

Smith, Sharon L.; O'Neill, H. Brendan; Isaksen, Ketil; Noetzli, Jeannette; Romanovsky, Vladimir E. (2022): The changing thermal state of permafrost. In *Nat Rev Earth Environ* 3 (1), pp. 10–23. DOI: 10.1038/s43017-021-00240-1.

Stammler, Melanie; Blöthe, Jan; Flöck, Fabian; Bell, Rainer; Schrott, Lothar (2025a): Dos Lenguas rock glacier kinematics stable despite warming trend (2016–2024): Surface changes and the role of topography and climate in the Dry Andes of Argentina. In *Earth Surface Processes and Landforms* 50 (11). DOI: 10.1002/esp.70151.

Stammler, Melanie; Blöthe, Jan; Flöck, Fabian; Bell, Rainer; Schrott, Lothar (2025b): UAV-based optical imagery, digital elevation models and hillshades of Dos Lenguas rock glacier / Argentinean Dry Andes (30ºS, 69ºW; 2016, 2018, 2022, 2024) and daily static optical imagery (2023-2024) [dataset]. In *PANGAEA*. Available online at https://doi.org/10.1594/PANGAEA.979876.

Stammler, Melanie; Cusicanqui, Diego; Bell, Rainer; Robson, Benjamin; Bodin, Xavier; Blöthe, Jan; Schrott, Lothar (2024): Vertical surface change signals of rock glaciers: combining UAV and Pléiades imagery (Agua Negra, Argentina). In *Proceedings of the 12th International Conference on Permafrost*. DOI: 10.52381/ICOP2024.138.1.

Strozzi, Tazio; Caduff, Rafael; Jones, Nina; Barboux, Chloé; Delaloye, Reynald; Bodin, Xavier et al. (2020): Monitoring Rock Glacier Kinematics with Satellite Synthetic Aperture Radar. In *Remote Sensing* 12 (3), p. 559. DOI: 10.3390/rs12030559.

Tapia Baldis, Carla; Trombotto Liaudat, Dario (2019): Rockslides and rock avalanches in the Central Andes of Argentina and their possible association with permafrost degradation. In *Permafrost and Periglacial Processes* 30 (4), pp. 330–347. DOI: 10.1002/ppp.2024.

Tedesco, M. (2014): Remote sensing and the cryosphere. In: Remote Sensing of the Cryosphere: John Wiley & Sons, Ltd, pp. 1–16.

Thorn, C. (1988): An Introduction to Theoretical Geomorphology. 1st ed.: Springer Dordrecht.

Trombotto, D.; Borzotta, E. (2009): Indicators of present global warming through changes in active layer-thickness, estimation of thermal diffusivity and geomorphological observations in the Morenas Coloradas rockglacier, Central Andes of Mendoza, Argentina. In *Cold Regions Science and Technology* 55 (3), pp. 321–330. DOI: 10.1016/j.coldregions.2008.08.009.

Trombotto, Dario (2000): Survey of cryogenic processes, periglacial forms and permafrost conditions in South America. In *Revista do Instituto Geológico* 21 (1-2), pp. 33–55. DOI: 10.5935/0100-929X.20000004.

Trombotto, Dario; Buk, Enrique; Hernández, José (1997): Monitoring of Mountain Permafrost in the Central Andes, Cordon del Plata, Mendoza, Argentina. In *Permafrost and Periglacial Processes* 8 (1), pp. 123–129. DOI: 10.1002/(SICI)1099-1530(199701)8:1<123::AID-PPP242>3.0.CO;2-M.

van der Sluijs, Jurjen; Kokelj, Steven; Fraser, Robert; Tunnicliffe, Jon; Lacelle, Denis (2018): Permafrost Terrain Dynamics and Infrastructure Impacts Revealed by UAV Photogrammetry and Thermal Imaging. In *Remote Sensing* 10 (11), p. 1734. DOI: 10.3390/rs10111734.

Villarroel, Cristian; Tamburini Beliveau, Guillermo; Forte, Ana; Monserrat, Oriol; Morvillo, Monica (2018): DInSAR for a Regional Inventory of Active Rock Glaciers in the Dry Andes Mountains of Argentina and Chile with Sentinel-1 Data. In *Remote Sensing* 10 (10), p. 1588. DOI: 10.3390/rs10101588.

Villarroel, Cristian Daniel; Forte, Ana Paula; Ortiz, Diana Agostina; Tamburini Beliveau, Guillermo; Güell, Arturo (2020): Active layer and permafrost thickness in rock glaciers derived from geophysical methods in the semiarid Andes of Argentina. In *Geomorphology* 365, p. 107249. DOI: 10.1016/j.geomorph.2020.107249.

Villarroel, Cristian Daniel; Ortiz, Diana Agostina; Forte, Ana Paula; Tamburini Beliveau, Guillermo; Ponce, David; Imhof, Armando; López, Andrés (2022): Internal structure of a large, complex rock glacier and its significance in hydrological and dynamic behavior: A case study in the semi-arid Andes of Argentina. In *Permafrost and Periglacial Processes* 33 (1), pp. 78–95. DOI: 10.1002/ppp.2132.

Vivero, Sebastián; Bodin, Xavier; Farías-Barahona, David; MacDonell, Shelley; Schaffer, Nicole; Robson, Benjamin Aubrey; Lambiel, Christophe (2021): Combination of Aerial, Satellite, and UAV Photogrammetry for Quantifying Rock Glacier Kinematics in the Dry Andes of Chile (30°S) Since the 1950s. In *Front. Remote Sens.* 2, Article 784015. DOI: 10.3389/frsen.2021.784015.

Vivero, Sebastián; Lambiel, Christophe (2024): Annual surface elevation changes of rock glaciers and their geomorphological significance: Examples from the Swiss Alps. In *Geomorphology* 467, p. 109487. DOI: 10.1016/j.geomorph.2024.109487.

Wahrhaftig, C.; Cox, A. (1959): Rock Glaciers in the Alaska Range. In *GSA Bulletin* 70 (4), p. 383. DOI: 10.1130/0016-7606(1959)70[383:RGITAR]2.0.CO;2.

Westoby, M. J.; Brasington, J.; Glasser, N. F.; Hambrey, M. J.; Reynolds, J. M. (2012): 'Structure-from-Motion' photogrammetry: A low-cost, effective tool for geoscience applications. In *Geomorphology* 179, pp. 300–314. DOI: 10.1016/j.geomorph.2012.08.021.

Wheaton, Joseph M.; Brasington, James; Darby, Stephen E.; Sear, David A. (2010): Accounting for uncertainty in DEMs from repeat topographic surveys: improved sediment budgets. In *Earth Surface Processes and Landforms* 35 (2), pp. 136–156. DOI: 10.1002/esp.1886.

Williams, Richard (2012): DEMs of difference. In *Geomorphological Techniques* 2 (3.2).

WMO; United Nations Environment Programme; International Science Council; Intergovernmental Oceanographic Commission of the United Nations Educational, Scientific and Cultural Organization (2022): The 2022 GCOS Implementation Plan (GCOS-244). World Meteorological Organization (WMO). Geneva, Switzerland.

Xiong, Liyang; Tang, Guoan; Yang, Xin; Li, Fayuan (2021): Geomorphology-oriented digital terrain analysis: Progress and perspectives. In *J. Geogr. Sci.* 31 (3), pp. 456–476. DOI: 10.1007/s11442-021-1853-9.

Zalazar, Laura Viviana; Ferri Hidalgo, Lidia; Castro, Mariano Agustin; Gargantini, Hernan; Giménez, Melisa Mariel; Pitte, Pedro Miguel et al. (2017): Glaciares de Argentina: Resultados preliminares del Inventario Nacional de Glaciares. In *Revista de Glaciares y Ecosistemas de Montaña* 2, pp. 13–22.

Appendix

Paper 1 **Stammler, M.**, Cusicanqui, D., Bell, R., Robson, B., Bodin, X., Blöthe, J., Schrott, L., 2024. Vertical surface change signals of rock glaciers: combining UAV and Pléiades imagery (Agua Negra, Argentina). Proceedings of the 12th International Conference on Permafrost **(**ICOP). Whitehorse / Canada. DOI: *10.52381/ICOP2024.138.1*

Paper 2 **Stammler, M.**, Blöthe, J., Flöck, F., Bell, R., Schrott, L., 2025. Dos Lenguas rock glacier kinematics stable despite warming trend (2016–2024): Surface changes and the role of topography and climate in the Dry Andes of Argentina. Earth Surface Processes and Landforms 50. DOI: *10.1002/esp.70151*

Including its supplementary material.

Paper 3 **Stammler, M.**, Blöthe, J., Cusicanqui, D., Ebert, S., Bell, R., Bodin, X. and Schrott, L., 2025. Glacial decline next to stable permafrost in the Dry Andes? Vertical glacier surface changes and rock glacier kinematics based on Pléiades imagery (Rodeo basin / Argentina, 2019-2025). The Cryosphere. *Submitted*.

As submitted to The Cryosphere and including its supplementary material.

Vertical surface change signals of rock glaciers: combining UAV and Pléiades imagery (Agua Negra, Argentina)

Melanie Stammler[1], Diego Cusicanqui[2], Rainer Bell[1], Benjamin Robson[3], Xavier Bodin[4], Jan Blöthe[5] & Lothar Schrott[1]

[1]*Department of Geography, University of Bonn, Bonn, Germany*

[2]*Institut des Sciences de la Terre (ISTerre), CNRS/Université Grenoble Alpes, Grenoble, France*

[3]*Department of Earth Science, University of Bergen, Bergen, Norway*

[4]*Laboratoire EDYTEM, CNRS/Université Savoie Mont-Blanc, Le Bourget du Lac, France*

[5]*Institute of Environmental Social Sciences and Geography, University of Freiburg, Freiburg, Germany*

ABSTRACT

Detailed analyses of rock glacier change are essential in the Dry Andes, where rock glaciers store essential waters whose input to hydrological systems are forecast to gain relative importance due to climate change. The rugged terrain and high elevation present challenges when conducting high-resolution monitoring with demanding UAV flying, and steep slopes that can be occluded. Degradation processes often manifest themselves in surface changes whose investigation of local patterns assists in understanding the landforms' runoff contribution.

We investigate vertical surface change on Dos Lenguas (San Juan, Argentina) using UAV flights and tri-stereo, panchromatic Pléiades imagery (austral summers 2022/2023). We compare three photogrammetric processing strategies to assess which method can be used to resolve the subtlest vertical rock glacier changes. The processing of Pléiades imagery in Agisoft Metashape Professional leads to the most appropriate representation of ridges and furrows, whereas the DEMs produced in Catalyst Professional contain noise larger than the magnitude of annual change. We find that processing Pléiades imagery in Ames Stereo Pipeline allows for the DEMs of Difference to reproduce vertical rock glacier surface change to an extent suitable for a geomorphological interpretation in terms of magnitude and pattern, with high similarity to UAV based results and low errors. We suggest combining UAV and Pléiades imagery to bridge detailed small-scale and less detailed regional assessment. We envision that this opens up novel possibilities for interpreting previously undetected change signals. These could provide new insights in our process-response understanding of the high Andean (peri)glacial landscape and its hydrological significance.

1 INTRODUCTION

Periglacial and cryogenic meltwaters represent an essential water source to domestic, agricultural and industrial water use in the Dry Andes and their foreland (Trombotto and Borzotta 2009; Schrott 1994; Schrott and Götz 2013), as in the study area of the Agua Negra catchment (San Juan Province/Argentina, 30ºS and 69ºW). Climate change induced melting of glaciers and snow, as well as the degradation of permafrost pose risk in terms of water scarcity. While glacial and cryogenic water storages are diminishing quickly (Dussaillant et al. 2019; Masiokas et al. 2020; Ferri et al. 2020; Pitte et al. 2022), rock glaciers show a delayed water release to surface runoff. Their ice and water storage capacities are primary controls on groundwater recharge (Halla et al. 2021; Geiger et al. 2014) and discharge contribution. Already today, (peri)glacial runoff contribution is specifically important in areas characterised by scarce precipitation; with increasing hydrological significance towards the future (Arenson et al. 2022; Masiokas et al. 2020).

Rock glaciers and glaciers which exist in close proximity suggest mutual (de)coupling relations (Cusicanqui et al. 2023). Examples are acting as mechanical entity (Etzelmüller and Hagen 2005) or water becoming an agent of transient interaction (Miesen et al. 2021). Surface changes are indicators of alterations in melting/thawing processes. Surface change analysis can explain not only local patterns of surface variations but also meltwater contribution to runoff (Blöthe et al. 2021; Halla et al. 2021; Vivero and Lambiel 2019). It is hypothesized, that co-existence of glacial and periglacial systems, e.g., moraine-derived rock glaciers, showcase diverging surface processes to non-glacially impacted periglacial systems, e.g., talus-derived rock glaciers, in terms of their magnitude and pattern due to interim water storage. Thus, it is important to move from single landform-focused analyses to investigating change signals for multiple landforms, over larger areas. For an accurate and precise understanding of the surface changes and related processes (thawing and (re)freezing of ice bodies and active layer, degradation of permafrost), highly resolved elevation data is crucial (Mueting et al. 2021; Robson et al. 2022).

Stereophotogrammetry allows for a generation of high-resolution DEMs which can be intercompared to derive elevation changes (Halla et al. 2021; Robson et al. 2022). While UAV surveying offers highest resolutions, these acquisitions are dependent on favourable weather conditions and can be challenging at high altitudes. Sub-metre tri-stereo satellite sensors such as Pléiades enable DEM generation with resolutions of up to 1 m (e.g., Bagnardi et al. 2016) at spatial coverage much higher than common UAV surveys.

https://doi.org/10.52381/ICOP2024.138.1

We test combining Pléiades and UAV imagery to interpret previously undetected change signals. This might provide new insight into our process-response understanding of the high Andean (peri)glacial landscape and its hydrological significance. We (i) generate high-resolution DEMs based on tri-stereo, panchromatic Pléiades data and repeated UAV flights (austral summers 2022/2023) for Dos Lenguas rock glacier, (ii) compare results from three software, (iii) evaluate the Pléiades DEMs of Difference (DoDs) against the UAV DoD, and (iv) apply the developed Pléiades workflow for El Paso rock glacier. This research is a proof of concept to allow future large(r) scale investigation.

1.1 Study area

The Agua Negra catchment is located in the Western part of San Juan Province, Argentina (30°S and 69°W). It is part of the Cordillera Principal, extents over 435 km² (Schrott 1994) and hosts glacial and periglacial landforms (Figure 1). Today's (peri)glacial high-alpine landscape in the catchment represents a 'geomorphic palimpsest' (Hewitt 2002) of relict, transient and replacement forms. As part of the Dry Andes, the catchment is characterized by extremely low mean annual precipitation (~250 mm) and constant high solar radiation (Croce and Milana 2002; Lliboutry et al. 1998; Schrott 1994). Surface temperatures and upper ground thermal regimes are mainly controlled by incoming solar radiation (Schrott 1994). The active layer in areas underlain by permafrost generally varies between 2–3 m; reduced to a few centimetres above 5000 m where continuous permafrost is present (Halla et al. 2021).

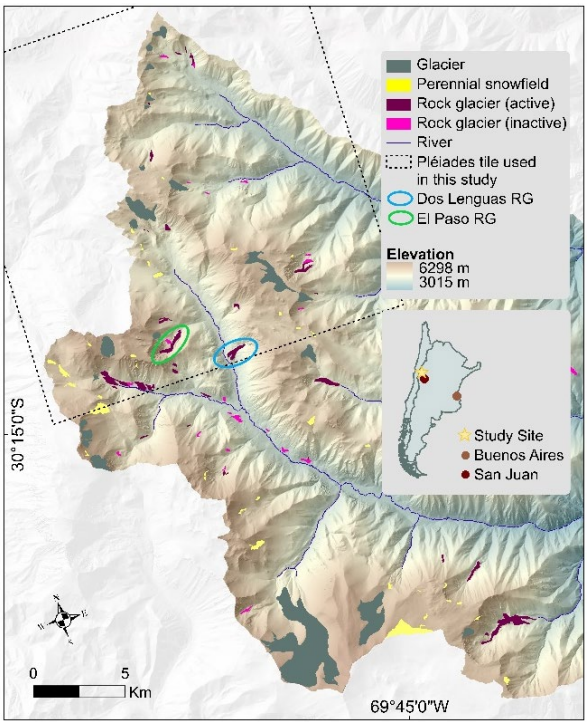

Figure 1. Upper part of the Agua Negra catchment with typical (peri)glacial landform distribution. Hillshade based on TanDEM-X DEM, elevation on Pléiades DEM. All landform polygons by IANIGLA-CONICET (2018).

2 METHODOLOGY

We use tri-stereo, panchromatic Pléiades data acquired in 2022/2023 for DEM and DoD generation on Dos Lenguas and El Paso rock glaciers. We apply three software to study their impact on the generated products. A Phantom DJI 4 RTK was used for conducting two UAV surveys on Dos Lenguas to obtain very high resolution DEMs to compare to the Pléiades DEMs (Table 1). UAV imagery was collected at constant elevation above a TanDEM-X DEM (12 m, 2011–2014). We measured 20 points with a Trimble DGNSS (R8s base/R2 rover, RTK) with vertical and horizontal precisions of < 0.02 m; for georeferencing (ground control points, GCPs) and quality check (control points, CPs).

Table 1. Acquisition parameters for UAV flights on Dos Lenguas (Figure 1) and the Pléiades data acquisition.

UAV model	Phantom 4 RTK (Terrain Awareness)	
Date (dd.mm.yy)	24.03.22	12.02.23
Number of images	1509	2160
Flight altitude, speed	40 m, 5 m/s	50 m, 5 m/s
Overlap (ver/hor.)	65/65 %	70/70 %
GCPs / CPs	15/5	15/5
Geometry	Tri-stereo (panchromatic, multi-spectral)	
Date (dd.mm.yy)	08.02. to 22.02.22	13.02. to 20.02.23

Agisoft Metashape Professional (Agisoft) utilizes structure-from-motion techniques to obtain DEMs (Smith et al. 2016) on UAV and satellite imagery. We base the sparse clouds on all imagery, independent of their date of acquisition (Cook and Dietze 2019; Haas et al. 2021), separate the aligned cameras per acquisition and georeference the UAV sparse cloud using 15 GCPs and 5 CPs (Figure 2A). For the Pléiades data, we rely on the rational polynomial coefficients (RCPs) for solving the exterior orientation and use higher key and tie point limits than for the UAV processing. We build dense clouds using the 'high' quality and 'moderate' depth filtering options before generating the DEMs.

Catalyst Professional (Catalyst) follows a traditional photogrammetric approach and is well used for glacial and periglacial change analysis. We create maximum overlapping epipolar images and generate DEMs using the semi-global matching algorithm (SGM), also making use of the RCPs.

Ames Stereo Pipeline (ASP, Beyer et al. 2018) is open source and freely available. We project the Pléiades imagery using a SRTM DEM (30 m) as seed DEM. We proceed with the projected imagery to derive DEMs applying the SGM algorithm using both tri-stereo pairs without GCPs. Given our local focus, we do not fill gaps (due to only minimal presence) and do not correct sensor undulations.

We co-register the 2023 Pléiades DEMs to the 2022 Pléiades DEMs clipped by study site and paired by software following Nuth and Kääb (2011) in DEMCOREG (Shean et al. 2016). During co-registration, we assume non-rock glacier surfaces to be stable with slopes < 40°, validated

using the GCPs/CPs. When evaluating the Pléiades DoDs against the UAV DoD, we focus on the rock glacier outlines by IANIGLA-CONICET (2018) as we use them to define stable terrain during co-registration (Figure 3BD).

3 RESULTS

3.1 Digital elevation models (DEMs)

With a maximum UAV DEM resolution for Dos Lenguas of 3.09 cm/pixel (2022) and 2.76 cm/pixel (2023), modelled GCP locations deviate approximately 1 cm from DGNSS measurements. The total error in x, y and z directions for 2022 is 0.6 cm, 1.0 cm, and 0.25 cm. The total error for 2023 is similar with 0.6 cm, 0.9 cm, and 0.3 cm. The DEM reproduces known points not included in the model (CPs) with a maximum distance of 10 cm. Deviations between the modelled CPs and DGNSS measurements are lower on stable terrain, and higher in the upper part of the rock glacier.

The Pléiades DEMs processed in Agisoft appear clearest and with furrows and ridges produced most similarly to the UAV DEMs (Figures 2B and 4). The processed Pléiades DEM in Catalyst leads to coarser surfaces and 'flattened' microtopography (Figures 2C and 4). The ASP results occur smoothest with limitations in representing boulders in the rock glaciers' upper part while portraying furrows and ridges (Figures 2D and 4). None of the DEMs has voids over the target site. All Pléiades DEMs are generated with a resolution of 1 m.

The offset between DEMs prior to co-registration is largest for Agisoft, followed by Catalyst and ASP (Table 2). ASP DEMs are most consistent in their offset compared to 20 DGNSS measurements (GCP/CPs; Figure 2A; Table 3). The spatial distribution of error (Eltner et al. 2016; James et al. 2019) is most consistent in time for the ASP DEMs, based on a comparison of the 5 highest Pléiades DEM deviations from the 20 DGNSS measurements. In 2022, errors are largest in the upper part of Dos Lenguas r (Agisoft, Catalyst; Figure 2B, C) and at the sides and front (ASP, Figure 2D). In 2023, largest errors occur at the center, front and the sides (Agisoft, Figure 2B) and only the front and sites (Catalyst, ASP; Figure 2C, D). While differences in absolute elevation exist between processing strategies, co-registration per processing strategy is efficient (Figure 4).

Table 2. Linear co-registration shifts calculated over stable terrain between respective Pléiades DEMs, relying on RCP files for DEM generation. Co-registration of 2023 Pléiades to 2022 Pléiades DEMs following Nuth and Kääb (2011) in DEMCOREG (Shean et al. 2016).

	Shift in x (m)	Shift in y (m)	Shift in z (m)
22/23: Agisoft	-35.84	15.06	15.22
22/23: Catalyst	-8.41	3.70	32.08
22/23: ASP	-0.35	-0.04	1.15

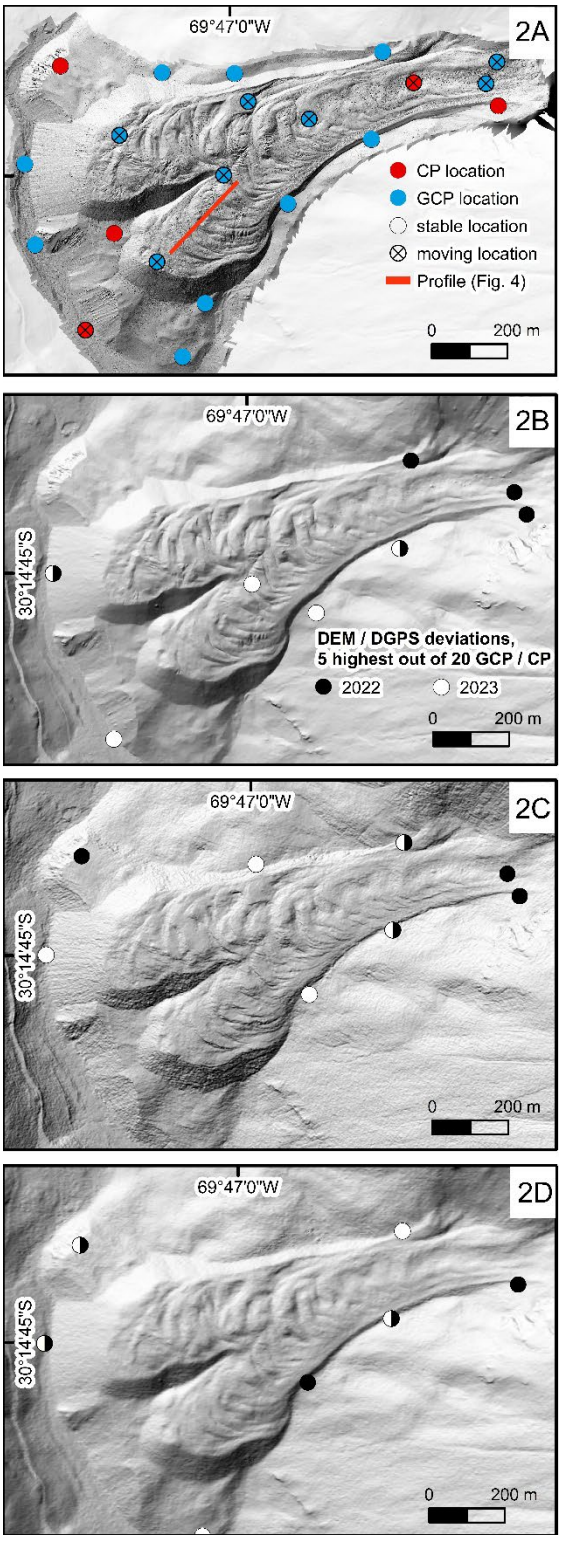

Figure 2. DEM visual appearance of Dos Lenguas rock glacier (2022) based on UAV/Agisoft (A), Pléiades/ Agisoft (B), Pléiades/Catalyst (C), and Pléiades/ASP (D). GCP/CP locations measured 2022 and 2023. Line indicates the profile location taken for Figure 4 (A). For explanation on deviations (2B-D), see chapter 3.1.

Table 3. Consistency of DEM offsets calculated as standard deviations (σ) of the differences between 20 known DGNSS points (each for 2022 and 2023) and the respective DEM, similar to Mueting et al. (2021). As we rely on the RCP files for DEM generation, none of the DGNSS measurements is included in the DEM.

	σ 2022	σ 2023
DGNSS to Agisoft DEM	6.46	2.48
DGNSS to Catalyst DEM	2.15	1.13
DGNSS to ASP DEM	0.83	1.02

3.2 DEMs of Difference (DoDs)

Given its very high resolution, the UAV DoD shows magnitude and distribution of vertical surface change on Dos Lenguas rock glacier between 2022 and 2023 in most detailed manner (Figure 3A; 5 cm resolution based on resampled UAV DEMs 2022 and 2023 for better comparison between UAV DEMs). The Pléiades DoD processed in Agisoft overestimates negative change throughout the entire surface of the rock glacier compared to the UAV DoD, yet appropriately represents ridges and furrows (Figure 3B). The Pléiades DoD processed in Catalyst overestimates negative change particularly towards the lower part of the rock glacier and does not adequately portray the microtopography, especially in comparison to the UAV DoD but despite being characterized by the same resolution also compared to the Pléiades DEM processed in Agisoft (Figure 3C). The processing of Pléiades imagery in ASP results in a DoD most similar to the UAV results in terms of magnitude as well as distribution of vertical surface change (Figure 3D).

Pixel frequencies for vertical surface change are unimodal and normally distributed independent of image source and processing strategy (Figure 5). Highest surface changes do not exceed ± 2 m with most changes occurring below zero. The UAV processing in Agisoft and the Pléiades processing in ASP show most similar distributions. The Pléiades processing in Agisoft and Catalyst leads to wider distributions with lower maxima, and with overall shifts to more negative values. The magnitude of calculated negative and positive surface changes between 2022 and 2023 (mean change below or above zero, uncertainty based on stable terrain for Pléiades DoDs) are higher for the Pléiades processing in Agisoft and Catalyst, and lower for the UAV processing in Agisoft and the Pléiades processing in ASP (Table 4).

Pléiades DoD based vertical surface change for El Paso rock glacier between 2022 and 2023 (Figure 1) is similar to vertical surface change on Dos Lenguas rock glacier during the same time period. This applies to the range of the pixel frequency distribution of vertical surface changes (below ± 2 m; Figures 5 and 6), the similarity of the magnitude of change of the Pléiades processing in ASP (Tables 4 and 5), and the lower mean negative and higher mean positive changes when processing Pléiades imagery in Agisoft and Catalyst in comparison to ASP (Figures 5 and 6; Tables 4 and 5).

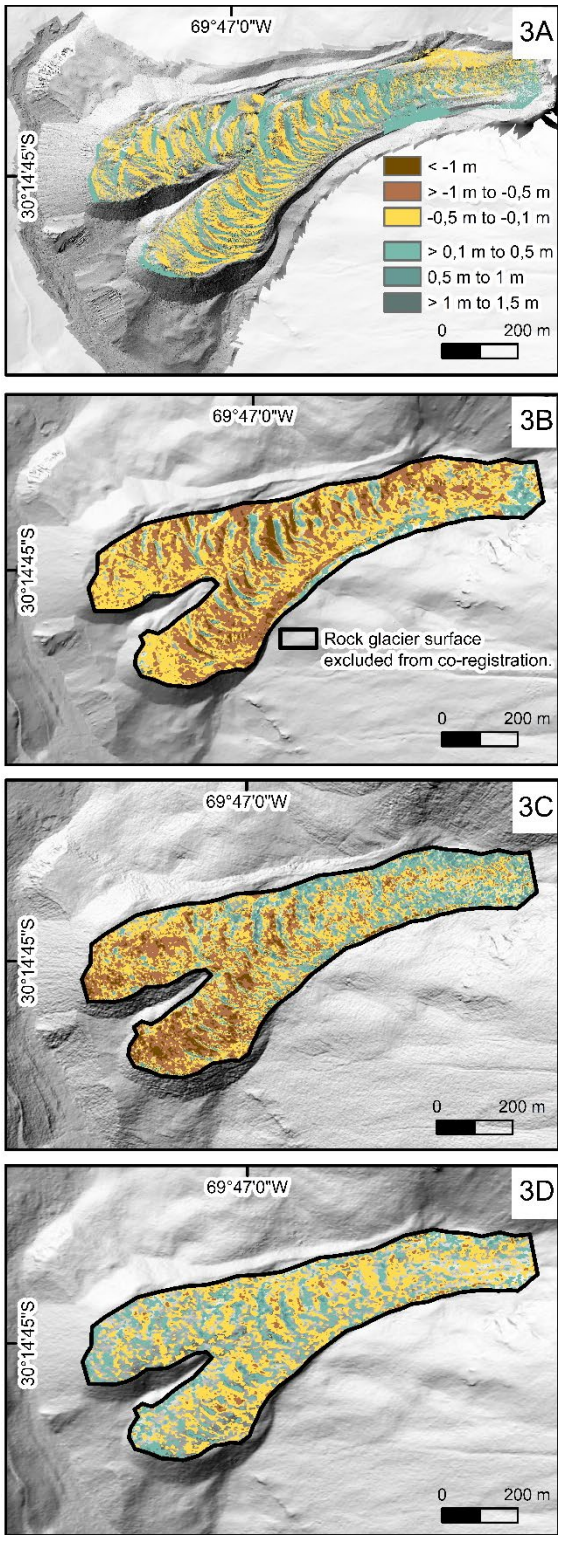

Figure 3. Vertical surface change (m) on Dos Lenguas rock glacier (2022/2023) based on UAV/Agisoft (A), Pléiades/Agisoft (B), Pléiades/Catalyst (C), and Pléiades/ASP (D). The rock glacier outline (3B–D) as mapped by IANIGLA-CONICET (2018) is used to exclude the rock glacier surface from co-registration.

Table 4. Mean negative and positive vertical surface changes (m) on Dos Lenguas rock glacier (2022–2023).

	Mean negative (m)	Mean positive (m)
UAV Agisoft	-0.16	0.16
Pléiades Agisoft	-0.49 ± 0.09	0.24 ± 0.09
Pléiades Catalyst	-0.47 ± 0.08	0.29 ± 0.08
Pléiades ASP	-0.19 ± 0.01	0.17 ± 0.01

Table 5. Mean negative and positive vertical surface changes (m) on El Paso rock glacier (2022 – 2023).

	Mean negative (m)	Mean positive (m)
Pléiades Agisoft	-0.28 ± 0.04	0.22 ± 0.04
Pléiades Catalyst	-0.26 ± 0.03	0.24 ± 0.03
Pléiades ASP	-0.19 ± 0.02	0.15 ± 0.02

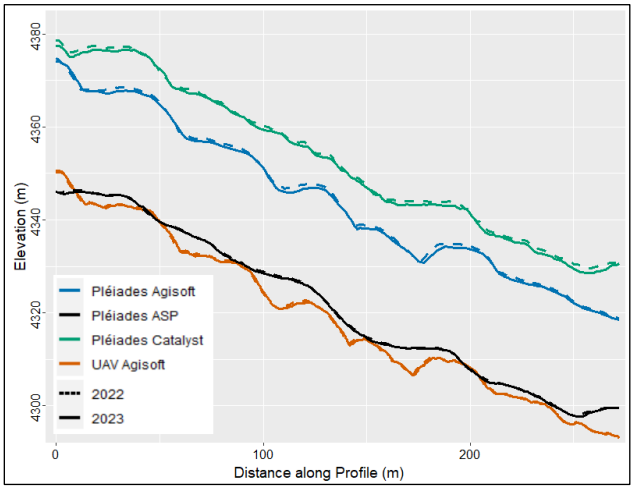

Figure 4. Surface profiles across the UAV and Pléiades DEMs on Dos Lenguas rock glacier, separated by processing strategy. For the profile location, see Figure 2A.

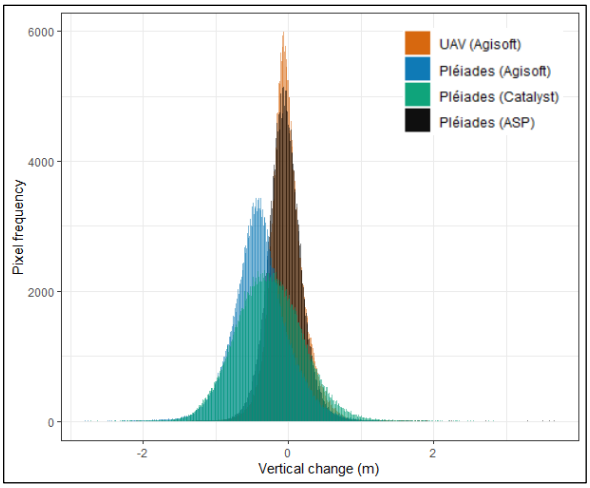

Figure 5. Vertical surface change (m) for Dos Lenguas rock glacier (2022–2023), separated by image source and processing strategy.

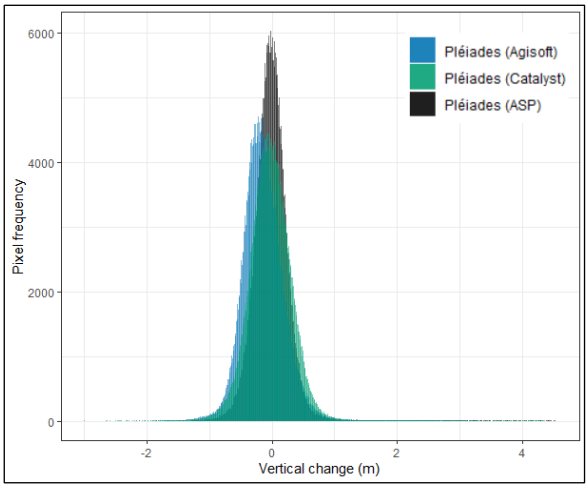

Figure 6. Vertical surface change (m) for El Paso rock glacier (2022–2023), separated by processing strategy.

4 Discussion

4.1 Comparison of processing strategies for DEM and DoD generation

Despite using the same Pléiades imagery as input, the DEMs vary distinctively in visual appearance (Figure 2B–D), quality and robustness (Tables 2 and 3) and absolute elevation (Figure 4). These variations caused by the three processing strategies propagate and lead to differences in calculated vertical surface change on Dos Lenguas rock glacier between 2022/2023 visually (Figure 3B–D), in pixel frequency distribution (Figure 5), and in terms of mean change values (Table 4). The differences not only hold true for Dos Lenguas but also for El Paso rock glacier (Figure 6; Table 5).

Our processing strategy for Pléiades imagery in Agisoft outperforms the Catalyst and ASP results in reproducing coherent furrows and ridges as well as landform neighbouring ridges and erosional gullies (Figure 2B). We assume that for this reason the Agisoft Pléiades processing is the sole strategy that shows deposition on the rock glacier's orographic right side slope (Figure 3B). Agisoft allows a combined processing of Pléiades tiles (Figure 1; extent of tile used for this study), enabling smooth transitions between overlapping tiles and direct, unrestricted investigation of rock glaciers located close to tile edges. We hypothesize that to the disadvantage, this combined processing causes distortions resulting in the shifts between the DEMs before co-registration and the poor consistency of offsets between DEMs and DGNSS measurements (Tables 2 and 3). We interpret the

inconsistency of the spatial error distribution throughout time as additional indication of low data robustness (Figure 2B). Potentially due to these limitations, the Agisoft Pléiades DoDs overestimate negative vertical surface change for the entire rock glacier, compared to the UAV results.

Our Pléiades processing strategy in Catalyst leads to 'flattened' and smoothed ridges on the DEMs (Figures 2C and 4). This effect propagates to the DoD with the vertical surface change in the lower part of the rock glacier being similar in magnitude to the Pléiades based results in Agisoft but less coherent with and confined to the microtopography (Figure 3C). The maximum of the Pléiades Catalyst based pixel frequency distribution is more similar to the UAV based results than the Pléiades Agisoft processing (Figure 5). However, this is caused by the balancing of overestimation of negative changes in the lower and of positive changes in the upper part compared to the UAV DoD (Figure 3C; Table 4), hence, is no sign of quality of the dataset.

The ASP processing of Pléiades imagery clearly stands out in its similarity of the pixel frequency distribution of vertical surface change and its mean negative and positive change in comparison to the Agisoft UAV DoD (Figure 5; Table 4). With the ability to gauge the errors of our UAV based results, we deem the ASP based results for the Pléiades data as most correct. This corresponds well to the highest overall data quality (Tables 2 and 3) and the highest consistency of spatial error (Figure 2D) of the ASP Pléiades analysis. The example highlights that Agisoft performs better when used for processing UAV imagery, than Pléiades imagery. For processing Pléiades data, ASP can clearly be attributed the best performance in terms of data quality and robustness. In terms of visualisation it lacks, e.g., the ability of reproducing single rocks on in the rock glaciers' root zone, in comparison to the Agisoft Pléiades DEM. We hypothesise that the smoothing performed when applying the SGM is causing this difference. This might also explain the similarity of the Catalyst and ASP derived profiles (Figure 4) as in both cases SGM is used for image correlation.

Co-registration significantly reduces shifts between the 2022 and 2023 Pléiades DEMs independent of processing strategy and notably improves the quality of the DoDs. The shift that occurs for our Agisoft and Catalyst results are uncommonly high (Table 2). Rieg et al. (2018) generate Pléiades based DEMs using a SGM algorithm available in ERDAS IMAGINE along with the RPC files and, depending on study site, automatically identified and manually controlled tie points (TPs) or GCPs. They investigate glaciers in the European Alps and the Khumbu Himal and encounter maximum offsets of 4 m, -3.2 m and 4.8 m in x, y and z directions. In comparison, the detected offsets for the ASP based Pléiades DEMs for Dos Lenguas rock glacier are minimal.

We decide on co-registering the 2023 to the 2022 Pléiades DEM per processing strategy to maintain independence between the photogrammetric software. We chose to not co-register the Pléiades DEMs to the UAV DEMs for a robust co-registration (UAV flights barely cover stable terrain) and to develop an UAV independent workflow for future use in larger regions. Despite well-performed co-registration of DEMs of the same processing strategy, absolute differences in elevation between the processing strategies occur (Figure 4). It is apparent that the UAV DEMs processed in Agisoft and the Pléiades DEMs processed in ASP are relatively similar in absolute elevation despite the difference in data source, in processing software and without any co-registration. We hypothesize that this is due to an unintended similarity in z values between the SRTM DEM used as seed DEM to generate the Pléiades DEM in ASP and the GCPs and CPs used for processing the UAV imagery in Agisoft.

4.2 Rock glacier surface change

We can confirm the ridge and furrow surface pattern as described by Halla et al. (2021) both in our UAV as well as in our Pléiades based DEMs, consequently also in all DoDs. Vertical surface change patterns are a compound signal of vertical and horizontal surface change with horizontal movements imprinting the vertical differences by shifting features, e.g., ridges, downslope from one year to the other. This results in negative change at the original location and positive change at the location downslope (Figure 3). While this causes strong changes in terms of vertical surface change pattern, the horizontal movement partially equals itself in terms of net surface change balance at locations where pronounced ridges are present (Halla et al. 2021).

None of the rock glaciers investigated expresses strong net negative vertical surface changes between 2022 and 2023, based on mean positive and negative changes (Tables 4 and 5). While this holds true for all processing strategies and data sources we focus on the UAV processing in Agisoft and Pléiades processing in ASP given the quality of the data (Tables 2–5; chapter 4.1). Halla et al. (2021) calculate UAV based annual net balances of vertical surface change on Dos Lenguas rock glacier of -0.36 m a^{-1} for 2016-2017 and +0.27 m a^{-1} for 2017–2018. These findings showcase interannual variability and similarities to our results.

Monnier and Kinnard (2017) calculate vertical rock glacier surface changes within Navarro complex of up to -1 m a^{-1} based on aerial photography and spaceborne DoDs, for the period 2000 to 2014. While the Navarro complex is located approximately 200 km south of our study area, the magnitude of vertical surface change is in agreement with our Pléiades result processed in ASP (Figure 5; minimum -1.32 m). Our UAV result processed in Agisoft exceeds these values (minimum -2.83 m). We attribute this to the difference in resolution (UAV DoD 5 cm, Pléiades DoD 1 m) and highlight the scale dependency of change values.

In the neighboring valley west of Agua Negra catchment (La Laguna catchment, Chile), Robson et al. (2022) calculate vertical surface changes of > -0.1 m a^{-1} on several rock glaciers between 2012 and 2020 which corresponds to the most frequent surface changes of our UAV based Agisoft and our Pléiades based ASP processed findings (Figures 5 and 6; Tables 4 and 5). The presented microtopography is similar to Dos Lenguas and El Paso rock glacier surfaces.

5 CONCLUSIONS

We present a local analysis on Dos Lenguas rock glacier (Dry Andes/Argentina) where we compare DEMs and DoDs based on repeated UAV surveys and Pléiades acquisitions (austral summer 2022 to austral summer 2023). We derive the Pléiades based results using three software, namely Agisoft, Catalyst and ASP. Further, we apply the Pléiades based approach to El Paso rock glacier which is located in the same study area.

We find that the choice of processing strategy strongly affects the Pléiades based results. While Pléiades based Agisoft derived DEMs and DoDs appear more appealing visually (less noise, appropriate ridges and furrows), we find their quality in terms of offset and distortion to cause an overestimation of negative vertical rock glacier surface change. Pléiades based DEMs and DoDs processed in Catalyst 'flatten' the furrows and ridges on the rock glacier surface and overestimate negative surface change particularly in the lower part. The Pléiades based results generated in ASP outperform the other processing strategies with highest consistencies of offsets to 20 known DGNSS locations, lowest shifts between DEMs before co-registration and strongest consistency of the spatial distribution of error. Pixel frequency distributions of vertical change are very similar to our UAV DoD processed in Agisoft and surface change values are in agreement with published results. Our example highlights the suitability of Agisoft for processing UAV imagery and of ASP for processing Pléiades imagery.

We can provide Pléiades based change analysis at El Paso rock glacier where we did not obtain UAV imagery. The findings allow for an interpretation of a more general behaviour in the study area. Given that the choice of software propagates to very similar impact when calculating vertical surface change for both rock glaciers, we conclude that attention should not only be focused on potential differences due to variability in co-registration techniques, but also to the choice of software for DEM generation.

A detailed analysis of surface change patterns is only possible with very high resolution DoDs, which clearly attributes benefit to UAV based DoDs. Pléiades DoDs, however, provide insight to general surface patterns. They can, using an appropriate processing strategy, deliver surface changes similar to UAV based investigation. Given the limitations of UAV surveys imposed by high-alpine conditions, such as for example strong winds, changing weather conditions, and/or limited access; Pléiades based DoDs enable vertical surface change magnitude and pattern analysis at the cost of spatial resolution but at the gains of increased spatial coverage, "access" to previously unvisited sites, and insights beyond the limitations of fieldwork.

We conclude that tri-stereo Pléiades imagery provides distinguishable benefits for analysing vertical rock glacier surface changes. We highlight the need for robust co-registration and prior knowledge of the study area to carefully assess the suitability of Pléiades DoDs at a specific location. We recommend processing Pléiades data in ASP and highlight the possibility to derive visually detailed Pléiades DEMs in Agisoft. We advocate perceiving these benefits as complementation to UAV surveys, so that highest spatial coverage is achieved by the first and highest spatial resolution by the latter. In view of permafrost degradation, we are certain that an analysis on both spatial scales is relevant.

6 ACKNOWLEDGEMENTS

This research is funded by the Deutsche Forschungsgemeinschaft (DFG, 461744503). We are thankful for the support received for acquiring the Pléiades imagery by the Centre National d'Etudes Spatiales (CNES). ASP computations presented were performed using the GRICAD infrastructure (gricad.univ-grenoble-alpes.fr), supported by Grenoble research communities. The authors thank all fieldwork campaign participants F. Flöck, F. Wester, D. A. Ortiz, T. Köhler, P. Reichartz, T. Wenzel, M. Cramer. MS further thanks A. Müting for all advice shared.

MS: conceptualization, resources, investigation, formal analysis (UAV, Pléiades; Agisoft, Catalyst), visualization, writing-original draft, writing-review and editing. DC: formal analysis (Pléiades, ASP), writing-review and editing. RB: conceptualization, resources, writing-review and editing. BR: resources, writing-review and editing. XB: resources, writing-review and editing. JB: supervision, writing-review and editing. LS: supervision, funding acquisition, writing-review and editing. All authors contributed to the final version of this manuscript.

7 REFERENCES

Arenson, L.U., Harrington, J.S., Koenig, C.E.M., Wainstein, P.A. 2022. 'Mountain Permafrost Hydrology - A Practical Review Following Studies from the Andes', *Geosciences* 12(2), 48 p. doi:10.3390/geosciences12020048.

Bagnardi, M., González, P.J., and Hooper, A. 2016. 'High-resolution digital elevation model from tri-stereo Pleiades-1 satellite imagery for lava flow volume estimates at Fogo Volcano', *Geophysical Research Letters* 43(12), pp. 6267–6275. doi:10.1002/2016GL069457.

Beyer, R.A., Alexandrov, O., and McMichael, S. 2018. 'The Ames Stereo Pipeline: NASA's Open Source Software for Deriving and Processing Terrain Data', *Earth and Space Science* 5(9), pp. 537–548. doi:10.1029/2018EA000409.

Blöthe, J.H., Halla, C., Schwalbe, E., Bottegal, E., Trombotto Liaudat, D., and Schrott, L. 2021. 'Surface velocity fields of active rock glaciers and ice-debris complexes in the Central Andes of Argentina', *Earth Surface Processes and Landforms* 46(2), pp. 504–522. doi:10.1002/esp.5042.

Cook, K.L. and Dietze, M. 2019. 'Short Communication: A simple workflow for robust low-cost UAV-derived change detection without ground control points', *Earth Surface Dynamics* 7(4), pp. 1009–1017. doi:10.5194/esurf-7-1009-2019.

Croce, F.A. and Milana, J.P. 2002. 'Internal structure and behaviour of a rock glacier in the Arid Andes of Argentina', *Permafrost and Periglacial Processes* 13 (4), pp. 289–299. doi:10.1002/ppp.431.

Cusicanqui, D., Bodin, X., Duvillard, P.-A., Schoeneich, P., Revil, A., Assier, A. et al. 2023. 'Glacier, permafrost and thermokarst interactions in Alpine terrain: Insights from seven decades of reconstructed dynamics of the Chauvet glacial and periglacial system (Southern French Alps)', *Earth Surface Processes and Landforms*, pp. 1–18. doi:10.1002/esp.5650.

Dussaillant, I., Berthier, E., Brun, F., Masiokas, M., Hugonnet, R., Favier, V. et al. 2019. 'Two decades of glacier mass loss along the Andes', *Nature Geoscience* 12(10), pp. 802–808. doi:10.1038/s41561-019-0432-5.

Eltner, A., Kaiser, A., Castillo, C., Rock, G., Neugirg, F., and Abellán, A. 2016. 'Image-based surface reconstruction in geomorphometry – merits, limits and developments', *Earth Surface Dynamics* 4(2), pp. 359–389. doi:10.5194/esurf-4-359-2016.

Etzelmüller, B. and Hagen, J.O. 2005. 'Glacier-permafrost interaction in Arctic and alpine mountain environments with examples from southern Norway and Svalbard', in *Geological Society, London*, Special Publication 242, pp. 11–27. doi:10.1144/GSL.SP.2005.242.01.02.

Ferri, L., Dussaillant, I., Zalazar, L., Masiokas, M.H., Ruiz, L., Pitte, P. et al. 2020. 'Ice Mass Loss in the Central Andes of Argentina Between 2000 and 2018 Derived From a New Glacier Inventory and Satellite Stereo-Imagery', *Frontiers in Earth Science* 8, 530997. doi:10.3389/feart.2020.530997.

Geiger, S.T., Daniels, J.M., Miller, S.N., and Nicholas, J.W. 2014. 'Influence of Rock Glaciers on Stream Hydrology in the La Sal Mountains, Utah', *Arctic, Antarctic, and Alpine Research* 46(3), pp. 645–658. doi:10.1657/1938-4246-46.3.645.

Haas, T. de, Nijland, W., McArdell, B.W., and Kalthof, M.W.M.L. 2021. 'Case Report: Optimization of Topographic Change Detection With UAV Structure-From-Motion Photogrammetry Through Survey Co-Alignment'. *Frontiers in Remote Sensing* 2-2021, Article 626810. doi:10.3389/frsen.2021.626810.

Halla, C., Blöthe, J.H., Tapia Baldis, C., Trombotto, D., Hilbich, C., Hauck, C., and Schrott, L. 2021. 'Ice content and interannual water storage changes of an active rock glacier in the dry Andes of Argentina', *The Cryosphere* 15, pp. 1187–1213. doi:10.5194/tc-15-1187-2021

Hewitt, K. 2002. 'Introduction: Landscape Assemblages and Transitions in Cold Regions', in K. Hewitt, M.L. Byrne, M. English, and G. Young (eds.), *Landscapes of Transition*. The GeoJournal Library, vol 68. Springer, Dordrecht.

IANIGLA-CONICET 2018. *Inventario Nacional de Glaciares y Ambiente Periglacial*. Informe de la subcuenca del río Blanco. Cuenca del Río San Juan. With assistance of Ministerio de Ambiente y Desarrollo Sustentable de la Nación.

James, M.R.; Chandler, J.H., Eltner, A., Fraser, C., Miller, P.E., Mills, J.P. et al. 2019. 'Guidelines on the use of structure-from-motion photogrammetry in geomorphic research', *Earth Surface Processes and Landforms* 44(10), pp. 2081–2084. doi:10.1002/esp.4637.

Lliboutry, L., Williams, R., and Ferrigno, J.G. 1998. 'Glaciers of Chile and Argentina', *US Geological Survey* Professional Paper 1386-I-6.

Masiokas, M.H., Rabatel, A., Rivera, A., Ruiz, L., Pitte, P., Ceballos, J.L. et al. 2020. 'A Review of the Current State and Recent Changes of the Andean Cryosphere', Frontiers in Earth Science 8, Article 99. doi:10.3389/feart.2020.00099.

Miesen, F., Dahl, Dahl, S.O., and Schrott, L. 2021. 'Evidence of glacier-permafrost interactions associated with hydro-geomorphological processes and landforms at Snøhetta, Dovrefjell, Norway', *Geografiska Annaler: Series A, Physical Geography* 103(3), pp. 273–302. doi:10.1080/04353676.2021.1955539.

Monnier, S. and Kinnard, C. 2017. 'Pluri-decadal (1955–2014) evolution of glacier–rock glacier transitional landforms in the central Andes of Chile (30–33°S)'. *Earth Surface Dynamics* 5(3), pp. 493–509. doi:10.5194/esurf-5-493-2017.

Mueting, A., Bookhagen, B., and Strecker, M.R. 2021. 'Identification of Debris-Flow Channels Using High-Resolution Topographic Data: A Case Study in the Quebrada del Toro, NW Argentina', *JGR Earth Surface* 126(12). doi:10.1029/2021JF006330.

Nuth, C. and Kääb, A. 2011. 'Co-registration and bias corrections of satellite elevation data sets for quantifying glacier thickness change', *The Cryosphere* 5(1), pp. 271–290. doi:10.5194/tc-5-271-2011.

Pitte, P., Masiokas, M., Gargantini, H., Ruiz, L., Berthier, E., Ferri Hidalgo, L., Zalazar, L., Dussaillant, I., Viale, M., Zorzut, V., Corvalán, E., Scarpa, J.P., Costa, G., and Villalba, R. 2022. 'Recent mass-balance changes of Agua Negra glacier (30°S) in the Desert Andes of Argentina', *Journal of Glaciology* 68(272), pp. 1197–1209. doi:10.1017/jog.2022.22.

Rieg, L., Klug, C., Nicholson, L., and Sailer, R. 2018. 'Pléiades Tri-Stereo Data for Glacier Investigations—Examples from the European Alps and the Khumbu Himal', *Remote Sensing* 10(10), 1563. doi:10.3390/rs10101563.

Robson, B.A., MacDonell, S., Ayala, Á., Bolch, T., Nielsen, P.R., and Vivero, S. 2022. 'Glacier and rock glacier changes since the 1950s in the La Laguna catchment, Chile', *The Cryosphere* 16(2), pp. 647–665. doi:10.5194/tc-16-647-2022.

Schrott, L. and Götz, J. 2013. *Forschen im Gebirge. Investigating the mountains*. Christoph Stadel zum 75. Geburtstag. Verlag der Österreichischen Akademie der Wissenschaften (IGF-Forschungsberichte, Band 5). Wien.

Schrott, L. 1994. *Die Solarstrahlung als steuernder Faktor im Geosystem der subtropischen semiariden Hochanden (Agua Negra, San Juan, Argentinien)*. Heidelberger Geographische Arbeiten 94.

Shean, D.E., Alexandrov, O., Moratto, Z.M., Smith, B.E., Joughin, I.R., Porter, C., and Morin, P. 2016. 'An automated, open-source pipeline for mass production of digital elevation models (DEMs) from very-high-resolution commercial stereo satellite imagery', *ISPRS Journal of Photogrammetry and Remote Sensing* 116, pp. 101–117. doi:10.1016/j.isprsjprs.2016.03.012.

Smith, M.W., Carrivick, J.L., and Quincey, D.J. 2016. 'Structure from motion photogrammetry in physical geography', *Progress in Physical Geography: Earth and Environment* 40(2), pp. 247–275. doi:10.1177/0309133315615805.

Trombotto, D. and Borzotta, E. 2009. 'Indicators of present global warming through changes in active layer-thickness, estimation of thermal diffusivity and geomorphological observations in the Morenas Coloradas rockglacier, Central Andes of Mendoza, Argentina', *Cold Regions Science and Technology* 55(3), pp. 321–330. doi:10.1016/j.coldregions.2008.08.009.

Vivero, S. and Lambiel, C. 2019. 'Monitoring the crisis of a rock glacier with repeated UAV surveys', *Geographica Helvetjca* 74(1), pp. 59–69. doi:10.5194/gh-74-59-2019.

Received: 6 January 2025 | Revised: 10 August 2025 | Accepted: 18 August 2025

DOI: 10.1002/esp.70151

RESEARCH ARTICLE

ESPL WILEY

Dos Lenguas rock glacier kinematics stable despite warming trend (2016–2024): Surface changes and the role of topography and climate in the Dry Andes of Argentina

Melanie Stammler[1] | Jan Blöthe[2] | Fabian Flöck[1] | Rainer Bell[1] | Lothar Schrott[1]

[1]Department of Geography, University of Bonn, Bonn, Germany

[2]Faculty of Environment and Natural Resources, University of Freiburg, Freiburg, Germany

Correspondence
Melanie Stammler, Department of Geography, University of Bonn, Bonn, Germany.
Email: stammler@uni-bonn.de

Funding information
This research is funded by the German Research Foundation (DFG, 461744503). M. Stammler further acknowledges funding by the German Scholarship Foundation.

Abstract

Rock glaciers are increasingly recognized for their hydrological significance, specifically relevant in regions with reduced water availability, like the Dry Andes. Despite their relevance, driving factors for rock glacier surface changes in vertical and horizontal direction, termed kinematics, are still poorly understood. Rock glacier kinematics allow to elucidate the local state of permafrost. Knowledge on the Andean state of permafrost, however, is scarce. This study investigates vertical and horizontal surface changes on Dos Lenguas rock glacier in the Dry Andes of Argentina (30°S) using quasi-biennial austral summer UAV datasets for 2016–2024. Given the very high resolution of the UAV datasets (11 cm), we are able to focus on resolving the magnitude and spatial pattern of surface changes within the landform in great detail. We generate DEMs for vertical change quantification. Further, we derive hillshades from these DEMs for feature tracking-based horizontal change quantification. We co-analyse these with slope and curvature as well as ERA5 air temperature and precipitation data provided by meteoblue for 1940–2024 to investigate the effect of topography and climate. Findings reveal spatial and temporal variability in surface kinematics, with maximum surface velocities up to 1.7 m/yr and mean velocities of 0.9 m/yr. The majority of vertical changes, reaching upto ±1.5 m, are predominantly influenced by compressional flow and ridge-furrow systems and correlate with topographic drivers like slope and curvature. In contrast to other regions in the world, high-resolution monitoring of Dos Lenguas rock glacier for the time period of 8 years (2016–2024) reveals vertical and horizontal surface change to be stable for almost one decade, despite increasing (winter) temperatures. We attribute the lack of snow sheltering due to extremely dry conditions and the comparatively high-altitude location of Dos Lenguas (4,400 m asl), the main controls of absent/delayed kinematic reaction to climatological change. We highlight the importance of high-resolution monitoring for resolving the magnitude and spatial pattern of rock glacier kinematics with low levels of detection.

KEYWORDS
DEMs of Difference, Dry Andes, Feature Tracking, permafrost, rock glacier kinematics, structure-from-motion, surface change, uncrewed aerial vehicles

1 | INTRODUCTION

The Dry Andes are characterized by a very high density of rock glaciers, ice-debris landforms creeping downslope under the force of gravity (Blöthe et al., 2021; IANIGLA-CONICET, 2018). As glaciers diminish under rising global temperatures, rock glaciers react with a certain delay time, potentially buffering water availability by storing and releasing water over extended periods (Arenson et al., 2022; Masiokas et al., 2020). The hydrological relevance is particularly pronounced in arid regions such as the Dry Andes, where precipitation is scarce and water availability is reduced.

Rock glacier kinematics are descriptive of the mechanical behaviour of rock glaciers, either evident as surface motion and/or internal deformation processes (Hu et al., 2025). Displacement in the rock glacier's shear horizon, ice-rich core and active layer contribute to surface motion, at different magnitudes (Cicoira et al., 2021). Recently incorporated into the essential climate variable permafrost (Global Climate Observing System, GCOS), rock glacier velocity (RGV) – surface movement in horizontal direction – traces climate change impact on multi-decennial scale, focusing on continuous and comparable monitoring (RGIK, 2023). RGV is monitored in-situ (GNSS, theodolite, total station), by close-range remote sensing applications (e.g., UAV-borne photogrammetry, terrestrial laser scanning) or far-range remote sensing applications (e.g., air- and spaceborne photogrammetry) (Hu et al., 2025). Vertical surface changes reveal volumetric variations and indicate flow dynamics, offering a window into the morphometric complexity of rock glaciers (Halla et al., 2021; Vivero & Lambiel, 2024). Vertical surface changes are commonly calculated by differencing correctly georeferenced or co-registered DEMs from two different points in time, at equal resolution (Williams, 2012). Together, horizontal and vertical rock glacier surface changes are indicative of changes in ground temperature and ice content (Halla et al., 2021; Jones et al., 2019; RGIK, 2023), thus, providing a surface indication of subsurface changes. Despite the hydrological significance of rock glaciers in the Dry Andes, long-term monitoring records of rock glaciers are limited (Blöthe et al., 2024, 2021; Cusicanqui et al., 2025; Vivero et al., 2021), contrasting sharply with the up to century-long datasets available for the Swiss Alps (Manchado et al., 2024) or North America (Kääb & Røste, 2024).

While the drivers of rock glacier surface change are multifaceted, temperature is regularly attributed a governing role (Kääb & Røste, 2024; Marcer et al., 2021). Warmer frozen debris typically moves at a faster rate due to the reduced viscosity of the warmer ice component and the effects of infiltrating meltwater (Arenson, Springman, & Sego, 2007; Cicoira et al., 2021; Moore, 2014), as by Glen-Nye flow law. In addition, local factors, such as material composition (different proportions of rock, ice and air, e.g. due to variability of grain size distribution), slope, ice content, internal shear horizons, water content and external inputs like rockfall, also significantly influence rock glacier kinematics (Cicoira et al., 2021; Hartl et al., 2023; Kääb & Røste, 2024). As the Dry Andes are underrepresented in the GCOS, measured decadal temperature data are not available for our study area.

Both an understanding of the driving factors of rock glacier kinematics as well as the Andean state of permafrost are limited. Here, we try to fill these gaps by examining the surface kinematics of the Dos Lenguas rock glacier in the Agua Negra catchment in the Dry Andes of Argentina (30°S) based on high-resolution UAV datasets collected in the austral summers of 2016, 2018, 2022 and 2024. We generate digital elevation models (DEMs) based on our UAV imagery using structure-from-motion techniques and calculate vertical surface change by the subtraction of correctly georeferenced DEMs, as well as horizontal surface change by automatic feature-tracking on DEM-based hillshades. This dataset represents the longest UAV time series for UAV-based rock glacier monitoring in the Dry Andes, enabling an unprecedented investigation into the magnitude and spatial patterns of changes in rock glacier surface morphology. Relying on our investigation of Dos Lenguas rock glacier kinematics at high resolution (11 cm), we address the following research questions:

- What is the magnitude and spatial pattern of vertical and horizontal surface changes on Dos Lenguas rock glacier?
- How do topography (slope, curvature) and climatological characteristics (air temperature and precipitation) correlate with the magnitude and spatial pattern of these changes?
- What state of permafrost do surface kinematics on Dos Lenguas imply for the wider region?

With our study, we contribute to a better understanding of spatial and temporal rock glacier kinematics to elucidate the current state of permafrost within Dos Lenguas rock glacier and its implications for the broader region.

2 | STUDY AREA

The catchment of the Agua Negra River is part of the Rodeo basin and is located in the Dry Andes (30°S and 69°W, Figure 1A). The region is characterized by extremely low mean annual precipitation (~ 250 mm), none to sparse vegetation and constant high solar radiation intensities (Croce & Milana, 2002; Halla et al., 2021; Lliboutry et al., 1998; Schrott, 1996) and is projected to become warmer (Pabón-Caicedo et al., 2020). The high Andean catchment is underlain by permafrost (continuous > 5,000 m asl) (Gruber, 2012) and hosts a region-typical distribution of glacial and periglacial landforms (Halla et al., 2021; Schrott, 1996, 1998), including 59 rock glaciers (IANIGLA-CONICET, 2018). Located in San Juan Province in Argentina, its meltwaters contribute to domestic, agricultural and economic water use with the downstream viticulture, olive and fruit production generating 35% of the regional economy (Contreras et al., 2011). Based on borehole measurements, rock glaciers in the Andes (27°-34°) are characterized by lower ground temperatures in comparison to non-rock glacier ground temperatures (e.g., glacial deposits, colluvium, bedrock) at similar altitude (Koenig et al., 2025).

In this study, we focus on the active, westward creeping, tongue-shaped and two-snouted Dos Lenguas rock glacier (Figure 1B, C). Located at 4400 m asl, the rock glacier covers an area of approximately 0.35 km^2 with a length and width of approximately 1,500 m and 500 m. Its surface is characterized by c-shaped downward-pointing ridges and furrows, strongly visible on the rock glacier surface across all episodes investigated in this study.

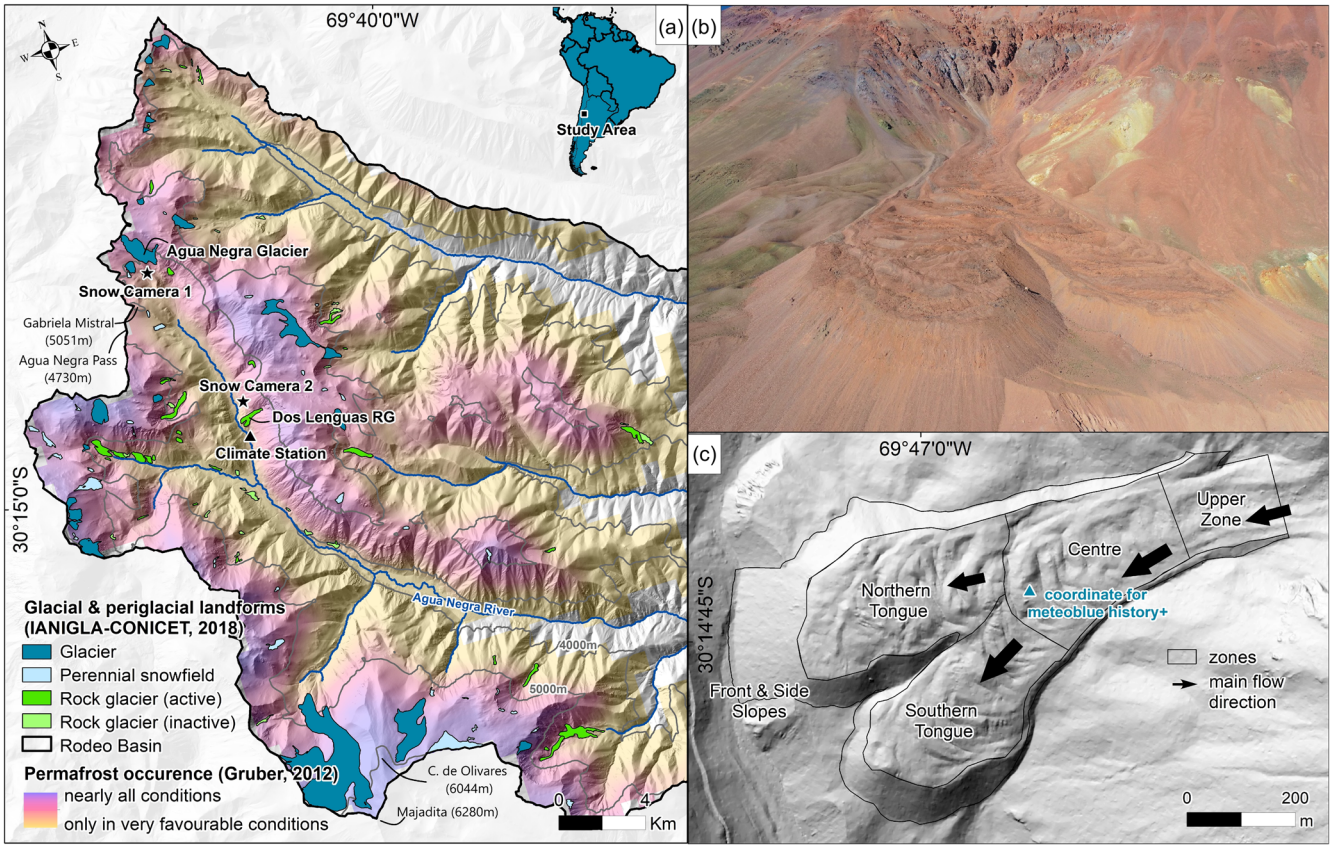

FIGURE 1 A) Rock glacier and glacier distribution in the high-altitude catchment of Agua Negra River, which is part of the Rodeo basin and located in the Dry Andes of Argentina (30°S and 69°W). The upper Rodeo basin is characterized by a distribution of (peri)glacial landforms representative of the region, the very limited presence of vegetation and the absence of populated areas. Landforms are inventoried by IANIGLA-CONICET (2018) and displayed on top of the permafrost occurrence map by Gruber (2012) and a TanDEM-X-based hillshade. B) Photo of Dos Lenguas rock glacier taken with a Phantom 4 RTK drone, March 2022. C) Geomorphological zones slightly adapted after Halla et al. (2021) and displayed on top of a Pléiades-based DEM of 1 m resolution. The Pléiades DEM is based on tristereo, panchromatic Pléiades imagery acquired between February 13th and 20th, 2023. For more information, see Stammler et al. (2024). Snow camera and climate station locations in A), the coordinate used for the extraction of ERA5 data provided through meteoblue history+ in C).

3 | METHODOLOGY AND METHODS

We use structure-from-motion (SfM) techniques to generate high-resolution DEMs for the Dos Lenguas rock glacier surface for four episodes based on quasi-biennial UAV flights between 2016 and 2024. Based on the georeferenced DEMs we calculate vertical surface changes as well as horizontal displacement. We analyse the vertical and horizontal surface changes, the latter gained through the feature tracking on hillshades, both on an annual scale as well as concerning their trends over time.

We co-analyse our rock glacier kinematics findings with the DEM derivatives slope and curvature, as well as historical air temperature and precipitation records for the location, with regard to their role as potential driving factors.

3.1 | UAV flights

During four field campaigns in the austral summers of 2016, 2018, 2022 and 2024, we obtained repeated UAV flights covering Dos Lenguas rock glaciers and its near proximity. The differences in data acquisition (e.g., mission type, duration of acquisition (Table 1) are not intended but caused by fieldwork constraints. All imagery is acquired in sunny and windy conditions, typical for the region's climate (cf. 2). Changing illumination conditions are minimized by conducting acquisition from start to finish, wherever possible. Flight heights, as specified below, are decided by balancing high ground resolution, battery demand and battery weight needed to be carried in the high-mountain terrain.

For the 2016 and 2018 flights we operate a DJI Phantom 3 Advanced (sensor: 1/2.3" CMOS, effective pixels: 12.4MP, focal length: 20 mm [35 mm equivalent], field of view: 94°, image size: 4000 × 3000, shutter type: electronic) in visual line-of-sight (VLOS) and 2D mode. To prevent maximum differences in ground sampling distance caused by the consistent flight height, we split data acquisition into two overlapping parts (approximately upper & centre zone, centre zone & tongues, cf. Figure 1C), starting both with a flight height of 40 m. In 2018, imagery acquisition spans multiple days due to constraining weather conditions. For normalizing vertical and horizontal surface change to full years, we select March 18th, 2018 as date. While Halla et al. (2021) produce DEMs from the 2016 and 2018 UAV flights, we use their imagery and ground control points (GCPs) for the generation of new DEMs in accordance with our workflow (cf. 3.3).

Starting 2022 we use a Phantom 4 RTK setup (sensor: 1" CMOS, effective pixels: 20MP, focal length: 24 mm [35 mm

TABLE 1 Data characteristics for UAV flights (TA = terrain awareness mode). Imagery previously used in publications (Halla et al., 2021; Stammler et al., 2024) is reprocessed using the workflow of this study. No imagery has previously been published. All imagery is available as part of an accompanying dataset publication (Stammler et al., 2025).

	2016	2018	2022	2024
Manufacturer & UAV Model	DJI Phantom 3	DJI Phantom 3	DJI Phantom 4 RTK	DJI Phantom 4 RTK
Mission type	2D	2D	TA	TA
Date (dd.mm.yy)	13.3.16	03.03.18 to 07.03.18	24.03.22	29.02.24
# acquired/aligned images	512/512	1537/1519	1472/1472	2183/2183
Flight altitude (m)	40 to 100	40 to 100	50	50
Vertical/horizontal Overlap (%)	60 to 70	60 to 70	65	70
Flight speed (m/s)	5	5	5.5	5
Ground resolution (cm/pix)	5.56	4.76	1.55	1.39

TABLE 2 Data characteristics for DGNSS measurements. The horizontal and vertical errors are given in meters and represent the mean of all DGNSS measurements used as GCPs and CPs during the respective year. For a spatial distribution of the measurement's errors, see supplementary material 1. For all DGNSS measurements, see Stammler et al. (2025).

	2017	2018	2022	2024
Date (dd.mm.yy)	23.02.17 & 24.02.17	01.03.18 & 02.03.18	17.03.22 & 21.03.22	10.02.24 & 12.02.24
# of points	16	34	20	15
# GCPs/CPs	12/4	26/8	15/5	11/4
Mean horizontal error GCPs/CPs (m)	0.01/0.01	0.01/0.01	0.01/0.01	0.01/0.01
Mean vertical error GCPs/CPs (m)	0.02/0.02	0.02/0.02	0.02/0.02	0.02/0.03

equivalent], field of view: 84°, image size: 5472 × 3648, shutter type: mechanical; application in combination with a D-RTK2 mobile station) in VLOS and terrain awareness (TA) mode, ensuring a constant flight altitude of 50 m over the entire rock glacier. Located on the moving rock glacier surface, we (re)measure (cf. 3.2) and insert the coordinate of the location of the D-RTK2 mobile station (2022: 424640.993, 6653872.988, 4370.320 m; 2024: 424640.053, 6653872.678, 4370.231 m; both WGS 84 UTM zone 19S (EPSG:32719) with errors of 0.01 m (horizontal) and 0.02 m (vertical)) prior to conducting the flights. Execution of both flights is within a single day to limit the influence of different light conditions. A DEM of the 2022 dataset is used for validation in Stammler et al. (2024). Similar to above, we reprocess the imagery and GCPs in this study.

3.2 | DGNSS measurements

We conduct repeated Differential Global Navigation Satellite System (DGNSS) measurements in the austral summers of 2017, 2018, 2022 and 2024 (Table 2). Marked on flat surfaces of selected large boulders (> 2 m axis) on the rock glacier surface and surrounding terrain (Figure 4A-C and supplementary material 1), 20 to 34 points per year are (re)measured using Trimble DGNSS equipment (R8 base, R2s rover, TSC3 handheld, RTK). The coordinate of the base station is fixed to the same coordinate for all years (424101.83, 6654084.621, 4247.137 m; WGS 84 UTM zone 19S (EPSG:32719)). DGNSS measurements serve as GCPs used for georeferencing and optimization of the internal model geometry during DEM generation (cf. 3.3), and check points (CPs) for quality estimation between the measured point and the generated DEM. The ratio between GCPs and CPs is approximately 2/3 to 1/3 for all time periods (Table 2). The acquisition dates of the 2018–2024 datasets differ by a maximum of 19 days (2024) from the corresponding UAV flight to ensure measurement representability. Due to a lack of DGNSS measurements in 2016, a set of 16 points off-site Dos Lenguas surface measured in 2017 is used for the generation of the 2016 DEM. We confirm the measurements to be located on stable terrain with mean 2017–2018 differences of 0.01 m ± 0.02 m (easting), −0.01 m ± 0.02 m (northing) and 0.01 m ± 0.03 m (altitude) (cf. supplementary material 1).

3.3 | Digital elevation model generation

We generate DEMs for Dos Lenguas rock glacier using SfM techniques and a standard photogrammetric workflow based on our quasi-biennial UAV missions (Table 1), in Agisoft Metashape Professional (version 2.0.4). All processing is conducted on a 13th Gen Intel(R) Core™ i9-13900K and a NVIDIA RTX A4500. We reprocess all UAV imagery to ensure algorithm reproducibility (Hendrickx et al., 2019). Both UAVs used (cf. Table 1) are equipped with a normal camera model with a field of view of 94° and 84° for the Phantom 3 Advanced and 4 RTK, respectively.

For our four UAV flights, we co-align all images independent of their date of acquisition to increase comparative accuracy between the time periods (Cook & Dietze, 2019; de Haas et al., 2021). We select the highest accuracy and key and tie point limits of 40′000 and 10′000, respectively. Our optimization parameters are f (focal length), cx and cy (principal point X and Y), k1-k3 (radial distortion coefficients) and p1-p2 (tangential distortion coefficients). We fit additional corrections and do not apply adaptive camera model fitting. We then separate the aligned images based on their date of acquisition and

georeference using our DGNSS measurements (Table 2) as GCPs and CPs (cf. Figure 3A-C). For co-processing with the UAV image coordinates, DGNSS measurements are converted from EPSG:32719 to WGS84 (EPSG:4326) in Agisoft Metashape Professional. Vertical and horizontal DGNSS measurement errors (cf. supplementary material 1) are included during georeferencing. We apply high-quality and moderate depth filtering during depth map generation, select the point cloud as source data during DEM generation and export the DEMs in GeoTIFF format. For an overview of the number of tie points and projections, as well as the reprojection error and the final optimized camera intrinsic parameters for each acquisition, see supplementary material 2.

3.4 | DEMs of difference and volumetric change

For DEMs of Difference (DoD) calculation, the spatially distributed and rasterized elevation values from subsequent DEMs are resampled to equal resolution using bilinear interpolation (11 cm, resolution 2016 data, Table 3) and subtracted from one another to calculate vertical surface change. All DoDs are time-normalized to their respective episodes. To ensure physical meaningfulness, we calculate all surface changes also for stable terrain, displayed as applicable. We assess both the bias and the random component of the vertical error by calculating the mean vertical error (bias) and the standard deviation (σ, random component) of the CP residuals, Table 3. The Limit of Detection (LoD) is calculated based on the propagation of the random component of vertical error between two DEMs, following the approach of Brasington, Langham, & Rumsby (2003) and Wheaton et al. (2010): $Propagated\ error = \sqrt{(\sigma\ error_{new})^2 + (\sigma\ error_{old})^2}$ where σ $error_{new}$ and σ $error_{old}$ refer to the random error component of the vertical errors of the newer and older DEMs used in the DoD calculation, respectively. This approach is applicable when the bias component is negligible compared to the random component. To account for cases where a systematic difference in bias exists, we include an additional term, resulting in the adapted formula: $LoD = |\ b_{new-}b_{old}\ | + \sqrt{(\sigma\ error_{new})^2 + (\sigma\ error_{old})^2}$ where b_{new} and b_{old} denote the mean vertical error (bias) of the respective DEM.

We calculate volumetric changes based on the DoDs at 11 cm resolution. For an estimation of potential error, we visualize the range between minimum and maximum volume change based on the LoD of each time period (Figure 3). These are calculated as $Min\ Volume\ Change = \sum([pixel\ value - LoD]^*pixel\ area)$ and $Max\ Volume\ Change = \sum([pixel\ value + LoD]^*pixel\ area)$, whereby pixel value and LoD depend on the time period and the pixel area is ($11cm^2$) based on the data's resolution.

3.5 | Feature tracking

All feature tracking is conducted in the Environmental Motion Tracking (EMT) software (Schwalbe & Maas, 2017) based on DEM-derived hillshades generated at 25 cm resolution. EMT matches image patches between consecutive hillshades in a two-step process, first using cross-correlation to estimate a pixel-precise shift, followed by a least-squares matching to achieve sub-pixel accuracies (Schwalbe & Maas, 2017). The use of DEMs and their derivatives for tracking surface displacement has been found to outperform orthoimages given their independency of lighting conditions and capability of enhancing subtle changes, especially over longer intervals (Dall'Asta et al., 2017; Fleischer et al., 2021). Given the two-year separation of the UAV surveys used in this study, orthoimages are subject to considerable spectral differences due to varying lighting conditions, partial snow cover and shadow effects between data acquisitions, cf. Table 1 (Dall'Asta et al., 2017; Halla et al., 2021).

On the rock glacier surface, we space patch centres at 2 m distance, leading to a resolution of 2 m in the final rock glacier velocity dataset. To quantify the residual positional mismatch between consecutive images, we place 1,000 randomly distributed points on stable terrain outside the rock glacier (supplementary material 3). Tracking these stable points, we quantify the LoD of our analysis using the 90th percentile of their apparent movement, see Blöthe et al. (2024) and supplementary material 3.

3.6 | Topographical analysis

To determine the impact of topographical characteristics on horizontal and vertical surface change on Dos Lenguas rock glacier, including their change through time, we generate scatterplots with elevation and the DEM derivatives slope (6 parameter 2nd order polygon, [Evans, 1979]) and curvature at 2 m, 5 m and 10 m resolution (Figure 6, selection). All products are resampled from their original resolution (11 cm for vertical change and elevation, 2 m for horizontal change) to the respective new resolution, applying bilinear interpolation.

We calculate Pearson correlation coefficients to better understand correlations between the different rasters (Figure 6 selection, supplementary material 4). Here, elevation, slope and curvature values are valid at the beginning of the respective time episode. For example, horizontal change from 2016 to 2018 is tested for correlation with the topographical characteristics for 2016, while horizontal change from 2018 to 2022 is tested for correlation with the topographical characteristics for 2018.

3.7 | Climatological data and validation

For the study area, no long time series of climatological data are available. The most proximate station is Capayán (4,754 m asl), where air temperature is measured since December 20th, 2016. Located 8.5 km north of Dos Lenguas and in front of Agua Negra glacier (Figure 1A), the station's data is very likely impacted by the glacier's presence, thus, not used in this study. We operate a climatological station 0.5 km south of Dos Lenguas near Agua Negra River (4,160 m asl, Figure 1A) as of February 14th, 2022, measuring air temperature with a HOBO air temperature sensor at 1.7 m above ground.

We analyse ERA5 data available through meteoblue history+ extracted for a point in the centre area of Dos Lenguas rock glacier (Figure 1C), at monthly resolution for the time period 1940 to 2024. For historical data, meteoblue history+ provides tailored access to the ERA5 dataset generated by the European Centre for Medium-Range Weather Forecasts (Hersbach et al., 2019). We use air temperature at 2 m elevation (°C), precipitation amount (mm/m^2) and snowfall

amount (cm/m^2), and compare one year of the ERA5 data provided by meteoblue to our measured data for validation (Figure 7A).

We installed SECACAM Pro Plus cameras at two locations in the catchment (Figure 1A). Location 1, close to the northern end of the Agua Negra valley at approximately 4,650 m asl provides an overview on the valley between February 6th, 2023 and February 25th, 2024. Location 2, at 1.5 km distance north from and with a view towards Dos Lenguas sheds light on snow conditions at Dos Lenguas between February 16th, 2023 and February 27th, 2024. Location 2 is equipped with metric-labelled poles for snow height estimation. As we do not have reliable, local precipitation measurements for the area, we proceed using the ERA5 precipitation without data-based validation and visually evaluate the presence of snow cover on optical photos automatically taken with the installed cameras. All photos taken are part of the paper accompanying dataset (Stammler et al., 2025).

4 | RESULTS

4.1 | DEMs and feature tracking

The error between the DGNSS-based GCPs and the generated DEMs (GCP error) and between the DGNSS points used as CPs and the generated DEMs (CP error) is highest for the 2016 dataset and lowest for the 2022 dataset (Table 3). For all time episodes, horizontal errors of the DGNSS measurements used as GCPs and CPs exceed their corresponding vertical errors (Table 2, supplementary material 1, Trimble DGNSS equipment). Errors do not vary by the measurements' application as GCPs and CPs (Table 2). While differences occur between the locations of the measurements (supplementary material 1), no distinct spatial patterns emerge.

An investigation of the CP-based z error reveals extremely low bias for the 2018 and 2022 DEMs compared to their random error components (Table 3). For 2024, the bias is slightly higher than for 2018 and 2022 but remains lower than 50% of the 2024 standard deviation. In contrast, the 2016 dataset exhibits a bias that exceeds the random error component. For 2022 and 2024, the mean CP errors normalized by flight height are 0.0084% and 0.0468%, respectively. For 2016 and 2018, non-dimensionalization by flight height is not feasible due to variable flight height (cf. Table 1).

Independent of using a DJI Phantom 3 or a DJI Phantom 4 RTK, the derived DEMs are classified as very high resolution DEMs with resolutions of 11 cm or even below (cf. Table 3). Point densities of the dense point cloud before generating the DEMs range from 0.081 points/cm^2 for the 2016 DEM to 0.105 points/cm^2 for the 2022 DEM. DEM resolutions for the 2022 and 2024 DEMs based on the Phantom 4 RTK flights exceed the resolutions of the 2016 and 2018 DEMs based on flights conducted with a DJI Phantom 3 (Table 1 & 3). Suitability of our UAV imagery for alignment is high across all datasets, based on comparing the number of UAV images taken and UAV images aligned (Table 1). Image characteristics such as spectral properties, presence of shadows and none to very little presence of snow is very similar across each dataset, with contrasting properties between the different datasets. LoDs for vertical change detection fall between ±4.1 cm/yr and ±27.5 cm/yr for vertical surface changes normalized to full years, depending on the DoD constituting DEMs and their error (cf. Table 3).

Using the 90th percentile of 1,000 randomly distributed points outside the mapped limits of the Dos Lenguas rock glacier, we estimate the residual mismatch between image pairs to fall between 0.35 pixel (2022–2024, minimum) and 1.63 pixel (2016–2022, maximum). Given the variable epoch length, this translates to LoDs between 3.1 and 17.9 cm/yr for surface velocities obtained by feature tracking.

4.2 | Dos Lenguas vertical surface changes

Annual vertical surface changes range in their majority from 1.5 to −1.5 m with singular values reaching 1.7 m (Figure 2). The overall pattern of vertical differences is similar over the three episodes, depicting ridge-and-furrow morphology displacement. Highest magnitudes for positive and negative vertical surface changes are reached in the central area of the rock glacier surface, followed by the southern tongue. The upper zone and northern tongue, the latter specifically towards the front slope, are characterized by a lower magnitude of vertical changes. A spatially coherent positive change is visible on the southern tongue's front (Figure 2, blue area on front).

Volumetric changes in the upper, centre, northern and southern tongue zones are predominantly negative (Figure 3). This leads to overall negative balances for the rock glacier surface in 5 out of 6 cases. In 3 out of these 5 cases, overall negative volumetric change on the southern tongue is of the highest magnitude compared to the upper, centre and northern tongue. This pattern is consistent for

TABLE 3 DEM characteristics per data-take include GCP and CP errors, the mean vertical error and the standard deviation of the CP residuals (all in cm). For GCP and CP details, see Table 1–2. GCP errors represent the discrepancies between DGNSS measurements used during DEM generation and the corresponding values extracted from the DEM. CP errors are calculated from DGNSS measurements not used in DEM generation, making them an independent measure of DEM quality. The mean vertical error quantifies the systematic bias of the DEM, whereas the standard deviation of the CP residuals reflects the random component of the vertical uncertainty. For a separation of the errors by GCP/CP location on the rock glacier surface or in the vicinity of the landform, see supplementary material 6.

	2016	2018	2022	2024
GCP error (x, y, z in cm)	±10.47, ±5.05, ±12.39	±3.44, ±5.30, ±3.90	±1.71, ±3.12, ±2.81	±3.87, ±4.80, ±4.29
CP error (x, y, z in cm)	±19.91, ±21.23, ±15.93	±2.80, ±6.55, ±3.51	±1.53, ±1.32, ±1.48	±4.80, ±6.45, ±5.33
Mean vert. CP error (cm)	−12.61	0.49	0.42	2.34
σ of CP residuals (cm)	11.25	3.72	1.59	5.53
DEM spatial resolution (cm/pixel)	11.0	9.51	3.09	2.89

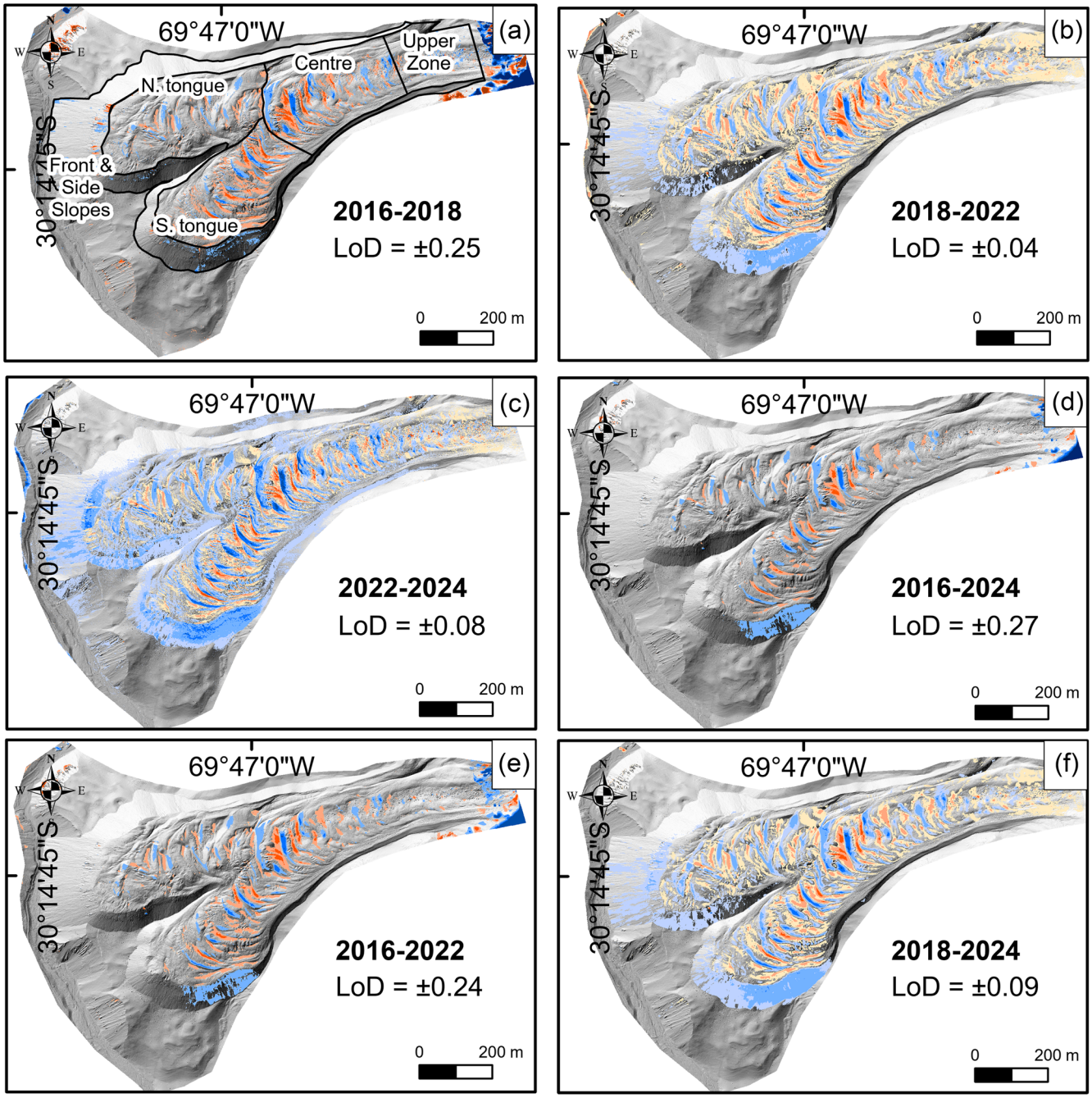

FIGURE 2 Vertical surface changes (m/yr) on Dos Lenguas rock glacier for the time periods 2016–2018 (A), 2018–2022 (B), 2022–2024 (C), 2016–2024 (D), 2016–2022 (E) and 2018–2024 (F), all normalized to years. UAV-based DEMs are generated at 11 cm resolution and displayed on top of the 2024 hillshade. The colour scheme of the legend is adapted to the respective LoD (m/yr). A) includes the delineation of geomorphological zones as referred to in the text. Vertical changes east of the upper zone (A, D, E) are related to the smaller extent of the 2016 flight compared to the other UAV flight campaigns. Vertical changes west of the rock glacier (B, C) are related to fluvial activity of Agua Negra River, cf. Figure 1.

the 2016–2018, 2018–2022, 2016–2024, 2016–2022 and 2018–2024 time episodes (Figure 3A, B, D-F). When pairing the 2022–2024 datasets (Figure 3C), vertical surface changes in all zones on the rock glacier surface are positive. Volumetric change on the front and side slopes is positive across all time episodes. Given the lower LoD of the 2016 dataset (Figure 2), the results for the 2018–2022, 2022–2024 and 2018–2024 time periods are considered to be more reliable (Figure 3B, C, F).

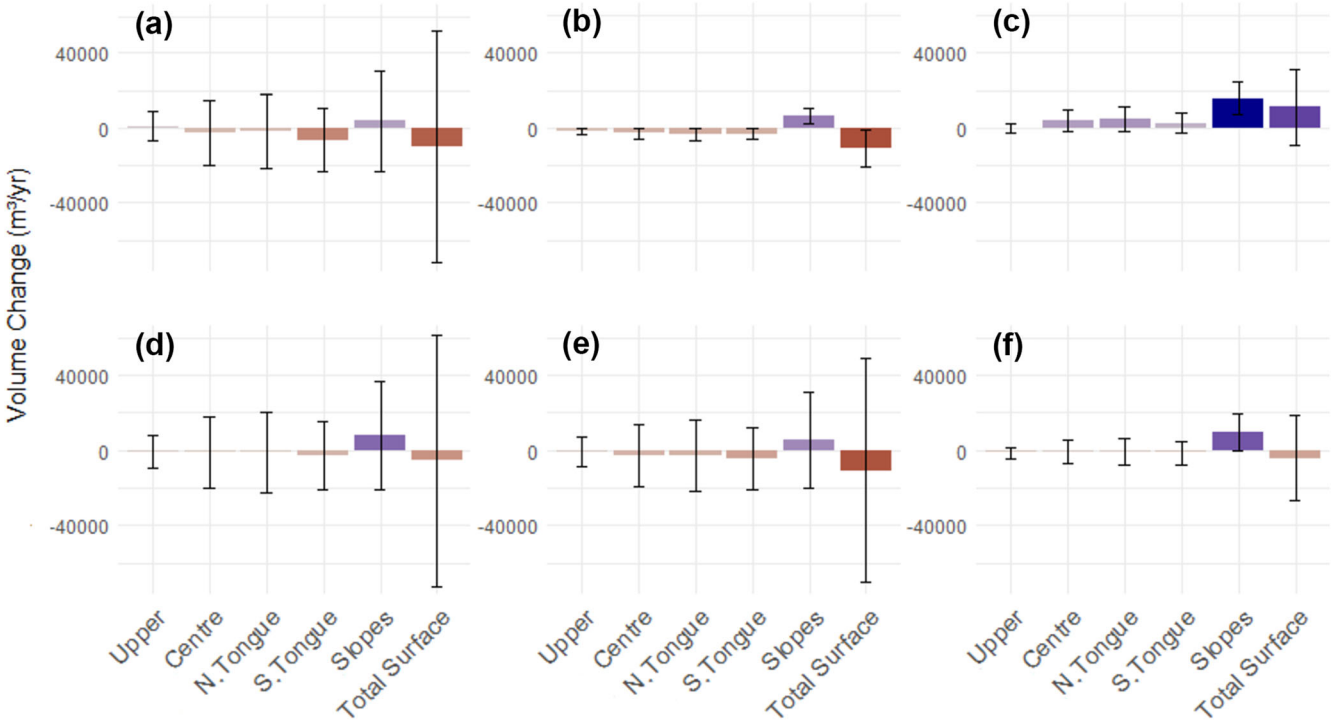

FIGURE 3 Volumetric changes (m^3/yr) on Dos Lenguas rock glacier for the different geomorphological zones and the time periods 2016–2018 (A), 2018–2022 (B), 2022–2024 (C), 2016–2024 (D), 2016–2022 (E) and 2018–2024 (F). Periods are normalized to years and 'total surface' refers to the upper, centre and tongue zones without front and side slopes. Based on UAV imagery generated DEMs at 11 cm resolution. Whiskers indicate the range between the minimum and maximum volume change based on the LoD of the respective time period; for calculation, see 3.4. For the delineation of the geomorphological zones, see Figures 1C or 2A. For time episode-specific LoDs, see Figure 2.

4.3 | Dos Lenguas horizontal surface velocities

Across all time periods (époques, EPs; 2016–2018, 2018–2022, 2022–2024, 2016–2024), the upper zone of Dos Lenguas rock glacier generally is characterized by highest values (1.5 to 2 m/yr), with a slowing trend towards the southern tongue (< 1.5 m/yr) (Figure 4). The northern tongue experiences lower values (< 1 m/yr), specifically closer to the centre, in comparison to the upper, centre or southern tongue, with a drastic slowdown traversing from the centre to the northern tongue. Along the entire rock glacier and across all time episodes, the edges on both sides are characterized by lowest velocities. The mean surface velocity for the rock glacier surface without front and side slopes is 0.88 m/yr (2016–2024, LoD ± 0.05 m/yr) and mean surface velocities are consistent in time (2016–2018: 0.88 m/yr with an LoD of ±0.18 m/yr, 2018–2022: 0.91 m/yr and ±0.04 m/yr, 2022–2024: 0.91 m/yr and ±0.05 m/yr). Further, the orientation of movement is consistent, with south-east–east (59.1–65.4%, all EPs) and south–south-east (22.2–27.5%, all EPs) representing the main directions of the rock glacier. The south–south-east direction is confined to the southern tongue and southern edge of the northern tongue, while the rest of the rock glacier is oriented in south-east–east direction (supplementary material 5).

Comparing quasi-biennial surface velocities to the 2016–2024 mean surface velocity reveals no significant change, with acceleration and deceleration to seldomly exceed the LoDs of the respective datasets (Figure 5). Detectable are a minimal increase in the upper zone for 2018–2022 (< 0.1 m/yr, Figure 5B) and a minimal increase in velocity in the tongue zone for 2022–2024 (< 0.1 m/yr, Figure 5C). In all cases, the magnitude of velocity change is minor and barely exceeds 0.1 m/yr (Figure 5 F-J).

4.4 | Surface kinematics and topography

Different magnitudes of horizontal rock glacier surface change are reached depending on their elevation (Figure 6A, B). This pattern is consistent through all time episodes and is independent of the resolution (supplementary material 7). Highest velocities are reached in the upper zone (Figure 2). At 10 m resolution, a two-grouped pattern of decreasing velocity frequencies is established in the centre of the rock glacier (purple, Figure 6A, B). The velocity group with a lower magnitude merges with the onset of the northern tongue (blue), and the velocity group with a higher magnitude continues to the southern tongue (green).

Slope decreases from the upper zone (yellow) to the centre of Dos Lenguas rock glacier (purple, Figure 6C, D). Characterized by lower slope at the beginning, the centre area increases in slope values towards the tongues. Both tongues are characterized by a similar slope at the beginning, with the slope decreasing at the northern tongue while increasing at the southern tongue.

Vertical surface changes reach the highest magnitudes in the centre area of the rock glacier, followed by the southern tongue (Figure 6E, F and Figure 2). Vertical surface changes on the northern tongue are of a lesser magnitude than on the southern tongue, while vertical surface change in the upper zone being of lowest magnitude. Maximum vertical surface changes, both centre and southern tongue,

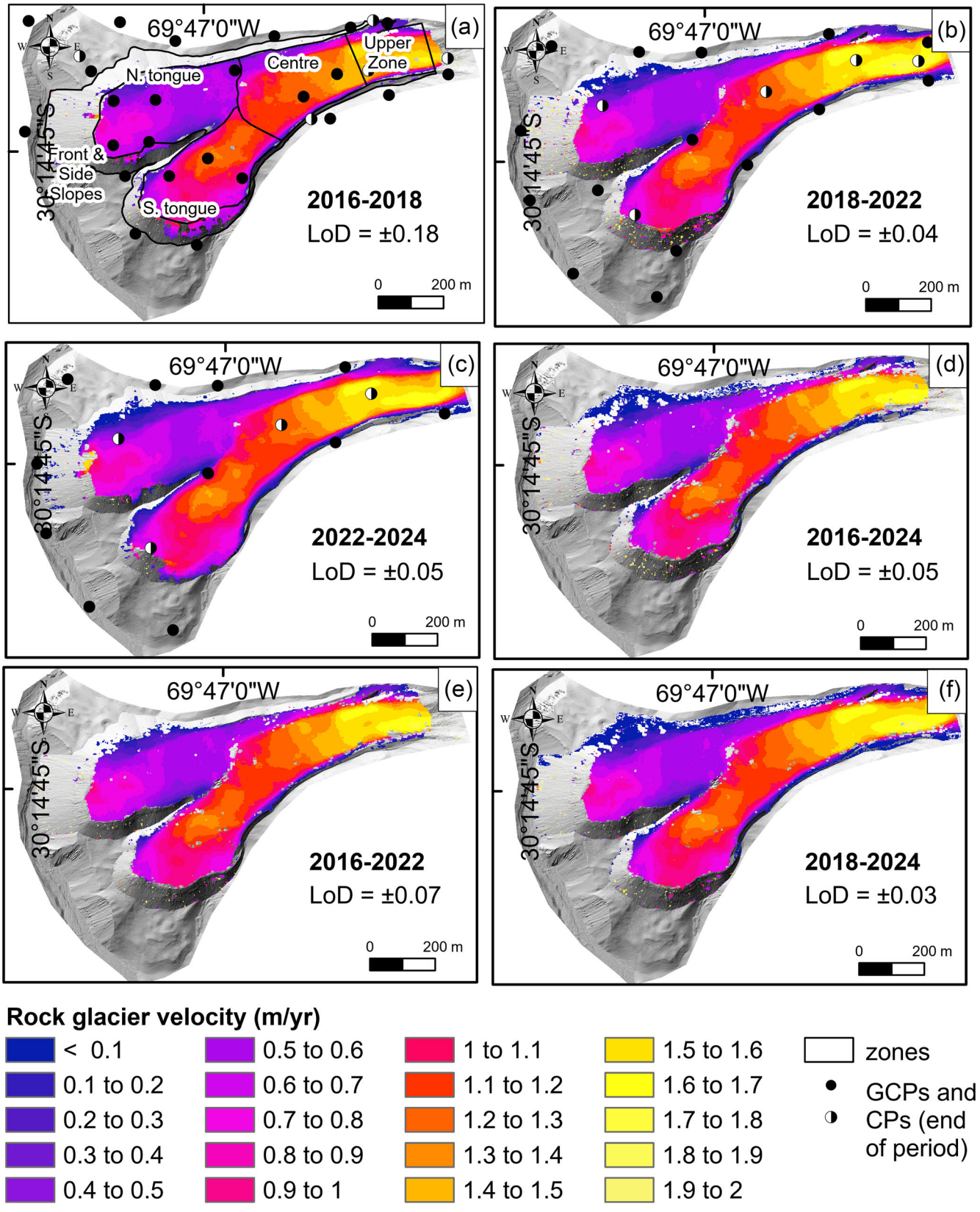

FIGURE 4 Surface velocities (m/yr) on Dos Lenguas rock glacier with 2 m resolution, based on feature tracking on UAV-based hillshades at 25 cm resolution. Time periods are 2016–2018 (A), 2018–2022 (B), 2022–2024 (C), 2016–2024 (D), 2016–2022 (E) and 2018–2024 (F). Surface velocities are displayed on top of the 2024 hillshade. Limits of Detection provided in m/yr). A), B) and C) further include the locations of DGNSS measured GCPs and CPs (cf. Table 2 and supplementary material 1) for the end of the period, e.g., for 2018 in A).

occur at velocities of more than 1 m/yr and less than 1.25 m/yr, vertical changes in areas with velocities below 1 m/yr or above 1.5 m/yr rarely exceed ±0.25 m/yr (Figure 6G, H).

Correlation coefficients (Pearson) calculated for upper-centre-northern (zone A) tongue and upper-centre-southern (zone B) tongue for all resolutions (2 m, 5 m, 10 m) and time episodes

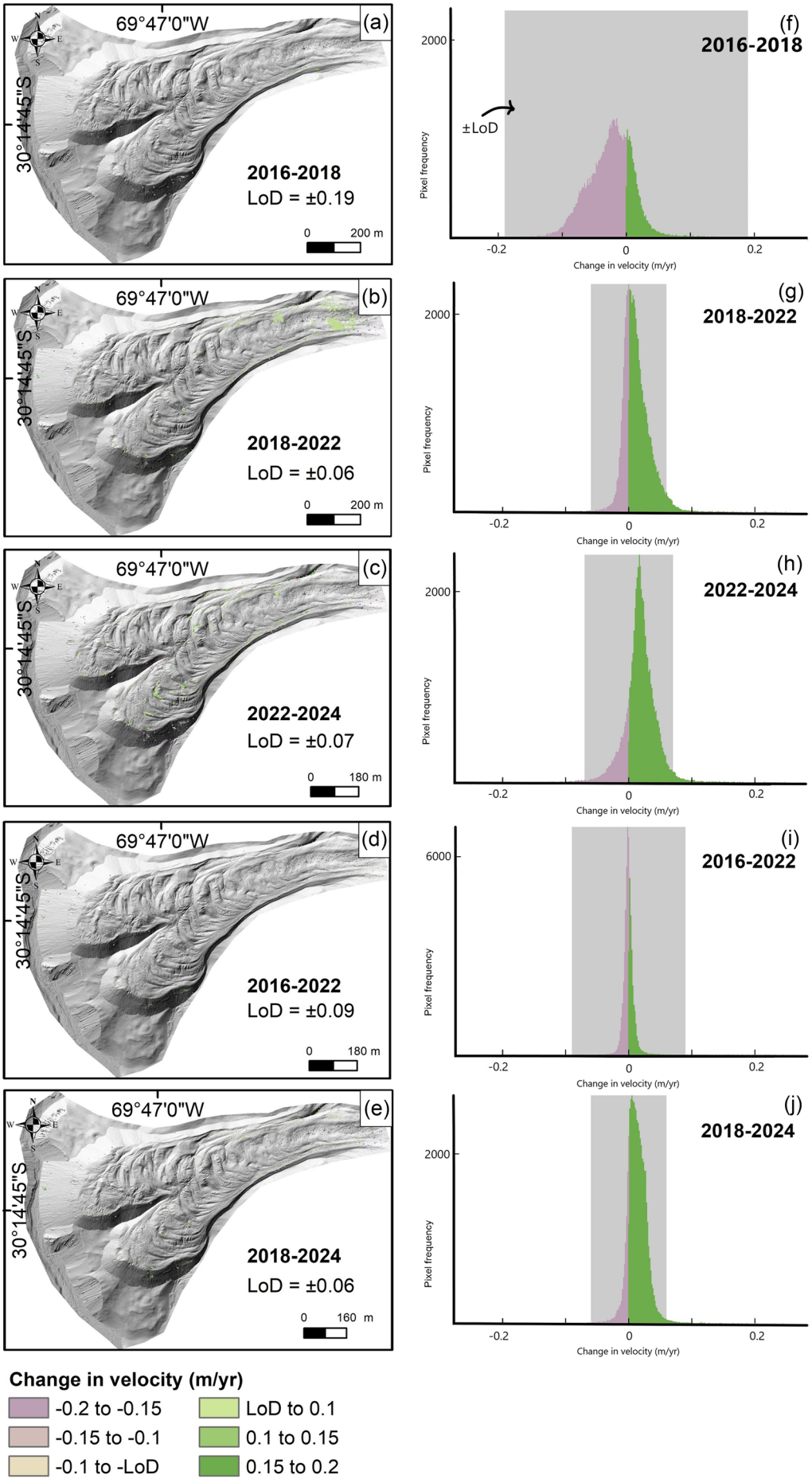

FIGURE 5 Legend on next page.

FIGURE 5 Acceleration and deceleration of annual surface velocities (m/yr) on Dos Lenguas rock glacier for episodes 2016–2018 (A, F), 2018–2022 (B, G), 2022–2024 (C, H), 2016–2022 (D, I) and 2018–2024 (E, J), all normalized to years and compared to the 2016–2024 mean. LoDs are propagated by summing the squares of the individual LoDs (cf. Figure 4) and taking the square root of the result. A-E: displayed with 2 m resolution on top of the 2024 hillshade. Values within LoDs are not visualized. F-J: values correspond to velocity change on the rock glacier surface only (no front and side slopes). LoDs are indicated with grey boxes.

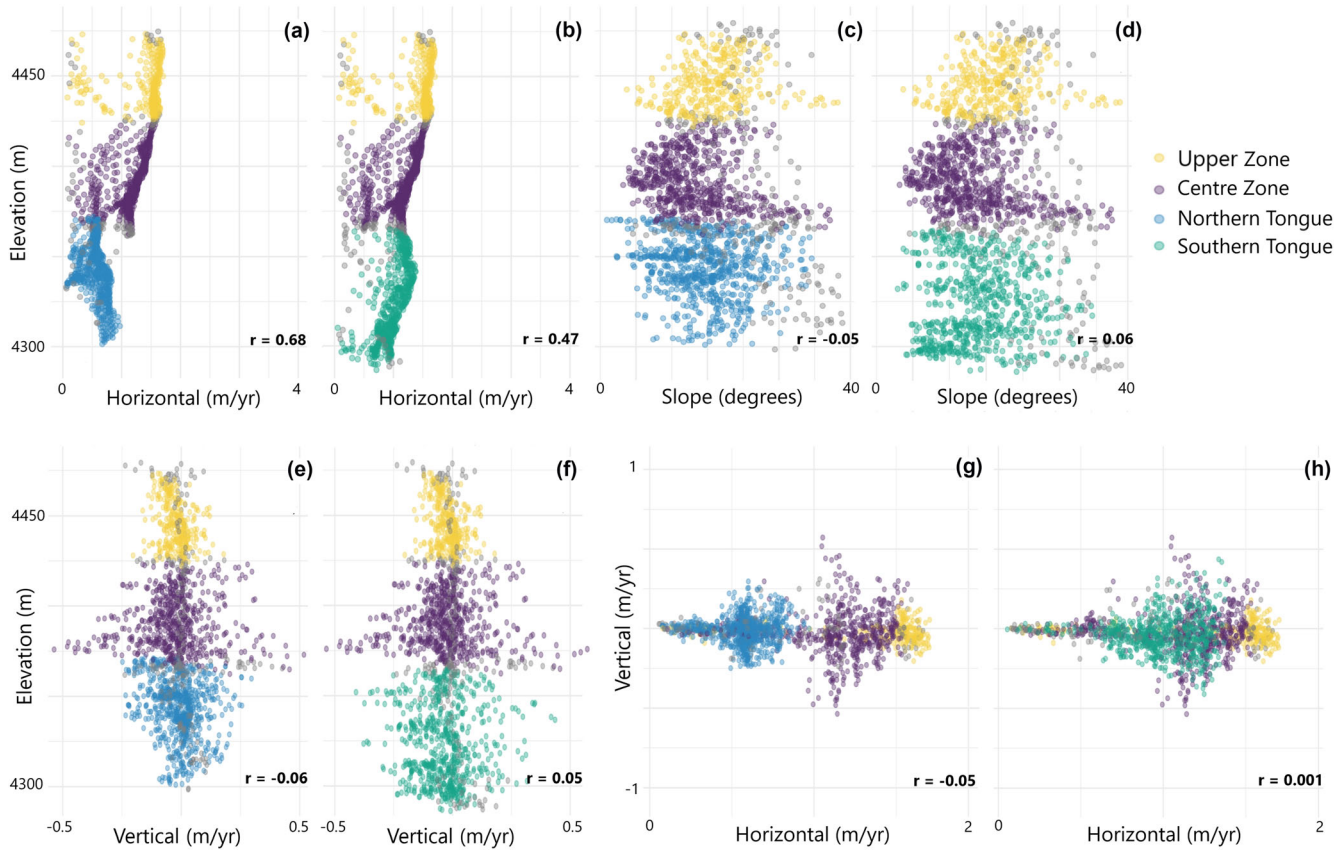

FIGURE 6 Dos Lenguas rock glacier kinematics and their concurrence with topographic characteristics based on 2016–2024 data (cf. Figure 2-4 D) at 10 m resolution. Plotted against elevation, horizontal surface change (A, B), slope (C, D) and vertical surface change (E, F) show unique patterns. Horizontal surface change is further plotted against vertical surface change (G, H). For each pair, the upper zone (yellow) and centre zone (purple) show the same data, with alteration for the northern tongue (blue; A, C, E, G) and the southern tongue (green; B, D, F, H). See Figures 1C, 2A, 4A for a delineation of the geomorphological zones.

(2016–2018, 2018–2022, 2022–2024, 2016–2024, 2016–2022, 2018–2024) show strongest positive correlations between elevation and horizontal surface change (A: 0.62 to 0.71; B: 0.36 to 0.47) (Figure 6, supplementary material 4). Highest values for zone A are reached for the 2016–2024 and 2016–2018 time episodes. For zone B, the correlation remains stable across time. For both zones, higher resolutions (2 m, 5 m) produce higher correlation coefficients. We find a weak but persistent positive correlation between vertical surface change and slope (A: 0.40 to 0.53; B: 0.40 to 0.55), consistent in time and increasing with higher resolutions. We find a weak negative correlation between vertical surface change and curvature at 5 m, and partially at 10 m resolution (A: −0.13 to −0.35; B: −0.11 to −0.43), stable through time.

4.5 | Climatologic records

ERA5 air temperature provided through meteoblue history+ (Figure 7A, red), constantly falls below the temperature data measured in front of Dos Lenguas (Figure 7A, grey) for the same time period (February 14th, 2022 to February 7th, 2023). This difference between the two datasets is larger for the austral winter months in comparison to the austral summer months. Air temperature evolution since 1940, based on the ERA5 data, shows a clear warming trend for the last decades (Figure 7B). Both austral summer (bright red, October to March) and austral winter (dark red, April to September) temperatures fall below their 1940–2024 mean (dashed lines) in the 90s. While austral summer temperatures have exceeded this mean since the early 2000s, the onset of winter temperatures exceeding their mean in 2017 coincides almost with the UAV monitoring period (2016–2024, grey box). Historical ERA5 precipitation in the austral summer months (Figure 7C) is less compared to the winter months (Figure 7D). This is independent of precipitation occurring as rain (dark blue) or snow (light blue).

Based on the visible inspection of repeated optical photos, we find that snow cover is present on 14 out of 377 days at the location close to Dos Lenguas rock glacier. It does not last for more than three consecutive days (June 20th, 2023 to June 23rd, 2023, August 19th,

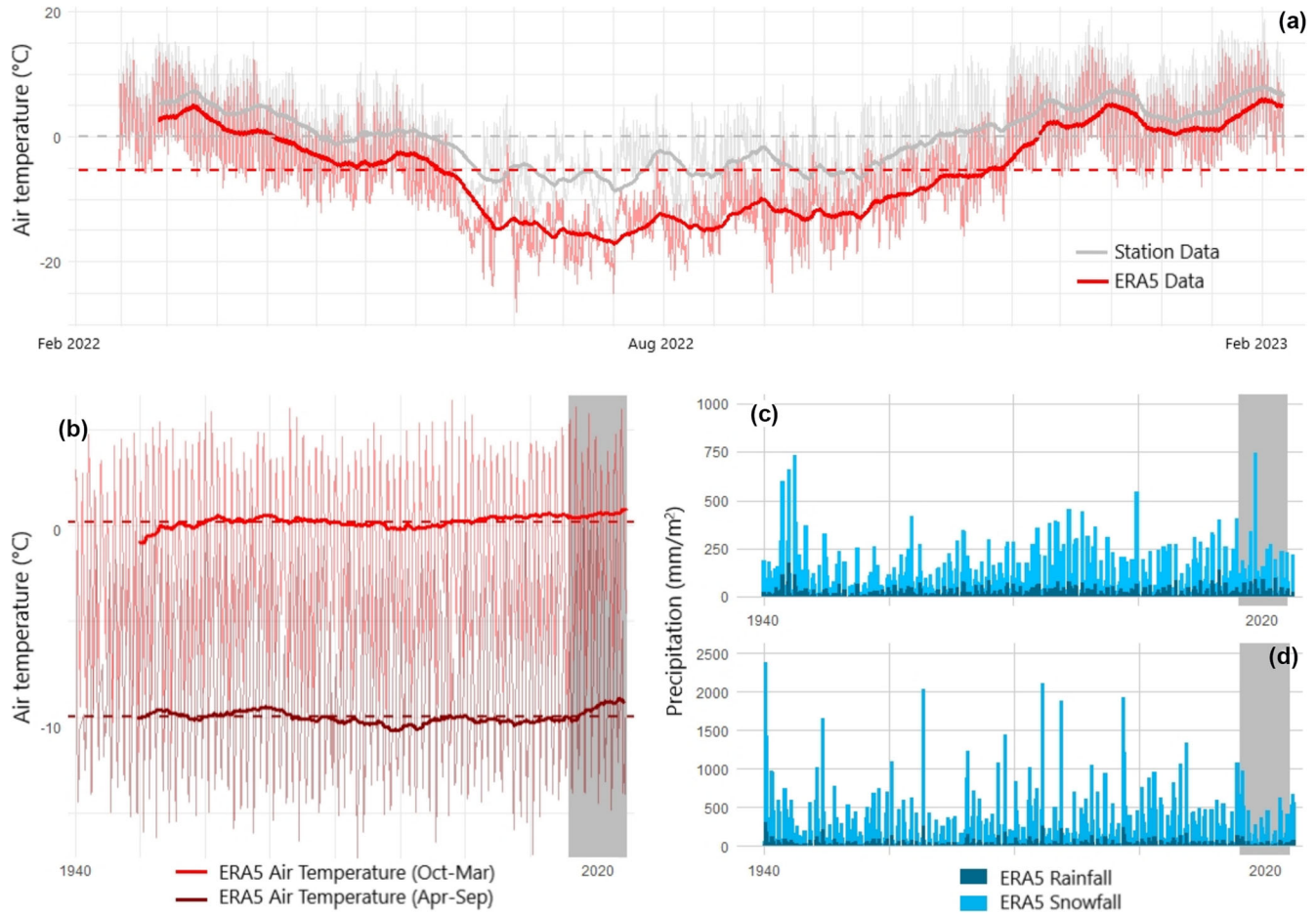

FIGURE 7 Air temperature and precipitation at Dos Lenguas rock glacier. Comparison of hourly ERA5 air temperature data provided through meteoblue history+ (red) to hourly measured air temperature (grey) for February 14th, 2022 to February 7th, 2023 (A). Dashed lines show mean colour-coded for the different datasets. Monthly ERA5 air temperature evolution over time for the October to March period (red) and April to September period (dark red) displayed as 5 year mean (solid lines) and mean temperature (dashed lines) (B). Monthly ERA5 precipitation as rainfall (dark blue) and snowfall (bright blue) for Dos Lenguas in the austral summer months (C) and the austral winter months (D). Note the different y-axis limits for the drier austral summers (C) compared to the wetter austral winters (D). The grey boxes correspond to the time period of the UAV-based monitoring.

2023 to August 21st, 2023). Snow height at this location does not exceed 10 cm, estimated based on poles. The camera located in the upper catchment shows snow on 147 out of 386 days whereby on 104 of these days snow is present as single patches, often located at the western slope only. Similar to the UAV imagery, these photos are available in the accompanying dataset publication (Stammler et al., 2025).

5 | DISCUSSION

5.1 | Data quality

The error between the DEMs and the DGNSS measurements used as CPs is <10 cm for the 2018, 2022 and 2024 DEMs (Table 3). It is higher for the 2016 dataset, coinciding with the highest GCP error and lowest resolution (Table 3). In comparison to the spatial resolution of the DEMs, the GCP and CP errors for the 2018–2024 DEMs fall below 1 pixel. Solely the 2016 GCP error (x, z) and the 2016 CP errors range between 1 to 2 pixels. A difference of the 2016–2018 DEM quality compared to the other DEMs is expected given the variability in ground sampling distance in the 2016–2018 datasets (Table 1) and the poorer performance capability of the Phantom 3 Advanced to the Phantom 4 RTK in terms of, e.g., pixel depth, impact of the shutter mechanism on image quality and capability of the sensors to resolve nuances (cf. 3.1, Table 1). The differences in DEM quality between the 2016 and 2018 DEMs are attributed to the few images used for the 2016 DEM generation, resulting in a lower point cloud density (cf. 4.1), in combination with the error introduced by using DGNSS measurements from 2017. The measurement error is comparable for all DGNSS measurements (Table 2). Error between the 2016 selected DGNSS points measured in 2017, compared to the 2018 DGNSS points (cf. 3.2), increases total error. Testing data robustness by plotting the 2016–2022 and 2016–2024 intervals (Figures 2D-E, 4D-E, 5D) and confirmation of the comparatively low error of the 2017 measurements (supplementary material 1) are, thus, essential.

When assessing the bias and the random component of the vertical CP-based errors, we find that for the 2018 and 2022 acquisitions, the bias is negligible compared to the random component (Table 3). For the 2024 acquisition, the bias is higher than for the other datasets but remains smaller than 50% of the random component, indicating a small positive offset. Likely, this impacts the, compared to the other

time episodes, slightly more positive vertical surface change in 2022–2024 (Figure 2C), leading to positive volume changes (Figure 3C). In contrast, the 2016 dataset exhibits a bias that exceeds the random error, suggesting a systematic vertical offset in the DEM. This systematic error in the 2016 dataset prevents the direct application of the error propagation formula by Brasington, Langham, & Rumsby (2003) and Wheaton et al. (2010), which assumes that DEM errors are dominated by random components with negligible bias. This systematic error in the 2016 dataset limits the quality of change detection for time periods involving this DEM. We account for the systematic error by addressing the bias in the LoD calculation (cf. 3.4) and decide for an application of the adapted error propagation for the calculation of all DoD LoDs. For a comparison of the effect of the adaptation of the formula, see supplementary material 8. As expected, the effect is almost minimal for the 2018–2022 DoD, slightly increased for DoDs involving the 2024 DEM and strongly increased for DoDs involving the 2016 DEM. The lower data quality of the 2016 datasets further leads to high uncertainty in volume calculation for time periods involving the 2016 acquisition (Figure 3A, D-E). We consider the results involving the 2016 to be reliable, given their similarities in spatial pattern and magnitude to the 2018–2022 dataset.

For all time episodes, quantified vertical and horizontal surface change is restricted to the rock glacier surface, sides and front. Otherwise, expected geomorphologically stable areas exhibit surface change below our LoDs, vertically and horizontally (Figures 2 & 4). This is supported by the DGNSS points measured outside the rock glacier surface (cf. Figure 4A-C), indicating high stability across all time periods (< 0.1 m/yr).

The defined 90% percentile as LoD during feature tracking results in comparatively low LoDs (Figure 4) in comparison to the magnitude of horizontal surface changes. DEM error propagates to feature tracking via hillshade generation and is accounted for by testing for stable terrain outside of the rock glacier surface during feature tracking.

5.2 | Dos Lenguas velocities: stable in time and in agreement with published data

In Dos Lenguas rock glacier's upper zone, debris moves rapidly without compressional flow, conveying debris and potentially ice to the lower zones (Figure 4, Halla et al., 2021). In the centre of the Dos Lenguas rock glacier, compressional flow and the development of ridges and furrows increases along with a slight decrease in overall velocities. Movement in the southern half of the upper and centre zone is already faster than in the northern half, at a magnitude much smaller than after tongue separation (Figures 4 and 6A, B). The main horizontal movement follows a 'streamline' from the upper to the southern tongue, with almost non-moving areas towards the edges of the rock glacier.

With our processing of the 2016 and 2018 UAV imagery, we reproduce the maximum surface velocities by Halla et al. (2021) in magnitude and pattern. In addition, we show that mean surface velocities of 0.9 m/yr (Figure 4) with maximum values of 1.7 m/yr in the upper zone (Figure 6) are consistent in time for all additional time episodes investigated in this study. Our velocities, particularly when focusing on the more active areas (cf. Figures 4, 6B), are in agreement with Strozzi et al. (2020) that quantify surface velocities for a location within Dos Lenguas upper zone ranging from 1.5 to 2 m/yr based on interferometric synthetic aperture radar (InSAR) and offset tracking for 2015–2020.

Robson et al. (2022) detect an average velocity of 0.54 ± 0.03 m/yr for rock glaciers in the La Laguna catchment (2012–2020), the neighbouring catchment on the Chilean side of the Andes, next to highlighting several rock glaciers with velocities of approximately 0.9 m/yr. While further detailed comparison is necessary, this highlights a potential for horizontal rock glacier surface change occurring with a similar magnitude on both slopes of the Andes.

With our UAV-based investigation, we detect stable surface velocity conditions on Dos Lenguas rock glacier for the time period 2016–2024 at 2 m resolution and with LoDs being low compared to the magnitude of the velocities. We find no deceleration outside our LoDs (±0.06 to ±0.19 m/yr, cf. Figure 5) for any of the time periods (2016–2018, 2018–2022, 2022–2024, 2016–2022, 2018–2024) and only two time periods where acceleration exceeds the LoDs of the respective time periods, but remains below 0.1 m/yr (Figure 5). This is in agreement with Blöthe et al. (2024) that find unchanged rock glacier velocities for 175 investigated rock glaciers in the Valles Calchaquíes region (Argentina) within three time episodes between 1986 and 2023 (1968–2009, 2009–2020, 2020–2023) based on optical feature tracking on historical aerial photographs, ALOS PRISM and CBERS-4A imagery.

We expect a future disconnection of the northern tongue kinematics from the rest of the rock glacier. As Halla et al. (2021) postulate an increase of ice volume for the northern tongue for 2016–2018, we argue that the decrease of velocity of the northern tongue is due to flow divergence and reduction of material through-put, coupled with a topographical effect, without a necessary decrease of ice content – as supported by the pattern and magnitude of vertical changes being stable in time. Halla et al. (2021) assume more massive ice in the upper zone and more spatially disconnected ice in the rock glacier centre and tongues based on geophysics and four-phase modelling. We encourage repeated geophysical investigation and a thorough investigation of the coincidence of ice content and surface kinematic characteristics for an investigation of their correlation.

Hartl et al. (2023) find localized velocity increase as starting point of rock glacier destabilization on the Äußeres Hochebenkar rock glacier in the Austrian Alps. Velocities on the northern tongue of Dos Lenguas rock glacier increase towards the front, consistent across all time episodes (Figure 3). While these values are not comparable in magnitude to Hartl et al. (2023) at the moment, potential future velocity increase at the front of Dos Lenguas northern tongue including possible front failure represent great hazard potential, as a collapsed front could dam the Agua Negra River, located right next to the Dos Lenguas' front, causing potential for a consequent outburst flood (cf. Figure 1A) and highlighting the importance of continued high-resolution monitoring.

5.3 | Dos Lenguas vertical change: Heterogeneous with predominantly negative volumetric change

The impact of the ridge and furrow system on Dos Lenguas' vertical surface change is apparent across all time episodes (Figure 2). We refrain from mean values given this heterogeneity of the vertical

change distribution in space. We experience a general trend of vertical change magnitude increase in Dos Lenguas rock glacier's centre, likely related to increased compressive flow leading to the formation of higher ridges. Slope values on Dos Lenguas are high in the upper zone, lower in the centre and increase again towards the tongues, specifically the southern tongue (Figure 6C, D). We anticipate the decrease in slope in the centre to represent a knickpoint which leads to a lowering of volume throughput, resulting in high furrows and ridges, explaining the weak positive correlation between vertical change and slope (5.4). Vertical changes on the southern tongue are much higher than on the northern tongue. We relate this to the slope control as described above as well as the magnitude of the main horizontal change streamflow (Figures 4, 5.2). While the northern tongue's front is characterized by gravitational movements, vertical change on the southern tongue's front indicates forward movement of the tongue (Figure 2, blue surface on front). We explain this difference by the spatial pattern of high-magnitude surface velocity that is focused on the upper-centre-southern tongue transect (Figures 4, 5.2).

Volumetric changes are overall negative for the rock glacier surface for the entire time period (Figure 3D). We interpret this as an imbalance of material input in relation to material throughput (e.g., negative balances for upper and centre zones, Figure 3), the latter visible via the continuous forward movement of the southern tongue (Figure 2). The 2022–2024 dataset strongly differs in terms of volumetric changes, displaying positive volumetric change for all geomorphological zones (Figure 3C). For horizontal surface change of rock glaciers, alternation in time of acceleration and deceleration is reported (Blöthe et al., 2024). Similarly, Vivero & Lambiel (2024) find average net elevation changes on three rock glaciers in the Western Swiss Alps to alternate between positive and negative values. Given the horizontal surface change for 2022–2024 not differing from the other time periods (Figure 4C), with acceleration below 0.1 m/yr and no deceleration present (Figure 5C), an investigation of volumetric change over a longer time period is needed to thoroughly ascertain this behaviour.

5.4 | Topography: A catalysator for surface change

Slope is heterogeneously present across elevation (Figure 6C-D), with the upper zone and southern tongue being characterized by the highest slopes, and the highest horizontal changes (Figure 6A, B). We can quantify (cf. 4.5) and exemplify at Dos Lenguas that slope acts as an important driver for horizontal rock glacier surface change, in agreement with the definition of rock glaciers by Barsch (1996) and many other studies. This is supported by the overall direction of flow on Dos Lenguas (south–south-east) being in agreement with the overall highest magnitudes of slope as well as the strong positive correlation of the two. In seeming contrast, high slope values at the most western location of the centre zone correspond with the lowest velocities in this unit. We argue that the higher slope values here are not related to the overall topography but to the highest ridges of the Dos Lenguas' ridge-furrow morphology, found at exactly this location.

Next to facilitating gravitational force on the rock glacier mass, knickpoints in slope control the degree of compression on the rock glacier surface. This degree of compression controls the magnitude of vertical change when observed with fixed pixel frames (impact of horizontal flow on vertical change) (Figure 4). With compressional flow, vertical changes are highest (both negative and positive) while velocity decreases (Figure 6E-F, cf. 5.2, 5.3). The observed weak negative correlation between vertical change and curvature is likely related to higher vertical change occurring on ridges or in furrows and not in the area of transition between both, the area with higher curvature. The correlation coefficients are higher at resolutions of 5 and 10 m, which pick up the pattern of ridges and furrows better, not obscured by, e.g., movement of big boulders.

The differences in behaviour of the tongues (lower magnitude of surface changes on northern tongue with increase in velocity towards the front; higher magnitude of velocities and vertical changes on the southern tongue stable in time) have been discussed as function of different slope and flow diversion by potential impact of bedrock topography (Halla et al., 2021; Schrott, 1996). Our data attests to these discussions (Figure 6A-B).

With elevation increase, we generally find higher velocities (Figure 6A, B) and correlation coefficients. This pattern is impacted most by the highest velocity values occurring in the upper zone. Correlation is much higher when looking at the upper, centre and northern tongue rather than the upper centre and southern tongue, as velocities on the northern tongue are lower. We expect this behaviour not only to be driven by the high slopes in the upper zone but also by the pull force of the compressed rock glacier mass in the rock glacier centre, supported by the increasing slope values on the southern tongue.

5.5 | Temperature: A foundation for surface change

For the time period covered by our air temperature measurements, ERA5 air temperature is constantly lower than measured at our climatological station in front of Dos Lenguas rock glacier (Figure 7A), particularly in the austral winter. We attribute this difference to the spatial resolution of the ERA5 data, causing areas of an altitude higher than Dos Lenguas, and even higher than the location of our climate station, to impact the dataset. As the change patterns between the ERA5 and measured data are similar, we consider relative change within the historical time period from 1940 to 2024 to resemble real change. For observations of absolute air temperature changes, we highlight the need for longer periods of in-situ measured data to ensure correct temperature approximation.

We do see an overall temperature increase with ERA5 austral summer air temperatures exceeding the 1940 to 2024 mean since the 2000s. Historical precipitation (rain and snowfall) for austral summers shows no clear trend (Figure 7C). Austral winter temperatures have continuously exceeded their 1940 to 2024 mean since 2017, coinciding with the monitoring period of our study. Historical precipitation data for austral winters is reduced for the period after 2017. Austral winter precipitation, in general, is higher than austral summer precipitation. The fact that winter precipitation is more affected by change than summer precipitation is in agreement with Rivera et al. (2021), who state that the regional drought from 2000 to 2021

affected the wet season most, in Rivera et al. (2021) describing April–October.

Due to the low precipitation and strong winds in the Dry Andes, snow cover is sparse and consistently scattered (as also perceived from daily images, cf. 4.6). With its location on the west-facing slope in the southern hemisphere, snow at the Dos Lenguas site is further exposed to higher sun activity, leading to rapid melting. Insolation effects on ground temperature are, hence, not comparable to the Alps, where temperature sheltering by snow cover (Bast et al., 2024) as well as the effect of the absence thereof (Koenig et al., 2025; Noetzli & Pellett, 2023) have been reported. This potentially enables a more direct effect of austral winter temperatures on rock glacier velocities. We hypothesize, that the absence of snow sheltering compensates temperature increase as cold winter temperatures – despite being warmer than before – are able to thoroughly penetrate the rock glacier.

Bast et al. (2024) conclude based on a rock glacier study in the Alps that winters with little snow in combination with dry summers are beneficial for rock glacier deceleration. For Dos Lenguas, warmer and drier austral winters in combination with warmer and generally dry austral summers are beneficial for unchanged velocities (Figure 5), enabling a generally stable state. A monitoring of seasonal kinematics of Dos Lenguas rock glacier potentially offers the opportunity to study the effects of (increasingly) arid conditions on rock glacier kinematics, focusing on the role of liquid water availability.

5.6 | Surface kinematics on Dos Lenguas: Implications for the regional state of permafrost

Dos Lenguas kinematics imply a stable state of permafrost conditions for the area. This is unexpected given increasing air temperatures in the region (Pabón-Caicedo et al., 2020; Pitte et al., 2022) and an unprecedented decrease of ice surface area and volume in the glacial domain (Pitte et al., 2022). Further, in comparison to findings on region-wide acceleration of rock glacier velocities in the Alps (Kellerer-Pirklbauer et al., 2024; Manchado et al., 2024) and North America (Kääb & Røste, 2024).

Stable rock glacier velocities on Dos Lenguas are in coherence with Blöthe et al. (2024) who find unchanged rock glacier velocities for the Valles Calchaguíes region (24° to 25°, Argentinean Andes) for 1968–2023. This supports that rock glacier kinematics in the Dry Andes are currently stable in time and behave differently from rock glaciers in other regions of the world. We attribute the stable kinematics to the lack of snow sheltering (cf. 5.5), allowing for winter temperature penetration and the location at high altitude, with a measured mean air temperature at 0°C (Figure 7A).

Unchanged surface velocities on Dos Lenguas rock glacier elucidate stable permafrost conditions at the location for the observed period in time. This corresponds with Koenig et al. (2025) who find no clear warming indication for ground temperatures in the Andes (27°S to 34°C) based on 53 boreholes at eight locations, spanning a maximum observation period of 9 years between 2006 and 2023. Similar in length of observation to this study, the authors discuss the possibility of short-term temperature fluctuations deviating from long-term trends, highlighting the need for ongoing monitoring efforts.

6 | CONCLUSION

Our UAV-based investigation of Dos Lenguas rock glacier kinematics between 2016 and 2024 allows a high spatio-temporal analysis of rock glacier kinematics. The mean rock glacier velocity for the entire Dos Lenguas surface is 0.9 m/yr (2016–2024). Spatially heterogeneous, the highest values of up to 1.7 m/yr are reached in the upper zone, with a decrease in velocity towards the centre and southern tongue. The northern tongue and northern parts of the Dos Lenguas centre are disconnected from the main spatial velocity pattern. We do not see an increase or decrease in surface velocity within the length of our 8-year study period. The majority of vertical surface changes reach ±1.5 m/yr. Highest magnitudes of vertical surface change are reached in Dos Lenguas centre and on the southern tongue.

We use scatterplot analysis and Pearson correlation coefficients to increase our understanding of forces that drive rock glacier kinematics. Analyses between rock glacier kinematics and topographic characteristics reveal a positive correlation of horizontal change and slope, highlighting the effect of gravitational forces. Further, we find the magnitude and pattern of rock glacier kinematics on Dos Lenguas to be strongly related to the location within the rock glacier surface perpendicular to and along with the flow direction (e.g., flow line vs. edges, extensional vs. compressional flow, disconnected northern vs. connected southern tongue). Vertical change and curvature are weakly, negatively correlated – supporting the impact of the ridge and furrow system. To understand the local variability of rock glacier kinematics within the landform, high-resolution UAV data – for both, horizontal and vertical changes - are essential.

We co-analyse Dos Lenguas surface changes over time with ERA5 air temperature and precipitation data to understand the observed kinematics implications for the local state of permafrost. In contrast to other regions in the world, high-resolution monitoring of Dos Lenguas rock glacier for the time period of 8 years (2016–2024) reveals horizontal surface change to be overall consistent in time, along with increasing (winter) temperatures. We attribute the lack of snow sheltering due to extremely dry conditions allowing for the penetration of winter temperatures through the rock glacier body, and the comparatively high-altitude location of Dos Lenguas (4,400 m asl), the main control of absent kinematic reaction to climatological change. We highlight the importance of high-resolution monitoring for resolving the magnitude and spatial pattern of rock glacier kinematics with low levels of detection.

Our findings contribute to a better understanding of the state of permafrost in the Agua Negra catchment, next to providing potentially transferable answers to the underlying drivers of rock glacier surface changes. With ongoing air temperature increase in the Dry Andes, a (delayed) reaction of the now-absent rock glacier kinematic response is expected in the near future. We emphasize the need for longer-term datasets of more than a decade to capture this rock glacier response and encourage an increase in monitoring efforts at this crucial point in time.

AUTHOR CONTRIBUTIONS

Melanie Stammler: conceptualization; funding acquisition; methodology (including methodological development); investigation; writing – initial draft; writing – reviewing and editing. **Jan Blöthe:**

methodology (including methodological development); investigation; resources (provision of data etc.); supervision; writing – initial draft; writing – reviewing and editing. **Fabian Flöck:** investigation; writing – reviewing and editing. **Rainer Bell:** conceptualization; writing – initial draft; writing – reviewing and editing. **Lothar Schrott:** funding acquisition; supervision; writing – reviewing and editing.

ACKNOWLEDGEMENTS

The historical climatological data is provided by www.meteoblue.com. The authors thank Tamara Köhler, Diana Agostina Ortiz, Philipp Reichartz, Till Wenzel, Manon Cramer, Florian Wester, Kathrin Förster and Gabriele Kraus for their help during fieldwork. We further thank our collaboration partners at IANIGLA-CONICET in Mendoza/ Argentina, particularly Fidel Roig and Dario Trombotto Liaudat as well as Cristian Villaroel (CIGEOBIO-CONICET, San Juan/Argentina). Open Access funding enabled and organized by Projekt DEAL.

CONFLICT OF INTEREST STATEMENT

The authors declare no conflict of interest.

DATA AVAILABILITY STATEMENT

All data used for this study are available at PANGEA.

Stammler, Melanie; Blöthe, Jan; Flöck, Fabian; Bell, Rainer; Schrott, Lothar (2025): UAV-based optical imagery, digital elevation models and hillshades of Dos Lenguas rock glacier/Argentinean Dry Andes (30°S, 69°W; 2016, 2018, 2022, 2024) and daily static optical imagery (2023–2024) [dataset]. Available online at https://doi.org/10.1594/PANGAEA.979876.

ORCID

Jan Blöthe https://orcid.org/0000-0001-9448-9561

REFERENCES

Arenson, L., Springman, S.M. & Sego, D.C. (2007) The rheology of frozen soils. *Applied Rheology*, 17(1), 1–14. Available from: https://doi.org/10.1515/arh-2007-0003

Arenson, L.U., Harrington, J.S., Koenig, C.E.M. & Wainstein, P.A. (2022) Mountain permafrost hydrology—A practical review following studies from the Andes. *Geosciences*, 12(2), 48. Available from: https://doi.org/10.3390/geosciences12020048

Barsch, Dietrich (1996) *Rockglaciers. Indicators for the present and former geoecology in high mountain environments*, Springer series in physical environment. Berlin, Heidelberg: Springer.

Bast, A., Kenner, R. & Phillips, M. (2024) Short-term cooling, drying, and deceleration of an ice-rich rock glacier. *The Cryosphere*, 18(7), 3141–3158. Available from: https://doi.org/10.5194/tc-18-3141-2024

Blöthe, J.H., Falaschi, D., Vivero, S. & Tadono, T. (2024) Rock glacier kinematics in the Valles Calchaquíes region, Northwestern Argentina, from multi-temporal aerial and satellite imagery (1968–2023). *Permafrost & Periglacial*, 36(1), 123–136. Available from: https://doi.org/10.1002/ppp.2260

Blöthe, J.H., Halla, C., Schwalbe, E., Bottegal, E., Trombotto Liaudat, D. & Schrott, L. (2021) Surface velocity fields of active rock glaciers and ice-debris complexes in the Central Andes of Argentina. *Earth Surface Processes and Landforms*, 46(2), 504–522. Available from: https://doi.org/10.1002/esp.5042

Brasington, J., Langham, J. & Rumsby, B. (2003) Methodological sensitivity of morphometric estimates of coarse fluvial sediment transport. *Geomorphology*, 53(3–4), 299–316. Available from: https://doi.org/10.1016/S0169-555X(02)00320-3

Cicoira, A., Marcer, M., Gärtner-Roer, I., Bodin, X., Arenson, L.U. & Vieli, A. (2021) A general theory of rock glacier creep based on in-situ and remote sensing observations. *Permafrost & Periglacial*, 32(1), 139–153. Available from: https://doi.org/10.1002/ppp.2090

Contreras, S., Jobbágy, E.G., Villagra, P.E., Nosetto, M.D. & Puigdefábregas, J. (2011) Remote sensing estimates of supplementary water consumption by arid ecosystems of central Argentina. *Journal of Hydrology*, 397(1–2), 10–22. Available from: https://doi.org/10.1016/j.jhydrol.2010.11.014

Cook, K.L. & Dietze, M. (2019) Short communication: A simple workflow for robust low-cost UAV-derived change detection without ground control points. *Earth Surface Dynamics*, 7(4), 1009–1017. Available from: https://doi.org/10.5194/esurf-7-1009-2019

Croce, F.A. & Milana, J.P. (2002) Internal structure and behaviour of a rock glacier in the Arid Andes of Argentina. *Permafrost and Periglacial Processes*, 13(4), 289–299. Available from: https://doi.org/10.1002/ppp.431

Cusicanqui, D., Lacroix, P., Bodin, X., Robson, B. A., Kääb, A. & MacDonell, S. (2025) Detection and reconstruction of rock glacier kinematics over 24 years (2000–2024) from Landsat imagery. *The Cryosphere*, 19(7), 2559–2581. Available from: https://doi.org/10.5194/tc-19-2559-2025

Dall'Asta, E., Forlani, G., Roncella, R., Santise, M., Diotri, F. & Di Morra Cella, U. (2017) Unmanned aerial systems and DSM matching for rock glacier monitoring. *ISPRS Journal of Photogrammetry and Remote Sensing*, 127, 102–114. Available from: https://doi.org/10.1016/j.isprsjprs.2016.10.003

de Haas, T., Nijland, W., McArdell, B.W. & Kalthof, M.W.M.L. (2021) Case report: Optimization of topographic change detection with UAV structure-from-motion photogrammetry through survey co-alignment. *Frontiers in Remote Sensing*, 2, 626810. Available from: https://doi.org/10.3389/frsen.2021.626810

Evans, I. S. (1979) An Integrated System of Terrain Analysis & Slope Mapping: Department of Geography, University of Durham. https://books.google.de/books?id=xMwaAQAAMAAJ

Fleischer, F., Haas, F., Piermattei, L., Pfeiffer, M., Heckmann, T., Altmann, M., et al. (2021) Multi-decadal (1953–2017) rock glacier kinematics analysed by high-resolution topographic data in the upper Kaunertal, Austria. *The Cryosphere*, 15(12), 5345–5369. Available from: https://doi.org/10.5194/tc-15-5345-2021

Gruber, S. (2012) Derivation and analysis of a high-resolution estimate of global permafrost zonation. *The Cryosphere*, 6(1), 221–233. Available from: https://doi.org/10.5194/tc-6-221-2012

Halla, C., Blöthe, J.H., Tapia Baldis, C., Trombotto, D., Hilbich, C., Hauck, C. & Schrott, L. (2021) Ice content and interannual water storage changes of an active rock glacier in the dry Andes of Argentina. https://doi.org/10.5194/tc-2020-29

Hartl, L., Zieher, T., Bremer, M., Stocker-Waldhuber, M., Zahs, V., Höfle, B., et al. (2023) Multi-sensor monitoring and data integration reveal cyclical destabilization of the Äußeres Hochebenkar rock glacier. *Earth Surface Dynamics*, 11(1), 117–147. Available from: https://doi.org/10.5194/esurf-11-117-2023

Hendrickx, H., Vivero, S., de Cock, L., de Wit, B., de Maeyer, P., Lambiel, C., et al. (2019) The reproducibility of SfM algorithms to produce detailed Digital Surface Models: The example of PhotoScan applied to a high-alpine rock glacier. *Remote Sensing Letters*, 10(1), 11–20. Available from: https://doi.org/10.1080/2150704X.2018.1519641

Hersbach, H., Bell, W., Berrisford, P., Horányi, A., Muñoz-Sabater, J. & Radu, N.R. (2019) Global reanalysis: Goodbye ERA-Interim, hello ERA5| ECMWF Newsletter. In European Centre for Medium-Range Weather Forecasts, 04/2019. https://www.ecmwf.int/en/elibrary/81046-global-reanalysis-goodbye-era-interim-hello-era5, checked on 4/4/2025.

Hu, Y., Arenson, L.U., Barboux, C., Bodin, X., Cicoira, A., Delaloye, R., et al. (2025) Rock glacier velocity: An essential climate variable quantity for permafrost. *Reviews of Geophysics*, 63(1), e2024RG000847.

IANIGLA-CONICET. (2018) ANIGLA-Inventario Nacional de Glaciares y Ambiente Periglacial. Informe de la subcuenca del río Blanco. Cuenca del río San Juan. With assistance of Ministerio de Ambiente y Desarrollo Sustentable de la Nación.

Jones, D.B., Harrison, S., Anderson, K. & Whalley, W.B. (2019) Rock glaciers and mountain hydrology: A review. *Earth-Science Reviews*, 193,

66–90. Available from: https://doi.org/10.1016/j.earscirev.2019.04.001

Kääb, A. & Røste, J. (2024) Rock glaciers across the United States predominantly accelerate coincident with rise in air temperatures. *Nature Communications*, 15(1), 7581. Available from: https://doi.org/10.1038/s41467-024-52093-z

Kellerer-Pirklbauer, A., Bodin, X., Delaloye, R., Lambiel, C., Gärtner-Roer, I., Bonnefoy-Demongeot, M., et al. (2024) Acceleration and interannual variability of creep rates in mountain permafrost landforms (rock glacier velocities) in the European Alps in 1995–2022. *Environmental Research Letters*, 19(3), 34022. Available from: https://doi.org/10.1088/1748-9326/ad25a4

Koenig, C. E. M., Hilbich, C., Hauck, C., Arenson, L. U. & Wainstein, P. (2025) Thermal state of permafrost in the central andes (27–34° s). *The Cryosphere*, 19(7), 2653–2676. Available from: https://doi.org/10.5194/tc-19-2653-2025

Lliboutry, L., Williams, R. & Ferrigno, J.G. (1998) Glaciers of Chilie and Argentina. Geological Survey professional paper. Washington.

Manchado, A.M.-T., Allen, S., Cicoira, A., Wiesmann, S., Haller, R. & Stoffel, M. (2024) 100 years of monitoring in the Swiss National Park reveals overall decreasing rock glacier velocities. *Communications Earth & Environment*, 5(1), 138. Available from: https://doi.org/10.1038/s43247-024-01302-0

Marcer, M., Cicoira, A., Cusicanqui, D., Bodin, X., Echelard, T., Obregon, R., et al. (2021) Rock glaciers throughout the French Alps accelerated and destabilised since 1990 as air temperatures increased. *Communications Earth & Environment*, 2(1), 81. Available from: https://doi.org/10.1038/s43247-021-00150-6

Masiokas, M.H., Rabatel, A., Rivera, A., Ruiz, L., Pitte, P., Ceballos, J.L., et al. (2020) A review of the current state and recent changes of the Andean cryosphere. *Frontiers in Earth Science*, 8, Article 99. Available from: https://doi.org/10.3389/feart.2020.00099

Moore, P.L. (2014) Deformation of debris-ice mixtures. *Reviews of Geophysics*, 52(3), 435–467. Available from: https://doi.org/10.1002/2014RG000453

Noetzli, J. & Pellett, C. (2023) Swiss permafrost bulletin 2022. Swiss Permafrost Monitoring Network (PERMOS). Available from: https://doi.org/10.13093/PERMOS-BULL-2023

Pabón-Caicedo, J.D., Arias, P.A., Carril, A.F., Espinoza, J.C., Borrel, L.F., Goubanova, K., et al. (2020) Observed and projected hydroclimate changes in the Andes. *Frontiers in Earth Science*, 8, Article 61. Available from: https://doi.org/10.3389/feart.2020.00061

Pitte, P., Masiokas, M., Gargantini, H., Ruiz, L., Berthier, E., Ferri Hidalgo, L., et al. (2022) Recent mass-balance changes of Agua Negra glacier (30°S) in the Desert Andes of Argentina. *Journal of Glaciology*, 68(272), 1197–1209. Available from: https://doi.org/10.1017/jog.2022.22

RGIK. (2023) Rock Glacier Velocity as an associated parameter of ECV Permafrost. Baseline Concepts Version 3.2.

Rivera, J.A., Otta, S., Lauro, C. & Zazulie, N. (2021) A decade of hydrological drought in central-western Argentina. *Frontiers in Water*, 3, 640544. Available from: https://doi.org/10.3389/frwa.2021.640544

Robson, B.A., MacDonell, S., Ayala, Á., Bolch, T., Nielsen, P.R. & Vivero, S. (2022) Glacier and rock glacier changes since the 1950s in the La Laguna catchment, Chile. *The Cryosphere*, 16(2), 647–665. Available from: https://doi.org/10.5194/tc-16-647-2022

Schrott, L. (1996) Some geomorphological-hydrological aspects of rock glaciers in the Andes (San Juan, Argentina). *Zeitschrift für Geomorphologie Supplementband*, 104, 161–173.

Schrott, L. (1998) The hydrological significance of high mountain permafrost and its relation to solar radiation. A case study in the high Andes of San Juan, Argentina. *Bamberger Geographische Schriften*, 15, 71–84.

Schwalbe, E. & Maas, H.-G. (2017) The determination of high-resolution spatio-temporal glacier motion fields from time-lapse sequences. *Earth Surface Dynamics*, 5(4), 861–879. Available from: https://doi.org/10.5194/esurf-5-861-2017

Stammler, M., Blöthe, J., Flöck, F., Bell, R. & Schrott, L. (2025) UAV-based optical imagery, digital elevation models and hillshades of Dos Lenguas rock glacier/Argentinean Dry Andes (30°S, 69°W; 2016, 2018, 2022, 2024) and daily static optical imagery (2023–2024) [dataset]. In *PANGAEA*. Available online at: https://doi.org/10.1594/PANGAEA.979876

Stammler, M., Cusicanqui, D., Bell, R., Robson, B., Bodin, X., Blöthe, J. & Schrott, L. (2024) Vertical surface change signals of rock glaciers: combining UAV and Pléiades imagery (Agua Negra, Argentina) Proceedings of the 12th International Conference on Permafrost. DOI: 10.52381/ICOP2024.138.1.

Strozzi, T., Caduff, R., Jones, N., Barboux, C., Delaloye, R., Bodin, X., et al. (2020) Monitoring rock glacier kinematics with satellite synthetic aperture radar. *Remote Sensing*, 12(3), 559. Available from: https://doi.org/10.3390/rs12030559

Vivero, S., Bodin, X., Farías-Barahona, D., MacDonell, S., Schaffer, N., Robson, B.A., et al. (2021) Combination of aerial, satellite, and UAV photogrammetry for quantifying rock glacier kinematics in the Dry Andes of Chile (30°S) since the 1950s. *Frontiers in Remote Sensing*, 2, 784015. Available from: https://doi.org/10.3389/frsen.2021.784015

Vivero, S. & Lambiel, C. (2024) Annual surface elevation changes of rock glaciers and their geomorphological significance: Examples from the Swiss Alps. *Geomorphology*, 467, 109487. Available from: https://doi.org/10.1016/j.geomorph.2024.109487

Wheaton, J.M., Brasington, J., Darby, S.E. & Sear, D.A. (2010) Accounting for uncertainty in DEMs from repeat topographic surveys: Improved sediment budgets. *Earth Surface Processes and Landforms*, 35(2), 136–156. Available from: https://doi.org/10.1002/esp.1886

Williams, R. (2012) DEMs of difference. In Geomorphological Techniques 2 (3.2). Available online at: https://eprints.gla.ac.uk/114527

SUPPORTING INFORMATION

Additional supporting information can be found online in the Supporting Information section at the end of this article.

How to cite this article: Stammler, M., Blöthe, J., Flöck, F., Bell, R. & Schrott, L. (2025) Dos Lenguas rock glacier kinematics stable despite warming trend (2016–2024): Surface changes and the role of topography and climate in the Dry Andes of Argentina. *Earth Surface Processes and Landforms*, 50(11), e70151. Available from: https://doi.org/10.1002/esp.70151

Supplementary Material

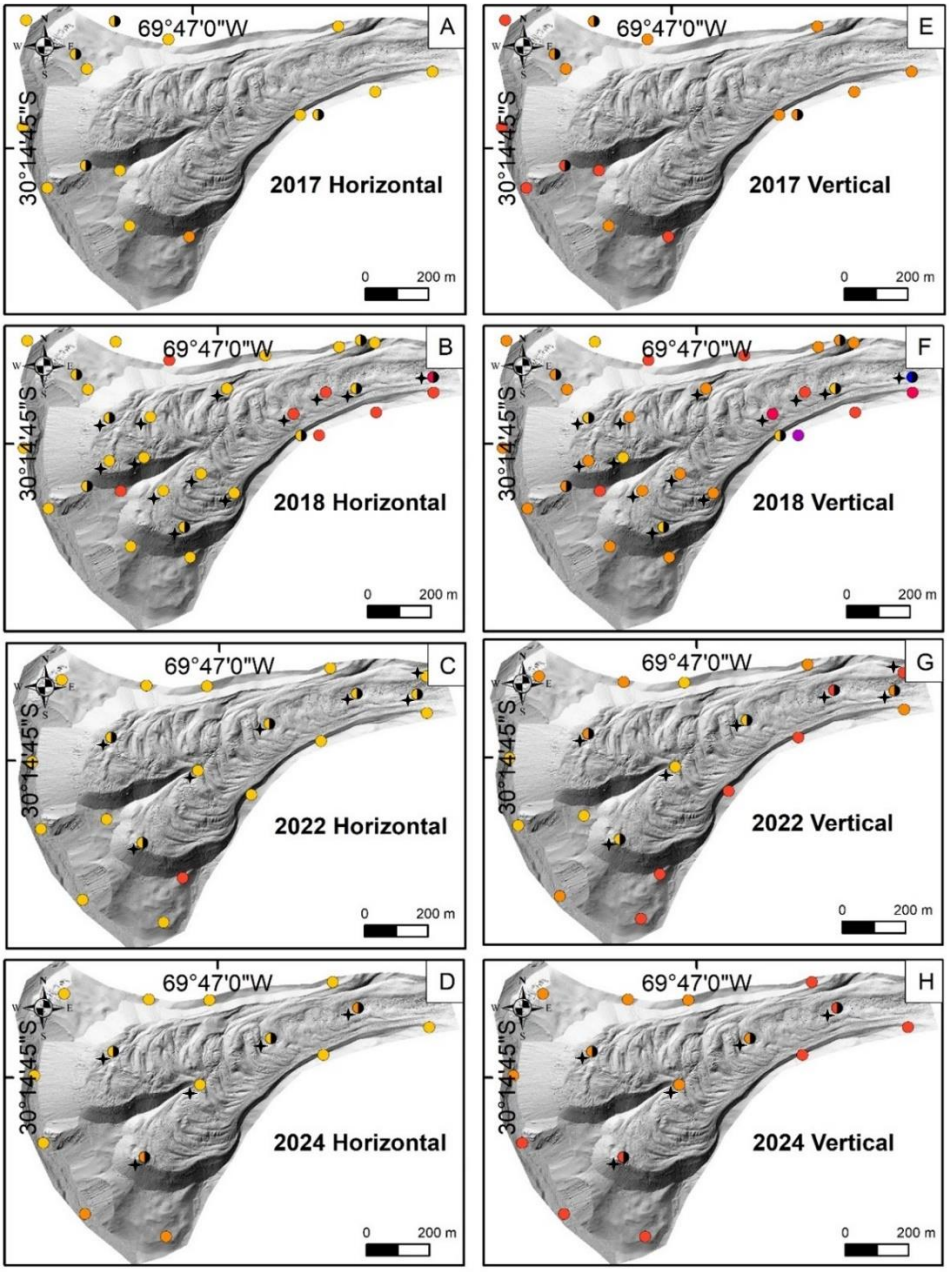

Supplementary Material 1 *Horizontal (A-D) and vertical (E-H) error of our DGNSS measurements displayed for all acquisitions. Data is measured with DGNSS equipment (R8 base, R2s rover, TSC3 handheld, RTK) and displayed in meter on top of the 2024 UAV-based hillshade. The 2017 DGNSS measurements (A, E) are used for the generation of the 2016 DEMs, cf. chapter 3.2. The positioning performance of the Trimble R8 base with RTK is 8 mm + 1 ppm RMS (horizontal) and 15 mm + 1 ppm RMS (vertical). The positioning performance of the Trimble R2s rover with RTK is 10 mm + 1 ppm RMS (horizontal) and 20 mm + 1 ppm RMS (vertical).*

Supplementary material 2 *Number of tie points, projections and projection errors as well as the final optimized camera intrinsic parameters for all UAV image acquisitions. F = focal length, Cx = Principal point X, Cy = Principal point Y, k1-k3 = radical distortion coefficients, p1-p2 = tangential distortion coefficients.*

	2016	**2018**	**2022**	**2024**
# of tie points	917’810	2’378’445	3’490’688	6’178’356
# of projections	3’122’850	7’766’774	10’407’311	19’337’977
Reproj. error (pix)	0.45	0.461	0.243	0.198
F	2334.72	2336.41	3700.11	3700.45
Cx	-2.57579	-3.35131	-8.05231	-39.349
Cy	-3.81541	-3.7087	-28.5707	-9.93101
k1	-0.0303257	-0.0330639	-0.267156	-0.273163
k2	0.0325742	0.0358024	0.0995295	0.106671
k3	-0.00487747	-0.00611871	-0.0219534	-0.0254349
p1	-0.000302105	-0.000429887	-0.000179467	0.000178524
p2	-0.000156312	-0.000134299	0.000134529	-0.000201599

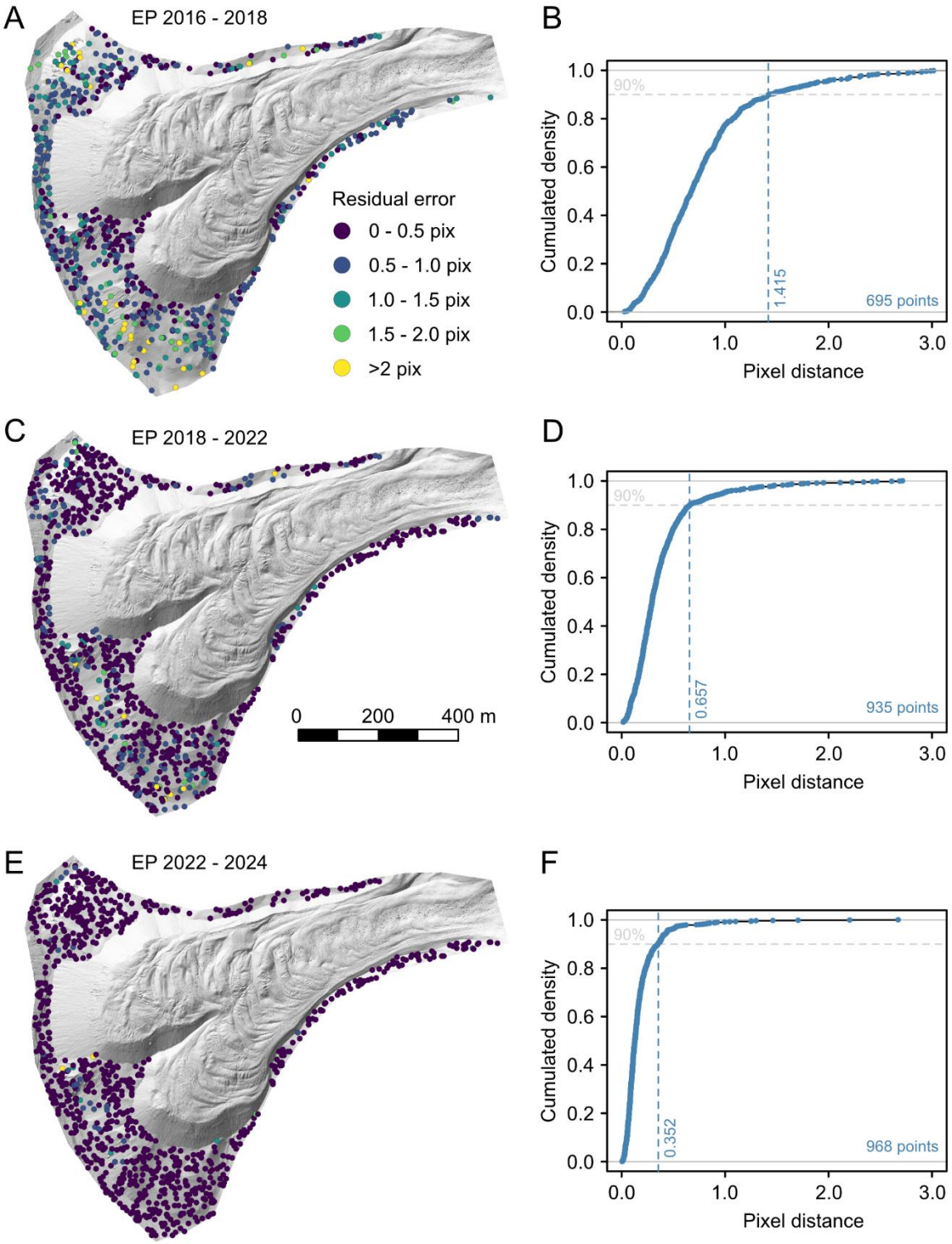
A
EP 2016 - 2018
Residual error
0 - 0.5 pix
0.5 - 1.0 pix
1.0 - 1.5 pix
1.5 - 2.0 pix
>2 pix
B
Cumulated density
90%
1.415
695 points
Pixel distance
C
EP 2018 - 2022
0
200
400 m
D
Cumulated density
90%
0.657
935 points
Pixel distance
E
EP 2022 - 2024
F
Cumulated density
90%
0.352
968 points
Pixel distance

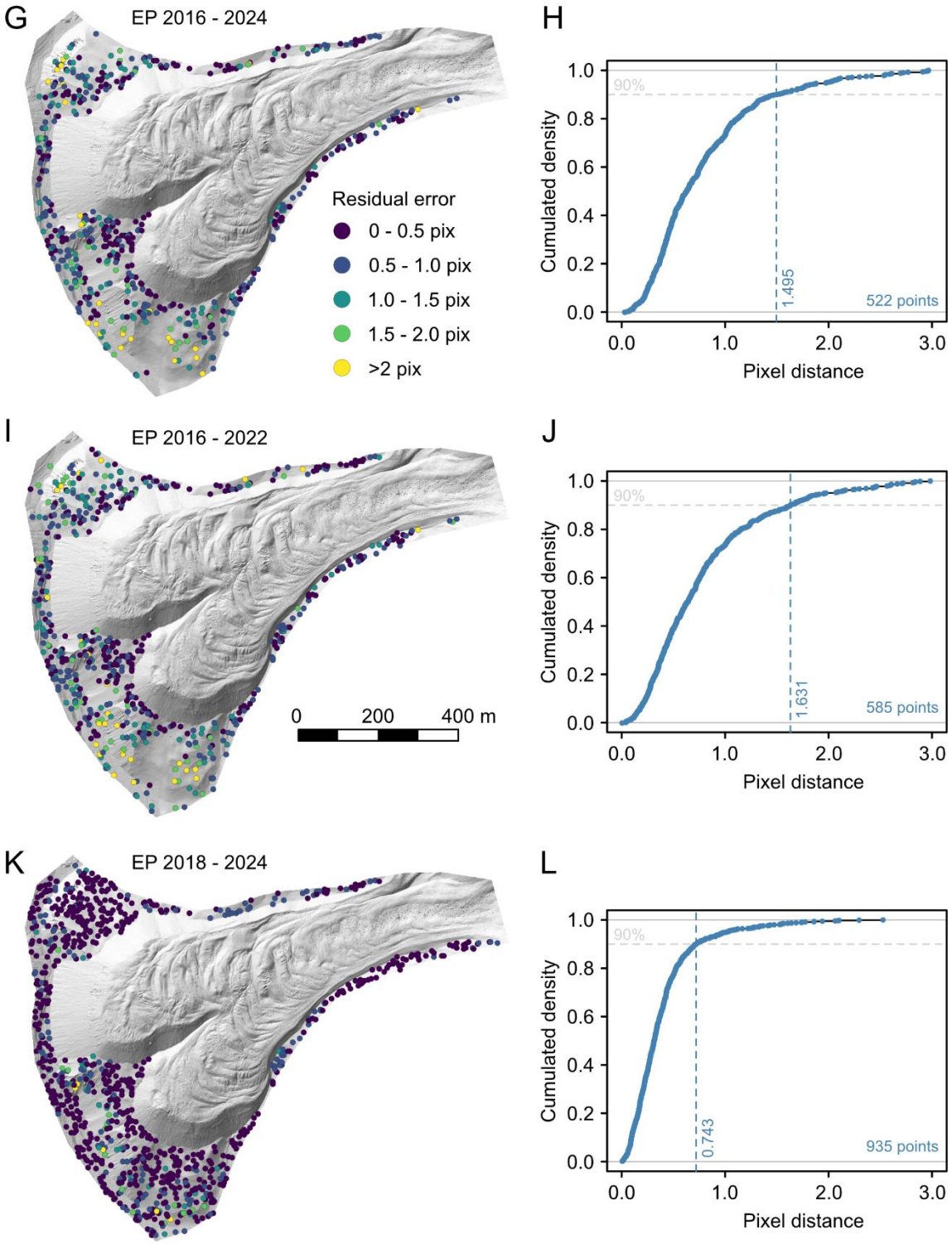

Supplementary Material 3 *Error assessment of the feature tracking approach. Locations of the randomly distributed points used to assess the residual matching error for all epochs (left) cumulated residual error calculated from the randomly distributed points, indicating the 90th percentile of the distribution used as the level of detection (right). Note that while we used 1000 randomly distributed points for tracking the residual motion, the number of successfully matched points that is available for determining the LoD is less.*

Supplementary Material 4 *Correlation coefficients (Pearson) for rasters of horizontal change, vertical change, elevation, slope and curvature for the time episodes 2016-2024, 2016-2018, 2018-2022, 2022-2024, 2016-2022, and 2018-2024 and for 2m, 5m and 10m resolution. Divided in upper zone-centre-northern tongue and upper zone-centre-southern tongue zones.*

Upper zone – Centre – Northern Tongue (A) 2m

1624		horizontal	vertical	elevation	slope	curvature
	horizontal	1	-0.03285	0.707525	-0.0405	-0.01048
	vertical	-0.03285	1	-0.05983	0.405624	-0.28192
	elevation	0.707525	-0.05983	1	-0.02351	0.005534
	slope	-0.0405	0.405624	-0.02351	1	-0.05895
	curvature	-0.01048	-0.28192	0.005534	-0.05895	1
1618		horizontal	vertical	elevation	slope	curvature
	horizontal	1	0.032407	0.669737	-0.04747	-0.00544
	vertical	0.032407	1	0.082612	0.468131	-0.19896
	elevation	0.669737	0.082612	1	-0.02549	0.004743
	slope	-0.04747	0.468131	-0.02549	1	-0.05683
	curvature	-0.00544	-0.19896	0.004743	-0.05683	1
1822		horizontal	vertical	elevation	slope	curvature
	horizontal	1	-0.03023	0.651651	-0.04553	-0.01067
	vertical	-0.03023	1	-0.06032	0.441326	-0.26783
	elevation	0.651651	-0.06032	1	-0.02655	0.007334
	slope	-0.04553	0.441326	-0.02655	1	-0.05834
	curvature	-0.01067	-0.26783	0.007334	-0.05834	1
2224		horizontal	vertical	elevation	slope	curvature
	horizontal	1	-0.07839	0.622632	-0.04807	-0.00464
	vertical	-0.07839	1	-0.16299	0.436298	-0.21046
	elevation	0.622632	-0.16299	1	-0.01354	0.003835
	slope	-0.04807	0.436298	-0.01354	1	-0.0667
	curvature	-0.00464	-0.21046	0.003835	-0.0667	1
1622		horizontal	vertical	elevation	slope	curvature
	horizontal	1	-0.00747	0.696055	-0.04356	-0.00779
	vertical	-0.00747	1	-0.01507	0.424899	-0.28362
	elevation	0.696055	-0.01507	1	-0.02587	0.008434
	slope	-0.04356	0.424899	-0.02587	1	-0.05997
	curvature	-0.00779	-0.28362	0.008434	-0.05997	1
1824		horizontal	vertical	elevation	slope	curvature
	horizontal	1	-0.05343	0.661375	-0.04379	-0.01069
	vertical	-0.05343	1	-0.10291	0.417367	-0.27886
	elevation	0.661375	-0.10291	1	-0.02607	0.010065
	slope	-0.04379	0.417367	-0.02607	1	-0.05983
	curvature	-0.01069	-0.27886	0.010065	-0.05983	1

Upper zone – Centre – Northern Tongue (A), 5m

1624		horizontal	vertical	elevation	slope	curvature
	horizontal	1	-0.03694	0.697686	-0.05822	-0.02944
	vertical	-0.03694	1	-0.06379	0.466976	-0.3513
	elevation	0.697686	-0.06379	1	-0.02517	0.008119
	slope	-0.05822	0.466976	-0.02517	1	-0.13802

	curvature	-0.02944	-0.3513	0.008119	-0.13802	1
1618		horizontal	vertical	elevation	slope	curvature
	horizontal	1	0.035257	0.66774	-0.06612	-0.01437
	vertical	0.035257	1	0.098943	0.510735	-0.12279
	elevation	0.66774	0.098943	1	-0.0275	0.007951
	slope	-0.06612	0.510735	-0.0275	1	-0.12562
	curvature	-0.01437	-0.12279	0.007951	-0.12562	1
1822		horizontal	vertical	elevation	slope	curvature
	horizontal	1	-0.0349	0.645308	-0.06402	-0.03027
	vertical	-0.0349	1	-0.06764	0.501817	-0.25461
	elevation	0.645308	-0.06764	1	-0.0297	0.011439
	slope	-0.06402	0.501817	-0.0297	1	-0.13341
	curvature	-0.03027	-0.25461	0.011439	-0.13341	1
2224	horizontal	vertical	elevation	slope	curvature	zone
	horizontal	1	-0.09232	0.611202	-0.06621	-0.02224
	vertical	-0.09232	1	-0.19106	0.48167	-0.12932
	elevation	0.611202	-0.19106	1	-0.01356	0.004539
	slope	-0.06621	0.48167	-0.01356	1	-0.14395
	curvature	-0.02224	-0.12932	0.004539	-0.14395	1
1622		horizontal	vertical	elevation	slope	curvature
	horizontal	1	-0.00922	0.691459	-0.06432	-0.02513
	vertical	-0.00922	1	-0.01364	0.486812	-0.31264
	elevation	0.691459	-0.01364	1	-0.02994	0.012466
	slope	-0.06432	0.486812	-0.02994	1	-0.13428
	curvature	-0.02513	-0.31264	0.012466	-0.13428	1
1824		horizontal	vertical	elevation	slope	curvature
	horizontal	1	-0.05937	0.650422	-0.06259	-0.02955
	vertical	-0.05937	1	-0.11444	0.481994	-0.31674
	elevation	0.650422	-0.11444	1	-0.02954	0.017349
	slope	-0.06259	0.481994	-0.02954	1	-0.13704
	curvature	-0.02955	-0.31674	0.017349	-0.13704	1

Upper zone – Centre – Northern Tongue (A), 10m

1624		horizontal	vertical	elevation	slope	curvature
	horizontal	1	-0.0462	0.692077	-0.11009	-0.06783
	vertical	-0.0462	1	-0.07217	0.51476	-0.31008
	elevation	0.692077	-0.07217	1	-0.04834	-0.0153
	slope	-0.11009	0.51476	-0.04834	1	-0.14012
	curvature	-0.06783	-0.31008	-0.0153	-0.14012	1
1618		horizontal	vertical	elevation	slope	curvature
	horizontal	1	0.034681	0.671294	-0.11305	-0.04442
	vertical	0.034681	1	0.125184	0.518616	-0.07694
	elevation	0.671294	0.125184	1	-0.04192	-0.00995
	slope	-0.11305	0.518616	-0.04192	1	-0.14794
	curvature	-0.04442	-0.07694	-0.00995	-0.14794	1
1822		horizontal	vertical	elevation	slope	curvature
	horizontal	1	-0.04687	0.650411	-0.1151	-0.06425
	vertical	-0.04687	1	-0.08001	0.530004	-0.18644
	elevation	0.650411	-0.08001	1	-0.05083	-0.001

	slope	-0.1151	0.530004	-0.05083	1	-0.13593
	curvature	-0.06425	-0.18644	-0.001	-0.13593	1
2224		horizontal	vertical	elevation	slope	curvature
	horizontal	1	-0.11961	0.623777	-0.10902	-0.05702
	vertical	-0.11961	1	-0.23519	0.481106	-0.08661
	elevation	0.623777	-0.23519	1	-0.02559	-0.01596
	slope	-0.10902	0.481106	-0.02559	1	-0.16515
	curvature	-0.05702	-0.08661	-0.01596	-0.16515	1
1622		horizontal	vertical	elevation	slope	curvature
	horizontal	1	-0.01689	0.687653	-0.11168	-0.06333
	vertical	-0.01689	1	-0.01393	0.524505	-0.25194
	elevation	0.687653	-0.01393	1	-0.04897	0.000108
	slope	-0.11168	0.524505	-0.04897	1	-0.12985
	curvature	-0.06333	-0.25194	0.000108	-0.12985	1
1824		horizontal	vertical	elevation	slope	curvature
	horizontal	1	-0.07616	0.658578	-0.11538	-0.07088
	vertical	-0.07616	1	-0.13405	0.520437	-0.24927
	elevation	0.658578	-0.13405	1	-0.05064	-0.0002
	slope	-0.11538	0.520437	-0.05064	1	-0.1313
	curvature	-0.07088	-0.24927	-0.0002	-0.1313	1

Upper zone – Centre – Southern Tongue (B), 2m

1624		horizontal	vertical	elevation	slope	curvature
	horizontal	1	0.002857	0.49796	0.002519	-0.00496
	vertical	0.002857	1	0.031482	0.404574	-0.30783
	elevation	0.49796	0.031482	1	0.041126	0.002029
	slope	0.002519	0.404574	0.041126	1	-0.05945
	curvature	-0.00496	-0.30783	0.002029	-0.05945	1
1618		horizontal	vertical	elevation	slope	curvature
	horizontal	1	0.063125	0.452308	0.000408	0.000508
	vertical	0.063125	1	0.226869	0.521257	-0.2412
	elevation	0.452308	0.226869	1	0.035525	-0.00114
	slope	0.000408	0.521257	0.035525	1	-0.05603
	curvature	0.000508	-0.2412	-0.00114	-0.05603	1
1822		horizontal	vertical	elevation	slope	curvature
	horizontal	1	-0.01577	0.425314	-0.00317	-0.00768
	vertical	-0.01577	1	-0.03006	0.48193	-0.31635
	elevation	0.425314	-0.03006	1	0.033796	0.006633
	slope	-0.00317	0.48193	0.033796	1	-0.05819
	curvature	-0.00768	-0.31635	0.006633	-0.05819	1
2224		horizontal	vertical	elevation	slope	curvature
	horizontal	1	-0.04145	0.381617	-0.03733	-0.00521
	vertical	-0.04145	1	-0.06983	0.489421	-0.25872
	elevation	0.381617	-0.06983	1	0.020131	-0.00089
	slope	-0.03733	0.489421	0.020131	1	-0.06199
	curvature	-0.00521	-0.25872	-0.00089	-0.06199	1
1622		horizontal	vertical	elevation	slope	curvature
	horizontal	1	0.020233	0.486902	0.009468	-0.00225
	vertical	0.020233	1	0.061615	0.446252	-0.31962

	elevation	0.486902	0.061615	1	0.039075	0.004373
	slope	0.009468	0.446252	0.039075	1	-0.06029
	curvature	-0.00225	-0.31962	0.004373	-0.06029	1
1824		horizontal	vertical	elevation	slope	curvature
	horizontal	1	-0.02708	0.431547	-0.00182	-0.00862
	vertical	-0.02708	1	-0.04491	0.436818	-0.31378
	elevation	0.431547	-0.04491	1	0.03515	0.008148
	slope	-0.00182	0.436818	0.03515	1	-0.05932
	curvature	-0.00862	-0.31378	0.008148	-0.05932	1

Upper zone – Centre – Southern Tongue (B), 5m

1624		horizontal	vertical	elevation	slope	curvature
	horizontal	1	-0.00058	0.47997	-0.01376	-0.03292
	vertical	-0.00058	1	0.03566	0.469816	-0.43421
	elevation	0.47997	0.03566	1	0.051414	0.003493
	slope	-0.01376	0.469816	0.051414	1	-0.15689
	curvature	-0.03292	-0.43421	0.003493	-0.15689	1
1618		horizontal	vertical	elevation	slope	curvature
	horizontal	1	0.071747	0.446879	-0.02108	-0.01455
	vertical	0.071747	1	0.266604	0.550803	-0.16716
	elevation	0.446879	0.266604	1	0.042479	-0.00419
	slope	-0.02108	0.550803	0.042479	1	-0.13691
	curvature	-0.01455	-0.16716	-0.00419	-0.13691	1
1822		horizontal	vertical	elevation	slope	curvature
	horizontal	1	-0.02015	0.415852	-0.02449	-0.03985
	vertical	-0.02015	1	-0.03289	0.542077	-0.33196
	elevation	0.415852	-0.03289	1	0.042272	0.007862
	slope	-0.02449	0.542077	0.042272	1	-0.14429
	curvature	-0.03985	-0.33196	0.007862	-0.14429	1
2224		horizontal	vertical	elevation	slope	curvature
	horizontal	1	-0.05074	0.364593	-0.058	-0.03126
	vertical	-0.05074	1	-0.08085	0.526652	-0.17901
	elevation	0.364593	-0.08085	1	0.031577	0.000427
	slope	-0.058	0.526652	0.031577	1	-0.15507
	curvature	-0.03126	-0.17901	0.000427	-0.15507	1
1622		horizontal	vertical	elevation	slope	curvature
	horizontal	1	0.019654	0.475966	-0.01501	-0.02636
	vertical	0.019654	1	0.068622	0.514224	-0.40224
	elevation	0.475966	0.068622	1	0.041591	0.007161
	slope	-0.01501	0.514224	0.041591	1	-0.15079
	curvature	-0.02636	-0.40224	0.007161	-0.15079	1
1824		horizontal	vertical	elevation	slope	curvature
	horizontal	1	-0.03238	0.416683	-0.02048	-0.0367
	vertical	-0.03238	1	-0.04984	0.504261	-0.40284
	elevation	0.416683	-0.04984	1	0.043518	0.0132
	slope	-0.02048	0.504261	0.043518	1	-0.14815
	curvature	-0.0367	-0.40284	0.0132	-0.14815	1

Upper zone – Centre – Southern Tongue (B), 10m

1624		horizontal	vertical	elevation	slope	curvature
	horizontal	1	0.001494	0.475108	-0.06025	-0.04359
	vertical	0.001494	1	0.049955	0.500402	-0.42712
	elevation	0.475108	0.049955	1	0.057876	-0.00654
	slope	-0.06025	0.500402	0.057876	1	-0.17245
	curvature	-0.04359	-0.42712	-0.00654	-0.17245	1
1618		horizontal	vertical	elevation	slope	curvature
	horizontal	1	0.0852	0.45387	-0.07066	-0.04639
	vertical	0.0852	1	0.332979	0.526653	-0.12616
	elevation	0.45387	0.332979	1	0.04615	-0.02203
	slope	-0.07066	0.526653	0.04615	1	-0.16438
	curvature	-0.04639	-0.12616	-0.02203	-0.16438	1
1822		horizontal	vertical	elevation	slope	curvature
	horizontal	1	-0.02381	0.420957	-0.06985	-0.05861
	vertical	-0.02381	1	-0.0369	0.543303	-0.27035
	elevation	0.420957	-0.0369	1	0.043356	-0.00205
	slope	-0.06985	0.543303	0.043356	1	-0.1617
	curvature	-0.05861	-0.27035	-0.00205	-0.1617	1
2224		horizontal	vertical	elevation	slope	curvature
	horizontal	1	-0.0675	0.382354	-0.11177	-0.05354
	vertical	-0.0675	1	-0.10257	0.496119	-0.11104
	elevation	0.382354	-0.10257	1	0.028677	-0.01934
	slope	-0.11177	0.496119	0.028677	1	-0.16689
	curvature	-0.05354	-0.11104	-0.01934	-0.16689	1
1622		horizontal	vertical	elevation	slope	curvature
	horizontal	1	0.025257	0.470499	-0.0471	-0.05702
	vertical	0.025257	1	0.094396	0.526413	-0.35323
	elevation	0.470499	0.094396	1	0.053918	-0.00194
	slope	-0.0471	0.526413	0.053918	1	-0.14929
	curvature	-0.05702	-0.35323	-0.00194	-0.14929	1
1824		horizontal	vertical	elevation	slope	curvature
	horizontal	1	-0.03636	0.424787	-0.06623	-0.06349
	vertical	-0.03636	1	-0.05503	0.520583	-0.35463
	elevation	0.424787	-0.05503	1	0.047957	0.002761
	slope	-0.06623	0.520583	0.047957	1	-0.15925
	curvature	-0.06349	-0.35463	0.002761	-0.15925	1

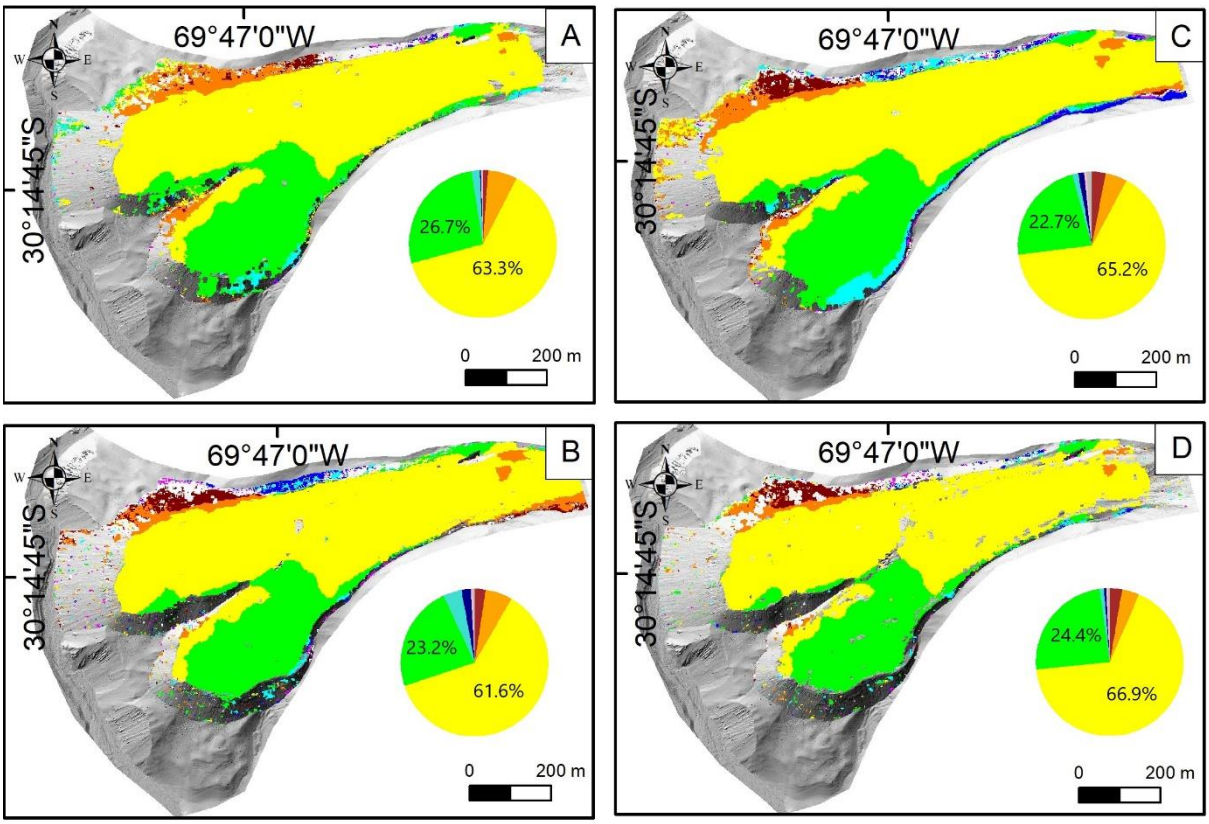

Supplementary Material 5 *Consistency in direction of rock glacier surface velocity on Dos Lenguas rock glacier with 2m resolution, based on feature tracking on UAV based hillshades at 25cm resolution. Time episodes are 2016-2018 (A), 2018-2022 (B), 2022-2024 (C), 2016-2024 (D). All velocity directions are displayed on top of the 2024 hillshade.*

Supplementary Material 6 *DEM characteristics per data-take separated by the location of the respective GCPs and CPs (all errors in cm). For a visualization of the location of the GCPs and CPs, cf. supplementary material 1. For 2016, no DGNSS measurements are available on the rock glacier surface, see text. For 2022, no CPs are located outside of the rock glacier surface, cf. supplementary material 1. For 2024, only 1 GCP is located at the rock glacier surface – restricting the calculation of errors. Similar to 2022, no CPs are located outside the rock glacier surface in 2024.*

	2016	**2018**	**2022**	**2024**
Mean GCP error (x, y, z in cm) for GCPs located **on** *the RG surface*	NA	-0.33, -0.37, -1.38	-1.17, 0.45, -2.82	NA
St. Dev. of the GCP error (x, y, z in cm) for GCPs located **on** *the RG surface*	NA	2.85, 5.21, 2.00	1.00, 0.87, 3.81	NA
Mean GCP error (x, y, z in cm) for GCPs located outside **outside off** *the RG surface*	-3.35, -0.44, 0.98	0.19, -1.40, 0.80	-0.41, -0.78, -0.46	0.02, -0.65, -0.36
St. Dev. of the GCP error (x, y, z in cm) for GCPs located **outside off** *the RG surface*	10.36, 5.26. 12.90	4.01, 5.52, 4.82	1.78, 3.38, 2.67	4.16, 5.26, 4.63
Mean CP error (x, y, z in cm) for CPs located **on** *the RG surface*	NA	0.94, 0.57, -1.01	0.86, -0.07, 0.42	-3.48, -4.70, 2.34
St. Dev. of the CP error (x, y, z in cm) for GCPs located **on** *the RG surface*	NA	4.72, 7.54, 3.30	1.41, 1.47, 1.59	3.82, 5.10, 5.53
Mean CP error (x, y, z in cm) for GCPs located **outside off** *the RG surface*	14.15, -0.97, -12.61	-0.37, -1.64, 1.39	NA	NA
St. Dev. of the CP error (x, y, z in cm) for GCPs located **outside off** *the RG surface*	16.18, 24.49, 11.25	1.93, 7.33, 4.00	NA	NA

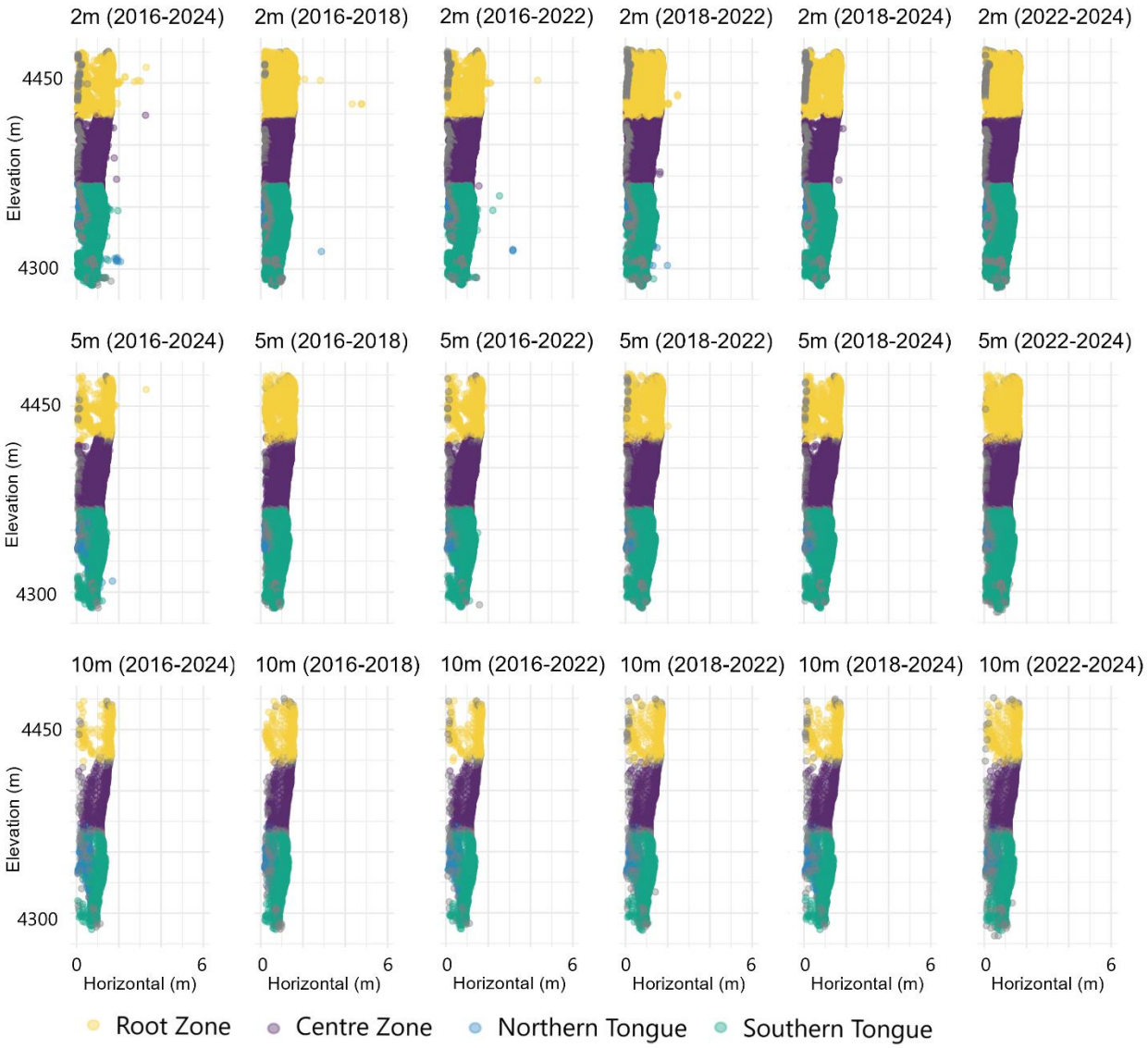

Supplementary Material 7 *Spatio-temporal independence of raster correlation exemplified for the scatterplots showing horizontal change (x axis) and elevation (y axis) for the upper zone (yellow), centre (purple), northern tongue (blue) and southern tongue (green) zones, the later overlapping to show the general pattern while keeping the number of subplots easy to compare. Figure shows 2m, 5m, and 10m resolution grouped by rows and 2016-2018, 2018-2022, 2022-2024, 2016-2024, 2016-2022, 2018-2024 time episodes grouped by columns. All horizontal change data is plotted against the elevation at the beginning of the respective time periods, e.g., the 2016-2018 horizontal change is plotted against the 2016 elevation dataset.*

Supplementary Material 8 Calculation of the levels of detection (in cm) based on the original formula by Brasington et al. (2003) and Wheaton et al. (2010) or by the bias corrected error propagation, cf. 3.4.

	Random error-based error propagation (cm)	**Bias-corrected error propagation (cm)**
LoD1618	±11.85	±24.94
LoD1822	±4.04	±4.11
LoD2224	±5.76	±7.67
LoD1624	±12.53	±27.48
LoD1622	±11.36	±24.39
LoD1824	±6.66	±8.51

Glacial decline next to stable permafrost in the Dry Andes? Vertical glacier surface changes and rock glacier kinematics based on Pléiades imagery (Rodeo basin, 2019-2025)

Melanie Stammler[1], Jan Blöthe[2], Diego Cusicanqui[3], Simon Ebert[2,4], Rainer Bell[1], Xavier Bodin[5], Lothar Schrott[1]

[1]Department of Geography, University of Bonn, Bonn, 53115, Germany (https://orcid.org/0000-0002-9626-7548)
[2]Faculty of Environment and Natural Resources, University of Freiburg, Freiburg, 79104, Germany
[3]Institut des Sciences de la Terre (ISTerre) CNES, CNRS, IRD, Univ. Grenoble Alpes, Grenoble, 38000, France (https://orcid.org/0000-0002-4681-1111)
[4]Department of Earth and Planetary Sciences, ETH Zurich, Zurich, 8092, Switzerland (current address)
[5]Laboratoire EDYTEM, CNRS/Université Savoie Mont Blanc, Le Bourget du Lac, 73370, France

Correspondence to: Melanie Stammler (stammler@uni-bonn.de)

Abstract. The presence and volume of high-mountain cryospheric features are drastically affected by rising air temperatures – on global scale. In the Dry Andes, precipitation is extremely scarce, shifting the hydrological significance towards the solid water storages, glaciers and ground ice. While glaciers decrease in surface area and volume, periglacially stored waters, e.g., in rock glaciers, react more retarded to atmospheric forcing, potentially buffering future water availability. Despite rising air temperatures, recent studies suggest stable permafrost conditions in the Dry Andes based on borehole investigation and rock glacier kinematics for the last decade.

We investigate vertical surface changes of 19 glaciers, three debris-covered glaciers and 59 rock glaciers in the Rodeo basin (Dry Andes, Argentina) for the time period 2019-2025. Further, we calculate rock glacier velocities for 47 of the 59 rock glaciers for which we have data for all time periods. We follow photogrammetric principles using (tri)stereo, panchromatic Pléiades imagery to generate projected optical imagery and DEMs in Ames Stereo Pipeline that we co-register prior to DEM differencing for vertical surface change calculation. We conduct feature tracking on the panchromatic Pléiades imagery for the calculation of rock glacier velocities.

We detect glacier surface lowering of up to -8.99 m (cumulative, 2019-2025) and dominantly negative annual surface lowering for all glaciers investigated. We find vertical surface lowering on debris-covered glaciers to be well below the magnitude of glaciers but higher than for rock glaciers – the latter not exceeding a decimetre. We quantify rock glacier velocities of in average 0.28 to 0.82 m/yr (LoDs: ±0.16, ±0.61) and can categorize three rock glacier groups – large and fast, small and fast and small and slow. Across the 47 rock glaciers investigated, we do not find a regional trend of increasing velocities.

In conclusion, we observe a declining glacial domain to contrast with rock glacier velocities which elucidate stable permafrost conditions. We infer a delayed reaction of the periglacial domain to the rising temperatures that lead to the surface lowering of glaciers and highlight the need for ongoing, long(er)-time surface change monitoring in this crucial, dynamic point in time.

1 Introduction

The cryosphere of the Dry Andes of Argentina is an important water reservoir, buffering periods of drought (Dussaillant et al. 2019) and sustaining water use by meltwater contribution to river runoff (Ferri et al. 2020; Masiokas et al. 2020; Pitte et al. 2022; Schrott and Götz 2013). All cryospheric components in this region are exposed to increasing temperatures (Pabón-Caicedo et al. 2020; Pitte et al. 2022) and high variability in magnitude and pattern of precipitation. Compared to glacially stored waters, periglacially stored waters express a longer and extended response time to climatic changes (Arenson et al. 2022). Particularly in arid regions, the detection and quantification of such solid water storages, e.g., ice lenses in permafrost settings, is crucial, with their hydrological relevance increasing in the future (Arenson et al. 2022).

Glaciers in the Dry Andes of Argentina decrease in surface area and volume (Dussaillant et al. 2019; Masiokas et al. 2020; Pitte et al. 2022; Hugonnet et al. 2021), with sublimation strongly affecting glacial ice loss (Ayala et al. 2016; Réveillet et al. 2020). Mass balances for Agua Negra Glacier, located in the study area, reach -3.67 m water equivalent (w.e.) (2020-2021) based on the glaciological method (Pitte et al. 2022). Independent of density parameters, surface lowering presents a first indication of glacier ice loss. For debris-covered glaciers, the debris cover thickness strongly affects the magnitude of ice volume loss (Ferri et al. 2020), thus, the magnitude of vertical surface change. While ablation patterns are heterogeneous, particularly in regions with supraglacial ponds and/or ice cliffs (Ayala et al. 2025; Bodin et al. 2010; Falaschi et al. 2021), thinning (Ayala et al. 2025; Lenzano et al. 2016) or thickening rather than terminus recession is reported as climate response of debris-covered glaciers (Falaschi et al. 2021). In terms of their hydrological significance, debris-covered glaciers are reported to contribute to streamflow in a magnitude similar to glaciers (Ayala et al. 2016).

(Dis)continuous permafrost conditions are present in approximately 11’000 km^2 of the Dry Andes (17°30 S to 35°S, (Borsdorf and Stadel 2013)), based on a Permafrost Zonation Index above 0.5 (Gruber 2012). They are present across a high variability of periglacial landforms, spanning block- and talus slopes (Köhler et al. 2025), protalus ramparts, and rock glaciers (Halla et al. 2021; Robson et al. 2022; Stammler et al. 2025a). Recent studies suggest stable permafrost conditions in the Dry Andes for the last decade based on borehole ground temperature measurements (Koenig et al. 2025) and the monitoring of rock glacier kinematics (Blöthe et al. 2024; Stammler et al. 2025a).

Rock glaciers, consisting of debris, air and ice, are characteristic of permafrost environments (Barsch 1992; RGIK 2022). Their surface kinematics comprise the vertical and horizontal component and are descriptive of the rock glaciers’ mechanical behaviour evident as internal deformation processes and/or surface motion (Hu et al. 2025). Surface movement in horizontal direction, termed rock glacier velocity (RGV), was recently incorporated into the essential climate variable permafrost and is, while focusing on continuous and comparable monitoring, indicative for kinematic changes within the rock glacier body (Hu et al. 2025; RGIK 2023). Rock glacier monitoring efforts in the Andes are scarce (Hu et al. 2025), with few studies on rock glacier kinematics (Blöthe et al. 2021, 2024; Cusicanqui et al. 2025; Halla et al. 2021; Robson et al. 2022; Stammler et al. 2025a; Strozzi et al. 2020; Villarroel et al. 2018; Villarroel and Forte 2020; Villarroel et al. 2022). Studies on vertical surface

changes on rock glaciers are even more rare, with vertical surface changes reported to be minimal (Halla et al. 2021; Robson et al. 2022; Vivero and Lambiel 2024).

Given the rock glaciers' permafrost indication and hydrological significance, the analysis of rock glaciers can greatly contribute to interdisciplinary studies, for example, focusing on a catchment's hydrology. However, rock glacier studies often focus on chosen single rock glaciers. Moreover, only few studies investigate changes in the glacial and periglacial domains (Bodin et al. 2010; Cusicanqui et al. 2023), even fewer on a catchment scale (Falaschi et al. 2025; Robson et al. 2022), providing a comprehensive picture on current changes in the high-mountain cryosphere.

Satellite-based photogrammetry, by now a standard method applied for RGV monitoring (Hu et al. 2025), enables an increased spatial extent and an access- and weather conditions independent study compared to field-based studies. Photogrammetric processing software allows for the generation of digital elevation models (DEMs) based on an overlap of satellite imagery. While DEM differencing of correctly co-registered DEMs enables the calculation of vertical surface changes across landforms, feature tracking on projected, panchromatic imagery allows for the calculation of the horizontal component. (Tri)stereo panchromatic Pléiades imagery has been used for change detection in the field of geosciences (Bagnardi et al. 2016; Beraud et al. 2023; Berthier et al. 2024), often with a focus on glaciology.

In this paper, we investigate the current state of the cryosphere in Rodeo basin (Dry Andes of Argentina, 30ºS and 69ºW) by analysing vertical surface change on 19 glaciers, three debris-covered glaciers, and 59 rock glaciers, as well as horizontal surface change on, due to data coverage, 47 of the 59 rock glaciers for 2019-2025 based on (tri)stereo panchromatic Pléiades imagery. This means that we focus on vertical surface change across all cryospheric landforms but in particular on velocities of rock glaciers in the Rodeo basin. With the study we intent to increase the knowledge on the high-Andean cryosphere in a changing climate, address the above-described gap of combined and catchment wide studies for the glacial and periglacial domains, and contribute to the understanding of the state of permafrost in the arid environment of the Dry Andes. We address the following research questions:

- Which vertical surface changes can be observed on glaciers and debris-covered glaciers and how do these changes compare to vertical surface changes of the rock glaciers in the study area?
- Which vertical and horizontal rock glacier surface changes can be observed across the Rodeo basin and what do these changes imply for the local permafrost conditions?
- What are the advantages and limitations of a Pléiades-based surface change monitoring of glaciers, debris-covered glaciers and rock glaciers in the Dry Andes?

By simultaneously addressing the glacial and periglacial domain as well as increasing the spatial scale of our surface change monitoring to a catchment resolution, we foresee to contribute to a better understanding of the current status of the regional solid water storages in the Dry Andes at a, given rising air temperatures, crucial moment in time.

2 Study Area

The Rodeo basin is located in the Dry Andes, in the Western part of the San Juan Province / Argentina (30ºS and 69ºW), Fig. 1. The high Andean basin hosts 19 glaciers, three debris-covered glaciers, and 59 rock glaciers (IANIGLA-CONICET 2018), representative of a region-typical (peri)glacial landform distribution with few glaciers located at high elevations, dominated by a large number of periglacial landforms (Halla et al. 2021; Köhler et al. 2025), Fig. 1A. With a basin size of 1315.7 km^2, the basin's upper part is strongly impacted by the Cordillera Principal in the west (< 6947.5 m asl) and is underlain by permafrost, with continuous permafrost present above 5000 m asl (Gruber 2012; Halla et al. 2021; Schrott 1996). Most of the basin's runoff discharges to the reservoir Cuesta del Viento located in the inter-mountainous basin between the Cordillera Principal and the Cordillera Frontal (Esper Angillieri 2017) near Rodeo, Fig. 1B, at approximately 1500m asl. Glaciers in the basin are larger in size than rock glaciers, Fig. 2B, are located at higher elevation and are characterised by higher surface slopes, Fig. 1C. As a consequence of valley structures and the rock glaciers' location closer to the valley bottom, they are most often oriented east or south-east, rarely north or west. Characterized by extremely low mean annual precipitation (~250 mm), a mean annual air temperature of -4.9 °C (1961-1990, ERA5) and constant high solar radiation intensities (Lliboutry et al. 1998; Schrott 1994), solid water storages in the form of glacial or ground ice and their meltwaters are essential to river runoff (Dussaillant et al. 2019; Masiokas et al. 2020), with the relative hydrological significance of periglacially stored ice increased in the future (Arenson et al. 2022). According to Caro et al. (2024), the glaciological zone which includes, e.g., Tapado glacier located in ca. 10 km distance west of Agua Negra Glacier in the Chilean Andes, is characterised by the highest vulnerability to glacier runoff scarcity across the Andes. Research in the periglacial domain of the study area has focused on Agua Negra catchment which is part of the upper Rodeo basin (Halla et al. 2021; Köhler et al. 2025).

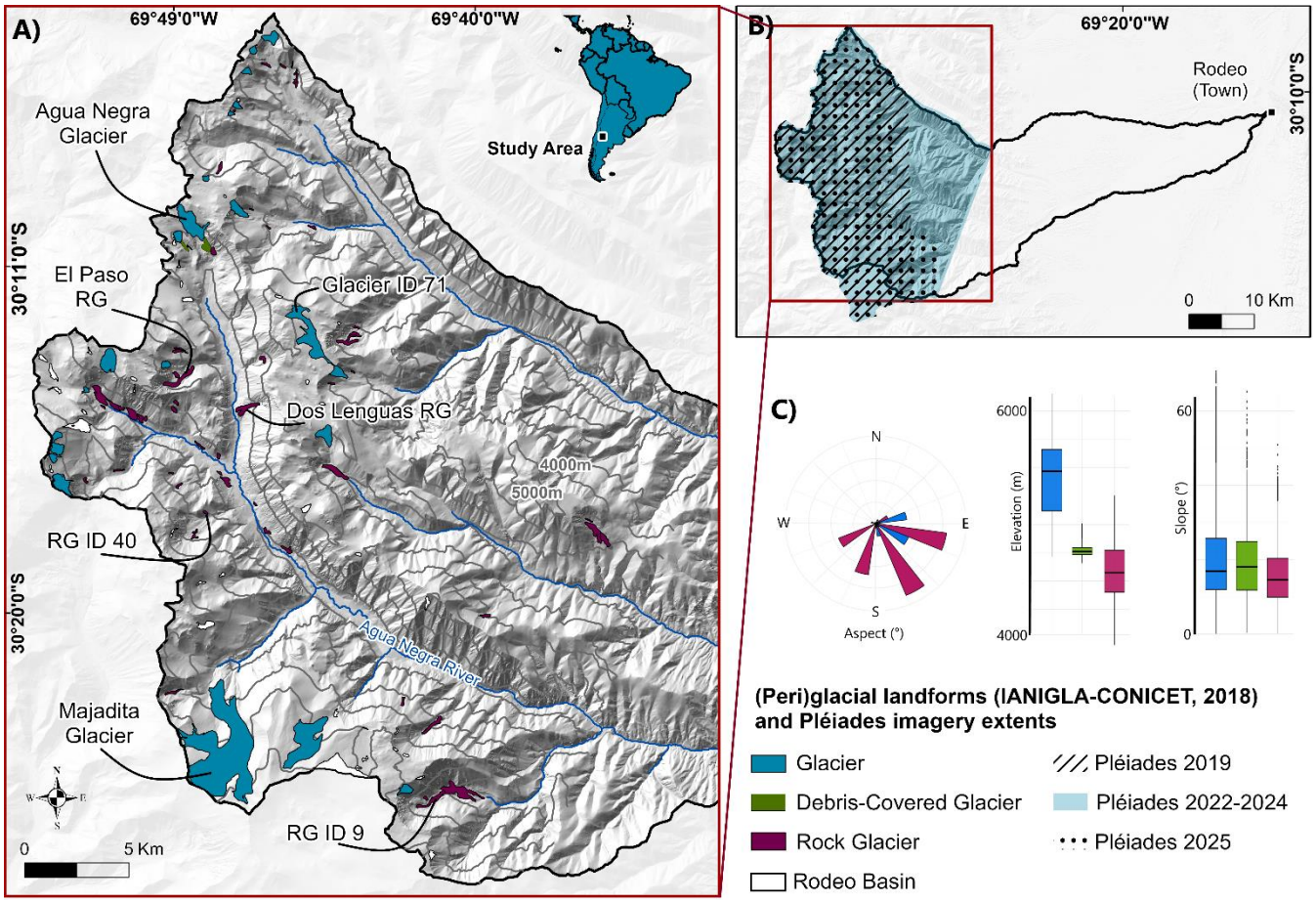

Fig. 1 A) Distribution of glaciers, debris-covered glaciers and rock glaciers as mapped by IANIGLA-CONICET (2018) in the upper part of Rodeo basin. All landforms labelled here are detailed in consequent figures. B) Rodeo basin including the extents of the Pléiades imagery acquisitions (cf. supplementary material A1). C) Aspect, elevation and slope characteristics of the (peri)glacial landforms of the study area, calculated from a 10 m DEM (based on the 2022 Pléiades data, Tab. 1) and its derivatives. Colour-scale for landform type applies to all subfigures.

3 Data and Methods

We analyse interannual vertical surface change on 19 glaciers, three debris-covered glaciers and 59 rock glaciers in the Dry Andes of Argentina for 2019-2025. Further, we investigate horizontal surface changes on 47 of the 59 rock glaciers consistently monitored for 2019-2025. We use (tri)stereo, panchromatic Pléiades imagery acquisitions for the austral summers of 2019, 2022, 2023, 2024 and 2025 for the generation of Pléiades-based DEMs and consequent DEMs of Difference (DoDs) for vertical change detection on all landforms. For rock glacier velocities, we conduct feature tracking on projected panchromatic Pléiades imagery.

3.1 National Inventory of Glaciers (Argentina)

Glaciers, debris-covered glaciers, rock glaciers (active/inactive) and perennial snowfields across the Argentinean Andes and South-Atlantic islands cover an area of 8484 km^2 and are documented in the National Inventory of Glaciers conducted by the Argentine Institute for Snow, Ice and Environmental Sciences (IANIGLA-CONICET) in collaboration with the Argentine Ministry of the Environment and Sustainable Development (Zalazar et al. 2017). With the aim of preserving glaciers and the periglacial environment, the dataset was established based on satellite imagery and ground-truthing as requirement of the law on Minimum Standards for the Preservation of Glaciers and the Periglacial Environment (span. Régimen de Presupuestos Mínimos para la Preservación de los Glaciares y del Ambiente Periglacial) (ibid.).

We rely on the National Inventory of Glaciers for glacial and periglacial feature boundaries in our study area and conduct our vertical and horizontal surface change analysis within these boundaries. For our analysis, we treat rock glaciers indifferent of their mapped state of activity allowing us to rely on measured activity rather than the visual interpretation of surface features as conducted during the establishment of the inventory (Zalazar et al. 2017).

3.2 Pléiades Imagery Acquisitions and Processing

The Pléiades 1A and 1B satellites were launched on December 17th 2011 and December 2nd 2012 respectively. With a sun-synchronous orbit type and repeat cycle 26 days, they offer panchromatic (resolution 0.5 m) and multispectral (resolution 2 m) imagery in stereo and tristereo mode (ASTRIUM 2012). Achieving the (tri)stereo cover during one pass over the area, a homogeneous product which allows for most precise DEMs to be generated is acquired despite the challenging terrain of the Andes - and allows for a suitable base-to-height (B/H) ratio. In contrast to radar imagery, the optical signal does not penetrate snow and ice, increasing suitability for cryospheric surface change detection (Berthier et al. 2014). All Pléiades data used in this study were tasked for austral summers, in stereo (2019) or tristereo (2022-2025) mode and processing level 1 corresponding to the primary product (ASTRIUM 2012), Tab. 1.

We process all Pléiades (tri)stereo pairs automatically using Ames Stereo Pipeline (ASP) software (Beyer et al. 2018). Processing is conducted without ground control points (GCPs) relying on rational polynomial coefficients (RPCs). We follow Berthier et al. (2024) and Cusicanqui et al. (2025) in using a STRM DEM as seed DEM during stereo processing and a semi-

global matching strategy. Here, either both stereo acquisitions or both pairs of the tri-stereo triplet are included. As a result, we generate DEMs at 1 m resolution. Given the data quality we do not fill gaps and proceed without correcting for sensor undulations.

Tab. 1 Acquisition dates and characteristics of the four (tri)stereo panchromatic Pléiades datasets. All dates are provided as dd.mm.yy. In the remaining paper, the overlapping image tiles acquired at different acquisition dates are referred to as top (T), bottom (B) and right (R) tiles. For the location of the three tiles, see supplementary material A1. B/H ratios are comparable with other studies, e.g., Beraud et al. (2023).

	2019	2022	2023	2024	2025
Image Acquisition Date(s) and Tile Locations (T, B, R)	17.03.19	14.02.22 (T)	13.02.23 (T)	12.02.24 (T)	02.03.25 (T)
		22.02.22 (B)	20.02.23 (B)	19.02.24 (B)	03.03.25 (B)
		15.02.22 (R)	14.02.23 (R)	09.03.24 (R)	-
Geometry	stereo	tristereo			
B/H	0.4	0.3 - 0.5			
Max Inc. Angle	< 20°				
Max Cloud Cover	< 5%				

3.3 DGNSS measurements for validation

We conduct 78 repeated Differential Global Navigation Satellite System (DGNSS) measurements on Dos Lenguas and El Paso rock glaciers as well in the Agua Negra Glacier forefield using Trimble DGNSS equipment (R8 base, R2s rover, TSC3 handheld, RTK), Tab. 2. Located on the landforms as well as surrounding terrain, the measurements are conducted in at least two consecutive years in the austral summers of 2022, 2023 and 2024; within maximum two consecutive days. Measured point locations are marked on flat surfaces of selected large boulders (> 2 m). The coordinate of the base stations are 424101.83, 6654084.621, 4247.137m for Dos Lenguas rock glacier; 422350.62, 6655630.667, 4723.248 m for El Paso rock glacier and 422783.389, 6661216.068, 4726.973 m for the Agua Negra Glacier forefield – all provided in WGS 84 UTM zone 19S. DGNSS measurements on Dos Lenguas rock glacier have been used for validation and georeferencing (Stammler et al. 2024; Stammler et al. 2025a) and are published in Stammler et al. (2025b). We publish the additional DGNSS measurements used in this study in the paper-accompanying dataset (Stammler et al. YEAR).

Tab. 2 Acquisition dates and characteristics of our DGNSS measurements, used for validation purposes. For rock glaciers, the number of points is split in onsite and offsite the landforms' surface. RG = rock glacier, AN forefield = Agua Negra glacier forefield. The DGNSS measurements of Dos Lenguas rock glacier are published in Stammler et al. (2025b). All other DGNSS data are published in Stammler et al. (YEAR).

	Dos Lenguas RG	El Paso RG	AN forefield
Acquisition Dates (dd.mm.yy)	17.03.22 - 21.03.22 16.01.23 - 12.02.23 10.02.24 - 12.02.24	- 01.02.23 - 02.02.23 14.02.24	08.03.22 17.01.23 26.02.24
# points	21 (8/13)	36 (26/10)	21
Mean accuracy hor./vert. (in m)	0.017 / 0.028	0.036 / 0.076	0.018 / 0.041

3.4 Vertical surface change by DEMs of Difference

We generate rectangular bounding boxes with minimum 500 m distance to each of the (debris-covered) glacier and rock glacier polygons to clip our Pléiades-based DEMs. We co-register the younger to the older clipped DEMs following Nuth and Kääb (2011) in Demcoreg (Shean et al. 2016), while masking the cryospheric landforms based on the National Inventory of Glaciers (IANIGLA-CONICET 2018). Single Pléiades tiles are processed separately to prevent distortion from mosaicking. If available for both acquisitions, each tile is co-registered respectively, e.g., 2023T to 2022T, 2023B to 2022B, 2023R to 2022R. For acquisitions with different extents and/or number of tiles, co-registration is only possible where data is available and is conducted as, e.g., 2022T to 2019, 2022B to 2019, 2022R to 2019. Co-registering clipped rasters allows for an adaption to the local setting of each landform, preventing larger distortion patterns to imprint on the DEM-based analysis while reducing processing times. Further, it enables temporal and spatial investigation of the x, y, z correction factors used during co-registration.

For vertical surface change quantification by DEM differencing, we subtract the co-registered newer DEMs from the original older DEMs. Vertical surface change across the cryospheric landforms in the Rodeo basin is compared as cumulative median or as vertical surface change normalized to full years, both calculated as median for the landforms' surfaces. Rock glaciers are attributed positive when vertical surface change plus and minus the LoD are above zero, and negative when both are below zero. Further, we derive elevation and slope from the Pléiades DEMs, all at a resolution of 1 m.

For the calculation of the LoDs of our vertical surface changes, we extract vertical surface change at 1000 random points distributed outside and in vicinity of each landform polygon and derive their median. Terrain outside the landform polygons is assumed stable. Having controlled vertical surface change in the areas outside the landform surfaces during co-registration, we directly accept the medians as LoDs.

3.5 Horizontal velocity by feature tracking

We use the projected panchromatic imagery at 0.5 m resolution to conduct feature tracking on all rock glaciers for which we have data for all time periods (47 out of 59) following the approach by Schwalbe and Maas (2017) which matches image patches between orthoimages with two different time stamps by applying cross-correlation for an estimation of a pixel-precise shift, and a least-squares matching for the achievement of sub-pixel accuracies. Originally implemented in the Environmental Motion Tracking (EMT) software, we adapt this approach to semi-automatically process a large quantity of rasters in python. For our stereo dataset (2019), we select the first image of the pair with a view angle tilted towards south. For the tristereo datasets (2022-2025), we select the second image of the triplet which is closest to nadir view (90°).

Similar to the DEMs, we clip the panchromatic orthoimages by our bounding boxes prior to feature tracking. After conducting an affine transformation for offset correction, identifiable pixels are tracked on the landform surface (no front and side slopes) using a set of equally, 5 m spaced points – leading to a 5 m spatial resolution of the calculated velocities. This approach benefits from using grey-scaled input which is independent of light conditions (Dall'Asta et al. 2017; Fleischer et al. 2021). To reduce

the impact of the polygon boundaries as included in the National Inventory of Glaciers (IANIGLA-CONICET 2018) on the feature tracking outcome, we apply a 200 m buffer on all polygons to determine the reference area used for aligning the images while we use a buffer of 50 m around the polygons for the actual image tracking. Horizontal surface change is presented normalized to full years.

Similar to the calculation of the LoDs for vertical surface changes, surface motion is tracked at 1000 randomly distributed points located outside of the landform surface for the calculation of the LoDs of the horizontal surface changes. We accept the median of the feature tracking results at these 1000 random points as LoD. This allows accounting for potential true surface change, e.g., related to fluvial processes, occurring outside the landform surface polygon.

We track the residuals of the affine transformation during our feature tracking approach to develop a criterion for the quality of the image alignment, which directly affects the feature tracking results. We detect the correlation of these residues in x, y space and use low correlation coefficients (0 to 0.5) as indication of a high-quality feature tracking and high correlation coefficients (0.5 to 1) as indication of a poorer feature tracking quality. The implementation of the correlation coefficient of the residues that arise during feature tracking as a quality control is based on the hypothesis that high correlation is indicative of a technical error, e.g., an image distortion, while true residues are expected to be independently distributed. We include this quality criterium as a metric and as categories.

4 Results

4.1 Co-registration, DEM differencing and feature tracking accuracies

The area's aridity and extremely limited cloud and vegetation cover yield perfectly suitable conditions for change analysis with remotely sensed optical imagery, such as Pléiades imagery. The summer conditions with very scarce and, if present, non-persistent snow coverage allow for largely uncovered terrain suitable for co-registration, supplementary material A1. For co-registration, X correction factors are of least magnitude in median through time, while Z correction factors are of highest, Tab. 3. A comparison of the T, B, and R tiles indicates no consistent pattern of spatial differences in co-registration factors. All correction factors used during co-registration are independent of the landform type, supplementary material A2.

Tab. 3 Co-registration corrections in x, y, and z direction based on the approach by Nuth and Kääb (2011) as applied in DEMCOREG (Shean et al. 2016). Shown as median of all co-registration factors (m) of the 81 clipped DEMs (number of landforms = 81). For all co-registration factors, see supplementary material A3.

	Shift in X (m)			Shift in Y (m)			Shift in Z (m)			Median (m)
	T	B	R	T	B	R	T	B	R	
2019-2022	-0.16	0.2	-0.18	0.24	0.23	0.44	1.22	1.04	2.62	**0.24**
2022-2023	-0.2	-0.08	0.00	-0.08	-0.01	-0.32	0.59	-0.56	-0.90	**-0.08**
2023-2024	0.26	-0.06	0.20	-0.47	-0.12	0.34	-0.76	0.81	0.58	**0.2**
2024-2025	0.05	-0.16	-	0.59	0.07	-	0.05	-1.55	-	**0.05**
Median (m)	**-0.06**	**-0.07**	**0**	**0.08**	**0.03**	**0.34**	**0.32**	**0.13**	**0.58**	

Vertical surface changes as extracted at 1000 randomly distributed points surrounding the landform polygons are independent of the landform type and time period and correspond to the respective LoD of our vertical surface changes, Tab. 4. They vary between ±0.1 to ±10 cm/yr when compared as median for all landforms of each landform type (glaciers, debris-covered glaciers, rock glaciers). Vertical change LoDs are lower than the LoDs calculated for horizontal surface changes. Median horizontal surface change at 1000 randomly placed points in vicinity of the rock glacier surfaces range between ±16 and ±61 cm/yr and represent our LoDs for horizontal surface change. The calculated LoDs for horizontal surface change are low for the 2019-2022 and 2023-2024 time periods, compared to 2022-2023 and 2024-2025.

Tab. 4 Vertical surface change (m/yr) on glaciers and debris-covered glaciers as well as vertical and horizontal surface change (m/yr) on rock glaciers shown as medians for all landforms within each category. VCh = Vertical surface change, HCh = Horizontal surface change, n = number of landforms, depending on the spatial extent of the image acquisition. LoDs for vertical and horizontal surface changes are based on the median of surface change at 1000 randomly distributed points in vicinity of the landforms, shown here as medians per landform category. For rock glacier velocities, we consider only surface change exceeding the respective LoD.

	Glaciers			Debris-c. Glaciers			Rock Glaciers					
	VCh	LoD	n	VCh	LoD	n	VCh	LoD	n	HCh	LoD	n
2019-2022	-1.28	±0.01	11	-0.09	±0.08	3	-0.01	±0.03	48	0.28	±0.16	38
2022-2023	-0.20	±0.001	18	0.02	±0.01	3	0.004	±0.003	59	0.64	±0.52	25
2023-2024	-1.50	±0.01	17	-0.22	±0.10	3	-0.01	±0.004	59	0.46	±0.17	28
2024-2025	-0.51	±0.001	17	0.16	±0.02	3	0.07	±0.001	54	0.82	±0.61	33

Correlation factors of the residues arising during our feature tracking approach range in median over time for the selected rock glaciers between 0.27 (ID44) and 0.64 (ID39), Tab. 5. This is representative for all polygons, with the least and highest correlation being 0.12 (ID25) and 0.66 (ID47), supplementary material A4. In total, 45 of the 57 polygons are characterised by low correlation coefficients of the residues (0 to 0.5), with 12 polygons exceeding a coefficient of 0.5 but none reaching a coefficient of 0.7. In median and independent of the different rock glacier polygons, the time period 2023-2024 is characterised by least correlation of the residues both for the selected rock glaciers (2023-2024: 0.26) as well as all polygons (2023-2024: 0.28). Thus, three out of the four time periods are characterized by low correlation coefficients with one exceeding a coefficient of 0.5 but remaining below 0.6, both for the selection as well as for all polygons.

Tab. 5 Correlation coefficients for residues arising during the affine transformation of our feature tracking approach on selected rock glaciers. Rock glaciers are selected based on their size and speed (large > 0.1 km^2, fast > 0.2 m/yr). For a full list of correlation coefficients, see supplementary material A4. We treat low correlation coefficients (0 to 0.5) as criterium for a high quality of the feature tracking approach and higher correlation coefficients (0.5 to 1) as a poorer quality of the feature tracking approach, cf. 3.5.

	Large and fast RG			Small and fast RG			Small and slow RG			Median (m)
	ID4	ID5	ID9	ID24	ID40	ID50	ID35	ID39	ID44	
2019-2022	0.64	0.62	0.21	0.79	0.55	0.32	0.44	0.74	0.42	**0.55**
2022-2023	0.20	0.34	0.45	0.22	0.72	0.11	0.85	0.66	0.80	**0.45**
2023-2024	0.33	0.02	0.26	0.29	0.12	0.29	0.41	0.08	0.12	**0.26**
2024-2025	0.51	0.53	0.57	0.53	0.25	0.44	0.29	0.61	0.13	**0.51**
Median (m)	**0.42**	**0.43**	**0.35**	**0.41**	**0.40**	**0.30**	**0.42**	**0.64**	**0.27**	

4.2 Pléiades-based vertical surface changes for (debris-covered) glaciers and rock glaciers in the Rodeo Basin

Vertical surface change across the cryospheric landforms in the Rodeo basin is highest in magnitude for glaciers, second highest for debris-covered glaciers and least for rock glaciers – independent of the time period, Fig. 2A. Calculated LoDs are very low compared to the vertical surface changes on glaciers, low compared to debris-covered glaciers and vertically dynamic rock glaciers, and high compared to rock glaciers with minimal vertical surface change when calculated as median for the landforms surface, Fig. 2 (whiskers) and Tab. 4.

All glaciers monitored in our study are characterized by negative vertical surface changes, leading to negative cumulative vertical surface change increasing in magnitude, Fig. 2A. This increase in magnitude is not linear over time and is highest for 2023-2024 (-1.50 m/yr, LoD ±0.01 m/yr) and lowest for 2022-2023 (-0.20 m/yr, LoD ±0.001 m/yr), Tab. 4. Cumulative vertical surface change is of highest magnitude for Agua Negra Glacier (1.09 km^2, 5012 m asl, 2nd largest glacier in the study area) amounting to a vertical elevation change in median for the glacier surface of -8.99 m for 2019-2025, detected with an LoD of ±0.11 m/yr. Annual vertical surface changes of Agua Negra Glacier are higher than of the largest glacier monitored with our Pléiades imagery for the full time period (ID71, 1.80 km^2, 5335.5 m asl), Tab. 6. In general, smaller glaciers are characterized by higher time-normalized median vertical surface change than large glaciers, Fig. 2B. Further, vertical surface change is highest in magnitude for glaciers at lower elevations, Fig. 2C, and independent of slope, Fig. 2D.

Only three debris-covered glaciers are present in the Rodeo basin with median vertical surface changes up to -22 cm/yr, detected with a LoD of ±10 cm, Tab. 6.

Rock glacier vertical surface change is minimal on Dos Lenguas and El Paso rock glaciers. This is representative for all rock glaciers monitored, Fig. 2A and Tab. 4. Rock glacier vertical surface changes are not correlated with median elevation or slope, Fig. 2C-D. However, rock glaciers in the Rodeo basin are characterized by an interannual variability of vertical surface change, with 47 rock glaciers alternating at least once between positive and negative median annual surface change between the observed time episodes (6 always negative, 4 always positive).

Tab. 6 Vertical surface change (VCh, m/yr) for the two largest glaciers, as median for the three debris-covered glaciers (DC = debris-covered, cf. Tab. 4), and for two selected rock glaciers (RG). For the location of the landforms, see Fig. 1A.

	Agua Negra Glacier		Glacier ID 71		DC Glaciers (median)		Dos Lenguas RG		El Paso RG	
	VCh	LoD	VCh	LoD	VCh	LoD	VCh	LoD	VCh	LoD
2019-2022	-1.51	±0.02	-0.67	±0.04	-0.09	±0.08	-0.08	±0.04	-0.04	±0.03
2022-2023	-0.59	±0.02	-0.09	±0.02	0.02	±0.01	-0.07	±0.09	0.005	±0.01
2023-2024	-1.85	±0.01	-1.13	±0.05	-0.22	±0.10	-0.04	±0.07	0.03	±0.05
2024-2025	-2.4	±0.04	-0.48	±0.01	0.16	±0.02	-0.03	±0.03	-0.07	±0.05

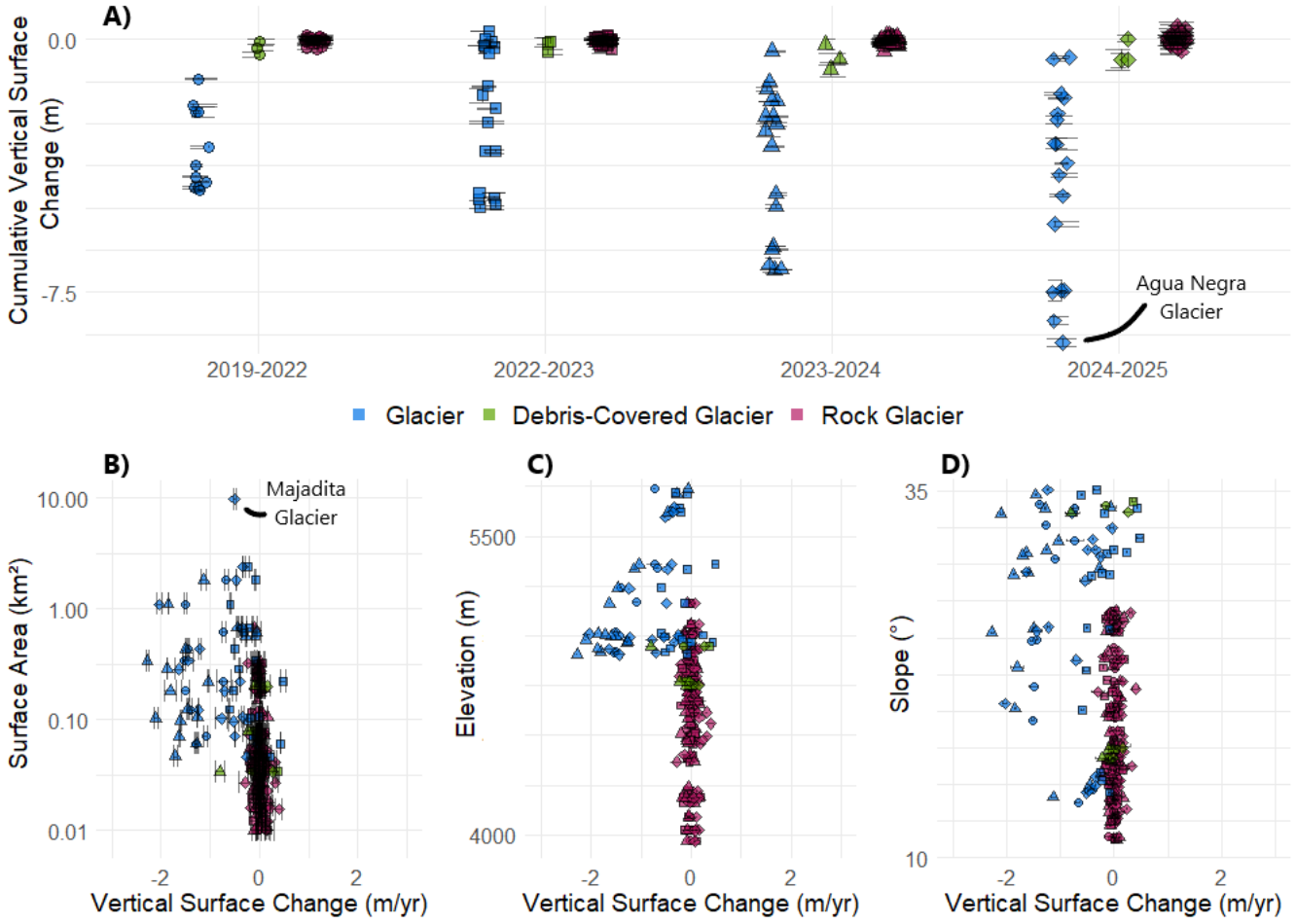

Fig. 2 A) Cumulative vertical surface change for glaciers, debris-covered glaciers and rock glaciers for 2019-2025. Calculated as median vertical surface change within the landform surfaces (e.g., no rock glacier fronts) based on DEM differencing between clipped, co-registered Pléiades DEMs. The number of the landforms investigated depends on the extent of the Pléiades acquisitions, cf. Fig. 1B. Bottom: Median annual vertical surface change normalized to full years and its concurrence with the landform surface area (B), with elevation (C) and slope (D). Elevation and slope are derived from the Pléiades-DEM at the beginning of the time period, e.g., 2019 for the 2019-2022 period. Symbol types correspond to the time periods as introduced in A). For the location of Agua Negra and Majadita Glaciers, see Fig. 1A.

Spatially, time-normalized vertical surface changes on Agua Negra Glacier are heterogeneously present with highest magnitudes on its west side and towards the glacier tongue, Fig. 3A. Vertical changes on the largest glacier (ID 71) are also heterogeneously present, with highest magnitudes reached in the centre and southern part, Fig. 3B. The glacier located next to El Paso rock glacier exhibits vertical surface changes particularly in its centre, Fig. 3C. Rock glacier vertical surface changes are spatially heterogeneous and often follow a ridge- and furrow morphology with alternating positive and negative areas, Fig. 3D. Rock glacier fronts are characterized by a coherent positive vertical surface change, Fig. 3C-D. For vertical surface changes of all monitored cryospheric landforms, see Fig. 3E.

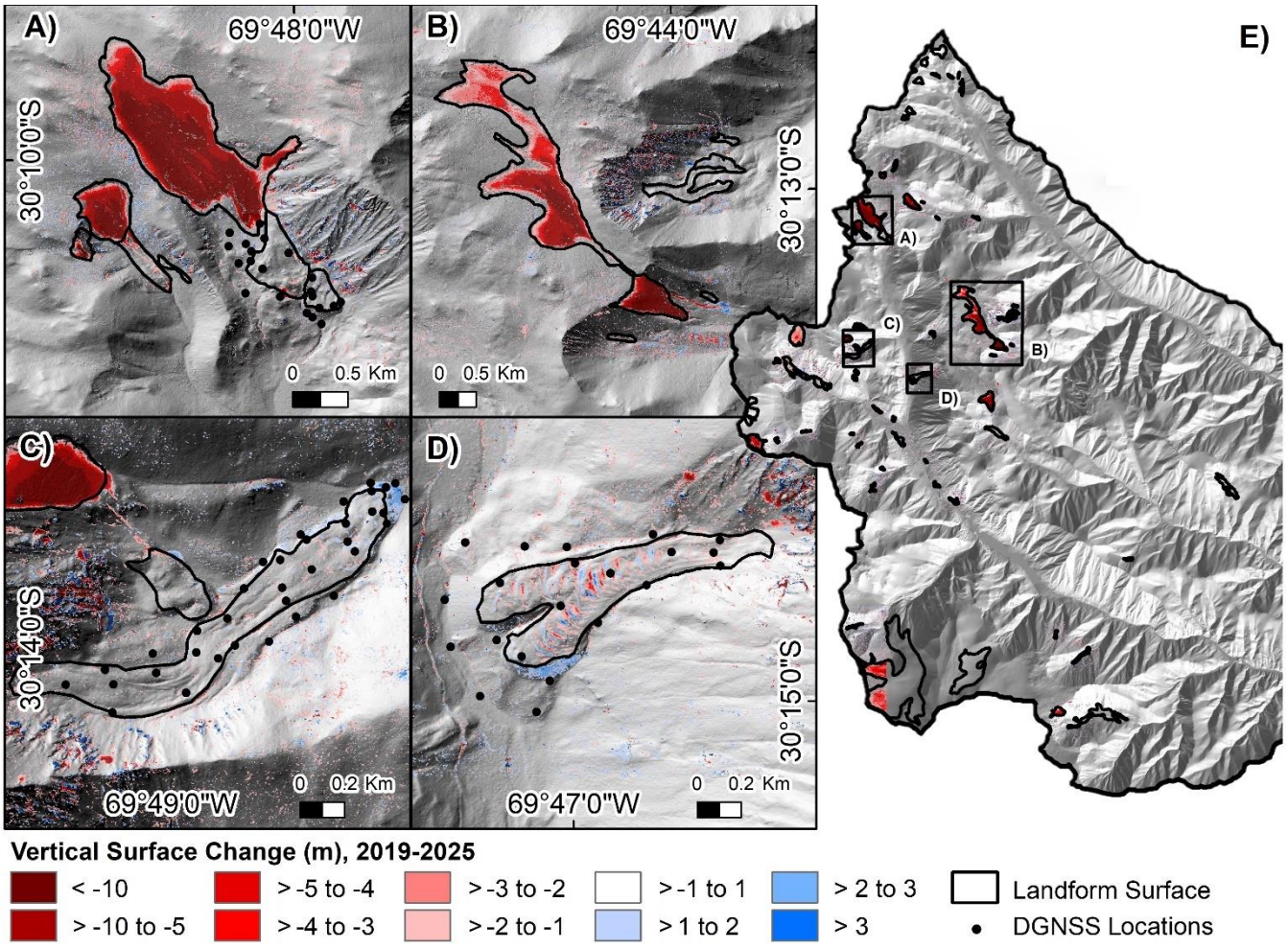

Fig. 3 Vertical surface changes (m) between 2019-2025, generated by DEM differencing of co-registered Pléiades DEMs for Agua Negra Glacier and proximate landforms (A), Glacier ID 71 and proximate landforms (B), El Paso rock glacier and proximate landforms (C), and Dos Lenguas rock glacier (D). For all vertical surface change results, including the locations of A) to D), see E). Polygons based on IANIGLA-CONICET (2018). Colour-scale for vertical surface change applies to all subfigures. A), C) and D) include DGNSS locations for repeated measurements, cf. Tab. 2.

4.3 Pléiades-based rock glacier velocities for Rodeo Basin in space and time

Rock glaciers in the Rodeo basin exhibit differences in the magnitude of their horizontal surface change in space with median rock glacier surface velocities being heterogeneously present in the Rodeo basin, Fig. 4. Their LoDs are independent of a rock glaciers locations, size and velocity. Out of the 47 rock glaciers, 1 rock glacier exceeds median velocities of > 1.25 m/yr for the time period 2019-2025 (Dos Lenguas rock glacier), while 7 rock glaciers fall between 1 and 1.25 m/yr (e.g., El Paso rock glacier), and 14 fall in the classes between 0.75 to 1 m/yr and 0.5 to 0.75 m/yr, respectively. Median rock glacier surfaces velocities based on all rock glaciers are heterogenous in time, with lowest velocities in 2019-2022 and highest in 2024-2025, Tab. 4. Increase in velocities is not linear, with the time period 2023-2024 being characterized by second lowest velocities.

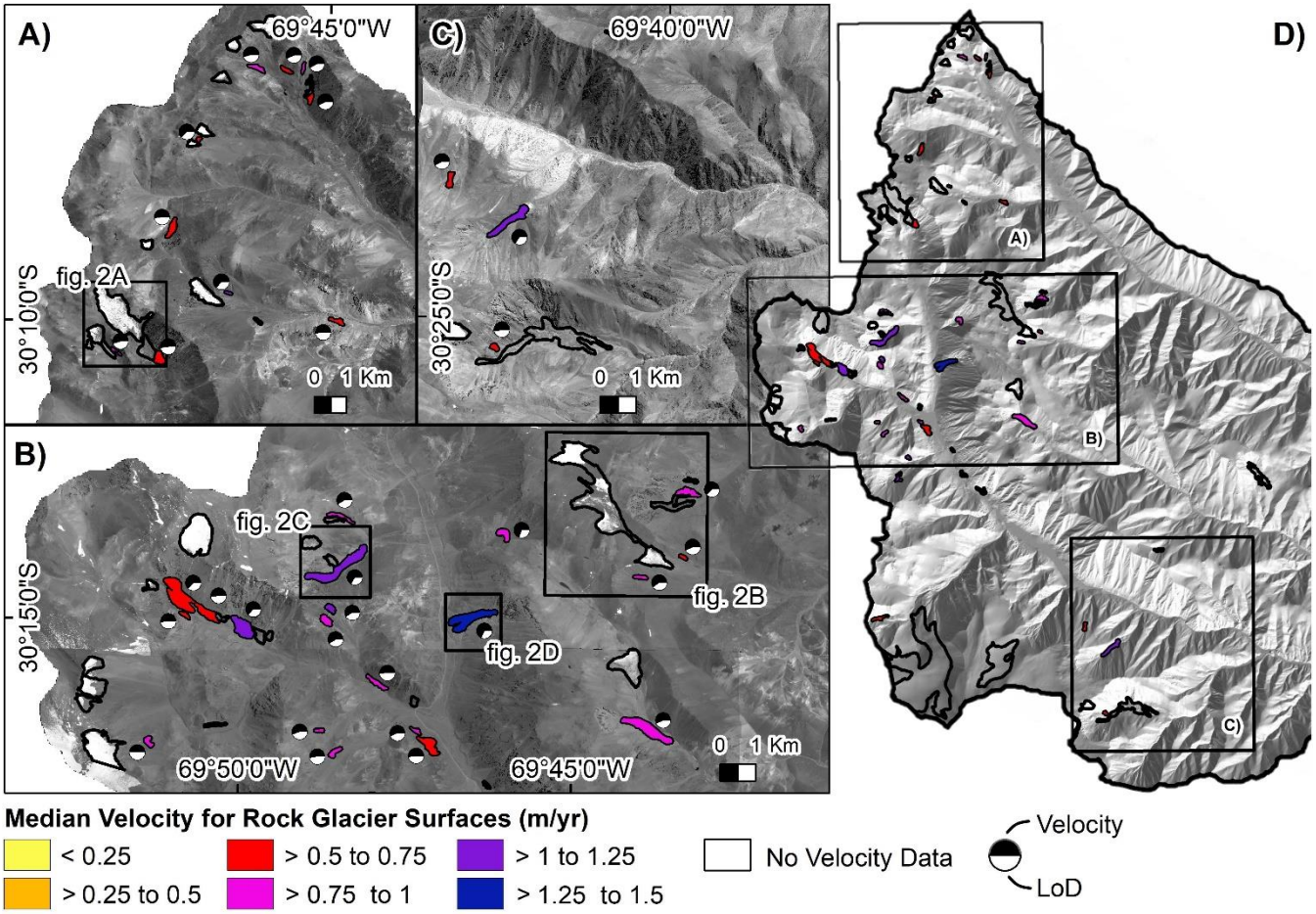

Fig. 4 Median velocities (m/yr) for rock glacier surfaces between 2019-2025, categorized and normalized to years. (Peri)glacial landforms as mapped by IANIGLA-CONICET (2018), portrayed on top of the Pléiades panchromatic orthophotos for 2024 (A-C) and a hillshade based on the 2022 Pléiades imagery (D). Ratios between the velocity (black) and LoD (white) of each landform are provided as pie charts (A-C). For specific location of the rock glaciers, see D. See black boxes referencing to Fig. 2 in A) and B).

While smaller rock glaciers (< 0.1 km^2) are characterized by various velocities from 0.0 to 1.23 m/yr, larger rock glaciers (> 0.1 km^2) in their vast majority exhibit velocities above 0.25 m/yr in all time periods, Fig. 5A. Rock glaciers located at elevations below 4100 m asl do not exceed velocities of 0.25 m/yr, while all rock glaciers located above 4300 m asl exceed velocities of 0.09 m/yr and reach up to 1.38 m/yr, Fig. 5B. Slope and rock glacier velocity are not correlated, Fig. 5C. Variability of median vertical change is dependent on the time period, with 2022-2023 characterized by more negative and 2023-2024 by more positive median vertical surface changes, Fig. 5D. We find three rock glacier categories in the Rodeo basin: large and fast, small and fast and small and slow rock glaciers. Large and fast rock glaciers are located at higher elevation, lower slope and are characterized by lower median vertical change. While small and fast rock glaciers are located at higher elevation and variable slope, small and slow rock glaciers are located at variable elevation and slope.

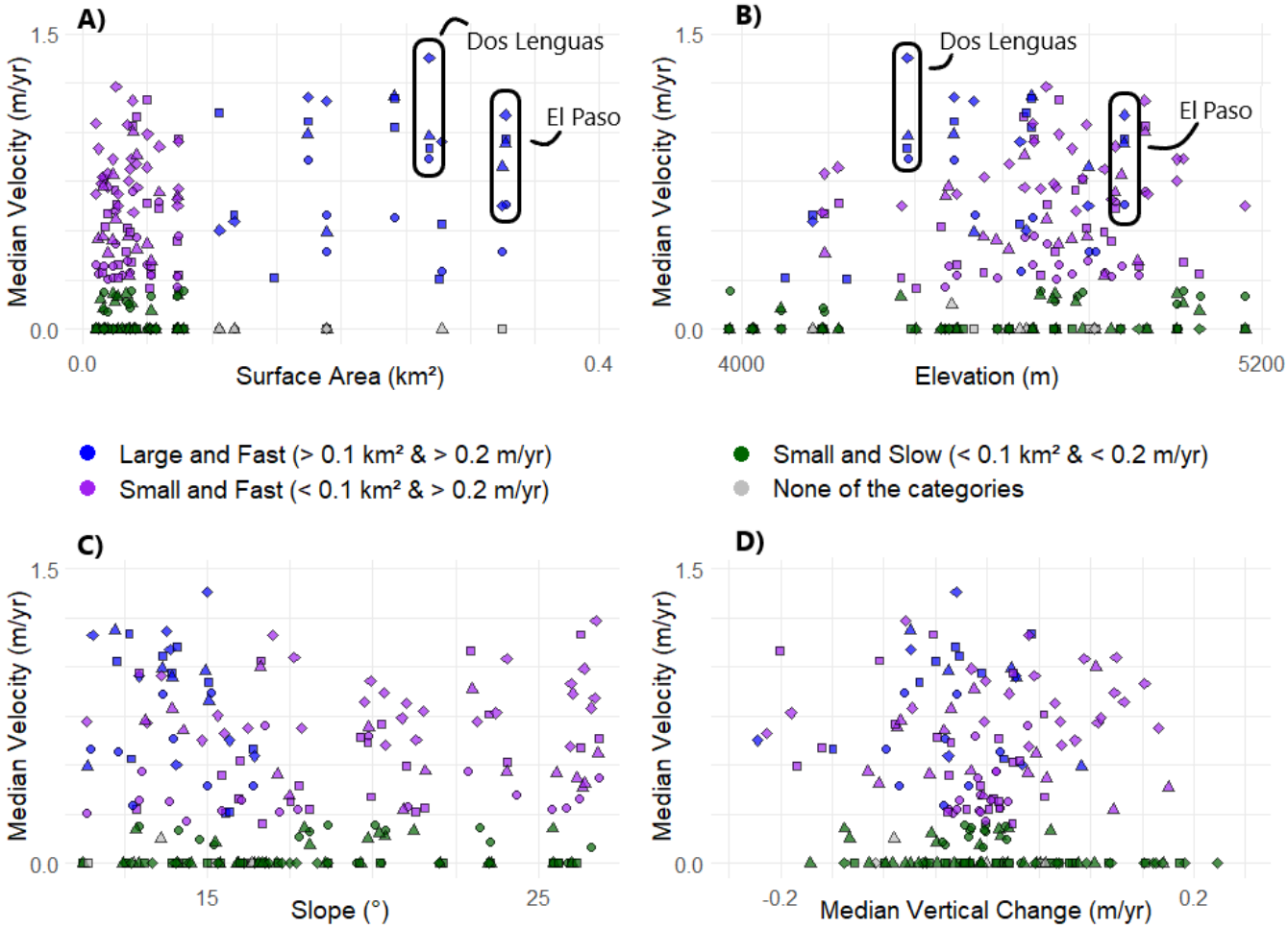

Fig. 5 Median velocities for rock glacier surfaces (m/yr) and their concurrence with the rock glacier polygon size (A), median elevation (B), median slope (C) and median vertical surface change (D), all calculated for the rock glacier surfaces. Elevation and slope are calculated for the beginning of each time period, leading to variability in values and to us refraining from marking Dos Lenguas and El Paso rock glaciers in C-D. Time periods are indicated by symbols (cf. Fig. 2), and rock glacier categories by colours.

Rock glacier velocities are spatially heterogeneous across the landforms, Fig. 6. El Paso rock glacier (ID 5) is in its upper part characterized by linear ridges in line with the flow direction that exhibit a faster velocity than the surrounding rock glacier surface, Fig. 6A. Highest velocities of up to 1.09 m/yr (2024-2025, LoD ±0.54 m/yr, Tab. 7) are reached in its lower part. Dos Lenguas rock glacier and rock glacier ID 9 are characterized by extensional flow in the upper area and c-shaped ridge and furrow morphologies oriented perpendicular to the direction of flow, commencing in the centre area, Fig. 6B-C. For both, highest velocities of up to 1.38 m/yr (2024-2025, LoD ±0.64 m/yr) and up to 1.17 m/yr (2024-2025, LoD ±0.95 m/yr) are reached in the upper part. The rock glacier with ID 40 is characterized by a lower magnitude increase in velocity in its lower part, particularly after 2024, Fig. 6D and cf. Fig. 7 ID40. Highest magnitudes of velocities correlate with rock glacier size, Fig. 6A-C compared to Fig. 6D.

Tab. 7 Median horizontal surface change (m/yr) reached on selected rock glaciers, compared to the median value for all rock glacier surface velocities, cf. Tab. 4.

	All RG surfaces		El Paso		Dos Lenguas		ID9		ID40	
	HCh	LoD	HCh	LoD	HCh	LoD	HCh	LoD	HCh	LoD
2019-2022	0.28	±0.16	0.64	±0.22	0.86	±0.15	0.57	±0.23	0.44	±0.06
2022-2023	0.64	±0.52	0.97	±0.54	0.92	±0.54	1.03	±0.52	0.64	±0.37
2023-2024	0.46	±0.17	0.95	±0.50	0.98	±0.36	1.18	±0.56	0.56	±0.16
2024-2025	0.82	±0.61	1.09	±0.54	1.38	±0.64	1.17	±0.95	1.23	±0.65
Size	0.05 km^2		0.33 km^2		0.27 km^2		0.24 km^2		0.02 km^2	

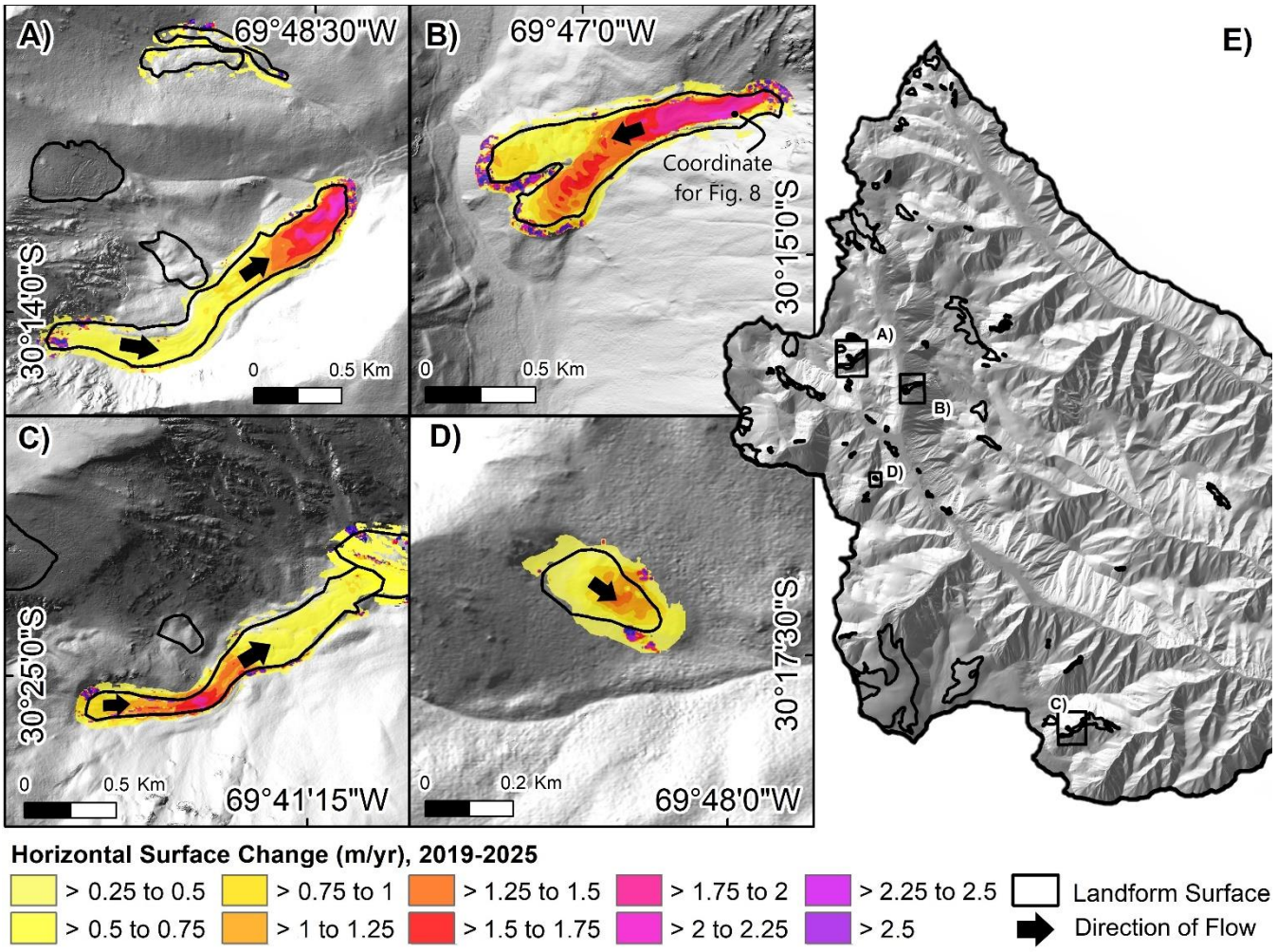

Fig. 6 Magnitude and pattern of our Pléiades-based rock glacier surface velocities between 2019-2025 (m/yr) for El Paso (A), Dos Lenguas (B) rock glaciers, as well as the rock glaciers with the IDs 9 (C), and 40 (D). Median rock glacier velocity generated based on our panchromatic Pléiades imagery and tracked on the landforms surface with equally, 5 m spaced points. Consequent velocities at 5 m resolution are shown on a hillshade based on the 2022 Pléiades imagery (cf. Tab. 1), together with the landform polygons as mapped by IANIGLA-CONICET (2018). Colour-scale for horizontal surface change applies to all subfigures.

The temporal evolution of rock glacier velocities for the 47 rock glaciers for which we have horizontal surface change data for all time episodes is heterogeneous, Fig. 7. Particularly the smaller (< 0.1 km^2) and slower (< 0.2 m/yr) rock glaciers do not show any changes in velocity over time, e.g., IDs 46-48. Within their respective LoDs, some of the faster rock glaciers show stable velocities for 2019 to 2024 and slightly higher velocities in 2024-2025, e.g., IDs 2, 3, 49 and Dos Lenguas rock glacier. Some rock glaciers exhibit alternations between higher velocities in 2022-2023 and 2024-2025 and lower velocities in 2019-2022 and 2023-2024, e.g., IDs 8, 13, 14, 51. Not one single rock glacier is fastest for all time periods but different rock glaciers, with highest magnitudes of 0.86 m/yr in 2019-2022 (LoD ±0.15 m/yr, Dos Lenguas), 1.16 m/yr in 2022-2023 (LoD ±0.87 m/yr, ID 23), 1.18 m/yr in 2023-2024 (LoD ±0.56 m/yr, ID 9) and 1.38 m/yr in 2024-2025 (LoD ±0.64 m/yr, Dos Lenguas).

4.5 Comparison of Pléiades- and DGNSS-based vertical and horizontal surface changes

Our DGNSS vertical errors at all three sites (El Paso and Dos Lenguas rock glaciers and Agua Negra Glacial Forefield) range from 0.008 m to 0.028 m (2022, median 0.019 m), 0.01 m to 0.076 m (2023, median 0.021 m) and 0.009 m to 0.041 m (2024, median 0.022 m). Horizontal errors are lower than vertical errors and range from 0.005 m to 0.017 m (2022, median 0.009 m), 0.006 m to 0.036 m (2023, median 0.012 m), and 0.006 m to 0.018 m (2024, median 0.011 m). With very few exceptions on Dos Lenguas rock glacier (2023), all horizontal errors are below 0.02 m/yr and are comparable between the landforms. For a spatial distribution, see supplementary material A5.

Vertical DGNSS error on El Paso rock glacier is lowest in the upper part, and for the lower part higher in 2024 than in 2023. DGNSS-based vertical surface change measured on the rock glacier surface is positive with 0.16 m/yr (2023-2024; LoD ±0.03 m/yr). Outside the rock glacier surface, DGNSS-based vertical surface change is 0.3 m/yr (2023-2024; LoD ±0.03 m/yr). Pléiades-based vertical surface change on El Paso rock glacier surface deviates in median by -0.02 m (2023-2024) from the DGNSS measurement, representing a difference of less than a pixel. Outside the rock glacier surface, difference in median is higher with -0.32 m (2023-2024). For horizontal surface changes on El Paso rock glacier, DGNSS measurements on the rock glacier surface are in median 0.66 m/yr (2023-2024, LoD ±0.11 m/yr). Outside the rock glacier surface, they are 0.07 m/yr (2023-2024, LoD ±0.11 m/yr). Given our feature tracking approach for quantifying horizontal surface changes, only DGNSS points within the landform polygon and the 50 m buffer can be compared. Pléiades-based horizontal surface change on El Paso rock glacier deviates in median -0.35 m (2023-2024) from the DGNSS measurements. Outside the rock glacier surface, difference in median is lower with 0.03m (2023-2024).

On Dos Lenguas rock glacier, vertical errors of the DGNSS measurements are lower in the northern part than in the southern part for 2022 and 2024 and higher for 2023. DGNSS-based vertical surface change is negative at all measured points located on the Dos Lenguas rock glacier surface, and similar in magnitude for both years (2022-2023: -0.19 m/yr, LoD ±0.04 m/yr; 2023-2024: -0.21 m/yr, LoD ±0.04 m/yr). DGNSS-based vertical surface change measured outside the rock glacier are in median 0 m/yr (2022-2023, LoD ±0.03 m/yr) and 0.07 m/yr (2023-2024, LoD ±0.04 m/yr). The difference between extracted Pléiades DoD raster values and DGNSS measurements for time-normalized vertical surface change is 0.08 m (2022-2023) or 0.16 m (2023-2024) on the rock glacier surface and 0.32 m (2022-2023) or -0.47 m (2023-2024) off-surface.

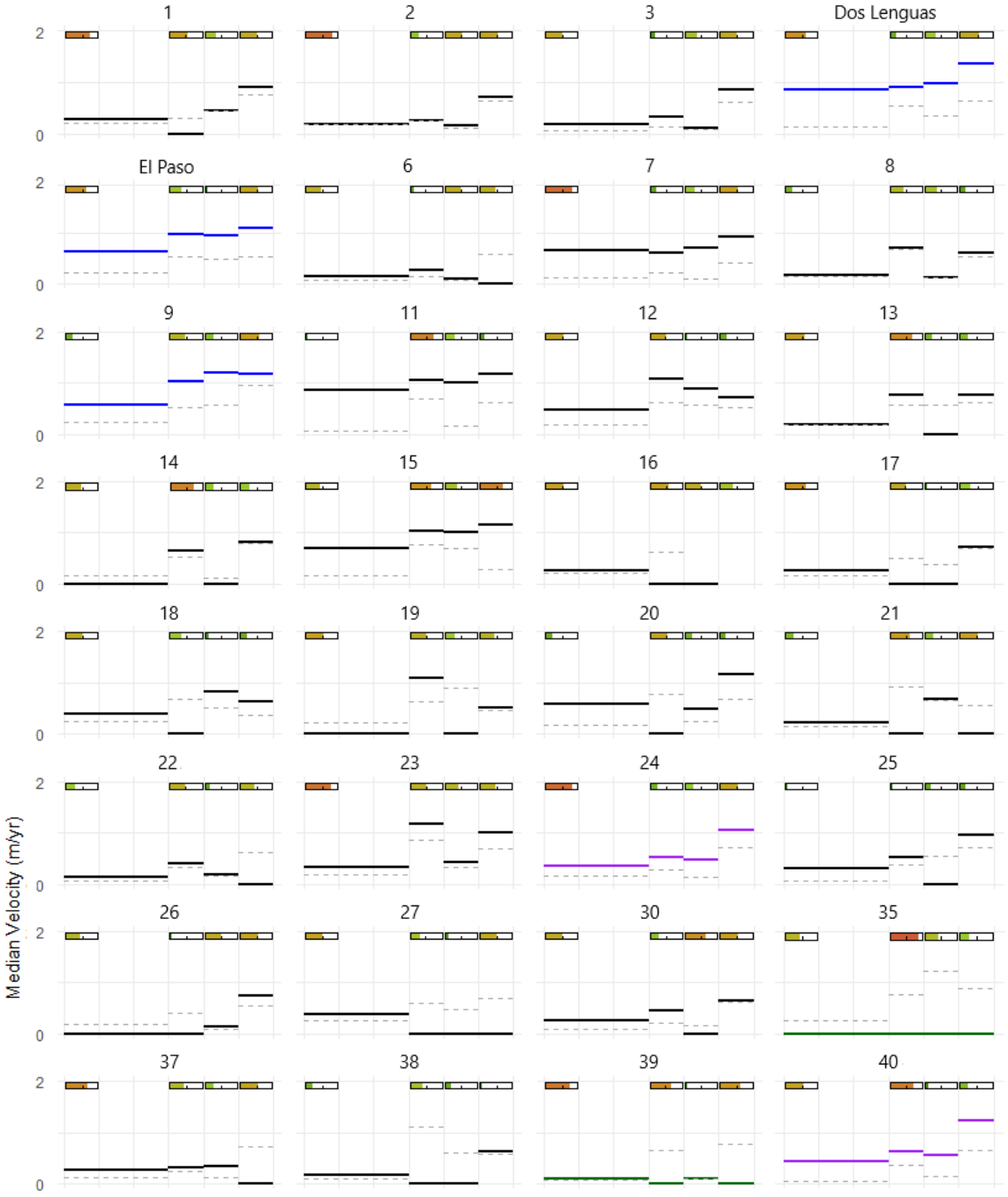
1
2
3
Dos Lenguas
El Paso
6
7
8
9
11
12
13
14
15
16
17
18
19
20
21
22
23
24
25
26
27
30
35
37
38
39
40
2
0
Median Velocity (m/yr)

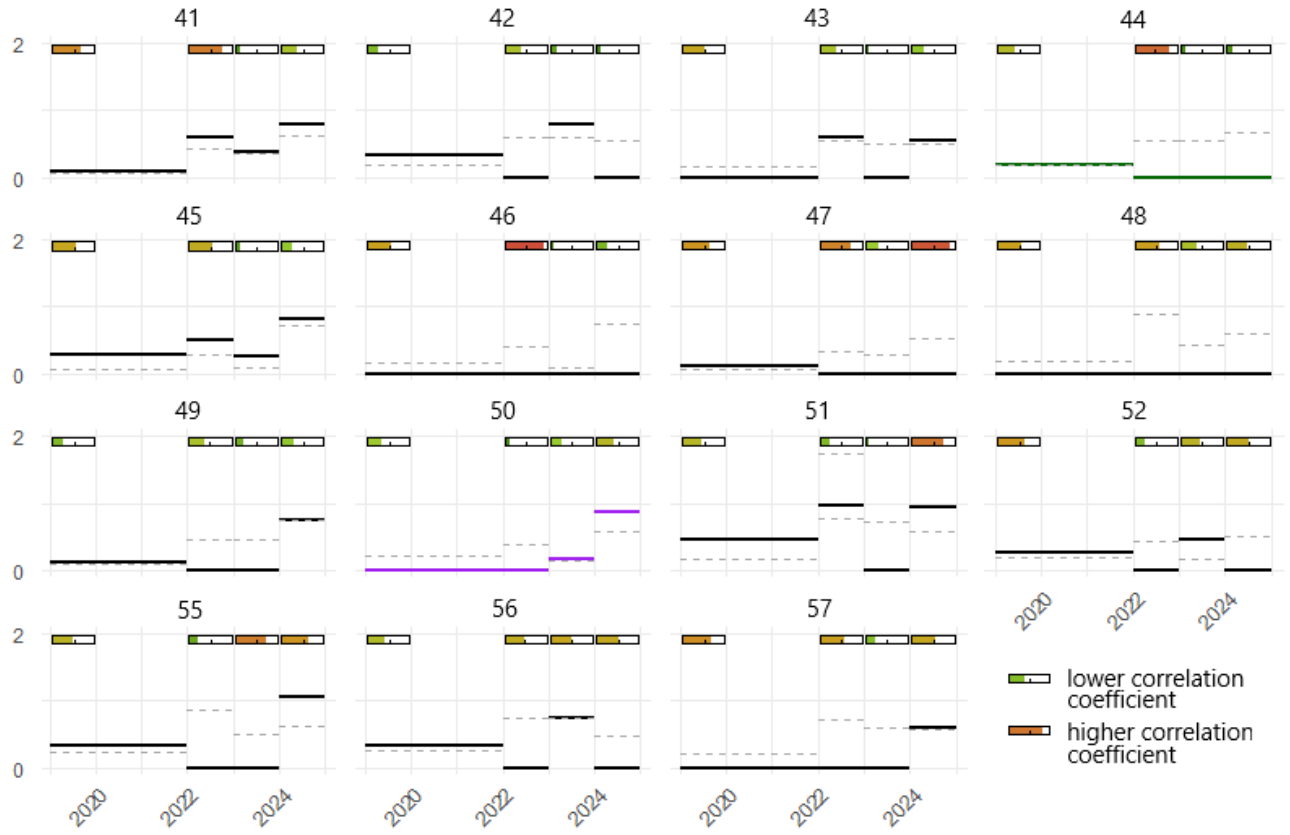

Fig. 7 (continued): Temporal evolution of median rock glacier surface velocities (m/yr) between 2019-2025 based on feature tracking on panchromatic Pléiades imagery (solid lines, colour-coding corresponds to Fig. 5). Median rock glacier velocity is calculated for the rock glacier surface based on tracked velocity at 5 m resolution. LoDs are shown as dashed lines. Residue correlation coefficients, our quality control for our feature tracking approach, are included as bars – one each per time period.

DGNSS-based horizontal surface changes on Dos Lenguas rock glacier are in median 0.80 m/yr (2022-2023, LoD ±0.02 m/yr) and 1.14 m/yr (2023-2024, LoD ±0.13 m/yr). Off-surface measurements result in 0.04 m/yr (2022-2023, LoD ±0.04 m/yr) and 0.04 m/yr (2023-2024, LoD ±0.11 m/yr). The difference between the DGNSS and the Pléiades-based velocities is -0.01 m (2022-2023) or 0.11 m (2023-2024) on the rock glacier surface and -0.63 m (2022-2023) or 0.01 m (2023-2024) off-surface. In the Agua Negra Glacier forefield, vertical errors are highest and more accurate for 2022 and 2023 compared to 2024. The DGNSS measurements indicate vertical and horizontal surface stability with median vertical surface change of 0 m/yr (2022-2023, LoD ±0.02 m/yr) and 0.05 m/yr (2023-2024, LoD ±0.03 m/yr) and median horizontal surface change of 0.04 m/yr (2022-2023, LoD ±0.01 m/yr) and 0.07 m/yr (2023-2024, LoD ±0.01 m/yr). The difference between the Pléiades-based and the DGNSS based surface changes in median is minimal (vertical: 2022-2023, 0.00m; 2023-2024, -0.18 m; horizontal: 2022-2023, 0.01 m; 2023-2024, -0.07 m). For a spatial distribution of the DGNSS-based surface changes, see supplementary material A6.

5 Discussion

5.1 Co-registration factors, DEM, and vertical and horizontal surface change quality

The offset between the acquired panchromatic Pléiades imagery is highest in z dimension compared to the x and y dimension, Tab. 3 and supplementary material A2. Linear co-registration shifts calculated over stable terrain excluding the landform surfaces do not exceed ±0.20 m (x) and ±0.59 m (y), Tab. 3. They indicate relatively good alignment between the panchromatic Pléiades acquisitions in x and y dimension even prior to our co-registration. Co-registration for the z dimension is of higher importance with correction factors up to -1.55 m (2024-2025, tile B) and 2.62 m (2019-2022, tile R), Tab. 3, respectively. While our shift in z direction is high compared to the x and y component, it is low compared to Rieg et al. (2018) (offsets x, y, z of 4 m, -3.2 m and 4.8 m, Pléiades-based DEMs in ERDAS IMAGINE) and Beraud et al. (2023) (offsets x, y, z of up to -9.89 m, 7.79 m, 12.40 m, Pléiades-based DEMs in ASP). As expected, our linear shifts are independent of the targeted location within the catchment, of time, and of the landforms type – supporting the technical nature of the need for co-registration. We do not see a difference in the magnitude of the correction factors needed to co-register the stereo dataset (2019), compared to the tri-stereo datasets (2022-2025). Based on the similarity of the 2019-2022 time period to the other time periods, cf. Fig. 2 & Fig. 7, we conclude the stereo acquisition to be suitable for vertical and horizontal rock glacier surface change monitoring in the Dry Andes. In comparison, Berthier et al. (2014) conclude a moderate effect of the tristereo benefit, including the reduction of the percentage of data voids.

Artefacts or missing values in our DEMs occur in areas with steep slope. These artefacts are not related to our DEM generation but to the Pléiades data-take which includes no data values for these steep slopes due to mismatches during image correlation. In the Rodeo basin and with our processing approach, we do not see generated spikes in the DEMs as described by Ruiz and Bodin (2015). The number of artefacts in our DEMs is very small. This is mainly due to the vegetation-freeness of the study area as well as the semi-global matching strategy whose tend to smooth the surface of the reconstructed DEMs. With a DEM resolution of 1m, the DEMs used in this study are of higher resolution than used in other studies (e.g., Beraud et al. 2023; Falaschi et al. 2023, 2025; Pitte et al. 2022).

Related to our DEM generation workflow, vertical surface change cannot be monitored on all glaciers. This is due to limited heterogeneity of glacier surface characteristics leading to gaps in the DEMs as the photogrammetric processing fails to generate elevation information for these areas, cf. 4.3, Fig. 3E. According to Berthier et al. (2014), the Pléiades imagery radiometric range (12bit) limits these effects compared to SPOT1-5 and ASTER. The effect is, however, also encountered by other studies (Beraud et al. 2023; Falaschi et al. 2023).

LoDs calculated as median vertical surface change at 1000 random points in the vicinity of the landforms leads to low LoDs in comparison to the magnitude of vertical surface changes, particularly for glaciers, cf. Tab. 4. Investigations of vertical surface change of rock glaciers are scarce (Vivero and Lambiel 2024), particularly for studies using Pléiades imagery (e.g., Falaschi et al. 2025). Thus, a comparison of our LoD calculation with other studies being extremely limited. For rock glacier velocities, all horizontal surface changes calculated exceed our LoDs calculated as median of 1000 random point in vicinity

of the rock glaciers, Fig. 6 & Fig. 7. Comparatively low LoDs highlight the stability of surfaces assumed to be stable and support the suitability of panchromatic Pléiades imagery for feature tracking.

Residue correlation coefficients, here used as quality control of the feature tracking approach, cf. 3.5, are in general below 0.5 in median – independent of the respective rock glacier polygon or time period. Their variability between the time periods is higher than between the landforms, highlighting the technical nature of the correlation, cf. Tab. 5 and supplementary material A4. The analysis of residue correlation characterises the time period 2023-2024 as particularly high in quality, not corresponding to the Pléiades tiles with the least co-registration needed, cf. Tab. 3. Though not fully portrayed in the residue correlation coefficient, we experience the effect of image distortion to be higher on rock glaciers located on steep slopes compared to locations closer to valley bottoms. This corresponds often with smaller landforms, as larger landforms with their elongated tongues 'flatten' the topography by building up bodies of rock and ice – rock glaciers.

While the use of the National Inventory of Glaciers for the landform boundaries allows upscaling our analysis, it restricts the landform surface to a static measure, rather than the surface being adapted for each year. This introduces error on the calculation of median vertical and horizontal surface changes and prevents the potential detection of new landforms. We reduce the impact of the inventory by calculating vertical surface change for bounding boxes with 500 m distance to the landform polygon and with buffered polygon outlines during feature tracking. We highlight the need to display the spatial distribution of surface changes within the landform, cf. Fig. 3 & Fig. 6, next to the calculated statistics and agree with Ferri et al. (2020) that highlight the effect of the choice of an inventory, e.g., a national versus a global one.

5.2 Validation of Pléiades-based surface changes with DGNSS data

Difference of our Pléiades-based vertical change to the vertical change measured with the DGNSS equipment is of lowest magnitude for the stable forefield of Agua Negra Glacier, cf. 4.2 and Fig. 3A. Higher difference correlates with a higher magnitude of vertical surface change dynamics at Dos Lenguas and El Paso rock glaciers, cf. 4.2 and Fig. 3C-D. However, difference between the DGNSS measurements and the Pléiades-based vertical surface changes is of lower magnitude for the rock glacier surface compared to the DGNSS measurements located off-site the rock glacier surfaces, cf. 4.2. We hypothesize this difference to be caused by higher vertical accuracies of our DGNSS measurements located at the rock glacier surfaces compared to the surrounding terrain, see supplementary material A5 – paired with a very dynamic off-surface environment for El Paso rock glacier, cf. Fig. 3C. Further, we hypothesize the higher accuracies of the DGNSS measurements on the rock glacier surfaces compared to their surroundings to stem from the elevated location on the surface allowing for a good connection between the DGNSS base and rover, compared to the off-surface DGNSS measurement locations partially obscured by the rock glacier body. Similar to the comparison of DGNSS- and Pléiades-derived vertical surface changes, difference between the DGNSS- and Pléiades-derived horizontal surface changes is smallest for the Agua Negra Glacier forefield, cf. 4.2. Despite low in general (all < 1 pixel), it is highest for El Paso rock glacier (-0.35 m, 2023-2024). At Dos Lenguas rock glacier, we encounter very little difference between DGNSS-based velocities and our Pléiades approach for the rock glacier surface (-0.01 m, 2022-2023 and 0.11 m, 2023-2024).

5.3 Vertical surface change of (debris-covered) glaciers in the Rodeo Basin

For our vertical surface changes, we find the time period 2022-2023 to contrast with rather low, partially even positive glacier vertical surface changes compared to the other time periods, cf. Tab. 4 and Fig. 2A. Using the panchromatic Pleiades imagery, see supplementary material A1, we can confirm partial snow cover in the surrounding of the majority of glaciers. The 2019, 2024 and 2025 Pléiades acquisitions are not impacted by snow, as expected in the arid study area.

Pitte et al. (2022) calculate mass balances ranging between -0.79 m w. e. (2014-2025, cumulative for entire glaciological year) and -3.67 m w.e. (2020-2021, see before) for Agua Negra Glacier based on the glaciological method (Cogley et al. 2011). Their annually repeated measurements are all negative and increase in time with one exception (2016-2017), indicating accelerated downwasting as in agreement with (Dussaillant et al. 2019; Masiokas et al. 2020; Ferri et al. 2020). Based on DEM differencing using, among others, Pléiades-based DEMs, Pitte et al. (2022) report a generalized thinning with high magnitudes at lower elevations which we can attest with our data, cf. Fig. 3A. Pitte et al. (2022) present vertical surface changes of ca. 1 m/yr between 2013-2019 in the Agua Negra centre and upper parts and changes of ca. 2 m/yr between 2013-2019 in the lower and western parts. This corresponds in magnitude with our vertical change results for Agua Negra Glacier as well as in pattern, Tab. 6 and Fig. 3A. Pitte et al. (2022) further report a 23 % reduction of the Agua Negra surface area between 1959 to 2019. While not part of this study we highlight the suitability of panchromatic and even multispectral Pléiades imagery to continue the assessment of surface area changes using our Pléiades acquisitions, cf. Tab. 1.

Ayala et al. (2025) estimate a 35 % area loss of the debris-free area of Tapado glacier between 1956-2024 located in the neighbouring catchment in Chile – elucidating a similarity of glacier response on both sides of the Andes while in contrast, observing an increase of the debris-covered area of Tapado glacier which reduces comparability to Agua Negra glacier that does not have a debris-covered part.

The glacier we refer to with ID 71 as mapped by IANIGLA-CONICET (2018), cf. Fig. 3B, is split in two WGMS glacier IDs (32927, 32920). Based on geodetic method, its mean annual elevation change is attributed values ranging from -0.2 m/yr (2000-2012) to -0.5 (2009-2014) for the first WGMS ID and predominantly around -0.4 m/yr for different measurement periods between 1999 and 2019 for the second (Dussaillant et al. 2019; Braun et al. 2019; Hugonnet et al. 2021). This contrasts with our Pléiades-based quantification of surface changes, Tab. 6, and strongly highlights the effect of glacier surface delineation (cf. 5.1), as also discussed by, e.g., by Ferri et al. (2020).

Our Pléiades-based vertical surface changes reveal glaciers at higher elevation and of larger size to be less prone to surface lowering, cf. Fig. 2B-C. This is in agreement with the temperature gradient and Al-Yaari et al. (2023) that find small glaciers to be affected by more pronounced loss – supporting the suitability of our approach. We refrain from calculating glacier mass balances given our limited in-situ knowledge on glacier ice density.

As expected, given their higher ice content compared to rock glaciers, vertical surface change is higher on the debris-covered glaciers in the Rodeo basin compared to the rock glaciers, Fig. 2A. This is in agreement with Ferri et al. (2020) that find mass balances of higher magnitude for debris-covered glaciers compared to rock glaciers based on the ASTERIX method

(Dussaillant et al. 2019) in the Central Andes (30° to 37°). For this study, however, we highlight that the three debris-covered glaciers are too little in number to draw representative conclusions upon their vertical surface change behaviour – particularly on detailed ablation patterns or the development of supraglacial ponds or ice cliffs as conducted, e.g., in Ayala et al. (2025) and Falaschi et al. (2021). Ayala et al. (2016) find similar streamflow contributions of debris-covered glaciers compared to glaciers, highlighting their hydrological significance. This significance contrasts with a strong underrepresentation of studies on debris-covered glaciers in glaciological studies (Masiokas et al. 2020).

Ferri et al. (2020) detect for the Central Andes (30° to 37°) highest mass balance losses for partly debris-covered glaciers, followed by clean ice glaciers and contrasting with completely debris-covered glaciers and rock glaciers characterised by almost zero mass balances (e. g., rock glaciers: -0.02 ± 0.19 m w.e. yr^{-1}, 2000-2018). Except for the partly debris-covered glaciers which we do not address here, this is well reflected in our results, cf. Fig. 2A. It highlights the strong differences in vertical surface change behaviour between the landforms. The question here is the comparability between the meaning of vertical surface changes on glaciers and rock glaciers, which is why we focus on rock glacier velocities as indicator of (in)stability of permafrost conditions in the next chapter.

5.4 Rock glacier kinematics in the Rodeo Basin

For Dos Lenguas rock glacier, our Pléiades-based rock glacier vertical surface changes, Tab. 6, and velocities, Tab. 7, are in good agreement with UAV-based rock glacier vertical and horizontal surface changes for Dos Lenguas rock glacier available for 2016-2018 (Halla et al. 2021) and 2016-2024 (Stammler et al. 2025a), both in terms of magnitude, Fig. 8, and pattern. In terms of pattern, highest values of 1.5 m/yr to 2 m/yr reached in the upper zone, cf. Fig. 6B (Halla et al. 2021; Stammler et al. 2025a).

Strozzi et al. (2020) quantify surface velocities ranging between 1.5 m/yr to 2 m/yr (2015-2020) for the upper part of Dos Lenguas rock glacier, based on interferometric synthetic aperture radar (InSAR) and offset tracking. These values are in good agreement with our Pléiades-based velocities, Fig. 8. While we acknowledge the challenges surrounding the comparison of optical and radar imagery-based rock glacier surface change quantification (view angles, different sources of error, different time periods, etc.) and caution a detailed comparison other than the comparison of general magnitude, we highlight the inter-methodological agreement of magnitude between the UAV-, Pléiades-, and InSAR-based investigations.

Except for Dos Lenguas rock glacier, no other rock glaciers in Rodeo basin have been monitored for surface change. This highlights the benefit of the remotely sensed analysis and its scalability compared to, e.g., UAV-based rock glacier surface change monitoring. Median horizonal surface changes for all rock glaciers investigated in this study, Tab. 4 & Tab. 6 are in agreement in terms of magnitude with average velocities of 0.54 ± 0.03 m/yr for rock glaciers in the neighbouring La Laguna catchment (Chile) as detected by Robson et al. (2022).

We hypothesize that the three groups we identify based on our basin-wide rock glacier surface change investigation, Fig. 5, are indicative of different driving mechanisms. Here, fast and large rock glaciers at high elevation and low slope are volume and creep dominated, see vertical surface change patterns in Fig. 3 and velocity pattern indicative of extensional and

compressional flow in Fig. 6A-C. As fast and small rock glaciers concur with high elevation with most importantly high slope, we infer gravitational force to have a strong impact – supported by missing creep surface morphology in, e.g., Fig. 6D. Small rock glaciers located at lower elevation with variable slope are slow to non-moving – potentially with the temperature gradient having the strongest effect on the low activity to inactivity. Fast rock glaciers, independent of their size, are characterised by coherent areas of positive vertical surface changes on the rock glaciers front, caused by the rock glaciers horizontal movement, Fig. 3C-D blue area on rock glacier front.

We do not detect a regional trend in increasing rock glacier velocities in the Rodeo basin between 2019-2025, Fig. 7. For many rock glaciers, including the fast and large and fast and small, the 2019-2024 period is characterised by very stable conditions, while the 2024-2025 time period is slightly higher. We cannot confirm the significance of this increase given our LoDs and the potential of an outlier year, but can confirm no similarly high velocities for 2019-2024, rendering them unprecedented in our dataset. Thus, we highlight the strong need for continued monitoring of rock glaciers in this basin in this potentially dynamic point in time. Slow and small rock glaciers do not show any activity above the LoD, confirming our conclusion on little activity.

This lack of a regional trend in increasing velocities elucidates stable permafrost conditions in Rodeo basin during 2019-2025. While we acknowledge the limitations of our short monitoring period, we highlight the data scarcity in this region of the world – particularly also for rock glacier monitoring (Hu et al. 2025). The detected lack of a regional trend is in agreement with a longer-term monitoring (1968-2023) by Blöthe et al. (2024) who identify unchanged rock glacier velocities in the Valles Calchaguíes region (24° to 25°S, Argentinean Andes) and Falaschi et al. (2025) who report a mixed signal of acceleration and deceleration of rock glacier velocities in Central Patagonia (47°S, Argentinean Andes) between 2018 and 2023. It contrasts with findings in the Alps (Manchado et al. 2024) or North America (Kääb and Røste 2024). Based on borehole measurements, Koenig et al. (2025) find no clear warming indication for ground temperatures in the Andes (27° to 34°) - further supporting the implication on permafrost conditions of our quantification of rock glacier velocities.

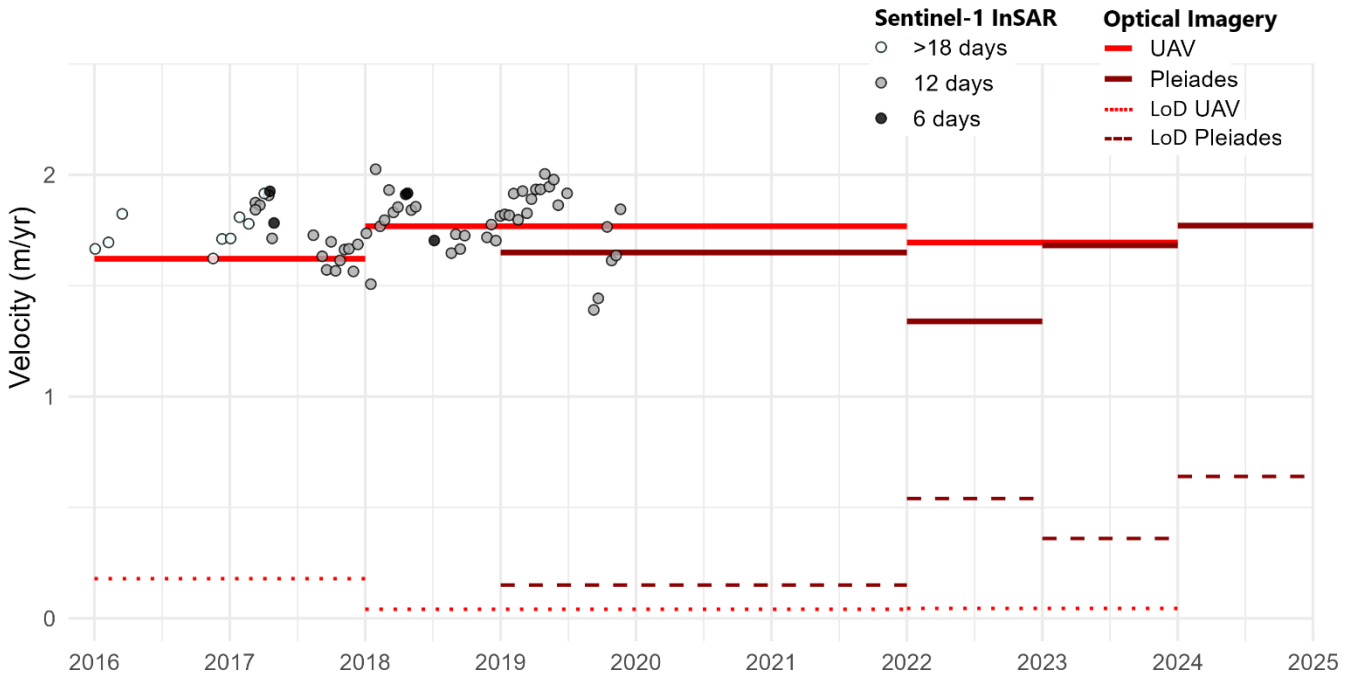

Fig. 8 Inter-method comparison between our Pléiades-based rock glacier velocity compared to Sentinel-1 InSAR (Strozzi et al. 2020) and UAV-based rock glacier velocity (Stammler et al. 2025a), all for a coordinate located in the upper part of Dos Lenguas rock glacier, see Fig. 6B. Note that velocities reached in the upper part of Dos Lenguas are higher than respective median values.

6 Conclusions

All glaciers in our study area of the Rodeo basin, located in the Dry Andes, are characterised by surface lowering. Agua Negra Glacier stands out with a maximum cumulative surface lowering of -8.99 m (2019-2025). Vertical surface change based on Pléiades DEM differing confirm smaller glaciers and glaciers at lower altitude to be prone to higher vertical surface lowering. Vertical surface changes on debris-covered glaciers are of a much lesser magnitude compared to glaciers, and of a higher magnitude than rock glaciers. Rock glaciers are characterised by minimal median vertical surface changes with high variability of negative and positive balances in time.

In contrast to the decline in the glacial domain, we do not see a regional trend of increasing rock glacier velocities for 2019-2025. Rock glacier velocities are heterogeneously present across the basin, with our monitoring for the entire basin allowing for a differentiation of driving mechanisms, such as dominance by creep and volume, gravity and temperature. Monitoring 47 rock glaciers further highlights that those velocities are heterogeneously present within the landforms, with similar magnitudes of change partially reached in the upper, and partially the lower part.

Both for vertical and horizontal surface change, our validation of the Pléiades-based quantification with repeated DGNSS measurements at three selected sites with in total 78 DGNSS measurements indicate minor differences below one pixel and supports the suitability of Pléiades imagery for cryospheric landform monitoring. An inter-method comparison of the rock

glacier velocities (Pléiades with UAV and InSAR) further enhances this conclusion. Pléiades imagery comes with the disadvantage of the need for tasking, particularly in areas characterized by data scarcity where archive coverage is poor. Initiatives like the Pléiades Glacier Observatory (Berthier et al. 2024) reduce this barrier by enabling access to selected image pairs and DEMs. Despite the remaining challenge in access, Pléiades imagery provides unseen opportunities specifically in remote areas where (physical) access is challenged. We find both stereo and tristereo acquisitions to be suitable for DEM generation at high resolution and error, while panchromatic Pléiades imagery particularly with its independence from colour nuances and changing lightning conditions provides a suitable basis for feature tracking. The possibility to increase the spatial coverage of the surface change monitoring to, e.g., catchment scale along with the benefit of monitoring surface change across landform types enables more interdisciplinary studies in the glaciological, geomorphological and hydrological fields.

Based on our comparison of vertical and horizontal surface changes in the glacial and periglacial domains of the Rodeo basin, we conclude a delayed response of the permafrost landforms to the increasing temperatures that are declining the glaciers and debris-covered glaciers alike. Given the hydrological significance of all meltwaters, we highlight the strong need for continued monitoring of surface changes in the glacial and periglacial domains, supported by interdisciplinary studies focusing on their potential interaction.

Author contributions

MS: a, b, c, d, h, i; JB: a, c, d, f, g, i, DC: c, d, e, f, i, SE: c, d, f, i, RB: e, i, XB: e, i, LS: b, g, i

(a) conceptualization; (b) funding acquisition; (c) methodology (including methodological development); (d) investigation; (e) resources (provision of data etc); (f) software (its provision and development); (g) supervision; (h) writing – initial draft; and (i) writing – reviewing and editing.

Data availability

The Pléiades imagery used in this study are commercial, but programs to facilitate academic access exist. These can be accessed via the CNES/Airbus DS Pléiades archive. The derived vertical surface changes for glaciers, debris-covered glaciers and rock glaciers, the derived rock glacier velocities and the DGNSS measurements used for validation will be published as dataset in PANGAEA. The repository with the image tracking framework will be made available on GITHUB.

Acknowledgements

This research is funded by the German Research Foundation (DFG, 461744503). M. Stammler further acknowledges funding by the German Scholarship Foundation. The generation of the Pléiades-derived products (DEMs and orthoimages) was performed using Ames Stereo Pipeline software (Bayer et al., 2018) and the GRICAD infrastructure (https://gricad.univ-grenoble-alpes.fr), which is supported by Grenoble research communities. We are thankful for the mapping efforts of the National Inventory of Glaciers without which studies like this would not be possible. The authors thank Tamara Köhler, Diana Agostina Ortiz, Fabian Flöck, Philipp Reichartz, Till Wenzel, Manon Cramer, Florian Wester, Kathrin Förster and Gabriele Kraus for their help during fieldwork. We further thank our collaboration partners at IANIGLA-CONICET in Mendoza/ Argentina, particularly Fidel Roig and Dario Trombotto Liaudat as well as Cristian Villaroel (CIGEOBIO-CONICET, San Juan/Argentina). Lastly, we thank Tazio Strozzi for sharing their Sentinel-1 InSAR data points.

References

Al-Yaari, Amen; Condom, Thomas; Junquas, Clementine; Rabatel, Antoine; Ramseyer, Victor; Sicart, Jean-Emmanuel et al. (2023): Climate Variability and Glacier Evolution at Selected Sites Across the World: Past Trends and Future Projections. In *Earth's Future* 11 (10), Article e2023EF003618, e2023EF003618. DOI: 10.1029/2023EF003618.

Arenson, Lukas U.; Harrington, Jordan S.; Koenig, Cassandra E. M.; Wainstein, Pablo A. (2022): Mountain Permafrost Hydrology—A Practical Review Following Studies from the Andes. In *Geosciences* 12 (2), p. 48. DOI: 10.3390/geosciences12020048.

ASTRIUM (2012): Pléiades Imagery User Guide. 2nd ed.

Ayala, A.; Pellicciotti, F.; MacDonell, S.; McPhee, J.; Vivero, S.; Campos, C.; Egli, P. (2016): Modelling the hydrological response of debris-free and debris-covered glaciers to present climatic conditions in the semiarid Andes of central Chile. In *Hydrol. Process.* 30 (22), pp. 4036–4058. DOI: 10.1002/hyp.10971.

Ayala, Álvaro; Robson, Benjamin; Navarro, Gonzalo; MacDonell, Shelley; Kinnard, Christophe; Vivero, Sebastián et al. (2025): Monitoring the physical processes driving the mass loss of Tapado Glacier, Dry Andes of Chile. In *J. Glaciol.* 71, e52. DOI: 10.1017/jog.2025.24.

Bagnardi, Marco; González, Pablo J.; Hooper, Andrew (2016): High-resolution digital elevation model from tri-stereo Pleiades-1 satellite imagery for lava flow volume estimates at Fogo Volcano. In *Geophys. Res. Lett.* 43 (12), pp. 6267–6275. DOI: 10.1002/2016GL069457.

Barsch, Dietrich (1992): Permafrost creep and rockglaciers. In *Permafrost and Periglacial Processes* 3 (3), pp. 175–188. DOI: 10.1002/ppp.3430030303.

Beraud, Luc; Cusicanqui, Diego; Rabatel, Antoine; Brun, Fanny; Vincent, Christian; Six, Delphine (2023): Glacier-wide seasonal and annual geodetic mass balances from Pléiades stereo images: application to the Glacier d'Argentière, French Alps. In *J. Glaciol.* 69 (275), pp. 525–537. DOI: 10.1017/jog.2022.79.

Berthier, E.; Vincent, C.; Magnússon, E.; Gunnlaugsson, Á. Þ.; Pitte, P.; Le Meur, E. et al. (2014): Glacier topography and elevation changes derived from Pléiades sub-meter stereo images. In *The Cryosphere* 8 (6), pp. 2275–2291. DOI: 10.5194/tc-8-2275-2014.

Berthier, Etienne; Lebreton, Jérôme; Fontannaz, Delphine; Hosford, Steven; Belart, Joaquin Munoz Cobo; Brun, Fanny et al. (2024): The Pléiades Glacier Observatory: high resolution digital elevation models and ortho-imagery to monitor glacier change. In *The Cryosphere* 18, pp. 5551–5571. DOI: 10.5194/tc-18-5551-2024.

Beyer, Ross A.; Alexandrov, Oleg; McMichael, Scott (2018): The Ames Stereo Pipeline: NASA's Open Source Software for Deriving and Processing Terrain Data. In *Earth and Space Science* 5 (9), pp. 537–548. DOI: 10.1029/2018EA000409.

Blöthe, Jan Henrik; Falaschi, Daniel; Vivero, Sebastián; Tadono, Takeo (2024): Rock Glacier Kinematics in the Valles Calchaquíes Region, Northwestern Argentina, From Multi-Temporal Aerial and Satellite Imagery (1968–2023). In *Permafrost & Periglacial*, Article ppp.2260. DOI: 10.1002/ppp.2260.

Blöthe, Jan Henrik; Halla, Christian; Schwalbe, Ellen; Bottegal, Estefania; Trombotto Liaudat, Dario; Schrott, Lothar (2021): Surface velocity fields of active rock glaciers and ice-debris complexes in the Central Andes of Argentina. In *Earth Surface Processes and Landforms* 46 (2), pp. 504–522. DOI: 10.1002/esp.5042.

Bodin, X.; Rojas, F.; Brenning, A. (2010): Status and evolution of the cryosphere in the Andes of Santiago (Chile, 33.5°S.). In *Geomorphology* 118 (3-4), pp. 453–464. DOI: 10.1016/j.geomorph.2010.02.016.

Borsdorf, Axel; Stadel, Christoph (2013): Die Anden. Ein geographisches Portrait. Berlin, Heidelberg: Springer.

Braun, Matthias H.; Malz, Philipp; Sommer, Christian; Farías-Barahona, David; Sauter, Tobias; Casassa, Gino et al. (2019): Constraining glacier elevation and mass changes in South America. In *Nature Clim Change* 9 (2), pp. 130–136. DOI: 10.1038/s41558-018-0375-7.

Caro, Alexis; Condom, Thomas; Rabatel, Antoine; Champollion, Nicolas; García, Nicolás; Saavedra, Freddy (2024): Hydrological response of Andean catchments to recent glacier mass loss. In *The Cryosphere* 18 (5), pp. 2487–2507. DOI: 10.5194/tc-18-2487-2024.

Cogley, J. G.; R. Hock; L.A. Rasmussen; A.A. Arendt; A. Bauder, R. BraithwaiteJ.; P. Jansson et al. (2011): Glossary of glacier mass balance and related terms. Paris, France (IHP-VII Techincal Documents in Hydrology No. 86, IACS Contribution No. 2, UNESCO-IHP). Available online at https://wgms.ch/downloads/Cogley_etal_2011.pdf.

Cusicanqui, Diego; Bodin, Xavier; Duvillard, Pierre-Allain; Schoeneich, Philippe; Revil, André; Assier, Alain et al. (2023): Glacier, permafrost and thermokarst interactions in Alpine terrain: Insights from seven decades of reconstructed dynamics of the Chauvet glacial and periglacial system (Southern French Alps). In *Earth Surf Processes Landf* 48 (13), pp. 2595–2612. DOI: 10.1002/esp.5650.

Cusicanqui, Diego; Lacroix, Pascal; Bodin, Xavier; Robson, Benjamin Aubrey; Kääb, Andreas; MacDonell, Shelley (2025): Detection and reconstruction of rock glacier kinematics over 24 years (2000–2024) from Landsat imagery. In *The Cryosphere* 19 (7), pp. 2559–2581. DOI: 10.5194/tc-19-2559-2025.

Dall'Asta, Elisa; Forlani, Gianfranco; Roncella, Riccardo; Santise, Marina; Diotri, Fabrizio; Di Morra Cella, Umberto (2017): Unmanned Aerial Systems and DSM matching for rock glacier monitoring. In *ISPRS Journal of Photogrammetry and Remote Sensing* 127, pp. 102–114. DOI: 10.1016/j.isprsjprs.2016.10.003.

Dussaillant, I.; Berthier, E.; Brun, F.; Masiokas, M.; Hugonnet, R.; Favier, V. et al. (2019): Two decades of glacier mass loss along the Andes. In *Nat. Geosci.* 12 (10), pp. 802–808. DOI: 10.1038/s41561-019-0432-5.

Esper Angillieri, María Yanina (2017): Permafrost distribution map of San Juan Dry Andes (Argentina) based on rock glacier sites. In *Journal of South American Earth Sciences* 73, pp. 42–49. DOI: 10.1016/j.jsames.2016.12.002.

Falaschi, Daniel; Bhattacharya, Atanu; Guillet, Gregoire; Huang, Lei; King, Owen; Mukherjee, Kriti et al. (2023): Annual to seasonal glacier mass balance in High Mountain Asia derived from Pléiades stereo images: examples from the Pamir and the Tibetan Plateau. In *The Cryosphere* 17 (12), pp. 5435–5458. DOI: 10.5194/tc-17-5435-2023.

Falaschi, Daniel; Blöthe, Jan; Berthier, Etienne; Tadono, Takeo; Villalba, Ricardo (2025): Monitoring recent (2018–2023) glacier and rock glacier changes in Central Patagonia using high-resolution Pléiades and ALOS PRISM satellite data. In *Front. Earth Sci.* 13, Article 1601249, p. 1601249. DOI: 10.3389/feart.2025.1601249.

Falaschi, Daniel; Rivera, Andrés; Lo Vecchio Repetto, Andrés; Moragues, Silvana; Villalba, Ricardo; Rastner, Philipp et al. (2021): Evolution of Surface Characteristics of Three Debris-Covered Glaciers in the Patagonian Andes From 1958 to 2020. In *Front. Earth Sci.* 9, Article 671854, p. 671854. DOI: 10.3389/feart.2021.671854.

Ferri, Lidia; Dussaillant, Inés; Zalazar, Laura; Masiokas, Mariano H.; Ruiz, Lucas; Pitte, Pierre et al. (2020): Ice Mass Loss in the Central Andes of Argentina Between 2000 and 2018 Derived From a New Glacier Inventory and Satellite Stereo-Imagery. In *Frontiers in Earth Science* 8, p. 530997. DOI: 10.3389/feart.2020.530997.

Fleischer, Fabian; Haas, Florian; Piermattei, Livia; Pfeiffer, Madlene; Heckmann, Tobias; Altmann, Moritz et al. (2021): Multi-decadal (1953–2017) rock glacier kinematics analysed by high-resolution topographic data in the upper Kaunertal, Austria. In *The Cryosphere* 15 (12), pp. 5345–5369. DOI: 10.5194/tc-15-5345-2021.

Gruber, S. (2012): Derivation and analysis of a high-resolution estimate of global permafrost zonation. In *The Cryosphere* 6 (1), pp. 221–233. DOI: 10.5194/tc-6-221-2012.

Halla, Christian; Blöthe, Jan Henrik; Tapia Baldis, Carla; Trombotto, Dario; Hilbich, Christin; Hauck, Christian; Schrott, Lothar (2021): Ice content and interannual water storage changes of an active rock glacier in the dry Andes of Argentina. In *The Cryosphere* 15 (2), 1187-1213 DOI: 10.5194/tc-15-1187-2021.

Hu, Yan; Arenson, Lukas U.; Barboux, Chloé; Bodin, Xavier; Cicoira, Alessandro; Delaloye, Reynald et al. (2025): Rock Glacier Velocity: An Essential Climate Variable Quantity for Permafrost. In *Reviews of Geophysics* 63 (1), Article e2024RG000847, e2024RG000847. DOI: 10.1029/2024RG000847.

Hugonnet, Romain; McNabb, Robert; Berthier, Etienne; Menounos, Brian; Nuth, Christopher; Girod, Luc et al. (2021): Accelerated global glacier mass loss in the early twenty-first century. In *Nature* 592 (7856), pp. 726–731. DOI: 10.1038/s41586-021-03436-z.

IANIGLA-CONICET (2018): ANIGLA-Inventario Nacional de Glaciares y Ambiente Periglacial. Informe de la subcuenca del río Blanco.Cuenca del río San Juan. With assistance of Ministerio de Ambiente y Desarrollo Sustentable de la Nación.

Kääb, Andreas; Røste, Julie (2024): Rock glaciers across the United States predominantly accelerate coincident with rise in air temperatures. In *Nat Commun* 15 (1), p. 7581. DOI: 10.1038/s41467-024-52093-z.

Koenig, Cassandra E. M.; Hilbich, Christin; Hauck, Christian; Arenson, Lukas U.; Wainstein, Pablo (2025): Thermal state of permafrost in the Central Andes (27–34° S). In *The Cryosphere* 19 (7), pp. 2653–2676. DOI: 10.5194/tc-19-2653-2025.

Köhler, Tamara; Schoch-Baumann, Anna; Bell, Rainer; Buckel, Johannes; Ortiz, Diana Agostina; Liaudat, Dario Trombotto; Schrott, Lothar (2025): Expanding cryospheric landform inventories – quantitative approaches for underestimated periglacial block- and talus slopes in the Dry Andes of Argentina. In *Front. Earth Sci.* 13, Article 1534410, p. 1534410. DOI: 10.3389/feart.2025.1534410.

Lenzano, María Gabriela; Lenzano, Luis; Barón, Jorge; Lannutti, Esteban; Durand, Marcelo; Trombotto Liaudat, Dario (2016): Thinning of the Horcones inferior debris-covered glacier, derived from five ablation seasons by semi-continuous GNSS geodetic surveys (Mt. Aconcagua, Argentina). In *andgeo* 43 (1), p. 47. DOI: 10.5027/andgeoV43n1-a03.

Lliboutry, L.; Williams, R.; Ferrigno, Jane G. (1998): Glaciers of Chilie and Argentina. Geological Survey professional paper. Washington.

Manchado, Alberto Muñoz-Torrero; Allen, Simon; Cicoira, Alessandro; Wiesmann, Samuel; Haller, Ruedi; Stoffel, Markus (2024): 100 years of monitoring in the Swiss National Park reveals overall decreasing rock glacier velocities. In *Commun Earth Environ* 5 (1). DOI: 10.1038/s43247-024-01302-0.

Masiokas, M. H.; Rabatel, A.; Rivera, A.; Ruiz, L.; Pitte, P.; Ceballos, J. L. et al. (2020): A Review of the Current State and Recent Changes of the Andean Cryosphere. In *Front. Earth Sci.* 8, Article 99. DOI: 10.3389/feart.2020.00099.

Nuth, C.; Kääb, A. (2011): Co-registration and bias corrections of satellite elevation data sets for quantifying glacier thickness change. In *The Cryosphere* 5 (1), pp. 271–290. DOI: 10.5194/tc-5-271-2011.

Pabón-Caicedo, José Daniel; Arias, Paola A.; Carril, Andrea F.; Espinoza, Jhan Carlo; Borrel, Lluís Fita; Goubanova, Katerina et al. (2020): Observed and Projected Hydroclimate Changes in the Andes. In *Front. Earth Sci.* 8, Article 61. DOI: 10.3389/feart.2020.00061.

Pitte, Pierre; Masiokas, Mariano; Gargantini, Hernán; Ruiz, Lucas; Berthier, Etienne; Ferri Hidalgo, Lidia et al. (2022): Recent mass-balance changes of Agua Negra glacier (30°S) in the Desert Andes of Argentina. In *J. Glaciol.* 68 (272), pp. 1197–1209. DOI: 10.1017/jog.2022.22.

Réveillet, Marion; MacDonell, Shelley; Gascoin, Simon; Kinnard, Christophe; Lhermitte, Stef; Schaffer, Nicole (2020): Impact of forcing on sublimation simulations for a high mountain catchment in the semiarid Andes. In *The Cryosphere* 14 (1), pp. 147–163. DOI: 10.5194/tc-14-147-2020.

RGIK (2022): IPA Action Group: Rock glacier inventories and kinematics. 22 Newsletter (04.02.3022): Rock glacier velocity as an associated parameter of ECV Permafrost. Available online at https://www.unifr.ch/geo/geomorphology/en/research/ipa-action-group-rock-glacier/, updated on 6/30/2023, checked on 6/30/2023.

RGIK (2023): Rock Glacier Velocity as an associated parameter of ECV Permafrost. Baseline Concepts Version 3.2.

Rieg, Lorenzo; Klug, Christoph; Nicholson, Lindsey; Sailer, Rudolf (2018): Pléiades Tri-Stereo Data for Glacier Investigations—Examples from the European Alps and the Khumbu Himal. In *Remote Sensing* 10 (10), p. 1563. DOI: 10.3390/rs10101563.

Robson, Benjamin Aubrey; MacDonell, Shelley; Ayala, Álvaro; Bolch, Tobias; Nielsen, Pål Ringkjøb; Vivero, Sebastián (2022): Glacier and rock glacier changes since the 1950s in the La Laguna catchment, Chile. In *The Cryosphere* 16 (2), pp. 647–665. DOI: 10.5194/tc-16-647-2022.

Ruiz, L.; Bodin, Xavier (2015): Analysis and improvement of surface representativeness of high resolution Pléiades DEMs: Examples from glaciers and rock glaciers in two areas of the Andes. In *Geomorphometry.org*. DOI: 10.13140/RG.2.1.4328.2963.

Schrott, Lothar (1994): Die Solarstrahlung als steuernder Faktor im Geosystem der subtropischen semiariden Hochanden (Agua Negra, San Juan, Argentinien). In *Heidelberger Geographische Arbeiten* 94.

Schrott, Lothar (1996): Some geomorphological-hydrological aspects of rock glaciers in the Andes (San Juan, Argentina). In *Zeitschrift für Geomorphologie. Supplementband* 104, pp. 161–173.

Schrott, Lothar; Götz, Joachim (2013): The periglacial environment in the semiarid and arid Andes of Argentina - hydological significance and research frontiers. In : Forschen im Gebirge / Investigating the mountains / investigando las Montanas, vol. 5.

Schwalbe, Ellen; Maas, Hans-Gerd (2017): The determination of high-resolution spatio-temporal glacier motion fields from time-lapse sequences. In *Earth Surf. Dynam.* 5 (4), pp. 861–879. DOI: 10.5194/esurf-5-861-2017.

Shean, David E.; Alexandrov, Oleg; Moratto, Zachary M.; Smith, Benjamin E.; Joughin, Ian R.; Porter, Claire; Morin, Paul (2016): An automated, open-source pipeline for mass production of digital elevation models (DEMs) from very-high-resolution commercial stereo satellite imagery. In *ISPRS Journal of Photogrammetry and Remote Sensing* 116, pp. 101–117. DOI: 10.1016/j.isprsjprs.2016.03.012.

Stammler, Melanie; Blöthe, Jan; Flöck, Fabian; Bell, Rainer; Schrott, Lothar (2025a): Dos Lenguas rock glacier kinematics stable despite warming trend (2016–2024): Surface changes and the role of topography and climate in the Dry Andes of Argentina. In *Earth Surf Processes Landf* 50 (11), Article e70151, e70151. DOI: 10.1002/esp.70151.

Stammler, Melanie; Blöthe, Jan; Flöck, Fabian; Bell, Rainer; Schrott, Lothar (2025b): UAV-based optical imagery, digital elevation models and hillshades of Dos Lenguas rock glacier / Argentinean Dry Andes (30ºS, 69ºW; 2016, 2018, 2022, 2024) and daily static optical imagery (2023-2024) [dataset]. In *PANGAEA*. Available online at https://doi.org/10.1594/PANGAEA.979876.

Stammler, Melanie; Cusicanqui, Diego; Bell, Rainer; Robson, Benjamin; Bodin, Xavier; Blöthe, Jan; Schrott, Lothar (2024): Vertical surface change signals of rock glaciers: combining UAV and Pléiades imagery (Agua Negra, Argentina) Proceedings of the 12th International Conference on Permafrost. DOI: 10.52381/ICOP2024.138.1.

Strozzi, Tazio; Caduff, Rafael; Jones, Nina; Barboux, Chloé; Delaloye, Reynald; Bodin, Xavier et al. (2020): Monitoring Rock Glacier Kinematics with Satellite Synthetic Aperture Radar. In *Remote Sensing* 12 (3), p. 559. DOI: 10.3390/rs12030559.

Villarroel, Cristian; Tamburini Beliveau, Guillermo; Forte, Ana; Monserrat, Oriol; Morvillo, Monica (2018): DInSAR for a Regional Inventory of Active Rock Glaciers in the Dry Andes Mountains of Argentina and Chile with Sentinel-1 Data. In *Remote Sensing* 10 (10), p. 1588. DOI: 10.3390/rs10101588.

Villarroel, Cristian Daniel; Forte, A. P. (2020): Spatial distribution of active and inactive rock glaciers and protalus ramparts in a sector of the Central Andes of Argentina. In *Geographical Research Letters* 46 (1), pp. 141–158. DOI: 10.18172/cig.4272.

Villarroel, Cristian Daniel; Ortiz, Diana Agostina; Forte, Ana Paula; Tamburini Beliveau, Guillermo; Ponce, David; Imhof, Armando; López, Andrés (2022): Internal structure of a large, complex rock glacier and its significance in hydrological and dynamic behavior: A case study in the semi-arid Andes of Argentina. In *Permafrost & Periglacial* 33 (1), pp. 78–95. DOI: 10.1002/ppp.2132.

Vivero, Sebastián; Lambiel, Christophe (2024): Annual surface elevation changes of rock glaciers and their geomorphological significance: Examples from the Swiss Alps. In *0169-555X* 467, p. 109487. DOI: 10.1016/j.geomorph.2024.109487.

Zalazar, Laura Viviana; Ferri Hidalgo, Lidia; Castro, Mariano Agustin; Gargantini, Hernan; Giménez, Melisa Mariel; Pitte, Pedro Miguel et al. (2017): Glaciares de Argentina: Resultados preliminares del Inventario Nacional de Glaciares. In *Revista de Glaciares y Ecosistemas de Montaña* 2, pp. 13–22. Available online at https://ri.conicet.gov.ar/handle/11336/60533.

Supplementary Material

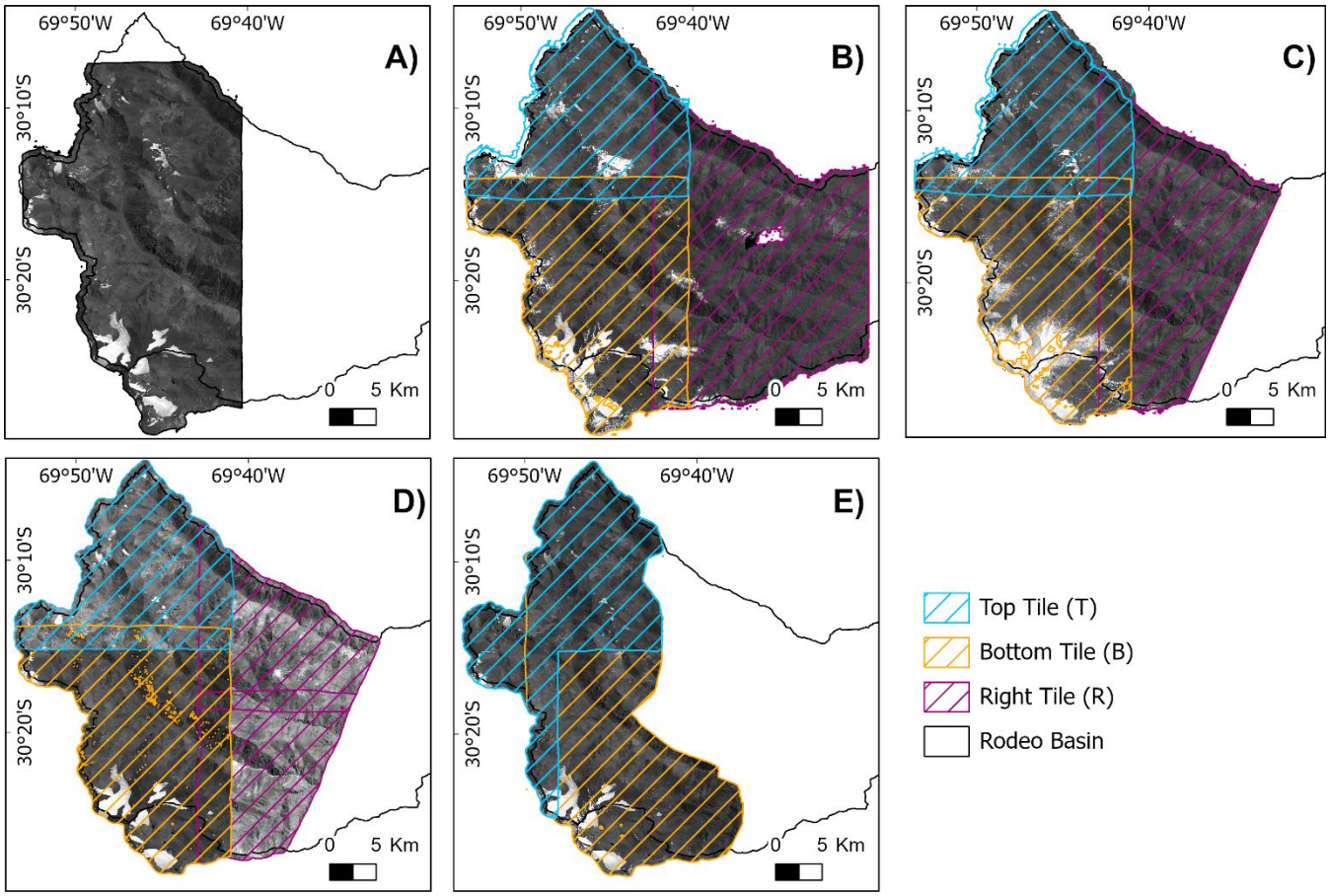

A1 Comparison of panchromatic Pléiades imagery with a focus on the distribution of acquisition tiles (T, B, R – see tab. 1) and differences in acquisition extent. Note that we do not separate in T, B and R for the 2019 acquisition as this imagery was acquired as one tile only. In addition, snow cover distribution at the respective date of the acquisitions is visible from the imagery. For the processing of the Pléiades imagery, see 3.2.

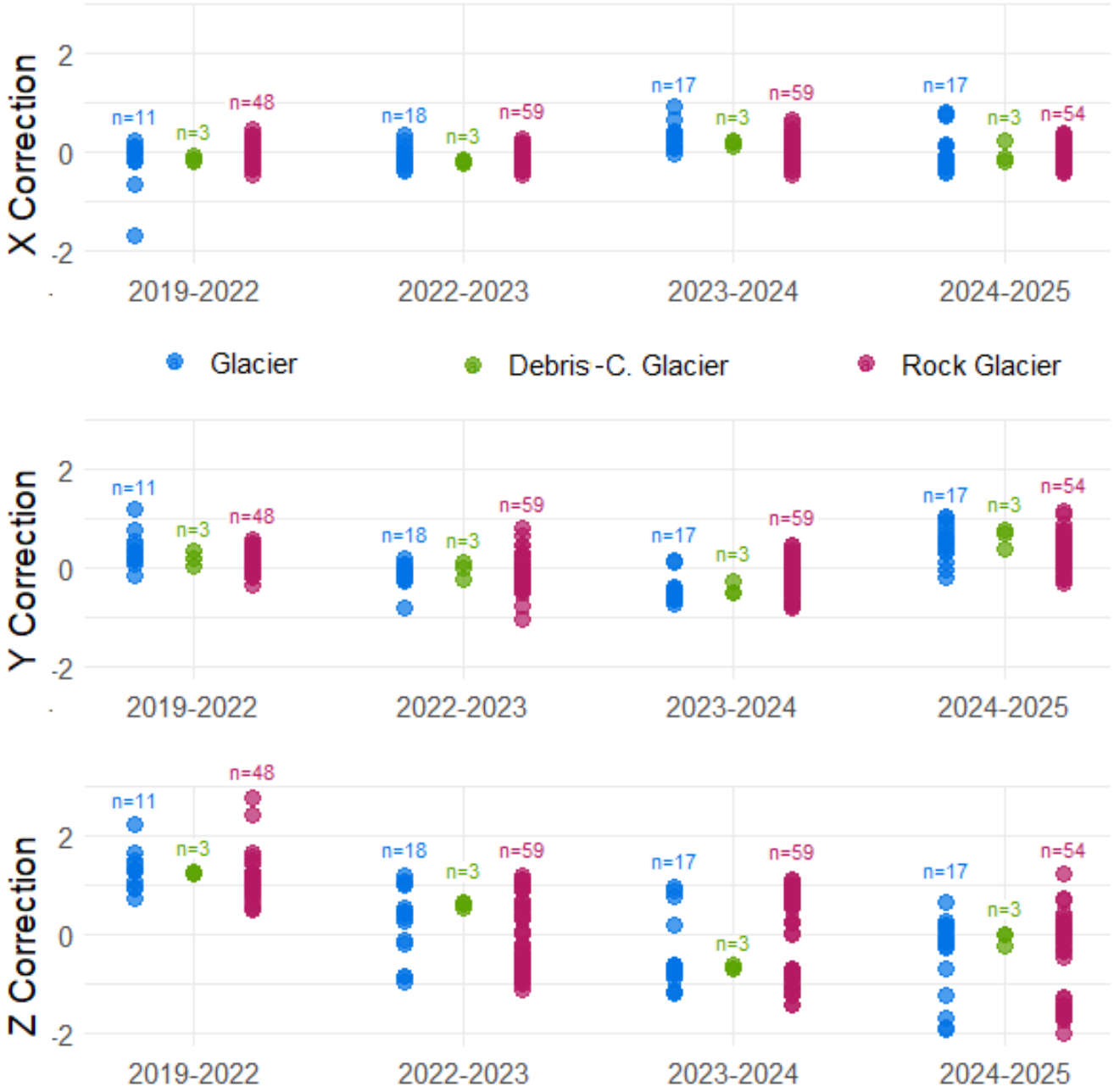

A2 Temporal and landform-specific analysis of the x, y and z correction factors (m) used during co-registration. For a full list of all correction factors, please see A3. Co-registration is achieved following the approach by Nuth and Kääb (2011) as applied in Demcoreg (Shean et al. 2016). The number of landforms in the respective category is given in each of the subplots and depends on the respective acquisition extents, see A1.

A3 Co-registration correction factors (m) for all clipped rasters based on the approach by Nuth and Kääb (2011) as applied in Demcoreg (Shean et al. 2016). For more background on the different polygon IDs, see Fig. 7.

Polygon ID	Tile	Start	End	X	Y	Z
1	T	19	22	-0.17	0.19	1.22
1	T	22	23	-0.21	-0.08	0.66
1	T	23	24	0.16	-0.47	-0.67
2	T	19	22	-0.16	0.43	1.24
2	T	22	23	-0.18	-0.18	0.72
2	T	23	24	0.31	-0.33	-0.69
3	T	19	22	-0.13	0.34	0.93
3	T	22	23	-0.25	-0.12	0.91
3	T	23	24	0.36	-0.35	-0.9
4	T	19	22	-0.16	0.14	1.05
4	B	19	22	0.27	0.29	1.02
4	T	22	23	-0.34	-0.06	1.15
4	B	22	23	-0.17	-0.16	-0.47
4	B	23	24	-0.08	-0.05	0.72
5	T	19	22	-0.31	0.23	1.2
5	B	19	22	0.21	0.06	0.39
5	T	22	23	-0.26	-0.03	1.05
5	T	23	24	0.58	-0.44	-1.23
6	T	19	22	-0.12	0.3	0.91
6	T	22	23	-0.2	-0.07	0.89
6	T	23	24	0.24	-0.34	-0.87
7	T	19	22	0.01	0.41	1.04
7	T	22	23	-0.19	-0.03	1.12
7	T	23	24	0	-0.72	-1.21
8	R	19	22	-0.02	0.4	2.7
8	B	19	22	0.32	-0.12	1.28
8	R	22	23	-0.02	-0.22	-0.93
8	B	22	23	-0.18	0.46	0.38
8	R	23	24	0.04	0.15	0.33
8	B	23	24	-0.01	-0.22	0.01
9	R	19	22	-0.16	0.38	2.78
9	B	19	22	0.08	-0.23	1.35
9	R	22	23	0.01	-0.28	-0.96
9	B	22	23	0.03	0.55	0.25
9	R	23	24	0.2	0.34	0.28
10	R	22	23	0.08	-0.35	-0.91
10	B	22	23	-0.15	0.73	0.2
10	R	23	24	0.24	0.48	0.23
11	R	19	22	-0.19	0.49	2.45
11	B	19	22	0.14	0.23	1.08
11	R	22	23	-0.03	-0.2	-0.8
11	B	22	23	0.09	0.03	0.17
11	R	23	24	0.11	-0.04	0.26
12	R	19	22	-0.25	0.56	2.44
12	B	19	22	0.14	0.44	0.92
12	B	22	23	0.21	0.26	0.09
12	R	23	24	0.15	-0.4	0.65
12	B	23	24	-0.08	0.48	0.04
13	B	19	22	0.04	-0.04	1.29
13	B	22	23	-0.47	0.05	-0.62
13	B	23	24	-0.12	-0.17	0.95
14	B	19	22	0.46	0.41	0.84
14	B	22	23	-0.37	-0.26	-0.98
14	B	23	24	0.08	0.08	1.12
15	B	19	22	0.12	0.37	0.53
15	B	22	23	-0.29	0.01	-0.21
15	B	23	24	-0.25	-0.17	0.92
16	T	19	22	-0.36	0.03	0.86
16	B	19	22	0.02	-0.02	1.04
16	B	22	23	-0.17	-0.32	-0.76
16	B	23	24	0.27	-0.12	0.81
17	T	19	22	0.21	0.06	1.22
17	B	19	22	0.23	0.6	1.04
17	T	22	23	-0.26	-0.15	1.07
17	B	22	23	0.15	-0.8	-0.22
17	B	23	24	0.15	0.06	0.59
18	T	19	22	0.08	0.19	1.28
18	B	19	22	0.49	0.67	0.83
18	T	22	23	-0.24	-0.17	1.08
19	T	22	23	-0.26	-0.11	1.13
19	B	22	23	-0.17	-1.09	-0.26
19	B	23	24	0	0.13	0.67
20	T	19	22	-0.32	0.03	1.06
20	B	19	22	0.27	0.34	1.08
20	T	22	23	-0.14	-0.21	1.17
20	B	22	23	-0.34	-0.77	-0.48
20	B	23	24	0.33	-0.08	0.68
21	T	19	22	-0.35	0.02	0.93
21	B	19	22	0.06	0.03	1.06
21	T	22	23	-0.15	-0.17	1.23
21	B	22	23	-0.17	-0.5	-0.69
21	B	23	24	0.28	-0.12	0.76
22	B	19	22	0.26	0.05	1.19
22	B	22	23	0.14	0.21	-0.88
22	B	23	24	-0.07	-0.18	0.92

23	T	19	22	-0.27	0.5	1.31
23	B	19	22	0.16	0.65	1.26
23	T	22	23	-0.39	-0.1	1.07
23	B	22	23	-0.13	-0.38	-0.54
23	B	23	24	0.66	-0.78	0.24
24	T	19	22	-0.11	0.34	1.29
24	B	19	22	0.34	-0.33	0.66
24	T	22	23	-0.38	-0.11	1.06
24	B	22	23	-0.04	0.26	0.06
24	B	23	24	-0.14	0.12	0.72
25	B	19	22	0.35	-0.18	1.06
25	B	22	23	-0.08	0.67	-0.67
25	B	23	24	-0.17	-0.34	0.82
26	T	19	22	-0.18	0.47	1.08
26	T	22	23	-0.28	0.03	1.19
26	T	23	24	0.48	-0.82	-1.4
27	T	19	22	-0.09	0.43	0.8
27	T	22	23	-0.2	-0.18	1.04
27	T	23	24	0.26	-0.55	-1.05
28	R	23	24	-0.04	0.29	1.03
29	T	22	23	0.05	-0.04	0.32
29	T	23	24	0.41	-0.5	-0.75
30	T	19	22	-0.08	0.15	1.59
30	T	22	23	-0.09	-0.19	0.55
30	T	23	24	0.22	-0.31	-0.75
31	T	22	23	-0.15	-0.05	0.4
31	T	23	24	0.22	-0.36	-0.69
32	T	22	23	-0.14	-0.02	0.38
32	T	23	24	0.22	-0.6	-0.77
33	T	22	23	-0.19	-0.02	0.35
33	T	23	24	0.21	-0.54	-0.8
34	T	22	23	-0.12	-0.2	0.36
34	T	23	24	0.22	-0.5	-0.74
35	B	19	22	0.29	0.39	0.86
35	B	22	23	-0.22	-0.41	-0.57
35	B	23	24	-0.39	0.18	0.97
36	R	22	23	-0.01	-0.46	-0.88
36	R	23	24	0.44	0.37	0.58
37	T	19	22	-0.3	0.29	1.2
37	T	22	23	-0.32	-0.06	1.05
37	T	23	24	0.41	-0.67	-1.18
38	B	19	22	0.2	-0.03	1.13
38	B	22	23	-0.2	0.33	0.02
38	B	23	24	0.03	-0.3	0.54
39	B	19	22	0.04	0.43	0.98
39	B	22	23	0.08	-0.28	-0.36
39	B	23	24	-0.39	0.31	0.77
40	B	19	22	0	0.1	0.98
40	B	22	23	-0.01	0.04	-0.37
40	B	23	24	-0.04	-0.05	0.68
41	B	19	22	0.3	-0.07	1.07
41	B	22	23	-0.18	0.81	-0.93
41	B	23	24	0.06	-0.51	0.95
42	B	19	22	0.21	0.23	0.54
42	B	22	23	-0.35	0.05	-0.18
42	B	23	24	-0.27	-0.22	0.89
43	B	19	22	0.33	-0.07	1.09
43	B	22	23	-0.02	0.48	-0.65
43	B	23	24	-0.06	-0.42	0.86
44	B	19	22	0.28	0.41	0.83
44	B	22	23	-0.16	-0.42	-0.54
44	B	23	24	-0.23	0.1	0.95
45	B	19	22	8.9	5	-9.47
45	B	22	23	0.14	0.11	-0.6
45	B	23	24	-0.47	-0.31	1.03
46	B	19	22	0.09	0.21	0.56
46	B	22	23	0.11	-0.31	-0.21
46	B	23	24	-0.27	0.26	0.81
47	B	19	22	0.05	0.6	1.14
47	B	22	23	0.09	-0.19	-1.1
47	B	23	24	-0.13	-0.22	1.1
48	T	22	23	-0.28	-0.11	1.17
48	B	22	23	-0.09	-1.02	-0.32
48	B	23	24	0.21	0.12	0.65
49	B	19	22	0.09	0.1	1.19
49	B	22	23	0.26	0.13	-0.66
49	B	23	24	-0.28	-0.15	0.95
50	T	19	22	0.07	0.32	1.12
50	B	19	22	0.11	0.12	0.34
50	T	22	23	-0.33	-0.08	1.11
50	T	23	24	0.26	-0.7	-1.42
51	T	19	22	-0.23	0.23	0.85
51	T	22	23	-0.05	0.01	0.94
51	T	23	24	0.34	-0.46	-1.06
52	T	19	22	-0.22	0.29	0.85
52	T	22	23	-0.21	-0.11	0.99
52	T	23	24	0.22	-0.32	-1.04
53	R	23	24	0.2	0.37	1
54	R	23	24	0.03	0.19	0.95
55	T	19	22	-0.47	0.39	1.65
55	T	22	23	-0.37	0.05	0.57
55	T	23	24	0.02	-0.33	-0.68

56	T	19	22	-0.35	-0.14	1.5
56	T	22	23	-0.3	-0.03	0.59
56	T	23	24	0.21	-0.39	-0.74
57	T	19	22	-0.25	0.04	1.44
57	T	22	23	-0.21	0.04	0.56
57	T	23	24	0.32	-0.44	-0.8
58	T	22	23	-0.21	-0.1	0.31
58	T	23	24	0.22	-0.43	-0.78
59	T	22	23	-0.3	0.03	0.52
59	T	23	24	0.27	-0.54	-0.73
60	T	19	22	-0.19	0.37	1.43
60	T	22	23	-0.16	-0.28	0.48
60	T	23	24	0.34	-0.61	-0.69
61	T	19	22	-0.04	0.46	1.08
61	T	22	23	-0.34	0.02	1.08
61	T	23	24	0.65	-0.71	-1.2
62	T	19	22	0	-0.13	1.3
62	T	22	23	-0.21	0.18	0.56
62	T	23	24	0.06	-0.45	-0.6
64	B	22	23	0.23	-0.03	-0.11
65	B	19	22	-1.68	1.21	2.25
65	B	22	23	0.35	-0.24	-0.19
65	R	23	24	0.6	-0.08	-0.06
65	B	23	24	0.08	0.17	0.22
66	T	19	22	0.1	0.21	1.33
66	B	19	22	0.24	0.16	0.56
66	T	22	23	-0.28	-0.06	1.03
66	T	23	24	0.37	-0.56	-1.16
67	B	22	23	-0.03	-0.07	-0.96
67	B	23	24	0.31	-0.64	0.97
68	T	19	22	-0.67	0.1	0.75
68	T	22	23	-0.23	-0.23	1.19
68	T	23	24	0.92	-0.47	-0.86
69	B	19	22	0.09	0.54	1.34
69	B	22	23	0.1	-0.8	-0.83
69	B	23	24	0.27	0.12	0.77
70	T	19	22	-0.37	0.69	0.79
70	B	19	22	-0.01	0.79	0.94
70	B	22	23	-0.08	0.06	-0.83
70	B	23	24	-0.05	-0.41	0.9
71	T	19	22	-0.14	0.34	0.96
71	T	22	23	-0.38	-0.23	1.07
71	T	23	24	0.38	-0.48	-1.15
72	T	19	22	-0.21	0.24	1.53
72	T	22	23	-0.04	-0.11	0.45
72	T	23	24	0.28	-0.39	-0.75
73	T	19	22	0.25	0.16	1.65
73	T	22	23	-0.09	0.09	0.48
73	T	23	24	0.42	-0.48	-0.81
74	T	22	23	0.04	-0.09	0.29
74	T	23	24	0.37	-0.54	-0.76
75	T	22	23	-0.03	-0.09	0.36
75	T	23	24	0.29	-0.49	-0.7
76	T	22	23	-0.19	-0.1	0.46
76	T	23	24	0.13	-0.42	-0.66
77	T	22	23	-0.07	-0.05	0.48
77	T	23	24	0.16	-0.41	-0.6
78	T	22	23	-0.1	-0.17	0.47
78	T	23	24	0.13	-0.41	-0.6
79	T	19	22	-0.06	0.03	1.27
79	T	22	23	-0.18	0.13	0.57
79	T	23	24	0.11	-0.51	-0.62
80	T	19	22	-0.15	0.37	1.26
80	T	22	23	-0.16	-0.24	0.68
80	T	23	24	0.21	-0.28	-0.67
81	T	19	22	-0.19	0.2	1.25
81	T	22	23	-0.23	-0.01	0.64
81	T	23	24	0.23	-0.49	-0.68

A4 Correlation coefficients of the affine transformation residues of the feature tracking approach, for all object IDs. While low correlation coefficients (0 to 0.5) correspond with a good quality of the feature tracking at that spatial location and time, higher correlation coefficients (0.5 to 1) correspond with a poorer feature tracking quality. For more background on this quality control, see 3.5.

Polygon ID	**2019-2022**	**2022-2023**	**2023-2024**	**2024-2025**	**Median**
ID1	0.73	0.57	0.35	0.50	0.53
ID2	0.79	0.28	0.52	0.53	0.53
ID3	0.52	0.15	0.38	0.51	0.45
ID4	0.64	0.20	0.33	0.51	0.42
ID5	0.62	0.34	0.02	0.53	0.43
ID6	0.48	0.01	0.49	0.48	0.48
ID7	0.79	0.18	0.32	0.56	0.44
ID8	0.22	0.41	0.37	0.17	0.30
ID9	0.21	0.45	0.26	0.57	0.35
ID11	0.06	0.70	0.31	0.15	0.23
ID12	0.54	0.53	0.10	0.20	0.37
ID13	0.57	0.66	0.23	0.25	0.41
ID14	0.49	0.69	0.28	0.29	0.39
ID15	0.43	0.62	0.37	0.70	0.53
ID16	0.56	0.56	0.50	0.38	0.53
ID17	0.61	0.51	0.09	0.30	0.40
ID18	0.50	0.33	0.12	0.20	0.27
ID19	0.56	0.48	0.30	0.45	0.47
ID20	0.20	0.54	0.22	0.19	0.21
ID21	0.24	0.58	0.27	0.56	0.42
ID22	0.31	0.48	0.17	0.44	0.37
ID23	0.76	0.47	0.44	0.47	0.47
ID24	0.79	0.22	0.29	0.53	0.41
ID25	0.07	0.04	0.19	0.17	0.12
ID26	0.43	0.05	0.50	0.54	0.46
ID27	0.55	0.35	0.14	0.50	0.43
ID30	0.51	0.27	0.64	0.56	0.54
ID35	0.44	0.85	0.41	0.29	0.42
ID37	0.67	0.41	0.28	0.53	0.47
ID38	0.22	0.37	0.19	0.07	0.20
ID39	0.74	0.66	0.08	0.61	0.64
ID40	0.55	0.72	0.12	0.25	0.40
ID41	0.67	0.73	0.13	0.36	0.52
ID42	0.24	0.38	0.17	0.10	0.20
ID43	0.53	0.37	0.09	0.28	0.33
ID44	0.42	0.80	0.12	0.13	0.27
ID45	0.54	0.51	0.14	0.28	0.39
ID46	0.56	0.89	0.00	0.23	0.40
ID47	0.62	0.69	0.30	0.86	0.66
ID48	0.56	0.57	0.39	0.48	0.52
ID49	0.24	0.37	0.21	0.28	0.26
ID50	0.32	0.11	0.29	0.44	0.30
ID51	0.44	0.24	0.04	0.75	0.34
ID52	0.61	0.24	0.47	0.52	0.49
ID55	0.46	0.19	0.72	0.62	0.54
ID56	0.41	0.50	0.53	0.52	0.51
ID57	0.65	0.57	0.25	0.53	**0.55**
Median	**0.53**	**0.47**	**0.28**	**0.47**	**0.47**

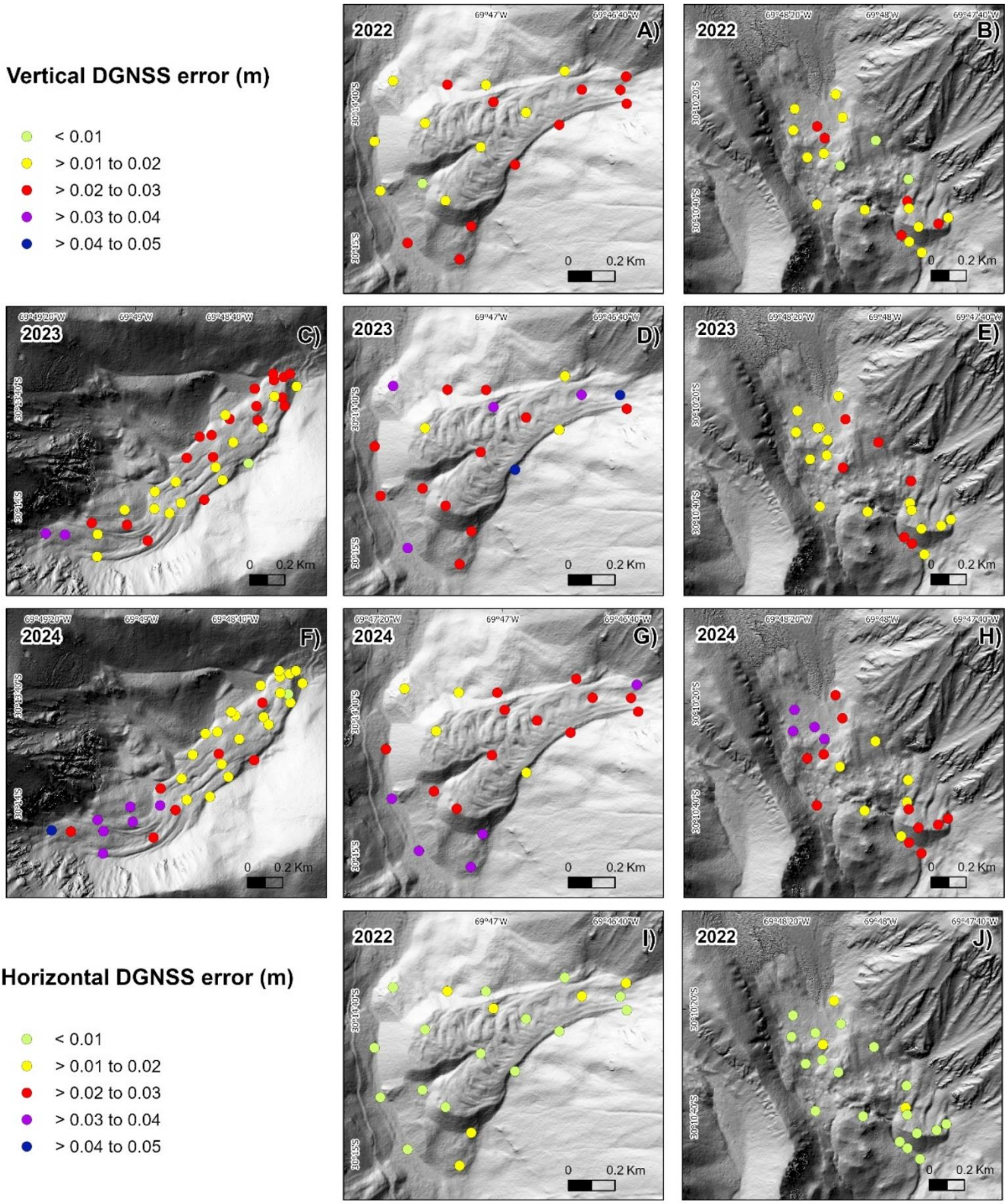
Vertical DGNSS error (m)
< 0.01
> 0.01 to 0.02
> 0.02 to 0.03
> 0.03 to 0.04
> 0.04 to 0.05
2022
A)
2022
B)
2023
C)
2023
D)
2023
E)
2024
F)
2024
G)
2024
H)
Horizontal DGNSS error (m)
< 0.01
> 0.01 to 0.02
> 0.02 to 0.03
> 0.03 to 0.04
> 0.04 to 0.05
2022
I)
2022
J)
0
0.2 Km

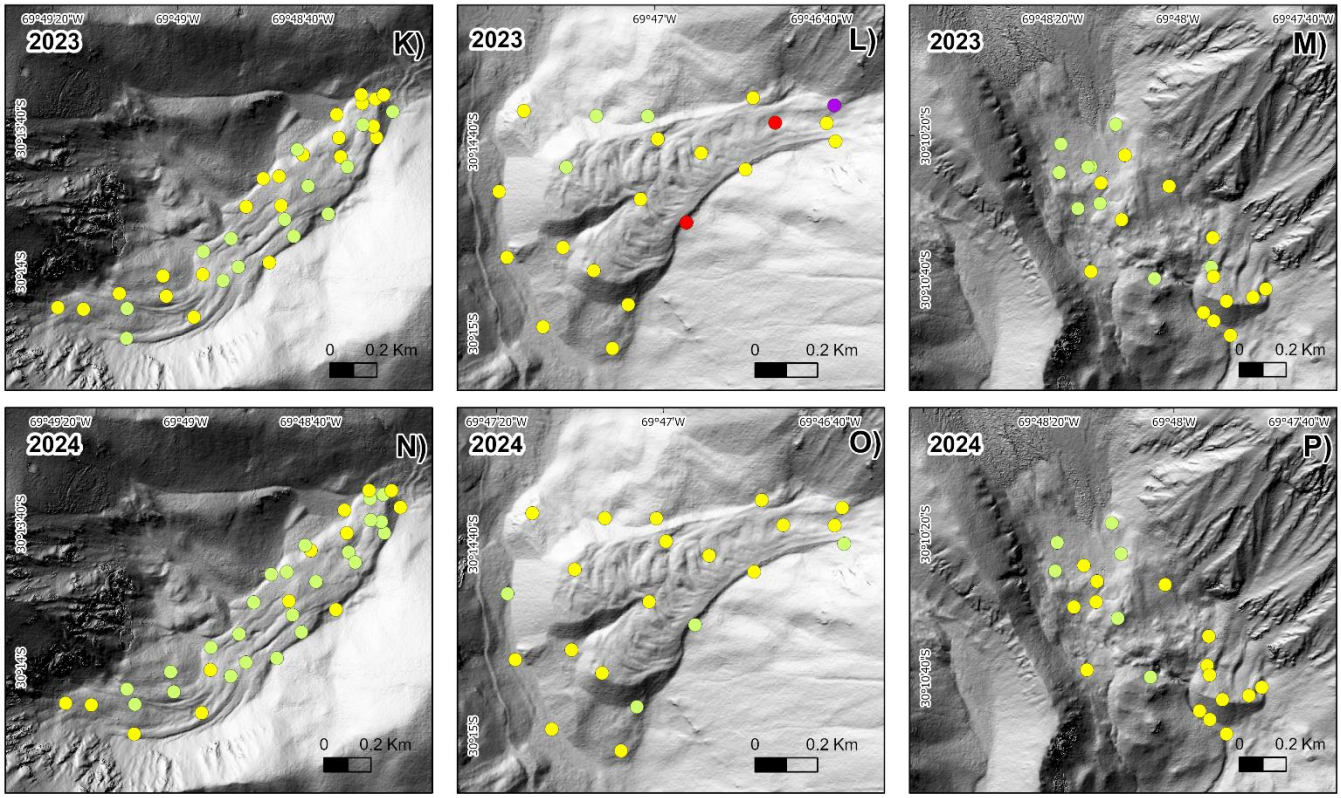

A5 continued Spatial distribution of the DGNSS errors (m) at El Paso rock glacier (left), Dos Lenguas rock glacier (centre) and the Agua Negra glacier forefield (right). Errors are provided for each acquisition (2022, 2023, 2024, as applicable) separated in vertical (A-H) and horizontal (I-P) error.

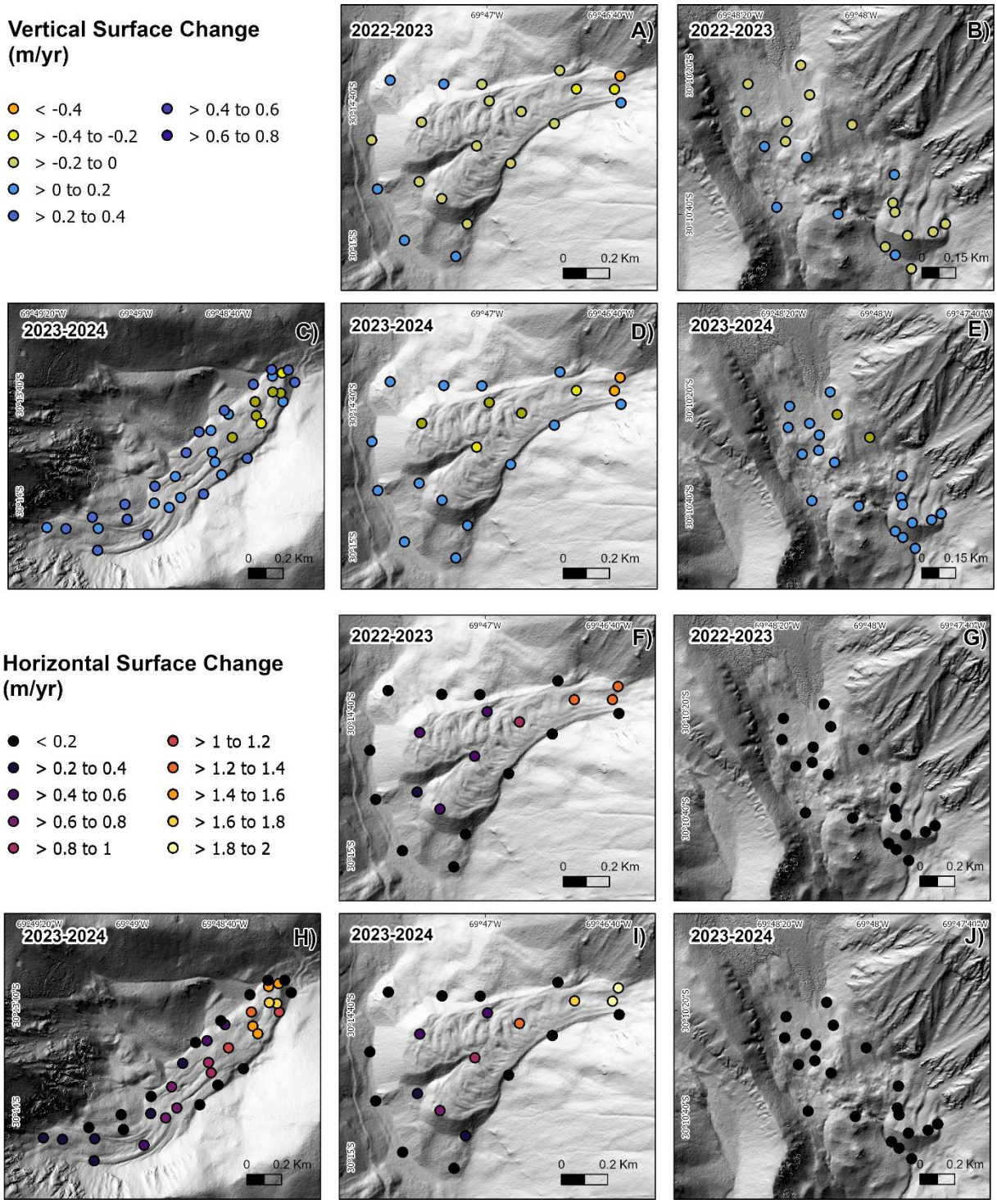

A6 Spatial distribution of the DGNSS-based surface changes (m/yr) at El Paso rock glacier (left), Dos Lenguas rock glacier (centre) and the Agua Negra glacier forefield (right). Surface changes are provided for each time period (2022-2023, 2023-2024, as applicable) separated in vertical (A-E) and horizontal (F-J) surface change.